



6th INTERNATIONAL CONFERENCE
ON ASIAN AND PACIFIC COASTS
(APAC2011)

Conference Programme
and Book of Abstracts



14-16 December 2011

Hong Kong, China



THE UNIVERSITY OF HONG KONG



Table of Contents

	Page
Welcome Message	1
Committees and Sponsors	2-6
General Information	7-9
APAC2011 Programme at a Glance	10-12
APAC2011 Oral Sessions	13-25
APAC2011 Poster Sessions	26-27
Keynote Lectures	29-72
Book of Abstracts	73-139

Welcome to APAC2011

It is our great pleasure to welcome you to this 6th International Conference on Asian and Pacific Coasts (APAC2011) and to the great city of Hong Kong. The Conference, hosted by The University of Hong Kong during December 14–16, 2011, aims to provide a platform where engineers and researchers can keep abreast of the current scientific and technological advancements in coastal and port-related research and practice.

The response to our Call for Papers announced in March 2011 was very heartening. We ended up receiving more than 300 submissions from more than 30 countries around the world. After peer review, some 250 papers have been accepted for presentation at the Conference.

This volume contains the APAC2011 Conference Programme and the Book of Abstracts. The programme consists of 6 keynote lectures, 4 invited lectures, 10 contributions to the Special Session on the 2011 East Japan Tsunami, and 237 other contributions arranged in various oral and poster sessions. These presentations cover a wide range of topics related to coastal, ocean and harbour engineering, such as beach erosion and morphodynamics, climate change and sea level rise, coastal management and shore protection, estuaries and ports, hydrodynamics of offshore and coastal structures, marine ecology and environment, marine and offshore wind energy, seawater intrusion, sediment transport, tsunami and storm surges, waves and tides, wastewater disposal and water quality, and so on. The full papers of these presentations are collected in the Proceedings of the Sixth International Conference on Asian and Pacific Coasts, which is published by World Scientific, 2011, ISBN: 978-981-4366-47-2.

We hope that you will find this Conference inspiring and stimulating for scientific interactions and informal discussions. The meeting should lead to more cooperation and collaboration within the scientific and engineering communities. Enjoy the Conference, and enjoy the great city of Hong Kong!

On behalf of the Local Organising Committee

Joseph Hun-Wei Lee

Chairman of APAC2011

December, 2011

APAC Council

CHOI, Byung Ho (Sungkyunkwan University, Korea) Chair
GODA, Yoshimi (Yokohama National University, Japan)
MIZUGUCHI, Masaru (Chuo University, Japan)
PYUN, Chong Kun (Myongji University, Korea)
QIU, Dahong (Dalian University of Technology, China)
XIE, Shileng (First Design Institute of Navigation Engineering, China)
ZUO, Qihua (Nanjing Hydraulic Research Institute, China)

International Steering Committee

CHENG, Liang (The University of Western Australia, Australia)
HUANG, Zhenhua (Nanyang Technological University, Singapore)
KIOKA, Wataru (Nagoya Institute of Technology, Japan)
LEE, Joseph Hun-Wei (The Hong Kong University of Science and Technology / The University of Hong Kong, Hong Kong, China)
LI, Yucheng (Dalian University of Technology, China)
LIN, Ming-Chung (National Taiwan University, Taiwan, China)
LIU, Philip L.F. (Cornell University, USA)
NADAOKA, Kazuo (Tokyo Institute of Technology, Japan)
OU, Shan-Hwei (Tajen University, Taiwan, China)
SHIBAYAMA, Tomoya (Waseda University, Japan)
SUH, Kyung-Duck (Seoul National University, Korea)
SUNDAR, Vallam (Indian Institute of Technology, Madras, India)
YAMASHITA, Takao (Hiroshima University, Japan)
YU, Xiping (Tsinghua University, China)
YUM, Ki Dai (Korean Ocean Research & Development Institute, Korea)

APAC2011 Local Organising Committee

LEE, Joseph Hun-Wei (The Hong Kong University of Science and Technology / The University of Hong Kong) Chairman

LI, C.W. (Hong Kong Polytechnic University) Vice-Chairman

MOK, Kai Meng (University of Macau) Vice-Chairman

NG, Chiu-On (The University of Hong Kong) Secretary

LAM, Kit Ming (The University of Hong Kong) Treasurer

CHAN, Pak Keung (Drainage Services Department, HKSAR Government)

CHOW, K.W. (The University of Hong Kong)

CLOSE Josie (City University of Hong Kong)

GAN, Jianping (The Hong Kong University of Science and Technology)

GHIDAoui, Mohamed S. (The Hong Kong University of Science and Technology)

KIKKERT, Gustaaf A. (The Hong Kong University of Science and Technology)

LAM, Hilda (Hong Kong Observatory, HKSAR Government)

LEE, Francis Man-chow (Civil Engineering and Development Department, HKSAR Government)

LO, Victor K.Y. (Development Bureau, HKSAR Government)

PUN, Kwok Leung (Chu Hai College of Higher Education, Hong Kong)

WAI, Onyx W.H. (Hong Kong Polytechnic University)

APAC 2011 International Scientific Committee

BAI, Yuchuan (Tianjin University, China)

CHIEW, Yee Meng (Nanyang Technological University, Singapore)

DAVIDSON, Mark (University of Canterbury, New Zealand)

HWUNG, Hwung-Hweng (National Cheng Kung University, Taiwan, China)

ISOBE, Masahiko (The University of Tokyo, Japan)

KAO, Chia Chuen, (National Cheng Kung University, Taiwan, China)

LARSEN, Ole (DHI-NTU Centre, Singapore)

LAW, Adrian Wing-Keung (Nanyang Technological University, Singapore)

LIN, Pengzhi (Sichuan University, China)

LIU, Cheng (International Research and Training Centre on Erosion & Sedimentation, China)

LIU, Hua (Shanghai Jiaotong University, China)

LO, Edmond Yat-Man (Nanyang Technological University, Singapore)

LU, Dong-qiang (Shanghai University, China)

TAJIMA, Yoshimitsu (University of Tokyo, Japan)

TAN, Soon Keat (Nanyang Technological University, Singapore)

TANAKA, Hitoshi (Tohoku University, Japan)

TAO, Jianhua (Tianjin University, China)

THANH, Vu Dinh (Ho Chi Minh City University of Technology, Vietnam)

WAN, Decheng (Shanghai Jiaotong University, China)

WANG, Xiaohua (The University of New South Wales, Australia)

YEH, Harry (Oregon State University, USA)

YUAN, Yeli (The First Institute of Oceanography, State Oceanic Administration, China)

ZHANG, Changkuan (Hohai University, China)

APAC2011 Supporting Organisations and Institutions



Korean Society of
Coastal and Ocean
Engineers



Chinese Ocean
Engineering Society



Japan Society of
Civil Engineers

International Association for Hydro-Environment Engineering and Research (IAHR)

International Association for Hydro-Environment Engineering and Research (IAHR) – Hong Kong Chapter (IAHR-HK)

The Hong Kong Institution of Engineers (Environmental Division)

The Hong Kong Institution of Engineers (Civil Division)

Chartered Institution of Water and Environmental Management (CIWEM) – Hong Kong

Civil Engineering and Development Department, HKSAR Government

Drainage Services Department, HKSAR Government

Hong Kong Observatory, HKSAR Government

Water Supplies Department, HKSAR Government

City University of Hong Kong – School of Energy and Environment

The Hong Kong University of Science and Technology

The Hong Kong Polytechnic University

Chu Hai College of Higher Education

University of Macau

Maritime Administration, Macao SAR Government

Meteorological and Geophysical Bureau, Macao SAR Government

APAC2011 Sponsors

K.C. Wong Education Foundation

Guangdong Provincial Changda Highway Engineering Co., Ltd.

Croucher Foundation

Dragages Hong Kong Limited

Nishimatsu Construction Co. Ltd.

Scottish Development International

World Scientific Publishing Co. Pte Ltd.

General Information

Conference Package

Each registrant will receive a conference bag, a name badge, a copy of the Proceedings on CD, a Conference Programme and Book of Abstracts, a receipt of the registration fee, and souvenirs. A certificate of attendance will be issued to participants upon request. Full-fee registrants and registered accompanying persons also receive an admission ticket to the banquet. All participants are requested to wear their conference badges throughout the conference. Refreshments will be served free of charge only to identifiable participants during the morning and afternoon breaks.

Oral Presentations

The time allotted to each speaker for presentation and discussion is as follows:-

Keynote speakers – 40 minutes

Invited speakers – 30 minutes

Other speakers – 15 minutes

Kindly respect each speaker's rights and adhere strictly to the time scheduled in the programme. Presenters are requested to do the following before the start of their session: (i) contact the session chair; (ii) load their presentation files onto the computer provided in the room of the session. Standard software packages (Office 2010, Acrobat, RealPlayer, Windows Media Player, etc) are installed on these computers, which run on Windows 7. Please test in advance your files (especially videos) with these computers. To save time and the trouble, presenters should not use their own computers for the presentation unless absolutely necessary.

Poster Presentations

Poster presentations are scheduled on 15, 16 December (Thursday and Friday). A poster can be mounted all day from 08:30, but not later than 12:00, on the day the presentation is scheduled, and must be removed by 16:30 the same day. Poster panels are 29 inches wide by 39 inches high (0.7 x 1.0 meter), and posters can be attached to them using magnets only (thumbtacks, glue and tapes are not allowed). Give the paper title and list all the authors at the top of the display. Recommended fonts are 36 pt. for title and 24 pt. for authors. All other texts should be 16 pt. or larger.

Lunches

Buffet lunches (for full-fee registrants) are served at the Sky Lounge on the 18th Floor of Sheraton Hotel.

Internet

Participants may have access to Wi-Fi, free of charge, for wireless connection of their computers to the internet at the conference venue.

Messages

Participants may leave messages or post notes on a notice board located near the registration desk. Please check the board frequently.

Banquet

The conference banquet is held at the East Ocean Restaurant, on Level 12 of The One, which is a shopping mall located about five blocks along Nathan Road (10 – 15 minutes walking) away from the conference venue. Please refer to the map shown on the back side of the banquet ticket, and present the ticket on attending the banquet.

Technical Visits

Participants are urged to join half-day technical visits to be held on 17 December. Please see the updated information posted on the notice board, and sign up at the registration desk.

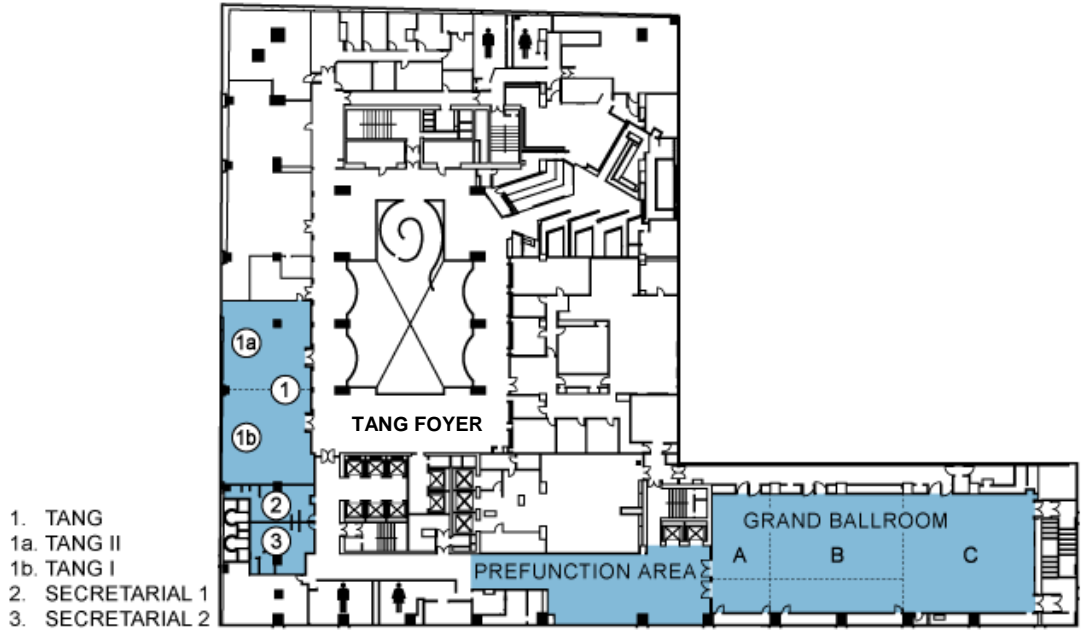
Conference Venue

Sheraton Hong Kong Hotel & Towers

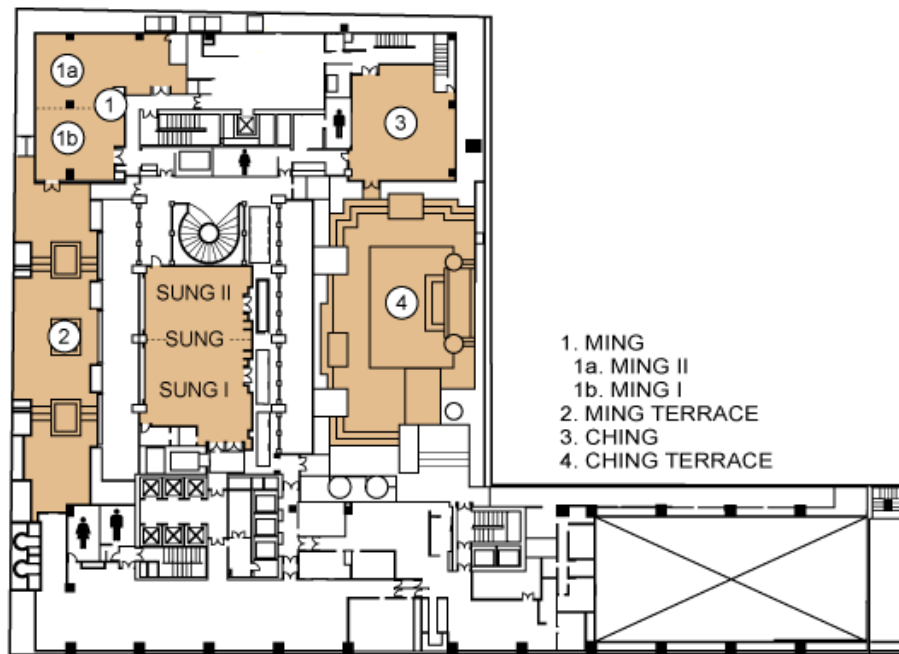
20 Nathan Road, Kowloon

Tel: (852) 2369 1111

Website: sheraton.com/hongkong



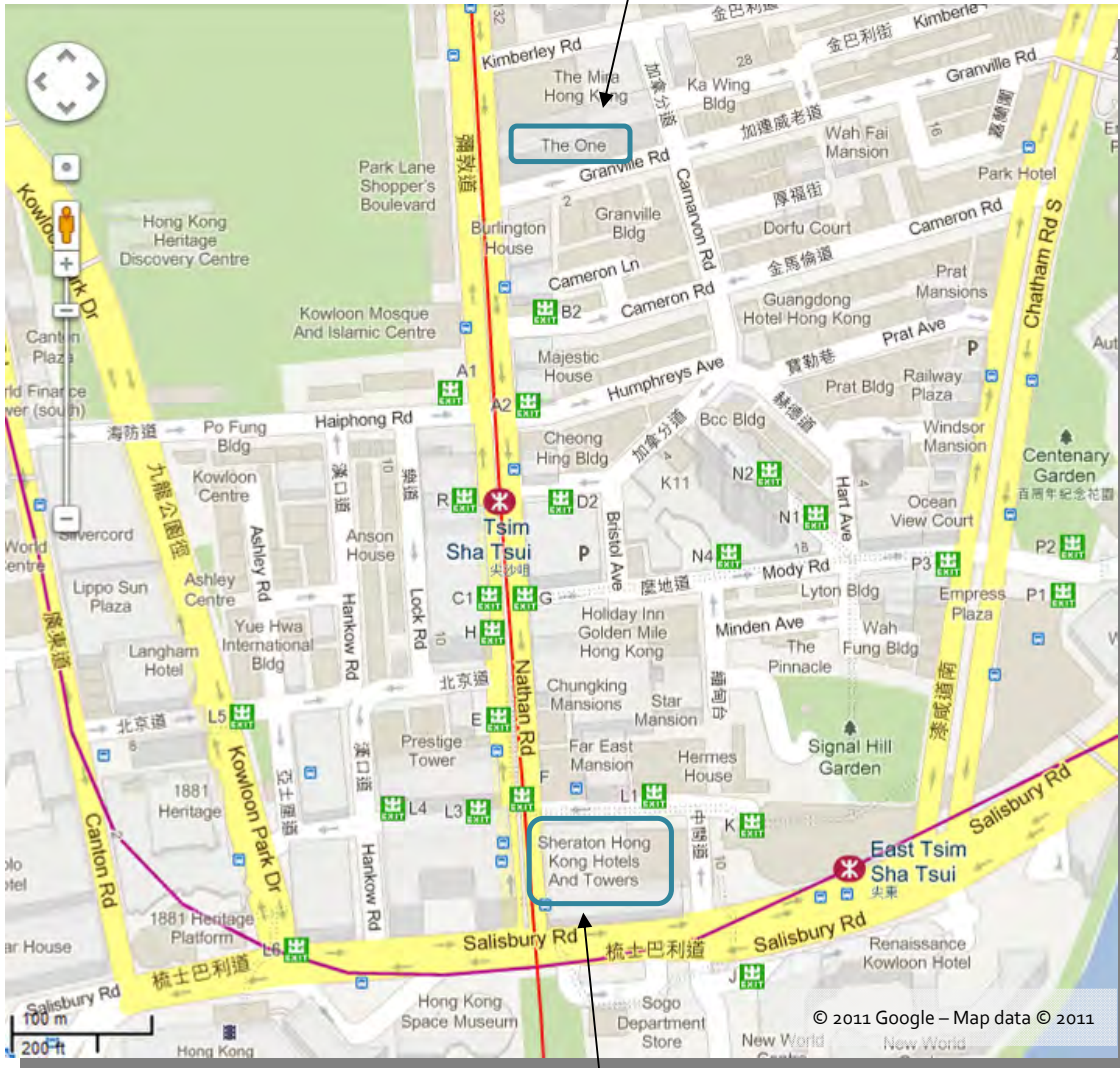
THIRD FLOOR



FOURTH FLOOR

Direction to Banquet venue
(~15 minutes' walk from Conference venue)

Banquet at East Ocean Restaurant
L12 The One, 100 Nathan Road



Conference venue
Sheraton Hong Kong Hotels & Towers

APAC2011 Programme at a Glance

Wednesday 14 December 2011	08:00 – 16:30	Registration	Tang Foyer
	09:00	Opening Ceremony (MC: Prof. K.M. Mok) Opening Remarks: Prof. Joseph H.W. Lee (Chairman, APAC2011 Local Organising Committee) Welcome Speech: Prof. Lap-Chee Tsui (Vice-Chancellor and President, The University of Hong Kong) Welcome Address: Mrs. Carrie Lam (Secretary for Development, Development Bureau, Hong Kong Government) APAC Address: Prof. Byung Ho Choi (Chair, APAC Council) Photo Taking and Presentation of Souvenirs	Ballroom
	09:35	Keynote Lecture 1 (Chair: Joseph H.W. Lee) Toward sustainable and secure coastal zones: roles of waves, tides, sediments, and turbulence <i>Harindra J.S. Fernando</i> (Univ. Notre Dame, USA)	Ballroom
	10:15	Keynote Lecture 2 (Chair: Takao Yamashita) Climate change effects on future waves and typhoons <i>Hajime Mase</i> (Kyoto Univ., Japan)	Ballroom
	10:55	Break	
	11:10	Keynote Lecture 3 (Chair: Qihua Zuo) Hydrodynamics research and application of the radial sand ridge in South Yellow Sea, China <i>Peidong Lu and Xiping Dou</i> (NHRI, China)	Ballroom
	11:50	Keynote Lecture 4 (Chair: Byung Ho Choi) Performance-based design of caisson breakwater incorporating wave height increase due to climate change <i>Kyung-Duck Suh</i> (Seoul National Univ., Korea)	Ballroom
	12:30	Lunch	Sky Lounge
	14:00	Parallel Session 1	
		Estuaries and Ports I	Ballroom C
		Climate Change and Sea Level Rise I	Ballroom B
		Coastal Management and Shore Protection I	Tang
	15:30	Break	
	15:45	Parallel Session 2	
		Estuaries and Ports II	Ballroom C
		Climate Change and Sea Level Rise II	Ballroom B
		Coastal Management and Shore Protection II	Tang
	17:30	Welcome Reception	Ching and Terrace

Thursday
15 December 2011

08:00 – 16:30	Registration	Ballroom Pre-function Area
08:30 – 09:10	Keynote Lecture 5 (Chair: Chong Kun Pyun) The challenges to be addressed if tidal energy is to become economically viable <i>Cameron M. Johnstone</i> (Nautricity Ltd., UK)	Ballroom
09:30	Parallel Session 3	
	Marine Energy I	Ballroom C
	Estuaries and Ports III	Ballroom B
	Marine Ecology and Environment I	Tang
	Hydrodynamics I	Ming II
	Wave Loading	Sung I
10:45	Break	
11:00	Parallel Session 4	
	Marine Energy II	Ballroom C
	Estuaries and Ports IV	Ballroom B
	Coastal Management and Shore Protection III	Tang
	Hydrodynamics II	Ming II
	Tsunami and Storm Surge	Sung I
12:30	Lunch	Sky Lounge
14:00	Parallel Session 5	
	Beach Erosion and Morphodynamics I	Ballroom C
	Estuaries and Ports V	Ballroom B
	Waves and Modelling I	Tang
	Hydrodynamics III	Ming II
	Numerical Methods and Simulation I	Sung I
15:30	Break	
15:45	Parallel Session 6	
	Beach Erosion and Morphodynamics II	Ballroom C
	Jets I	Ballroom B
	Waves and Modelling II	Tang
	Hydrodynamics IV	Ming II
	Numerical Methods and Simulation II	Sung I
08:30 – 16:30	Poster Session 1	Ballroom A

Friday 16 December 2011	08:00 – 16:30	Registration	Ballroom Pre-function Area
	08:30 – 09:10	Keynote Lecture 6 (Chair: C.W. Li) Tsunami amplification and breaking along a vertical wall <i>Harry Yeh and Wenwen Li</i> (Oregon State Univ., USA)	Ballroom
	09:30	Parallel Session 7 Special Session: The 2011 East Japan Tsunami I Jets II Marine Ecology and Environment II Waves and Modelling III Numerical Methods and Simulation III	Ballroom C Ballroom B Tang Ming II Sung I
	10:45	Break	
	11:00	Parallel Session 8 Special Session: The 2011 East Japan Tsunami II Wastewater Disposal and Water Quality I Sediment Transport I Waves and Modelling IV Numerical Methods and Simulation IV	Ballroom C Ballroom B Tang Ming II Sung I
	12:30	Lunch	Sky Lounge
	14:00	Parallel Session 9 Beach Erosion and Morphodynamics III Wastewater Disposal and Water Quality II Sediment Transport II Waves and Modelling V Properties of Materials	Ballroom C Ballroom B Tang Ming II Sung I
	15:30	Break	
	15:45	Parallel Session 10 Beach Erosion and Morphodynamics IV Seawater Intrusion Marine Ecology and Environment III Waves and Modelling VI Construction and Structures	Ballroom C Ballroom B Tang Ming II Sung I
	08:30 – 16:30	Poster Session 2	Ballroom A
	19:00	Banquet	East Ocean Restaurant

Programme for Oral Presentations

Wednesday, 14 December

Parallel Session 1 (14:00 – 15:30)

	Ballroom C Estuaries and Ports I Chair: <i>Xiping Dou, Moonsu Kwak</i>	Ballroom B Climate Change and Sea Level Rise I Chair: <i>Tsung-Lin Lee, Hisamichi Nobuoka</i>	Tang Coastal Management and Shore Protection I Chair: <i>Insik Chun, Onyx W.H. Wai</i>
14:00	Invited Talk Master plan of tidal flat reclamation along Jiangsu coastal zone <i>Changkuan Zhang and Jun Chen</i>	Oceanic oscillation and rainfall distribution in the Indonesian Archipelago <i>Takao Yamashita, Hendri, Takashi Okamoto and Tsuyoshi Ikeda</i>	Feasibility study of coastal reservoir for water supply to Southeast Queensland, Australia <i>Shu-Qing Yang</i>
14:15		Extreme wave climate change projection at the end of the 21st Century <i>Tomoya Shimura, Nobuhito Mori, Sota Nakajo, Tomohiro Yasuda and Hajime Mase</i>	Reliability analysis of quarter-circular caisson breakwater <i>Luwen Qie, Yinan Qin, H.Q. Ding, X. Zhang and Xuelian Jiang</i>
14:30	Simulation of the hydrodynamic influence for the HZM bridge project in the estuarine areas of Pearl River <i>Jie He, W.J. Xin and J.Y. Hou</i>	Long term trends of the regional sea level changes in Hong Kong and the adjacent waters <i>Kin Wai Li and Hing Yim Mok</i>	Directional wave spectrum in shallow water waves using an array of pixel brightness on video images <i>Muhammad Zikra, Noriaki Hashimoto, Masaki Yokota, Masaru Yamashiro and Kojiro Suzuki</i>
14:45	Tidal flat evolution at the central Jiangsu Coast, China <i>Zheng Gong, Zhengbing Wang, M.J.F. Stive and Changkuan Zhang</i>	Prediction of future tropical cyclone characteristics using global stochastic tropical cyclone model <i>Sota Nakajo, Nobuhito Mori, Tomohiro Yasuda and Hajime Mase</i>	Research on armor units stability in 3d and 2d physical model <i>Ci-Heng Zhang, Ziauddin Abd Latif, Han-Bao Chen and Yu-Fen Cao</i>
15:00	Analysis of the decadal change in the riverbed of the Tedor River, Japan and its correlation with neighboring coasts <i>Minh Hai Dang, Shinya Umeda, Ryosuke Matsuda and Masatoshi Yuhi</i>	Projection of future storm surge due to climate change and its uncertainty – a case study in the Tokyo Bay <i>Tomohiro Yasuda, Nobuhito Mori, Sota Nakajo, Hajime Mase, Yuta Hayashi and Yuichiro Oku</i>	Preliminary design of decision support system for seawall safety management <i>Zhengping Zhou, Qihua Zuo and Chi Wang</i>
15:15		Statistical downscaling of multi-site multivariate daily extreme temperature series for climate-related impact assessment studies <i>Van-Thanh-Van Nguyen and Malika Khalili</i>	Development of coastal observation system using a network camera and its application to Hachigasaki Beach, Japan <i>Hiroshi Kurosaki and Masatoshi Yuhi</i>

Parallel Session 2 (15:45 – 16:45)

	Ballroom C Estuaries and Ports II Chair: Changkuan Zhang	Ballroom B Climate Change and Sea Level Rise II Chair: Noriaki Hashimoto	Tang Coastal Management and Shore Protection II Chair: Han-Bao Chen, Luwen Qie
15:45	Influence on flood control when building tidal sluice in Mulan Creek Estuary, Fujian Province, China <i>Xiaodong Zhao, Xiangming Wang, Xuesong Xu and G.H. Chen</i>	Assessment of coastal vulnerability to sea level rise using remote sensing (RS) and geographic information systems (GIS): a case study of Bolinao, Pangasinan, Philippines <i>Sheryl Rose Reyes and Ariel Blanco</i>	From dynamic sand beach to static rubble mound <i>Frans Rabung and Jon B. Hinwood</i>
16:00	Numerical study on the siltation in harbor area of the Hongqili Waterway, Pearl River Delta <i>C.W. Xu, L.Q. Zuo and H.X. Liu</i>	Application of artificial neural network to estimate the long term sea level in 2020 <i>Tsung-Lin Lee, Chih-Chung Wen, Ching-Jer Huang and Tai-Wen Hsu</i>	Training work at the mouth of tidal inlet for protection of approach channel to fishing harbor <i>Dipak Kumar Maiti, M.D. Kudale and A.V. Sitarama Sarma</i>
16:15	The evolution tendency of the south channel of the Changjiang River Estuary, China, in the past 150 years <i>Huiming Huang, Yi-Gang Wang, Tong-Jun Yang and Juan Zhao</i>	Vulnerability change in coastal zones of Vietnam and Japan <i>Hisamichi Nobuoka and Mai Van Cong</i>	Development of deformable rubber membrane parapets <i>Insik Chun and Sunsin Kim</i>
16:30			Analytical research on the reliability of sea dike structure safety <i>Qing Jun Liu, Qi Hua Zuo, Deng Ting Wang, Zheng Ping Zhou and Jin Wang</i>

Parallel Session 3 (09:30 – 10:45)

	Ballroom C Marine Energy I Chair: <i>Josie Close, Cameron M. Johnstone</i>	Ballroom B Estuaries and Ports III Chair: <i>Zheng Gong, Masatoshi Yuhi</i>	Tang Marine Ecology and Environment I Chair: <i>Satoquo Seino, Wai Thoe</i>	Ming II Hydrodynamics I Chair: <i>Adrian Wing-Keung Law, Wataru Kioka</i>	Sung I Wave Loading Chair: <i>Liang Cheng, Guohai Dong</i>
09:30	Invited Talk Design of offshore wind farms <i>Andrass Ziska Davidsen and Flemming Jakobsen</i>	Preliminary analysis of the effects on the Yangtze Estuary after Three-Gorge Reservoir operation <i>Xiping Dou, Xiqing Chen and Yixin Yan</i>	Capture and clogging behavior of organic mud in sand beds <i>Narong Touch, Nakashita Shinya, Tadashi Hibino and Shoji Fukuoka</i>	Experimental study on wave crest height on a gravity type complex structure <i>Haiyuan Liu, Baoyou Zheng, Hanbao Chen and Baolei Geng</i>	Experimental investigation of wave loads on offshore platform with inverted cone column <i>Jing Zhao, Yanlong Qin and Shipeng-Wang</i>
09:45		The research on hydrodynamic mechanism of morphology revolution of the Xiaomiaohong tidal channel in radial sand ridges, Jiangsu Province, China <i>Kefeng Chen and Liangliang Yu</i>	Spatio-temporal patterns and the variation mechanism of nutrients in the Yangtze Estuary <i>Yanping Cui, Guoxian Huang, Qiuwen Chen and Simin Qu</i>	Wave-field flow structures developing around large-diameter vertical circular cylinder <i>Giancarlo Alfonsi, Agostino Lauria and Leonardo Primavera</i>	Research of wave force on the submerged caisson for pile-gravity complex wharf <i>Baolei Geng, Baoyou Zheng, Hanbao Chen and Haiyuan Liu</i>
10:00	Physical experiments on the discharge capability of the sluice caisson of tidal power plant <i>Sang-Ho Oh, Dal Soo Lee, Kwang Soo Lee and Se-Chul Jang</i>	Numerical simulation of tidal wave deformation in lower reach caused by floodgate in estuary <i>Xinzhou Zhang, Xiping Dou, X.M. Wang, Xiaodong Zhao and Xuesong Xu</i>	The variation trend of nutrient flux from Yangtze River and related impact on Yangtze Estuary <i>Guoxian Huang, Qiuwen Chen, Yanping Cui, F. Ye and Baodong Wang</i>	Analysis of wave interaction with a submerged slightly inclined porous plate with a partially reflecting sidewall <i>Yong Liu and Yucheng Li</i>	Numerical modelling of breaking wave impact pressure on a vertical wall <i>N. Senthil Kumar and S.A. Sannasiraj</i>
10:15	Upstream wake effect on performance of the horizontal axis tidal current power <i>Chul Hee Jo, Kang-Hee Lee, Jun Ho Lee and Cristian Nichita</i>	Flow change induced by shift and modification of submerged weir installed at Han River Estuary <i>Kyong-Oh Baek</i>	Multivariate statistical analysis of the seasonal variation of chlorophyll distribution in the north Indian Ocean <i>Sushant Das, Girija Jayaraman and Beena Kumari</i>	Numerical modelling of wave-induced soil response around breakwater heads <i>Dong-Sheng Jeng, Yu Zhang, Jisheng Zhang, Chi Zhang and Philip L-F Liu</i>	Experiment study on spectrum of wave and force on cylinder structure <i>Hanbao Chen, Haiyuan Liu and Haicheng Liu</i>
10:30	Development of real-time control and monitoring system for wave energy converters <i>Shin-Yeol Park, Byung-Hak Cho, Dong-Soon Yang and Kyung-Shik Choi</i>		Impact of oil and gas production activities on cohesive sediment and biological adaptation <i>Margaret Chen, Stanislas Wartel and Frank Fiers</i>	Coastal erosion caused by cavitation bubble implosion: micro-view on the bubble dynamics <i>Yuan Xiang Yang, Soon Keat Tan and Qian Xi Wang</i>	Wave induced pressures on crown wall of KOLOS armoured breakwater <i>Avaneendran Arunjith, Sannasi Annamalai Sannasiraj and Vallam Sundar</i>

Parallel Session 4 (11:00 – 12:30)

	Ballroom C Marine Energy II Chair: <i>Chul Hee Jo, Philippe Gourbeville</i>	Ballroom B Estuaries and Ports IV Chair: <i>Keisuke Nakayama, Y.Y. Wan</i>	Tang Coastal Management and Shore Protection III Chair: <i>Xuelian Jiang, Shu-Qing Yang</i>	Ming II Hydrodynamics II Chair: <i>Mohamed Ghidaoui, Dong-Sheng Jeng</i>	Sung I Tsunami and Storm Surge Chair: <i>K.W. Chow, Seungbuhm Woo</i>
11:00	Tidal range and tidal current energy resources in neighboring seas of Korea <i>Byung Ho Choi and Byung Il Min</i>	Effect of large scale tidal flat reclamation on hydrodynamic circulation in Jiangsu coastal areas <i>Jianfeng Tao, Ting Yang, Fan Xu and Jing Yao</i>	Evacuation modelling to develop risk management strategies for the cities of Padang and Pariaman, West Sumatra <i>Manuela Di Mauro, Kusnowidjaja Megawati and Zhenhua Huang</i>	Effects of pneumatic chambers on the performance of moored floating breakwaters: an experimental study <i>Fang He, Zhenhua Huang, Adrian Wing-Keung Law and Wenbin Zhang</i>	Magnetic anomaly induced by tsunami waves in open oceans <i>Benlong Wang and Hua Liu</i>
11:15	Morphological effect of flapping-type tidal power generator <i>Jin Hwan Ko, Jin-Soon Park, Kwang-Soo Lee, Tuyen Quang Le and Doyoung Byun</i>	Long-term hindcasting of wave climate for Jiangsu coast <i>Yongping Chen and Changkuan Zhang</i>	A dynamic 3-dimensional coastal information management system for the Pearl River Estuary, China <i>J.Z. Lu, B.Y. Chen, Onyx W.H. Wai and X.L. Chen</i>	Application of the wave pump concept to simulate tidal anomalies in Conjola Lake, NSW, Australia <i>Thuy T. T. Vu, Peter Nielsen, David P. Callaghan and David J. Hanslow</i>	Numerical solution of landslide tsunami propagation over a uniformly sloping beach <i>Seung Nam Seo and Philip L.-F. Liu</i>
11:30	Performance of tidal stream turbine adapted to bridge pier protection structures <i>Sang-Ho Oh, Jin-Hak Yi, Se-Chul Jang, Gunwoo Kim and Sang Ryul Lee</i>	Measurements of tidal current and surface current in Tokyo Bay by HF radar <i>Yusuke Ozawa and Kazuo Murakami</i>	Monitoring coastal shoreline and bathymetry based on space imagery <i>Shotaro Funatake, Yoshimitsu Tajima, Wickramaarachchi Bandula, Samarakoon Lal and Shinichi Sobue</i>	Vortex-induced vibration of a circular cylinder near a plane wall <i>Xikun Wang, Soon Keat Tan and Zhiyong Hao</i>	Rising seawall for prevention of tsunamis and storm surges <i>Yuichiro Kimura, Masaki Inui, Kyoichi Nakayasu, Yoshito Yamakawa, Tetsuya Hiraishi and Hajime Mase</i>

11:45	<p>Study of the influence of tropical cyclone on offshore wind turbine generator system</p> <p><i>Liang Pang, Zhi-Qiang Li and Hong-Rui Yang</i></p>	<p>Investigation on overtopping rate of north bank seawall in Qiantang Estuary due to super typhoons</p> <p><i>Shichang Huang, Jinchun Hu, Yali Xie and Xin Zhao</i></p>	<p>Wave run-up, run-down studies on berm breakwater with concrete cubes as armour units</p> <p><i>Subba Rao, Kiran G Shirlal, Balakrishna Rao K and Prashanth Janardhan</i></p>	<p>An introduction to O-tube</p> <p><i>Hongwei An, Chengcai Luo, Liang Cheng, Dave White and Tuarn Brown</i></p>	<p>Modelling of winds, precipitation, storm surge, and waves during the passage of typhoon Morakot using an atmosphere-waves-ocean coupled model</p> <p><i>Han Soo Lee, Fei Ding, Hendri, Takao Yamashita and Haggag Mohammed</i></p>
12:00	<p>Development of in-stream hydro power pilot plant in Korea</p> <p><i>Y.C. Park, C.S Myung, Ki-Dai Yum and Shin Taek Jeong</i></p>	<p>Computer simulation of Yeong-II man new harbor for seiche reduction</p> <p><i>Moonsu Kwak, Yongho Moon and Chongkun Pyun</i></p>	<p>The combination of low crested breakwater with mangroves to reduce the vulnerability of the coast due to climate change</p> <p><i>Muhammad Arsyad Thaha and Achmad Bakri Muhiddin</i></p>	<p>Bottom roughness and flow characteristics for combined near-orthogonal wave-current flows over smooth and rippled bottoms</p> <p><i>Kian Y. Lim, Ole S. Madsen and Hin F. Cheong</i></p>	<p>Tsunami induced shear stresses along submarine canyon off southeast coast of India</p> <p><i>Jaya Kumar Seelam and Tom E. Baldock</i></p>
12:15	<p>Experimental and numerical simulation tools for floating wind turbines</p> <p><i>Pierre Ferrant, Jean-Marc Rousset, Adrien Courbois and Maxime Philippe</i></p>		<p>Land use spatial model for building based on availability and capacity of land in territory of coastal city (case study: Palu City)</p> <p><i>Amar Akbar Ali, Mary Selintung, Roland A. Barkey and M. Arsyad Thaha</i></p>	<p>A modeling approach of combined simulation of tide, wind and wave on the west coast of Korea</p> <p><i>Seungwon Suh, Hyeonjeong Kim and Hwayoung Lee</i></p>	<p>Influence of velocity distribution and density stratification on generation or propagation of tsunamis</p> <p><i>Taro Kakinuma, Kazuo Nakamura, Kei Yamashita and Keisuke Nakayama</i></p>
12:30	<p>Assessment of wave energy source near Dangan Islands</p> <p><i>Zhe Ma, Hong Da Shi and Zhen Liu</i></p>				

Parallel Session 5 (14:00 – 15:30)

	Ballroom C Beach Erosion and Morphodynamics I Chair: <i>D.A. Suriamihardja, Jianping Gan</i>	Ballroom B Estuaries and Ports V Chair: <i>Jun Chen, Yongping Chen</i>	Tang Waves and Modelling I Chair: <i>Young-Taek Kim, Xiping Yu</i>	Ming II Hydrodynamics III Chair: <i>Seungwon Suh, Xikun Wang</i>	Sung I Numerical Methods and Simulation I Chair: <i>Hirohide Kiri, Benlong Wang</i>
14:00	Invited Talk Beach nourishment projects in China <i>Cuiping Kuang, Yi Pan, Lulu He, Yanxiong Yang and Feng Cai</i>	Wetlands restoration and protection in Yellow River Delta, China <i>Yanyan Hua, Baoshan Cui and Wenjie He</i>	Experimental research on computing method of wave pressure for immersed vertical barrier of open-type breakwater <i>Liehong Ju, Peng Li and Qihua Zuo</i>	Numerical experiments on strong vertical mixing under strong winds in the coastal zone <i>Nobuhito Mori, Yusuke Tanaka, Sota Nakajo, Tomohiro Yasuda and Hajime Mase</i>	Potential and application of hydrodynamic modelling on unstructured grids <i>Adri Verwey, Herman W.J. Kernkamp, Guus Stelling, M.L. Tse and W.C. Leung</i>
14:15		A study on the seawater flow characteristics for various shrouds used in tidal current generation systems <i>Jong-Won Kim, Yu-Hyun Choi and Sang-Ho Lee</i>	Effects of diffraction and directional asymmetry of random wave loads on a long structure <i>Jae-Sang Jung, Changhoon Lee and Yong-Sik Cho</i>	Experimental and numerical study on current velocities and vertical profiles of undertow over a submerged breakwater <i>Siddique Mohsin, Yoshimitsu Tajima and Shinji Sato</i>	RANS-VOF for a solitary wave flow around a 3d vertical cylinder <i>Decheng Wan, Hongjian Cao and Yuanchuan Liu</i>
14:30	Modelling the change of beach profile under tsunami waves: a comparison of selected sediment transport models <i>Linlin Li and Zhenhua Huang</i>	Monitoring fluid mud in the north passage navigation channel of Yangtze Estuary, China <i>Y.Y. Wan and J.A. Roelvink</i>	Particle trajectories in nonlinear interfacial water waves <i>Hung-Chu Hsu, Chiu-On Ng and Hwung-Hweng Hwung</i>	Oscillatory flow around a pair of cylinders of different diameters <i>Kun Yang, Hongwei An, Liang Cheng and Ming Zhao</i>	Three-dimensional numerical study on bore driven swash <i>Bin Deng, Changbo Jiang, Liping Zhao and H.S. Tang</i>
14:45	Effect of beach nourishment using gravel and tracking movement of gravel <i>Toshinori Ishikawa, Takaaki Uda and Toshiro San-Nami</i>	Advances in development and management of estuarine and coastal mudflats <i>Y.J. Lu, Q.Z. Hou, Y. Lu, Y.H. Wang, C.W. Xu and R.Y. Ji</i>	Revision of regional frequency analysis method for extreme wave heights <i>Yoshimi Goda, Masanobu Kudaka and Hiroyasu Kawai</i>	The role of steady streaming in sheetflow transport <i>Kyikyilwin, Haijiang Liu and Shinji Sato</i>	Internal generation of waves on an arced band in an unstructured grid system <i>Gunwoo Kim and Changhoon Lee</i>
15:00	Erosion of Hirota ruins due to storm waves associated with Typhoon 0514 <i>Takaaki Uda, Yukino Kowaki and Takahiro Ishido</i>		Power of a piston wave maker by numerical method <i>Hanbin Gu, Derek M. Causon, Clive G. Mingham, Ling Qian, Zhihua Ma, Hanbao Chen and Zilong Zheng</i>	The variation of water level and flow velocity in semi-closed water area by wind and boat wave <i>Kohji Uno, Gozo Tsujimoto and Tetsuya Kakinoki</i>	Numerical study on the water exchange of the Bohai Sea under the combined action of wave, tide and surge <i>Bo Xia, Qinghe Zhang, Yuan Li and Changbo Jiang</i>

Parallel Session 6 (15:45 – 16:45)

	Ballroom C Beach Erosion and Morphodynamics II Chair: <i>Yongjun Lu, Zheng Bing Wang</i>	Ballroom B Jets I Chair: <i>K.M. Lam, Il Won Seo</i>	Tang Waves and Modelling II Chair: <i>Yong-Sik Cho, Hung-Chu Hsu</i>	Ming II Hydrodynamics IV Chair: <i>Changhoon Lee, Yong Liu</i>	Sung I Numerical Methods and Simulation II Chair: <i>Decheng Wan</i>
15:45	Prediction of long-term topographic changes of Tenryu River Delta associated with sand bypassing at dam in upper basin assuming no coastal facilities <i>Shiho Miyahara, Takaaki Uda, Toshinori Ishikawa, Kou Furuike and Masumi Serizawa</i>	Vertical spreading of surface jets <i>Manh Tuan Nguyen and Soon Keat Tan</i>	Study on characteristics of solitary wave simulation in laboratory <i>Jin Wang, Deng-Ting Wang, Qi-Hua Zuo and Qing-Jun Liu</i>	Spacing of Langmuir circulations in ocean <i>Ming Zhao, Mohamed Ghidaoui and Zhenhua Huang</i>	Numerical simulation of sloshing in 2d rectangular tank based on SPH method with an improved boundary treatment approach <i>Kai Gong, Hua Liu and Soonkeat Tan</i>
16:00	Beach profile changes under the action of solitary waves: Boussinesq modeling and comparison with laboratorial measurements <i>Jie Chen, Zhenhua Huang, Changbo Jiang, Linlin Li and Hongtao Nie</i>	Turbulent jets: a comparative study of point-source and CFD simulation results <i>Bidya Sagar Pani and B.M. Aruna</i>	Laboratory study of breaking events of deep-water wave packets by Hilbert-Huang Transform <i>Yanli He, Guohai Dong, Yucheng Li, Yuxiang Ma and Wei Zhang</i>	Three dimensional model of the flow around a fishing plane net <i>Yunpeng Zhao, Chun Wei Bi, Guohai Dong, Yucheng Li</i>	Optimum open boundary conditions for coupled numerical model of tide, surge and wave <i>Soo Youl Kim, Yoshiharu Matsumi, Tomohiro Yasuda and Hajime Mase</i>
16:15	Long term extension of the sand spit and change of the surrounding coastal morphology around Damietta Promontory, Nile River Delta <i>Mostafa Ahmed, Yoshimitsu Tajima and Shinji Sato</i>	Numerical study on flow characteristics of a single jet and four tandem jets in crossflow <i>Yang Xiao, Hongwu Tang, Dongfang Liang and Jiuding Zhang</i>	Numerical study on the movement of muddy seabed under waves <i>Xiaojing Niu and Xiping Yu</i>	Dynamical analysis of a soft yoke moored FPSO in shallow waters <i>S.Q. Wang, S.Y. Li and X.H. Chen</i>	Numerical experiments on a permeable breakwater by using numerical wave tank, CADMAS-SURF/3D <i>Kenya Takahashi, Koichirou Anno, Takeshi Nishihata and Tsunehiro Sekimoto</i>
16:30	Beach erosion as long-term topographic response to avalanche and landslide associated with the 1923 Kanto Earthquake <i>Toshiro San-Nami, Toshinori Ishikawa, Takaaki Uda, Takao Harumi, Kazue Akita</i>	Mean cross-sectional flow structures of oblique jets released in a moving ambient <i>Xia Wang and Gustaaf Kikkert</i>	An experimental study on the wave control by environment-friendly artificial reef <i>Kyu-Han Kim, Sungwon Shin, Wontaek Lim, Yongho Moon and Chongkun Pyun</i>	Diffraction of water waves by a modified V-shaped breakwater <i>Kao-Hao Chang, Deng-How Tsaur and Liang-Hsiung Huang</i>	

Parallel Session 7 (09:30 – 10:45)

	Ballroom C Special Session: The 2011 East Japan Tsunami I Chair: <i>Harry Yeh, Sung Bum Yoon</i>	Ballroom B Jets II Chair: <i>Gustaaf Kikkert, Bidya Sagar Pani</i>	Tang Marine Ecology and Environment II Chair: <i>Margaret Chen, Tadashi Hibino</i>	Ming II Waves and Modelling III Chair: <i>Keisuke Murakami, E Van Groesen</i>	Sung I Numerical Methods and Simulation III Chair: <i>Susumu Araki, Changbo Jiang</i>
09:30	Overview of the 2011 Tohoku Earthquake Tsunami survey results <i>Nobuhito Mori</i>	Characteristic behaviours of a vertical round jet under different spectral waves <i>Zhenshan Xu, Yongping Chen, Chi-Wai Li and Changkuan Zhang</i>	Influence of sea surface temperature on coastal urban area - case study in Osaka Bay, Japan <i>Junichi Ninomiya, Nobuhito Mori and Hiroyuki Kusaka</i>	Large amplitude solitary waves due to solitary resonance <i>Keisuke Nakayama, Taro Kakinuma, Hidekazu Tsuji and Masayuki Oikawa</i>	Three dimensional numerical simulation of flow around four circular cylinders in an in-line square configuration <i>Feifei Tong, Liang Cheng, Ming Zhao and Xiao-Bo Chen</i>
09:45	Field survey of the 2011 off the Pacific Coast of Tohoku Earthquake Tsunami disaster and future tsunami protection <i>Tomoya Shibayama</i>	Two-phase velocity measurements in horizontally-discharging buoyant sediment jets <i>Peng Liu and K.M. Lam</i>	A study of pelagic plankton distribution patterns in the gulf of Alaska using a coupled population dynamics – physical mixing model <i>Jifeng Peng</i>	Empirical formula for regular wave breaking over currents <i>Yu Liu, Xiaojing Niu and Xiping Yu</i>	Currents past gravity anchors astride offshore pipelines: a direct numerical simulation <i>Xu Zhao, Ming Zhao, Liang Cheng and Wei He</i>
10:00	Field survey of suffering appearances due to Tohoku Earthquake Tsunami <i>Y. Kimura, Y. Yamakawa and H. Mase</i>	Hydraulic characteristics of the submerged plane jet formed at the lee side of a silt screen <i>Thu-Trang Vu and Soon-Keat Tan</i>	Monitoring topographic and habitat changes in natural sand dunes after setting back a seawall at Nakatsu tidal flat, Oita, Japan <i>Satoquo Seino, Yukiko Ashikaga, Takaaki Uda, H. Mihara and S. Watanabe</i>	Wave setup over fringing reef with a shallow reef crest: a hydraulic theory for flows under critical conditions <i>Zhenhua Huang, Yu Yao, Stephen Monismith and Edmond Lo</i>	Tidal current simulation of the Ariake Sea using the sigma-coordinate finite element model <i>Hirohide Kiri, Eisaku Shiratani, Hajime Tanji and Kyoji Ishita</i>
10:15	A brief overview on the post-tsunami survey in the Sanriku Coast, Japan <i>Haijiang Liu, Tomohiro Takagawa, Yoshimitsu Tajima, Shinji Sato, Takenori Shimozone, Akio Okayasu and Hermann M. Fritz</i>	The near-field jet behavior of 60 degrees dense jets discharged into a perpendicular crossflow <i>Chris C.K. Lai and Joseph Hun Wei Lee</i>	Integrated use of electrical resistance tomography and radon monitoring for characterizing submarine groundwater discharge dynamics in a fringing reef <i>Ariel C. Blanco, Kazuo Nadaoka and Atsushi Watanabe</i>	Mild-slope equations for random waves inside and over porous layers <i>Changhoon Lee, Seolwha Park and Hajime Mase</i>	Numerical simulation of free surface flow using a three-dimensional numerical model <i>Jin Woo Lee, Kyu-Hak Seo and Yong-Sik Cho</i>

Parallel Session 8 (11:00 – 12:30)

	Ballroom C	Ballroom B	Tang	Ming II	Sung I
	Special Session: The 2011 East Japan Tsunami II Chair: <i>Nobuhito Mori, Tomoya Shibayama</i>	Wastewater Disposal and Water Quality I Chair: <i>Kazuo Murakami, Aijia Zhu</i>	Sediment Transport I Chair: <i>Zhenhua Huang, Haijiang Liu</i>	Waves and Modelling IV Chair: <i>Kyung-Duck Suh, D.H. Zhang</i>	Numerical Methods and Simulation IV Chair: <i>Gunwoo Kim, Soo Youl Kim</i>
11:00	Hindcast simulation of 2011 great East Japan Earthquake Tsunami <i>Byung Il Min, Byung Ho Choi, Kyeong Ok Kim, Victor M. Kaistrenko and Efim N. Pelinovsky</i>	Assessment of seawater quality along northern coast of Oman <i>Ahmad Sana and Mahad Baawain</i>	A study on sedimentation of tidal rivers and channels flowing into Deep Bay with a Delft3D model <i>Z.B. Wang, M.L. Tse and S.C. Lau</i>	Development of mild-slope equation for irregular waves over mud layers <i>Tae-Hwa Jung and Changhoon Lee</i>	Verification of numerical simulation method for motion of cubic armor block <i>Susumu Araki, Saki Fujii and Ichiro Deguchi</i>
11:15	Numerical simulation of 2011 Tohoku Tsunami propagation over Pacific Ocean <i>Jae Seok Bae, Choong Hun Shin and Sung Bum Yoon</i>	Modelling dispersion characteristics in Rambler Channel <i>K.L. Pun, T.N. Fung, X.L. Chen and S.W. Lu</i>	Estimating settling velocity of mud flocs using laser diffraction particle size analyzer <i>Takeshi Koeda, Narong Touch and Tadashi Hibino</i>	Wind wave spectral analysis in north-central coastal waters of Jiangsu <i>W.B Feng, Bin Yang, Jin Sheng Xia and Yanbo Li</i>	A new technique for nested boundary conditions in hydrodynamic modeling <i>Qinghua Ye, Robin Morelissen, Erik De Goede, Maarten Van Ormondt and Jan Van Kester</i>
11:30	Propagation characteristics of 2011 North-East Japan Tsunamis towards Korean peninsula <i>Sung Bum Yoon, Jae Seok Bae and Chae-Ho Lim</i>	Hydrodynamic and water quality changes due to Saemangeum Project in Korea <i>Seungwon Suh, Hwayoung Lee and Hyeonjeong Kim</i>	Simulation study on deposition downstream estuarine gates <i>Xiping Dou, Hongling Qu, Xiangming Wang and Xinzhou Zhang</i>	Ship wave crests in intermediate-depth water <i>Changhoon Lee, Byeong Wook Lee, Yong Jae Kim and Kwang Oh Ko</i>	Numerical simulation of hydrodynamic behavior on wave-flap structure interactions with a SPH model <i>Da-Wei Chen, Shiaw-Yih Tzang, Neng-Yao Zeng, Chi-Ming Hsieh, Jiahn-Horng Chen and Rong-Jiann Robert Hwang</i>
11:45	11 March 2011 great East Japan Tsunami inundation modelling of four coastal areas using simplified source descriptions <i>Stefan Leschka, Ole Larsen, Nanis Sakti Ningrum, Floriane Dubonnet and Peter Skovgaard Rasch</i>	Numerical tracking blue algal bloom in Taihu Lake based on fractional Brownian motion <i>Cuiping Kuang, Xiaodan Mao, Ling Deng, Lulu He, Jing Huang and Jie Gu</i>	Model for predicting formation of slender sand bar due to shoreward sand transport on shallow tidal flats <i>Masumi Serizawa, Takaaki Uda and Shiho Miyahara</i>	Wave attenuation through an array of rigid circular cylinders: an experimental study <i>Zhenhua Huang and Wenbin Zhang</i>	Numerical simulation of forces on particles in the oscillatory boundary layer flow over a rough bed using Lattice Boltzmann Method <i>Lei Ding and Qinghe Zhang</i>

<p>12:00</p>	<p>Waveform evolution of the 2011 East Japan Tsunami <i>Harry Yeh, Shinji Sato and Yoshimitsu Tajima</i></p>	<p>Pollution control in urban drainage system - interception of dry weather flow in multi-cell box culvert <i>Gabriel T.O. Woo, Elaine Y.L. Wong, Kelvin N.F. Lau and Glenn T.H. Chan</i></p>	<p>Variation pattern analysis of the suspended sediment concentration in Busan New Port, Korea <i>Hongyeon Cho, Jangwon Chae, Kyeong-Ho Ryu and Youngmin Oh</i></p>	<p>Wave transformation and breaking on gentle slope <i>Peng Li, Junning Pan and Hongchuan Wang</i></p>	<p>Computation of wave overtopping on slope plate <i>Hyoseob Kim, Changhwan Jang, Hojun Yoo and Mansoon Song</i></p>
<p>12:15</p>	<p>Aftermath of the 3/11 tsunami in Tohoku Region of Japan <i>A.W. Jayawardena</i></p>	<p>Level 2 performance based design of coastal drainage pumping stations <i>Hajime Tanji and Hirohide Kiri</i></p>		<p>Time-accurate AB-simulations of irregular coastal waves above bathymetry <i>E Van Groesen and Andonowati</i></p>	

Parallel Session 9 (14:00 – 15:30)

	Ballroom C Beach Erosion and Morphodynamics III Chair: <i>Hajime Mase, A.W. Jayawardena</i>	Ballroom B Wastewater Disposal and Water Quality II Chair: <i>Cuiping Kuang, K.L. Pun</i>	Tang Sediment Transport II Chair: <i>Mengguo Li, Ole S. Madsen</i>	Ming II Waves and Modelling V Chair: <i>Taro Kakinuma, Dong-qiang Lu</i>	Sung I Properties of Materials Chair: <i>In-Sung Jang, Inyeol Paik</i>
14:00	Invited Talk Coral reef islands of Spermonde: morphodynamics and prospect <i>D.A. Suriamihardja</i>	Effects of tidal flat on water quality improvement in the Tokyo Port wild bird park <i>Nana Sasaki, Kazuo Murakami, Yusuke Umeda, Tomohiro Kuwae, Eiichi Miyoshi and Kouta Nakase</i>	Innovative monitoring and 3d modeling of dredging induced sediment plumes in the port of Los Angeles <i>Ying Poon, Sherilyn Kimura, Brent Mardian, Kathryn Curtis and Andrew Jirik</i>	Wave overtopping on flaring shaped seawall under oblique incident waves <i>Keisuke Murakami, Daisuke Maki and Naoto Takehana</i>	Experimental research on constitutive model of the saturated clay with seepage <i>Yuanzhan Wang, Linnan Hao, Zhong Xiao, Xi Cheng and Dianguang Ma</i>
14:15		Biomonitoring of pollution status in the Daya bay using protozoan communities with the bottled PFU method <i>Aijia Zhu, Zhanzhou Xu, Jingqin Liu, Hongda Fang, Chuguang Huang, Jianrong Huang and Hongbo Li</i>	Numerical study of sediment transport in Yangon River and Estuary <i>Toe Toe Aung, Takenori Shimozono and Akio Okayasu</i>	Steep standing waves against a vertical wall on a sloping beach <i>Wataru Kioka, Toshikazu Kitano, Masashi Okajima and Naoki Miyabe</i>	Investigation of chloride ion profiles of harbor concrete structure based on in-situ cores <i>Sanghun Han, Woosun Park and Jangwon Chae</i>
14:30	Prediction of deposition of sand on gravel layer formed by beach nourishment and onshore movement of gravel during storm <i>Masayuki Koya, Akio Kobayashi, Takaaki Uda and Yasuhito Noshi</i>	Numerical analysis of dispersion characteristics of cooled water discharge from LNG plant <i>Il Won Seo, Chang Geun Song, Hwang Jung Choi and In Hwan Park</i>	Wave shape effect on sheetflow sediment transport <i>Le Phuong Dong and Shinji Sato</i>	Wave reflection and transmission by vertical slotted barrier <i>Chang-Hwan Ji, Kyung-Duck Suh and Bum Hyoung Kim</i>	Predicting the hydraulic conductivity of Makassar marine clay using field penetration test (CPTu) results <i>Tri Harianto, Lawalenna Samang, Achmad Zubair, Dadang Suriamihardja and Takenori Hino</i>

14:45	<p>Three-dimensional morphodynamic model to sandy beach with shore reef area</p> <p><i>Masamitsu Kuroiwa, Yuhei Matsubara, Naotsugu Yamamoto, Yasushi Ichimura, Tomoyoshi Koizumi, Ken Yoshizu and Masami Sannoh</i></p>	<p>Real-time forecast of marine beach water quality in Hong Kong</p> <p><i>Wai Thoe and Joseph Hun Wei Lee</i></p>	<p>Evaluation on the sediment movement along the Miyazaki coast in terms of feldspar luminescence features</p> <p><i>Haijiang Liu and Shinji Sato</i></p>	<p>Wave overtopping of gentle slope revetment placed behind artificial reef</p> <p><i>Takao Ota, Yoshiharu Matsumi, Yuichi Kurata and Kenichi Ohno</i></p>	<p>Influence of sea water on the mechanical properties of porous asphalt containing liquid asphalt</p> <p><i>Nur Ali, Lawalenna Samang, M.W. Tjaronge and Abdul Rahman Djamaluddin</i></p>
15:00	<p>Experimental study on effects of the beach nourishment using the coarser sand</p> <p><i>Yoko Shibutani, Yuhei Matsubara, Masamitsu Kuroiwa and Noriko Yao</i></p>	<p>Field studies of E. coli decay rate at a coastal beach in Hong Kong</p> <p><i>Yuen Man Chan, Wai Thoe and Joseph Hun Wei Lee</i></p>	<p>Application of ROMS for simulating evolution and migration of tidal sand waves</p> <p><i>Zhipeng Zang, Liang Cheng and Fuping Gao</i></p>	<p>Study on the relationship between mooring force and wave period for a mooring oil tanker</p> <p><i>Xiangwei Meng, Feng Gao, Yunpeng Jiang and Haicheng Liu</i></p>	<p>Effect of sea water on the strength of porous concrete containing Portland composite cement and micro monofilament polypropylene fibre</p> <p><i>M.W. Tjaronge, Rudy Djamaluddin, Fatriady and Amirullah</i></p>
15:15			<p>Littoral transport estimate from the field measurement along north Chennai coast of Tamil Nadu, India</p> <p><i>K.V. Anand, Vallam Sundar, S.A. Sannasiraj, K. Murali, V. Rangarao and B.R. Subramanian</i></p>		

Parallel Session 10 (15:45 – 16:45)

	Ballroom C Beach Erosion and Morphodynamics IV Chair: <i>Liancheng Sun</i>	Ballroom B Seawater Intrusion Chair: <i>Elena Dolgoplova, Ken Wong</i>	Tang Marine Ecology and Environment III Chair: <i>H.J.S. Fernando, Girija Jayaraman</i>	Ming II Waves and Modelling VI Chair: <i>Jong-In Lee, Takao Ota</i>	Sung I Construction and Structures Chair: <i>Sanghun Han</i>
15:45	Short and medium-term evolution of the northern bank, Hangzhou Bay <i>Z.J. Dai, J.F. Li, X.L. Zhang and H.Y. Yao</i>	Water resource management in Macao SAR to tackle its sea water intrusion problem <i>Kai Meng Mok, Hou Wong and Xiao Jun Fan</i>	Durability of water environment restoration by covering layer of granulated coal ash in brackish-water lake <i>Tadashi Saito, Junji Hiraoka, Tadashi Hibino and Narong Touch</i>	Random wave generation using the internal wave maker in the Navier-Stokes equation-based model <i>Taemin Ha, Jihun Kim, Yong-Sik Cho and Pengzhi Lin</i>	Experimental study on lateral behavior of DSCT column <i>Taek Hee Han, Jong-Sun Kim, Deok Hee Won and Young Jong Kang</i>
16:00	Study on dynamic process of tombolo topography at Chiringa-Shima Island by image data based on point camera observation <i>Akio Nagayama and Toshiyuki Asano</i>	Formation of tidal bore and its effect on sea water intrusion <i>Elena Dolgoplova</i>	Research about the effect of reclamation on marine ecology in the northeast of Zhoushan Island <i>Maoming Sun, Yongqiang Ni, Shanshan Wang and Lihu Xiong</i>	Numerical study of wave breaking over a muddy seabed <i>Yi Hu, Yi Liu, Xin Guo and Lian Shen</i>	Development of unmanned underwater excavation equipment for port construction <i>In-Sung Jang, Woo-Tae Kim, Jin-Hwan Ko, Tae-Sung Kim, Kun-Woo Park and Min-Ki Lee</i>
16:15	Analysis of the causes of sediment loss at Golden Beach, Hong Kong <i>Hakeem Johnson, Peter Shek and Francis Lee</i>	Numerical study on impacts of discharge changes caused by major water conservancy projects on salinities at water intakes in the Changjiang Estuary <i>Jing Huang, Cuiping Kuang, Mingtao Jiang, Jie Gu and Bo Sun</i>	Properties of granulated coal ash and its effects on sludge purification <i>Tadashi Hibino, Narong Touch and Tadashi Saito</i>	Waves due to a disturbance in a two-layer fluid covered by an elastic plate <i>D.Q. Lu and C.Z. Sun</i>	Experimental study on seismic performance of non-dispersible underwater concrete short columns <i>Wei-Qiu Zhong, Zhi-Wei Zhang and Ye Ma</i>
16:30		Numerical investigation of circulation and nutrient transport in the Mirs Bay <i>Jianping Gan, Linlin Liang, Tingting Zu</i>	Modeling chlorophyll A of Bohai Bay based on structural equation model and Bayesian networks <i>Xiaofu Xu, Xianquan Xiang and Jianhua Tao</i>		

Programme for Poster Presentations

Thursday, 15 December

Poster Number	Ballroom A 08:30 – 16:30
1	Morphodynamics responses of the Erfenshui beach ridge on the Tiaozini sandbank in Jiangsu coast, China <i>Jun Chen, Xiao Qing Wei and Yong Zhou</i>
2	Hydraulic model test and field experiment on beach nourishment at large scale tidal flat beach <i>Gil-Pyo Hong, Kee-Sok Yang, Byeong-Kyu Kim and Jung-Seok Moon</i>
3	Evaluation of coastal erosion in the Nandu River Delta <i>Lianqiang Shi, Gang Hu, Shuhua Zuo and Jiaxin Wu</i>
4	Impact of sea level rise on Semarang coastal city Indonesia <i>Ir Suhelmi</i>
5	Effectiveness of GFRP-bar reinforcement on performance of new wave dissipating block <i>Inyeol Paik and Yong-Min Oh</i>
6	Wave period effects on wave overtopping of vertical structure <i>Young-Taek Kim and Jong-In Lee</i>
7	An analysis of causes of downtime in Pohang new harbor through long-term investigation of waves and winds <i>Kyong-Ho Ryu, Weon Mu Jeong, Won-Dae Baek and Gunwoo Kim</i>
8	Tide asymmetry in Mokpo coastal zone <i>Tae Sung Jung and Jong Hwa Choi</i>
9	Effect of stopping flow in one branch of bifurcated tidal estuary on hydrodynamic sediment environment <i>Mengguo Li and Wendan Li</i>
10	Ebb-dominant tidal currents characteristics in the Han-River Estuary, South Korea <i>Byung Il Yoon, Seung Buhm Woo and Yong Sik Song</i>
11	The characteristic of mass flux at Yeomha channel, Gyeonggi Bay <i>Dongwhan Lee and Seungbuhm Woo</i>
12	Mathematical modeling of the effect of constructing LNG terminal on hydrodynamic environment <i>Wendan Li, Mengguo Li and Wei Liu</i>
13	Verification of rip current simulation using HAECUM compared with field observational data <i>Jooyong Lee, Junglyul Lee and Inchul Kim</i>
14	Experimental study on hydraulic characteristics and vorticity interactions of floating breakwaters <i>Jaeseon Yoon, Don Namgung and Yong-Sik Cho</i>
15	Hydrodynamic analysis of heave plates of the truss spar platform <i>Jiang Xueliang and Sang Song</i>
16	Luo-Xia model and numerical simulations of dual synthetic jets <i>Zhen-Bing Luo, Zhi-Xun Xia, Lin Wang, Bing Liu and Qinghua Zeng</i>
17	Interaction between hydrodynamics and salt marsh dynamics: an example from Jiangsu coast <i>Zhan Hu, Marcel J.F. Stive, T.J. Zitman, Qinghua Ye, Zheng Bing Wang, Arjen Luijendijk, Zheng Gong and Tomohiro Suzuki</i>
18	Modelling chlorophyll a of Bohai bay based on CA-SVM using remote sensing data <i>Xianquan Xiang, Xiaofu Xu and Jianhua Tao</i>
19	Experimental study on wave energy concentration and control measures in limited sheltered basin area <i>Haicheng Liu and Yunjiang Wang</i>
20	Numerical investigation on water discharge capability of sluice caisson of tidal power plant <i>Gunwoo Kim, Sang-Ho Oh, Kwang-Soo Lee, In Suk Han, Jang Won Chae and Suk-Jin Ahn</i>

Friday, 16 December

Poster Number	Ballroom A 08:30 – 16:30
1	Mooring line dynamics for a floating wave energy converter <i>Dongho Jung, Seungho Shin, Hyeonju Kim and Hosaeng Lee</i>
2	Design and control of a 50kw class rotating body type wave energy converter <i>Byung-Hak Cho, Shin-Yeol Park, Dong-Soon Yang, Kyung-Shik Choi and Byung-Chul Park</i>
3	Dam break simulation using level-set finite volume method for solving two phase incompressible flows <i>Kil Seong Lee, Kidoo Park and Woo Yeon Sunwoo</i>
4	Direct numerical simulation of wave deformation around submerged structures using IB method <i>Min-Ji Kim, Jung-Hyun Park, Yong-Won Seo, Do-Sam Kim, Kwang-Ho Lee and Norimi Mizutani</i>
5	Numerical study on the tidal effect of seawater intrusion in Liao Dong Bay coastal plain, China <i>Fei Ding, Takao Yamashita, Han Soo Lee and M. Haggag</i>
6	Spatial and temporal variations and hydrodynamics explanation to suspended sediment concentration in the Changjiang (Yangtze) estuary, China <i>Shuhua Zuo, Jiufa Li and Lianqiang Shi</i>
7	Research on sediment deposition in deep-water compound navigation channel <i>Liancheng Sun and Na Zhang</i>
8	Three-dimensional numerical simulation of cohesive sediment transport due to a typhoon <i>Na Zhang, Hua Yang, Bing Yan and Hongbo Zhao</i>
9	Diagnosis and improvement for status and problems of dredging and ocean disposal of coastal sediment in Korea <i>Ki-Hyuk Eom, Dae-In Lee and Gui-Young Kim</i>
10	On the wintertime abnormal storm waves along the east coast of Korea <i>Han Soo Lee and Takao Yamashita</i>
11	Evaluation of tsunami fluid force acting on a bridge deck subjected to plunging breaker bores and surging breaker bores <i>Gaku Shoji and Yu Hiraki</i>
12	Discussion on calculation of wave forces on submerged quarter circular breakwater under irregular waves <i>Xuelian Jiang, Yanbao Li and Luwen Qie</i>
13	Steady streaming and set-ups due to gravity-capillary waves in a viscous fluid <i>Chiu-On Ng and Hung-Chu Hsu</i>
14	Numerical analysis of abnormal long wave “abiki” generated by local meteorological disturbance <i>Hendri, Takao Yamashita and Tomoaki Komaguchi</i>
15	Numerical study for waves propagating over submerged porous breakwater <i>Yongzhou Cheng, Chengxiang Liu, Yun Pan and Qingfeng Li</i>
16	Study on the wave making and wake washes of trimaran <i>Lilan Zhou and Gao Gao</i>
17	Wave calculations for seawall rehabilitation in Hangzhou Bay <i>Jinhai Zheng and Shangfei Lin</i>
18	Numerical modelling of Kandy Lake, Sri-Lanka in preparation for water quality improvement <i>J.H. Pu, K.B.S.N. Jinadasa, W.J. Ng, S.K. Weragoda, C. Devendra and S.K. Tan</i>
19	Evaluation of the vertical and horizontal undrained bearing capacities of suction buckets for wind turbines in clay <i>Chi Hung Le, Sungryul Kim and Myounghak Oh</i>
20	Application of cement stabilization sediment dredged as subgrade road of rigid pavement <i>Hamzah Yusuf, Muhammad Saleh Pallu, Lawalenna Samang, M. Wihardi Tjaronge and Amar Akbar Ali</i>

6th International Conference on
Asian and Pacific Coasts (APAC2011)

**With the Compliments of
Nishimatsu Construction Co. Ltd.**

Room 508, Star House, 3 Salisbury Road, Kowloon, Hong Kong

Phone: +852 2736-6461

Fax: +852 2730-1512

KEYNOTE LECTURES

TOWARD SUSTAINABLE AND SECURE COASTAL ZONES: ROLES OF WAVES, TIDES, SEDIMENTS, AND TURBULENCE

H.J.S. FERNANDO

Environmental Fluid Dynamics Laboratories, Civil Engineering & Geological Sciences & Aerospace & Mechanical Engineering, University of Notre Dame, Notre Dame, IN USA 46530

The coastal zone, or the transition region between land and ocean, is of great importance because of its economic, security and recreational utility and its impact on contiguous human settlements and ecosystems. Hydrodynamic and biogeochemical processes of different scales, their interactions and climate-related changes such as eustatic sea level rise lead to continuous evolution of coastal circulation, water quality and land cover. In addition, anthropogenic activities weaken natural beach-defense mechanisms and geomorphic stability, thus making coastal communities vulnerable to natural disasters such as hurricanes and tsunamis. Effluent releases to coastal areas affect water quality and impair marine life. In conflict zones, underwater mines are a weapon of choice and their burial in sediments is an impediment for detection and safe removal of mines. Further offshore, density stratification plays an important role, thus supporting internal waves, meso-scale eddies and turbulent mixing. All these application areas are entwined with fundamental physical, geological, chemical and biological processes of the coastal zone, the understanding of which is imperative for making informed decisions on coastal zone management.

1. Introduction

Coastal zones, defined as the areas where processes and activities depend on strong interactions of marine and terrestrial environments, have disproportionate economic impacts on nations. More than 50% of urban population of the world lives in coastal areas, which continues to increase despite the challenges facing coastal developments. Moreover, about 13% of the world's urban population lives in Low Elevation Coastal Zones (LECZ; elevation < 10m), and ten countries that occupy most LECZ constitute 73% of the global LECZs [1]. Coastal zones bear the brunt of natural disasters, including storm surges, tsunamis and sea-level rise, which in turn affect coastal infrastructure, erosion, temporary flooding and permanent inundation. Human demands for coastal tourism, high-end urban development, oil drilling, mineral extraction, fisheries - imperatives for economic sustainability - have overtaxed the environment to the extent that in some areas environmental degradation is conspicuous and has stymied ecosystem services (resources supplied by nature, e.g. drinking water and fisheries). This in turn has affected long term sustainability of coastal cities, although they are rapidly expanding. For example, about 14% of the U.S. coastlines have been developed in 2007 (compared to 4% along the interior waterways), but this is expected to be increased to 25% by 2025 [2].

The south Asian region has some of the richest coastal ecosystems replete with coral reefs and mangroves, and over 70% of the population of ASEAN countries lives within 400km from the coast. In China, more than 60% of its 1.2 billion population lives in the 12 coastal provinces [3]. Operation of coastal areas are subjected to many regulatory restrictions, for example, Coastal Zone Management Act, Endangered Species Act, Migratory Birds Act, Drinking Water Act, to name a few in the US. In the international arena, the UN Convention on the Law of the Sea (UNCLOS) defines the rights and responsibilities of nations to use the world's oceans. Included therein is the Exclusive Economic Zones (EEZs) that allow nations to harness adjoining oceans out to a distance of 200 nautical miles (which may include territorial sea and even the continental sea beyond this limit).

In addition to the impacts of coastal urban development on natural resources, coastal cities are vulnerable to security threats such as terrorism, drug and human trafficking, piracy and incursions. Some plausible countermeasures include mine and submarine warfare, patrolling and anti-invasion monitoring assets [4]. As a result, the recent "National Security and Federal Lands Protection Act" in the U.S. would cede the authority of the Secretary of Interior over coastal public lands to the Secretary of Homeland Security, which would grant a waiver for land managers to forgo compliance with environmental laws within 100 miles of a coast.

As mentioned, coastal areas are becoming ever more complex to manage and plan for, and integrated planning methodologies have been proposed for sustainable and secure coasts. The available holistic modeling systems are currently insufficient to handle such challenges, a task which is further predicated by political, industrial, real estate and navigational interests. For various coastal areas, especially those stressed anthropogenically, management plans are in place although to what extent they are being enforced is unclear. Below we briefly discuss a case where a coastal area is at risk due to anthropogenic stress, and the role of environmental hydraulics in seeking solutions. Thereafter an example is given on how scientific knowledge can be utilized in problems involving coastal security, focusing on mine burial in coastal zone.

2. Coastal Louisiana – Can it be sustainable?

The Louisiana Coastal Area (LCA) is a clear example of an anthropogenically stressed coast, as evidenced by flooding that followed hurricane Katrina on August 29, 2005. The natural and human landscapes of LCA are determined by complex interactions between flow, sediment, ecosystems and geology. The natural course of the Mississippi river that

empties into the gulf via LCA changes every few thousand years, and in its eastern alignment the sediment accretion rates exceed subsidence, leading to deltaic formation as well as wetlands growth. When the river is in western alignment, sediments are deprived in the eastern delta, but accretion, long-shore transport and sediment reworking occurs in the western delta. This balance of alternative sediment growth and loss has led to natural building up of land in the deltaic plains. Post-industrial engineering of the river for economic benefits, yet paying little attention to its ecological and geological health, has led to an unsustainable coast.



Figure 1a. Large engineering structures, such as the storm surge barrier recently completed in Louisiana, needed to be designed in harmony with environmental needs (courtesy: Dr. Barbara Kleiss).



Figure 1b. The West Bay diversion. It currently operates at ~ 20,000 cfs, and is expected to develop 9,831 acres in 20 years; So far it has not been successful for land building.

The engineering of Mississippi river has been multifaceted. Introduction of levees and rip-rap along the river over the past century has reduced the sediment load by about 60-70%, thus impeding the land building. Moreover, a land loss of ~ 7 sq miles per year is currently occurring due to sediment compaction and sea level rise. Oil and gas exploration started in the early 1960s has lent to reduction in geologic pressure, contributing to accelerated land loss; since then about 2100 square miles of land has disappeared, resulting in saltwater intrusions. Also destroyed were the wetlands, which provide hurricane protection by acting as a buffer between the coast and populated areas. If healthy, greenbelts may absorb 70-90% of the energy of storm surges [5]. In 2004, the Louisiana Wetlands Conservation and Restoration Authority suggested that storm surge height is reduced by ¼ ft per mile of wetland marsh along the central Louisiana coast. Computer modeling conducted by the U.S. Army Corps of Engineers (USACE) using the ADCIRC model indicates that, in the absence of the wetlands, the storm surge height in New Orleans during Hurricane Katrina would have been 3-6 ft higher. All these point to the role of natural environment as a buffer for coastal disasters and the need to protect and nurture it. Of course, the natural defenses are insufficient to fully protect burgeoning coastal cities, and engineering structures will be imperative but in harmony with the natural environment (Figure 1a).

Post-Katrina reconstruction of the Louisiana coast is expected to provide multiple protections via natural means, in addition to engineering structures. These aspects include: restoration of wetlands, marshes and barrier islands to ensure resilience of the coast; reduction of sediment losses and placing diversions at critical locations to feed new sediments into marshes (Figure 1b); restoration and maintenance of regional water flow patterns; promoting increase of soil formation and organic matter production by reducing flooding and salinity stress on vegetation; and maintenance of ecosystems diversity to improve fish and shellfish abundance.

Diversions are designed to provide river water and sediments to nearby marshes to promote deltas and sub-deltas, thus sustaining wild life, promoting ecosystem functions and mitigating natural disasters. Diversions are the only way of effectively capturing river sediments, and they are classified into land building and land sustaining diversions. Experiences with past natural delta building mechanisms (e.g., crevasses and splays) suggest that large diversions (say >50,000 cfs) are necessary to form new land. This is a new paradigm, which relies on sedimentation over the project area quite uniformly and creation of wetlands from river water irrespective of water quality. Diversions can take the form of crevasses, siphons (small) and flood control spillways, and their success is dependent on the amount of sediment accretion over the years.

While there are about twenty four diversions along the lower Mississippi, only one of them (the West Bay diversion, opened in 2004) has been designed as a land building diversion. All are smaller diversions (<50,000 cfs), except the intermittently operated structures such as Bonnet Carre spillway. Artificial distributaries (e.g. Wax lake outlet) are deep conveyance channels (>100,000 cfs) that protrudes into a bay or a lake. Freshwater diversions blunt saltwater intrusions in to marshes and provide freshwater for marsh creation, and some of the diversions also have created new land. While plausible, no studies have demonstrated that large diversions can build land continuously or that artificial diversions are effective in land building. Other first-order issues may arise, for example, the ability of

freshwater to create wetlands because of high nutrient loads in the river, alteration of hydrology, increased salinity due to turbulent mixing of fresh and salty water as well as effects on fisheries.

Another successful method of land buildings is the beneficial use of sediments, where dredged sediments are pipelined to specific sites. The practicality of this method can be questioned, however, on the basis of cost and that artificial introduction of sediments may not work the same way as natural land building, thus requiring frequent nourishment of newly formed land.

Undoubtedly, physicochemical processes in diversions are complex and interconnected, and there are no reported systematic studies on them. The drivers are the climatic and oceanic conditions, inputs of water and sediments and geometric features. Model validations will be imperative in numerical studies, since the ability of models to represent salient processes is questionable. A few diversions have received detailed scrutiny (e.g., West Bay) but others (e.g., Bayou Lamoque) are ill documented.

Many questions remain on the utility of diversions on land building: How large should the diversion be; where should be it placed; how much water should be diverted; should it be gated or natural; what optimal geometry and sill height be used; how do the characteristics of receiving area respond to sedimentation; when should sediment trapping devices be introduced; should water be diverted continuously or pulsating; how much land building is expected in near, intermediate and long term; what is the useful life of a diversion; and should each diversion be operated independently or as a group? Related issues also arise on bio-geo-physical interactions such as adverse effects of high nutrient loads carried by the river in creating dead zones. The impacts on navigation are important, and fluid mechanical arguments suggest, and some existing diversions indicate, that shoaling is unavoidable in straight river reaches. The influence of curvature and secondary circulation need to be understood so as the basin scale implications. Another critical question is: can beneficial use of sediments be an alternative, not a supplement, to diversions? These are captive research topics for the future.

A careful review of past diversions provides following information that will help design future diversions:

1. Extensive monitoring programs are required to establish data bases for research and model validation. Setting up of field scale prototypes for research and enhanced monitoring of existing diversions will be useful.
2. Although controlled structures provide flexibility of operation, allowing diversions to evolve naturally (after an initial trigger) should be considered.
3. Moderate and large diversions lead to downstream shoaling, thus affecting navigation. Also affecting diversions are their location and river geometry (e.g. curvature that leads to secondary flows).
4. Strongly three-dimensional (3D) nature of processes, especially at the entrance, requires the use of 3D models in simulations, although their use has been rare.
5. Maintaining sheet flow at the entrance allows sufficient time for sediment distribution. The sill depth ought to capture the maximum sediment concentration.
6. Violation of sheet flow conditions lead to scour and continuous modification of diversion geometry. In general, sub-delta building lasts for a limited time period, whence a delta enters a degradation stage. Reduction of sediment supply upon reaching a critical sill depth (the upper layers are devoid of sediment), increase of bed erosion with decreasing depth and exacerbated turbulence effects on shallower water column are some reasons for this stage. Interestingly, the collapse of delta building starts at the entrance.
7. Large diversions appear to have more land building capacity, but the actual gain of land strongly depends on the design, climatic factors and storm activities of the area. Without their inclusion, the modeling may not predict the performance of diversions correctly.

3. Coastal Security: Mine Countermeasures

As discussed, there is an increasing need for nations to protect coastal areas in the realms of environmental and national security, and a host of hydraulics issues underlie such related activities as navigation, underwater surveillance, chemical plume sensing, waves and circulation and mine and submarine countermeasures. When buried in the seabed, mines are difficult to detect or distinguished from benign objects, and thus areas of buried mines as well as burial mechanisms under different oceanic conditions are of great interest. The burial of mines upon their release depends on their initial impact on the sea floor upon falling through the water column (“impact” burial) and evolution of surrounding sand after it settles on the bed (“subsequent” burial). The extent of impact burial is highly dependent on the orientation and velocity of the mine at the impact and the properties of sediments [6]. The subsequent burial mainly occurs due to local morphological changes of the seabed such as scour, shakedown, tumbling or covering by migrating sand waves. The liquefaction occurs due to increase of sediment pore pressure above the confining pressure during the passage of water wave crests, causing the bearing strength of sediments to vanish. While impact burial has been subjected to a fair number of investigations, until recently only a handful of studies have focused on subsequent burial [7]. There are many shapes and designs of mines depending on the zone of operation, however, most of the anti-ship mines and larger munitions take approximately cylindrical shape.

Keynote Lecture by Fernando

For simplicity, consider a cylindrical mine (diameter D_c , length L_c) placed at time $t = 0$ on a layer of sand (grain size d , density ρ_s) in oscillating water flow (frequency ω , horizontal velocity amplitude U , water density ρ and viscosity ν) that mimics wave action. The cylinder axis has an angle θ relative to the flow direction. The full set of primary external parameters determining a particular scour/burial characteristic, say A , of the cylinder is given by [8]

$$A = F(D_c, L_c, d, \rho_s, t, U, \omega, \rho, \nu, g, \theta), \quad (1)$$

where g is the gravitational acceleration and F a function. Using standard dimensional analysis and general physical arguments, (1) can be reduced and written in dimensionless (asterisks) form as

$$A^* = F^*(Re, KC, Sh, \theta, \tau, a), \quad (2)$$

where $Re = D_c U / \nu$ is the Reynolds number; $KC = 2\pi U / D_c \omega = 2\pi \varepsilon / D_c$ the Keulegan-Carpenter number ($\varepsilon = U / \omega$ - amplitude of horizontal water particle excursion); $Sh = (f/2)\psi$ the Shields parameter [$\psi = U^2 / g^* d$ - mobility parameter, $g^* = g(\rho_s / \rho - 1)$, f the friction coefficient]; $\tau = \omega t$ the non-dimensional time; and $a = L_c / D_c$ the aspect ratio.

For the simple case of $\theta = const (= 0)$ and $a = const (= 5, \text{ a typical value})$, and assuming Reynolds number similarity, (2) becomes

$$A^* = \Phi^*(KC, Sh, \tau), \quad (3)$$

thus simplifying the problem considerably. For steady state, $\tau \gg 1$, only two parameters remain in (3). Laboratory experiments were conducted [8] in a large wave tank with a sloping bottom (slope 1:24) to evaluate the functional form in (3). In addition, a number of experiments were conducted without the slope. It was possible to match KC and Sh between the ocean and laboratory, but there is a large mismatch of Re which can be discounted on the basis of Reynolds number similarity [9]. The experiments on object burial delved into several issues, in particular, burial mechanisms and scour around mines. A scour/burial regime diagram was developed (Fig. 2a) for the case of steady forcing, and four main scour/burial regimes and the sheet flow regime were identified [10] on this diagram.

Regime I - no scour ($KC < KC^* \approx 2$, $Sh < Sh^* \approx 0.018$; this occurs when the local velocity is less than a critical velocity for the initiation of sediment motion).

Regime II - initial scour ($KC > KC^*$ and $Sh > Sh^*$; scour usually occurs on the onshore side of the cylinder due to wave nonlinearity, but for weakly nonlinear waves similar patterns could also be formed on the offshore side).

Regime III - expanded scour ($KC^* < KC < KC^{**} \approx 14$ and $Sh > Sh^{**} \approx 0.054$. When the background water motion is sufficiently energetic to form ripples, regime II becomes unstable and transforms into an expanded scour. If the cylinder diameter is larger than the ripple height, the flow disturbances due to cylinder are dominant, the expanded scour pattern is stable and it persists for many hours).

Regime IV - ripple dominated scour with possible periodic burial ($KC > KC^{**} \approx 14$ and $Sh > Sh^{**} \approx 0.054$. If the ripple height is larger than the cylinder diameter, the expanded scour pattern transforms into regime IV, wherein the cylinder is buried periodically under traveling ripples).

Regime V - sheet flow regime ($Sh > Sh_0 \approx 0.83$; at such high values of the Shields parameter, bottom features are "washed" away to form a planar bathymetry).

Theoretical arguments (not discussed here, dashed lines) together with experimental results were used to develop the following transitional boundaries between various burial regimes:

$$KC = KC^* + (Sh^{**} - Sh) / (Sh - Sh^*), \quad (\text{between regimes I and II}) \quad (4a)$$

$$KC = KC^* + (Sh_0 - Sh)^5 / (Sh - Sh^*), \quad (\text{between regimes II and III}) \quad (4b)$$

$$KC = KC^{**} + 1 / (Sh - Sh^{**})^{2/3}, \quad (\text{between regimes III and IV}) \quad (4c)$$

which broadly match with the solid lines. These relationships could be used to understand the behavior of mines in field situations, as shown in Figure 2b. Note that the field observations in the latter have been taken during the Indian Rock Beach field experiment [7], and the situation shown corresponds to regime III ($KC = 9.9$, $Sh = 1.1$). The agreement is good and gives credence to the laboratory modeling of mine burial processes. The dimensionless scour depth prediction based on laboratory-based parameterization was $S/D = 0.5$ and the length of scour $L^*/D = 3.5$, which compares well with Field Observations $S/D = 0.75$ and $L^*/D = 2.5 - 5$. Laboratory and field observations of this ilk have been used to develop physics-based and statistical (experts systems) mine burial predictions models by security agencies. Improved predictability therein points to the importance of process level understanding and the need for extensive data sets covering disparate beach types and mine configurations.

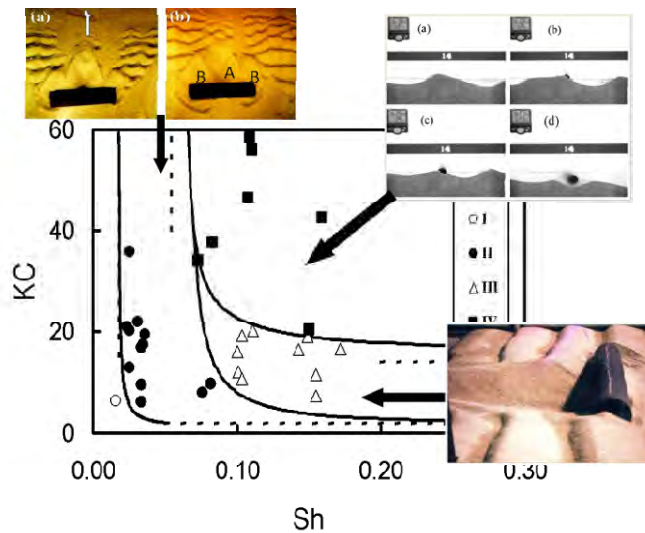


Figure 2a. Scour/burial regime diagram showing four different regimes (I-IV) depending on the values of KC and Sh parameters. Dashed lines - estimated limiting asymptotes, solid lines – actual transition curves between different regimes (i.e., parameterization 4).



Figure 2b. A field situation during the Indian Rock Beach Experiment off coast of Florida. Dashed line - expanded scour boundary.

4. Summary

Coastal areas are becoming the epicenters of human settlements and industrial/economic hubs, and also have long been the attraction for leisure and recreation activities. Environmental and physical securities are becoming ever more important for coastal areas, as they are in the frontier of cities and nations. Sustainable coastal cities entail environmental preservation to maintain ecosystems services and providing security against natural disasters (tsunamis, storm surges) and environmental variability (e.g., coastal erosion, sea level rise, subsidence). Furthermore, they need to be protected against incursions and security breaches. Progress in coastal hydraulics is imperative for facing these challenges.

Asian and Pacific coasts are of particular interest, given the rapid exploitation of natural resources, in step with on-going massive expansion. Overexploitation of fisheries resources, water and air pollution, threats to seagrass and coral beds are some of the immediate issues. Island nations of Asia Pacific face disproportionate climate woes, contributed by land loss due to sea level rise, coral bleaching and coastal erosion as a result of climate change [11]. Facing coastal challenges in Asia-Pacific region indeed will be daunting in the 21st century.

References

1. M. Fragkias, Interactions and responses to Global Environmental Change (GEC) and their implications for human security in urbanized coastal zones - a synthesis. International Human Dimensions Program on Global Environmental Change, Update, 2. 25-27 (2007).

Keynote Lecture by Fernando

2. D. Beach, *Coastal Sprawl: The Effects of Urban Design on Aquatic Ecosystems in the United States*. Pew Oceans Commission (2002). http://www.pewtrusts.org/our_work_report_detail.aspx?id=30037.
3. D. Hinrichsen, *Coastal Waters of the World: Trends, Threats, and Strategies*. Washington D.C. Island Press (1998).
4. Linkov, I., Kiker, G.A., Wenning, R. J. (Eds.), *Environmental Security in Harbors and Coastal Areas*, NATO Security through Science Series C: Environmental Security, 492 (2007).
5. UNEP, *In the front line - Shoreline protection and other ecosystem services from mangroves and coral reefs*. UNEP-WCMC, 2006. *Biodiversity Series No 24*. ISBN: 92-807-2681-1 (2006).
6. R.A. Arnone and L.E. Bowen, "Prediction of the Time History Penetration of a Cylinder Through the Air-Water-Sediment Phases", Naval Coastal Systems Center, Panama City, FL, TN 734-36 (1980).
7. R. Wilkens, R. and M.D. Richardson, M.D., *IEEE J. Ocean Eng.*, **32** (1), 3-9 (2007).
8. S.I. Voropayev, F.Y. Testik, H.J.S. Fernando and D.L. Boyer, *Ocean Eng.*, **30**(13), 1647-1667 (2003).
9. F.Y. Testik, S.I. Voropayev, H.J.S. Fernando, "Flow around a short horizontal bottom cylinder under steady and oscillatory flows," *Phys. Fluids*, **17**(4) (2005).
10. F.Y. Testik, S.I. Voropayev, H.J.S. Fernando, and S. Balasubramanian, *IEEE J. Ocean Eng.*, **32**(1), 204-213 (2007).
11. Chuenpagdee and D. Pauly, *Coastal Management*, **32**, 3-15 (2004).

About the speaker



Professor Joe Fernando received his Ph.D. (1983) in Geophysical Fluid Dynamics from Johns Hopkins University. In 2010, he joined the University of Notre Dame as Wayne and Diana Murdy Endowed Professor of Engineering and Geosciences, with the primary affiliation in the Department of Civil Engineering & Geological Sciences and a concurrent appointment in the Department of Aerospace & Mechanical Engineering. Prof. Fernando's research interests are very broad, including environmental fluid dynamics and hydraulics, geophysical fluid dynamics, air pollution; alternative energy sources, coastal and deep water oceanography, meso and micro-scale meteorology, particularly in complex terrain, fluid dynamics of urban areas, climate variability, industrial fluid dynamics, and so on. He was elected to the European Academy in 2009. In 2007, he was featured in the *New York Times*, *International Herald Tribune* and a dozen international news media for his work on hydrodynamics of beach defenses.

CLIMATE CHANGE EFFECTS ON FUTURE WAVES AND TYPHOONS

H. MASE

Disaster Prevention Research Institute, Kyoto University, Gokasho, Uji, Kyoto 611-0011, Japan

This paper introduces projection of future wave climate and analysis of differences between present and future ocean wave climate using the data of high-resolution atmospheric General Circulation Model and a global wave model. Secondly, a stochastic typhoon model for estimating characteristics of typhoons in both present and future climate conditions is described. Differences of statistical characteristics between present and future typhoons estimated from the GCM projections are taken into account in the stochastic model of future typhoons. Finally, the failure probability of seawalls is briefly described concerning the effects of sea level rise and waves.

1. Introduction

Research of global climate change due to green house effects on the earth environment is changing from understanding phenomena to impact assessment, mitigation and adaptation strategies for future development of human society. Sea level rise greatly impacts human activity near the coastal zone by inundating low level areas and increases the vulnerability of coastal regions to other physical processes (e.g., storm surges, storm waves). Ocean waves and storm surges of future climate are also expected to be changed from the present. If extreme weather events will become stronger than those in the present climate, it is necessary to consider the impacts of these dynamic extreme phenomena for coastal disaster prevention and reduction.

The future wave climate projection has been conducted by a few researchers (Hemer *et al.*, 2006). These studies have shown an increase in wave height due to increased wind speeds associated with mid-latitude storms in many regions of the mid-latitude oceans. Zhang *et al.* (2004) and Wang and Swail (2006) made statistical projections of global wave height from the empirical relationships between sea-level pressure and significant wave height.

Intensity of tropical cyclones (typhoons, hurricanes and cyclones) in the future will increase with the increase of sea surface temperature (IPCC AR4, 2007). Intensity enhancement of tropical cyclone, in other words, increase of wind speeds and decrease of atmospheric depressions cause severe coastal disasters due to extreme waves and storm surges (i.e. Mori *et al.*, 2010). A deterministic evaluation of storm surges in a particular bay in future is difficult since the data of typhoons causing damages on a specific region is very few. Since extreme event analyses are necessary for disaster reduction planning, the number and intensity of projected typhoons by a single GCM cannot provide enough information; therefore, a stochastic typhoon model is necessary for engineering purposes.

This paper summarizes recent studies of The Maritime Disasters Section, Disaster Prevention Research Institute, Kyoto University. Firstly, this paper introduces projection of future wave climate and analysis of differences between present and future ocean wave climate using the data of high-resolution atmospheric General Circulation Model (GCM) developed by Japanese Meteorological Research Institute and Japan Meteorological Agency (MRI-JMA) and a global wave model. Secondly, a stochastic typhoon model for estimating characteristics of typhoons from cyclogenesis to cyclolysis in both present and future climate conditions is described. Differences of statistical characteristics between present and future typhoons are estimated from the projections by the GCM, and these differences are taken into account in the stochastic model of future typhoons. Finally, the failure probability of seawalls is briefly described concerning the effects of sea level rise and waves by using the reliability analysis of Level 3.

2. Analysis Methods on Climate Change Effects

2.1. Climate Projection

This research uses product of global climate projections on the basis of 20km high-resolution GCM developed by JMA. The 20km high-resolution MRI-JMA GCM is the single atmospheric GCM with T959L60 resolution following A1B scenario and is newly developed in Kakushin (2007) program. Kakushin (2007) program is a Japanese governmental supported climate prediction project and a part of its objectives is quantitative prediction of extreme weather around the East Asia and Japan. The external forcing of the GCM is sea surface temperature (SST) and the ensemble averaged warmer SST and related oceanic conditions, projected by different coupled atmosphere-ocean GCM runs used in the IPCC AR4 (CMIP3), are used as bottom boundary conditions for the future climate projection, although the observed SST is used in the present climate computation. The time-slice experiments were conducted for three climate periods at 1979-2004 (present climate), 2015-2031 (near future climate) and 2075-2100 (future climate) following A1B scenario, respectively. By using the data computed from the GCM, disaster and environmental changes that may lead to natural disasters have been evaluated (i.e., Mori *et al.*, 2009; Yasuda *et al.*, 2009).

Here, the differences between the present wave conditions and future ones are mainly focused. The global wave climate projections for three periods were simulated by the SWAN (Simulating WAVes Nearshore) model (Booij *et al.*,

1999) using sea surface wind at 10 m height U_{10} of the GCM. The global wave computations were carried out using a spherical coordinate in the latitude range of 80N-80S with 1.25 degree resolution (289×126 grids).

The computed wave projection was verified by the long-term observed data. Over 25 years' observation data in the Pacific Ocean were selected for the validation. The averaged mean H_s is 11% underestimated, although the averaged mean U_{10} is 7% overestimated. On the other hand, the averaged standard deviation of H_s is 2.3% underestimated and the averaged standard deviation U_{10} is 5% underestimated. There are non negligible error of wave computation in average and the computed of wave height, therefore, includes same order of error. However, it is possible to estimate the ratio of wave climate change from the present to future climate, quantitatively.

2.2. Stochastic Typhoon Model

Stochastic Typhoon Models (STM) have been developed for engineering applications. STMs give the central pressure, travelling speed and direction along its trajectory. The construction of our STM uses the typhoon data of Best Track of 1468 observed typhoons in the northwest Pacific Ocean from 1951 to 2005 to get two-dimensional probability density functions (2D-pdfs) for each area of (1° x 1°) in the target area (0°N-70°N, 100°E-200°E), where a 2D-pdf consists of an input value and its local variation; for example, the central atmospheric pressure p at an original location and its variation Δp to the next location. These 2D-pdfs are constructed for the track direction, velocity and central atmospheric pressure.

The independence of typhoon parameters was firstly examined by using the BT. It was found that there is strong correlation in consecutive values such that correlation coefficients of moving direction, moving speed and central pressure are 0.68, 0.82, and 0.98, respectively. We employed principal component analysis to estimate the 2D-pdfs.

Indicative typhoon data from the GCM was selected by the method of Oouchi *et al.* (2006). Murakami and Sugi (2010) tuned the typhoon identification method of Oouchi *et al.* (2006) to obtain a number of typhoons similar to the observed data in the Northwest Pacific area. However, weaker typhoons were included into the total count and there are still large biases about the intensity. Although it is difficult to represent typhoon magnitude perfectly, the biases of present and future typhoons produced by a dynamical model GCM are assumed to be consistent each other (Mori *et al.*, 2011). Then, we took the changes of typhoon characteristics estimated from the GCM's typhoons into account to our STM.

3. Results and Discussion

3.1. Mean wave climate change

The important characteristics of future projection are not only extreme wave climate but also daily wave climate. Before discussing the extreme wave climate change, the period averaged (mean) H_s is discussed first. Figure 1 shows the mean of H_s (denotes H_s hereafter) in the present and future climates (Florida area is excluded for the analysis following validation results). Regarding the differences of H_s between the present and future climates, there are regional dependencies for H_s similar to U_{10} (Mori *et al.*, 2009). There are remarkable characteristics of large scale pattern change of averaged H_s from the present to future climate. First, the small wave height region on the equator is expanded to both north and south directions. On the other hand, large wave height region in the Antarctic Ocean is expanded from the present to future climate.

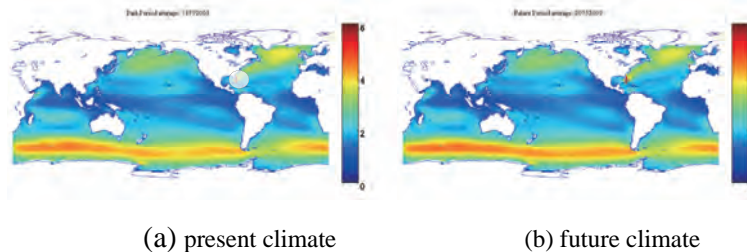


Figure 1. Period averaged significant wave height.

Figure 2 shows the normalized difference between the future and present climate (future minus present divided by present). The future H_s in the Pacific Ocean on the equator will be decreased about 7% which corresponds to a 0.1 m decrease of averaged wave height. The future H_s in the latitude range of 30N - 45N in the North Pacific and the North Atlantic Ocean will be decreased 7% which corresponds to 0.15 m of averaged wave height, approximately. The east offshore of Japan in the Pacific Ocean belongs to this decreased region and is expected 5–10% decreased in the future.

On the other hand, the future wave height in the Antarctic Ocean will be increased 6–9% which corresponds to more than 0.2 m increase of averaged wave height. The similar trends to the Antarctic Ocean can be observed in the Bering Sea and the Hudson bay in the northern hemisphere. These changes are caused by the Ferrel cell movement to the polar areas. To summarize the characteristics of averaged wave height change in the future, there are clear latitude dependence. Both positive and negative future wave climate changes are possible depending on the latitude and region. This result shows that the future daily wave climate will change as lower mean wave height in the middle latitudes, and the higher mean wave height in the high latitudes and equator areas.

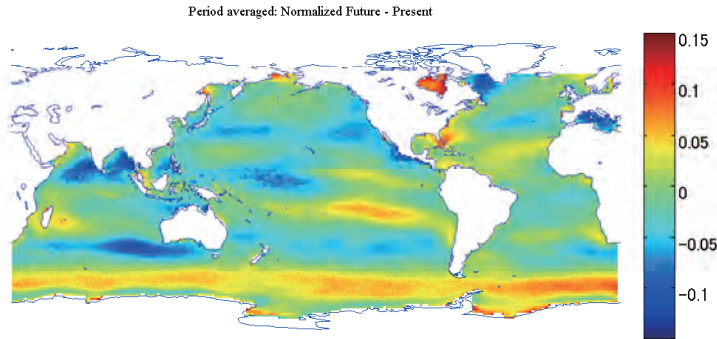


Figure 2. Difference of period averaged significant wave height Period averaged significant wave height.

3.2. Extreme wave climate change

The quantitative measure of extreme condition is arbitrary and is sensitive to the choice of parameters. The general discussion should be conducted to compare with the extreme value distribution or probability density functions of targets (Shimura *et al.*, 2010). Figure 3 shows the spatial averaged cumulative distribution of H_s over 99% value up to its maximum in four areas. The Antarctic Ocean indicates the latitude range of 70S - 40S and longitude range of 0 - 360, the Southern Indian Ocean indicates the latitude range of 40S - 10S and longitude range of 15 - 90, the south of Japan in the Pacific Ocean indicates the latitude range of 25N - 35N and longitude range of 100 - 130, and the east of Japan in the Pacific Ocean indicates the latitude range of 35N - 45N and longitude range of 115 - 140, respectively. The both the cumulative distributions of H_s in the present and future climates in the Antarctic Ocean and the east of Japan are quite similar and their maximum heights are about 16 m. On the other hand, the future cumulative distributions in the Southern Indian Ocean and the south of Japan in the Pacific Ocean side are different from the present climate. The differences of distributions between the present and future conditions are significant and these differences are departed from the probability of $10^{-2} - 10^{-3}$. The future spatial

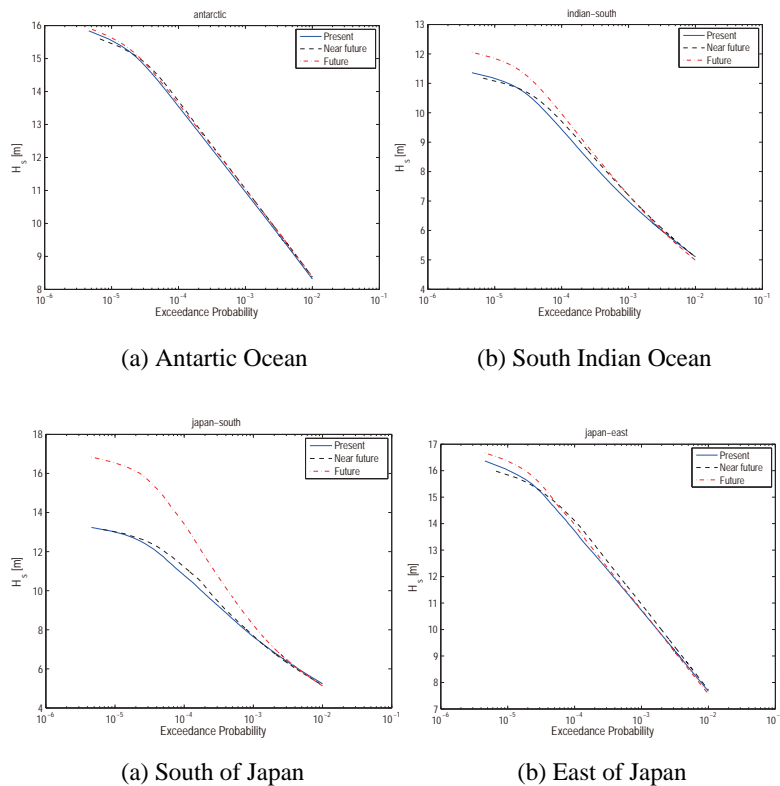


Figure 3. Cumulative distribution of wave height over 99%.

averaged maximum H_s in these areas are 0.5 meters and 3 meters larger than that of present climate, respectively. The extreme wave condition in the south of Japan in the Pacific Ocean side will be increased, although the mean H_s in this area will be decreased. The future cumulative distributions of U_{10} in these areas show similar deviations from the present climate but the differences in H_s are much larger than that of U_{10} . The wind stress to the wave energy is proportional to U_{10}^2 and therefore the extreme wave climate is more sensitive than that of wind climate.

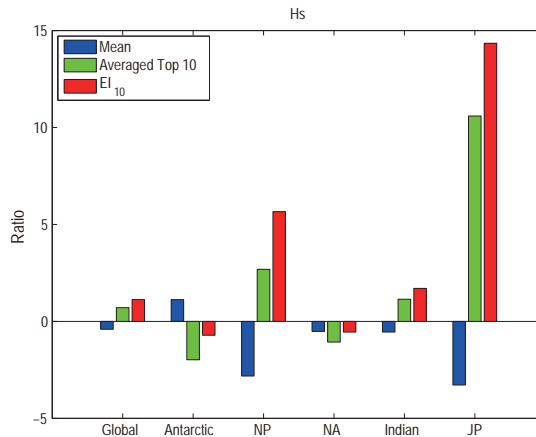


Figure 4. Spatial averaged mean, top 10 and EI of wave height (NP: Northern Pacific, NA: Northern Atlantic, JP: Pacific Ocean near Japan).

Figure 4 shows spatial averaged characteristic properties of H_s at several oceans. The blue, green and red colored bars are temporal-spatial averaged mean, averaged top 10 value and extreme index (EI) of H_s , respectively. The averaged top 10 value indicates characteristics extreme value computed the averaged top 10 value of cumulative distribution of H_s (i.e. Figure 3) to avoid statistical sensitivity. The EI indicates the averaged top 10 value divided by its mean value, and it corresponds to the ratio of extreme value to mean value. The area averaged mean H_s will be slightly increased in the Antarctic Ocean but it will be decreased significantly in the Northern Pacific Ocean. The other areas will be slightly decreased but changes are not significant. On the other hand, the averaged top 10 values will be decreased in the Antarctic Ocean but will be increased in the Northern Pacific Ocean. This inverse relation is caused due to tropical cyclone effects. The GCM model produces intense tropical cyclones in the West Pacific Ocean. Therefore, the future extreme wave condition in the Northern Pacific Ocean, especially near Japan area, will become more severe than the present climate.

3.3. Verification of STM outputs

The STM has applied to hindcast (present climate) by using BT from 1951 to 1995. Although the STM simulation has a little bias in genesis area compared to the observation, trajectory pattern of typhoons is well reproduced. For example, some typhoons go straight toward China and some other typhoons turn to northeast near Taiwan. When examining typhoons that landed near the Osaka bay (134.5E~135.5E, 34N~35N) from 1951 to 1995, it showed a fairly good agreement such that 25 typhoons had passed this area for 45 years and the average number of 10,000 years' run is 28 and standard deviation is 5.

Concerning the occurrence probability of central atmospheric pressure, the average and standard deviation of observed typhoon are 981 hPa and 17.7 hPa while the STM ones are 985 hPa and 22.0 hPa. The error is very small, and the difference of average value is only 4hPa. For the occurrence probability of typhoon moving speed, the average and standard deviation of BT are 45.5 km/h and 15.9 km/h while the STM ones are 49.8 km/h and 11.9 km/h. The average of typhoon moving speed simulated by STM is about 5 km/h faster than observed one, but it is not significant large error.

3.4. Future Typhoon Projection by STM

The number of typhoons projected by GCM for the present climate is inaccurate and insufficient to discuss the probabilistic characteristics of typhoon for the STM. Figure 6 shows the track of detected typhoons for the MRI-GCM present (1979-2004) and future (2075-2100) data. It is obvious that the typhoon genesis area is changed west of Philippine. The pdfs (the log-normal distribution fitted) for latitude and longitude of typhoon genesis locations are estimated by analyzing the GCM data. The modes of latitude pdf are 17.6° and 18.5° for the present (1979-2004) and the future (2075-2100). As for the longitude, the modes are 131.5° and 132.5°. The locations of typhoon cyclolysis

were also analyzed. The modes of latitude pdfs are 19.3° and 21.7° , and the modes of longitude pdfs are 116.1° and 120.8° , respectively.

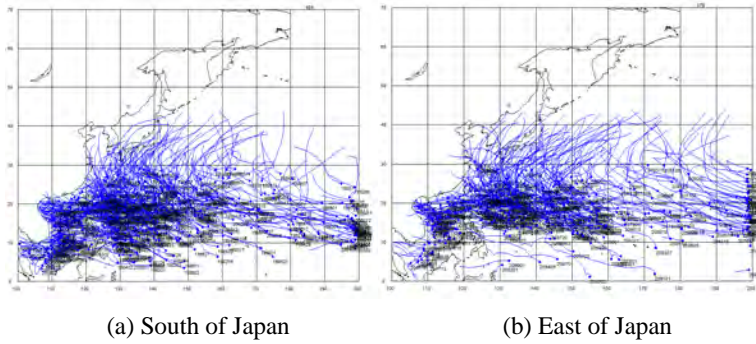


Figure 5. Typhoon tracks simulated by GCM.

To utilize the changes in typhoon characteristics projected by GCM, a modification based on these analyzed differences was applied to the BT data so as to simulate future typhoons. The locations of cyclogenesis and cyclolysis of BT data are changed proportionally according to the lognormal pdf's change. The stochastic procedure in the future experiment follows that for BT. Since the number of typhoons in the future climate is estimated to decrease from 20 to 16 by AGCM, the average number of typhoon genesis in the log-normal pdf will decrease from the observed average of 24.7 to 19.5 and the standard deviation will also decrease from the current 5.6 to 4.3. These averaged statistical characteristics are taken into account to the STM.

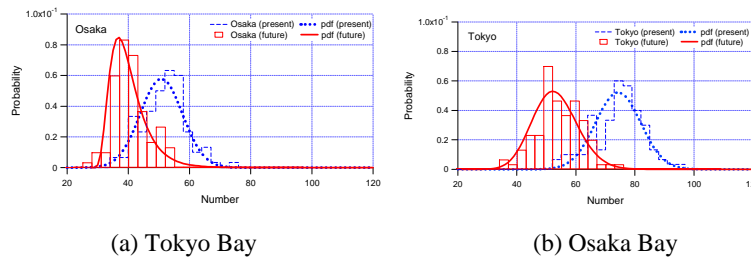


Figure 6. Probabilistic number of attacking typhoons in 100 years projected by STM.

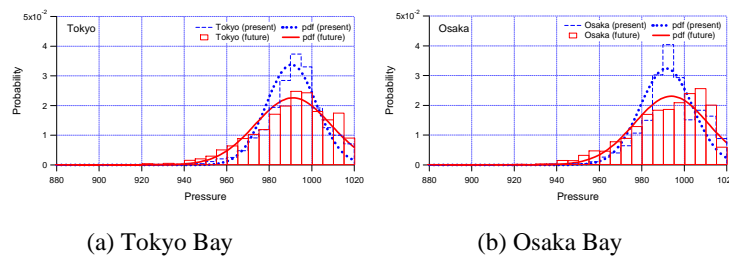


Figure 7. Lowest central atmospheric pressure of attacking Typhoons in 100 years projected by STM.

As shown in Fig.6, the number of possible typhoon events will decrease in Osaka Bay area. This is expected because the number of future cyclogenesis is given smaller than present climate. However, the number of future cyclogenesis is decreased about 21% in the whole do-main but number of future typhoon approaching to Osaka bay is decreased 30%. This is the influence of shift of typhoon tracks and cyclolysis. The both typhoon number and track information are important to discuss projections of future typhoon characteristics. The lowest central atmospheric pressures of the typhoons passing over major bays will stay approximately the same in the future as shown in Fig.7. One of the most significant results is the suggestion that for all three major bays the possibility of intense typhoons with central atmospheric pressure lower than 960 hPa will increase in the future. Although the average typhoon intensity will not change, extreme conditions will become more severe (Yasuda et al., 2011).

3.5. Failure Probability of Seawalls

In Japan, many coastal structures were designed in the late 1950s. In the future, coastal structures must be designed by taking into account the changes of coastal environmental forces accompanying with the climate change. This section shows the failure probabilities for coastal seawalls with three different conditions by using a reliability method of Level 3. The target failure modes are 1) failure due to wave overtopping, 2) subsidence due to overtopping wave pressure, and 3) parapet collapse due do wave pressure.

Considering the sea level rise and wave storminess, failure probabilities are estimated by a reliability analysis of Level III (Tamada and Mase, 2011). Probabilistic methods provide a powerful framework for the design of coastal defences. Three typical seawalls in field, South Coast of Sendai, Suruga Coast and Kochi Coast, were selected. Present design conditions, such as seawall's cross-section, bottom slope and so on, were used as in the present and future conditions. Wave heights, periods and tidal variations were given by some probabilistic distributions under a target design wave and mean sea level rise.

Figure 8 is a sample of results to show the change of failure probabilities due to wave height increase (figure (a)) and sea level rise (figure (b)) for Tsuruga Coast where the bottom slope is 1/10. It is seen that the effect of wave height increase is more important for seawall safety than that of sea level rise. At another site of Kochi Coast where the bottom slope is gentle, the sea level rise has more important effect than the wave height increase. By analyzing failure probabilities against the parameters such as crown height of seawalls and depth of toe of the structures, we can estimate the crown height, for example, to keep the same safety level in future climate.

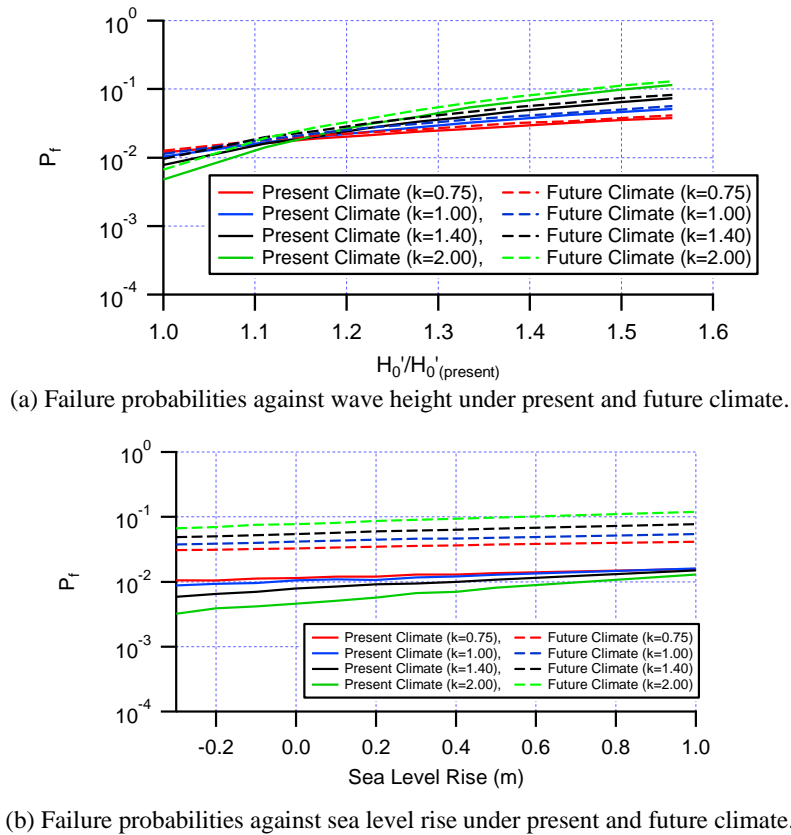


Figure 8. Failure probabilities for case of seawalls at Tsuruga Coast (failure mode due to wave overtopping).

4. Conclusions

This paper summarized resent studies of our research group, especially on projection of future wave climate and analysis of differences between present and future ocean wave climate, development of a stochastic typhoon model and probabilistic characteristics of future typhoons using the data of high-resolution atmospheric General Circulation Model developed by Japanese Meteorological Research Institute and Japan Meteorological Agency. In addition, the failure probability of seawalls is briefly described concerning the effects of sea level rise and waves by using the reliability analysis of Level 3.

Acknowledgments

A part of this study was supported by a fund of The Service Center of Port Engineering.

References

1. N. Booij, R. Ris and L. Holthuijsen, *Jour. of Geophy. Res.*, **104** (C4), 7649–66, 1999.
2. M. Hemer, J. Church, V. Swail and X. Wang, *Atmosphere-Ocean Interactions* **2**, 185–218, 2006.
3. IPCC Climate Change, Cambridge University Press, UK, 996p., 2007.
4. Kakushin, <http://www.kakushin21.jp/>, 2007.
5. N. Mori, T. Yasuda, R. Iwashima, T. H. Tom, H. Mase and Y. Oku, *Coastal Dynamics 2009*, ASCE, No.135, 2009.
6. T. Shimura, N. Mori, T. Yasuda and H. Mase, *The 32nd International Conference on Coastal Engineering*, 2010.
7. N. Mori, T. Yasuda, H. Mase, T. Tom and Y. Oku, *Hydrological Res. Letters*, Vol. **4**, pp.15-19. doi:10.3178/hrl.4.15, 2010.
8. H. Murakami and M. Sugi, *Scientific Online Letters on the Atmosphere*, **6**, 73-76. doi:10.2151/sola. 2010-019, 2010.
9. K. Oouchi, J. Yoshimura, H. Yoshimura, R. Mizuta, S. Kusunoki and A. Noda, *Jour. of Meteo. Soc. of Japan*, **84**(2), 259-276. doi:10.2151/jmsj.84.259, 2006.
10. N. Mori, S. Nakajo, H. Murakami, T. Yasuda and H. Mase, Ensemble Model Projection of Future Tropical Cyclone Characteristics, submitted to *Geophysical Research Letters*, 2011.
11. T. Yasuda, H. Mase, R. Takada, S.-Y. Kim, N. Mori and Y. Oku, *Proceedings of 33rd IAHR Congress*, 2009.
12. T. Yasuda, H. Mase and N. Mori, *Hydrological Res. Letters*, **4**, 65-69, doi:10.3178/HRL.4.65, 2010.
13. T. Yasuda, S. Nakajo, N. Mori, H. Mase, Y. Hayashi, S. Kunitomi, *Proceedings of 11th International Conference on Applications of Statistics and Probability in Civil Engineering*, 2011.
14. M. Sugi, H. Murakami, J. Yoshimura, *Scientific Online Letters on the Atmosphere*, **5**, 164-167. doi:10.2151/sola. 2009-042, 2009.
15. X. Wang and V. Swail, *Atmosphere-Ocean Interactions* **2**, 185–218, 2006.
16. K. Zhang, B. Douglas and S. Leatherman, *Climatic Change* **64** (1), 41–58, 2004.

About the speaker



Professor Hajime Mase received his Doctor degree in Engineering from Kyoto University in 1986. He is currently the professor in charge of maritime disasters in the Division of Atmospheric and Hydrospheric Disasters of the Disaster Prevention Research Institute, Kyoto University, Japan. His research is in the field of water control science, covering the following issues: nearshore wave transformation, dynamic and stochastic random wave characteristics, estimation of wave climate, wave action to coastal structures, extreme sea wave statistics, seabed response to sea waves, neural network application to coastal engineering, storm surge risk assessment, wave forecasting, climate change effects on coastal disasters, and so on. Professor Mase was awarded in 2007 the Paper Award of the Japanese Association for Coastal Zone Studies.

HYDRODYNAMICS RESEARCH AND APPLICATION OF THE RADIAL SAND RIDGE IN SOUTH YELLOW SEA, CHINA

PEIDONG LU

Nanjing Hydraulic Research Institute, Nanjing 210029, China

XIPING DOU

Key Lab of Port, Waterway and Sedimentation Engineering of the Ministry of Transport, Nanjing 210029, China

In this paper, the following are analyzed, the formation, the recent development, the long term evolution trends and the exploit of the radial sand ridges at the South Yellow Sea, China. A radial tidal current field is formed from the interactions between two tidal systems. The radial tidal current pattern is regarded as the driven force to generate and maintain this morphological feature. An analysis on the tide, wave and morphological changes of the tidal channels and sand ridges was carried out. The reclamation of Xiaomiaohong tidal flat and the construction of the artificial island for Yangkou Harbor provided engineering practice. Thus we claim that the key point for a consistent development of the radial sand ridges is to limit human interference, in the form of land reclamation on the tidal flat and the exploit of harbor development, so as to adapt to the natural evolution of hydrodynamic conditions and morphological changes.

1. Introduction

Sand ridges are massive sand bodies, mainly located in shallow coastal areas with rich sources of loose sediment material and strong tidal force. Sand ridges and the channels between them distribute alternatively along the direction of tidal currents. Most sand ridges are composed of sandy material, with a few meters to tens meters in height, a few hundred kilometers in width and a few kilometers to tens kilometers or more in length.

Various types of tidal sand ridges are found on the continental shelf of China, for example, the radial Sand ridges in South Yellow Sea (Figure 1), the comb type sand ridge in Yalu River estuary, the fingerlike sand ridges in Liao Dong Shoal area located at the East Bohai Sea, the crescent sand ridges at Taiwan Shoal area, and the fingerlike sand ridges located at Qiongzhou Strait (Figure 2). Specifically, the radial Sand ridges in South Yellow Sea are distinct for their wide distribution area, huge magnitude, and complex hydrodynamics and complicated formation mechanisms.

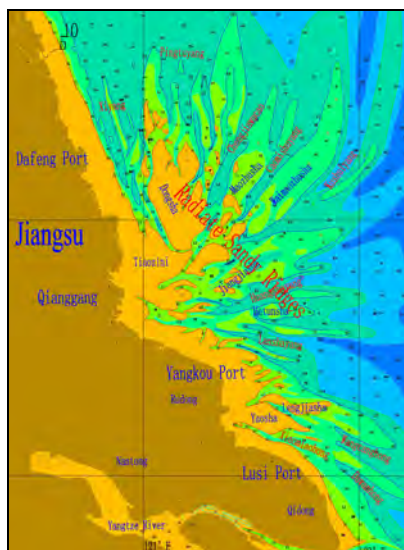


Figure 1: The Radial sand ridges at South Yellow Sea, China.

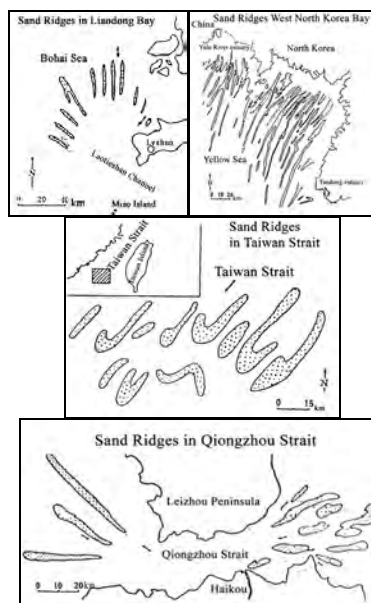


Figure 2: Tidal sand ridges in China.

The radial sand ridges consist of 70 sand ridges and tidal channels between them, which extend 199.6 km ($32^{\circ}00'N \sim 33^{\circ}48'N$) from north to south, 140 km ($120^{\circ}40'E \sim 122^{\circ}10'E$) from east to west. The sand ridges and tidal channels fan out with a central angle of about 160 degrees in the N, NE, E and SE, with Jianggang, in Dongtai City of Jiangsu, as the radial center. 8 large sand ridges cover an area of 2000 km² land above the LLWL. The tidal channels between these 8 sand ridges are usually deeper than 10 m.

The radial sand ridges have been formed under a long term interaction between continental shelf and ocean dynamics. In the past 40 years, quite some multidiscipline investigation and survey on the formation and evolution of the large morphological features have been carried out. The area of radial sand ridges covers an immersed tidal flat and

shallow water area, which provides many possibilities for land reclamation. In this case, the wide and deep channels between the sand ridges offer good conditions for harbor development. In the past 20 years, lots of investigation and engineering practice on land reclamation and harbor development have been carried out. This large morphological feature is obtaining increased public attention.

2. Formation of the radial sand ridges

2.1. Sediment sources

The radial sand ridges have been formed under a long term interaction between the continental shelf and ocean dynamics at the south Yellow Sea. As early as Holocene, the paleodelta of the Yangtze River has already presented a morphological foundation of the radial sand ridges. Later with enormous amount of the fine sediment, the Yellow River began to act as another important sediment source. The south coast of Yellow Sea has received a huge amount of sediments from both the ancient Yangtze River and the ancient Yellow River, which provided the material basis for the formation of the radial sand ridges with thick, loose sediment.

As early as the Holocene Epoch, the Yangtze River discharged into sea at Jianggang, the central point of the radial Sand ridges at present stage. Later on, the Yangtze River mouth moved southwards to the present position. During these long-term processes, a series of sandy islands, underwater sand ridges and river delta have been formed, which provided the morphological foundation of the radial sand ridges.

During 1128~1855 AC, the Yellow River took over the downstream course of the Huaihe River and discharged into the Yellow Sea. The huge amount of sediment carried by the Yellow River diffused southwards to the radial sand ridges area and increased the height of the underwater sand bodies. Till the early 1800's, the southern part of the radial sand ridge was already in radial shape. And till the mid 1900's, the middle part of the radial sand ridge also showed a primitive radial shape.

After 1855AC, the main channel of the Yellow River moved back in the north to Bohai Sea. The land side sediment source of the radial sand ridges was blocked. The only sediment source then was the erosion of coastal and underwater delta. Part of the eroded fine sediment was transported southwards by longshore current and settled at the north part of radial sand ridges. The sediment from the Yangtze River is mainly transported southwards, thus this sediment source has very limited contribution to the present radial sand ridges.

2.2. Main forces

Tidal force is regarded as the main force for the formation of the radial sand ridges. The tidal system in southern Yellow Sea has special characteristics: it is relatively stable; the progressive wave from the Pacific Ocean propagates from its southeast towards the East China Sea; part of the progressive wave is reflected by the Shandong peninsula; these two tidal currents merge to form a circular tidal system; the two tidal systems converge at Jianggang, the central point of the radial sand ridges at the south Yellow Sea. Since the tidal energy is centralized at this area, the tidal range increases to an abnormal height (Figure 3). As one of the largest tidal ranges along the Chinese coastal area, the measured tidal range at Xiao Yangkou Harbor, close to Jianggang, could be as high as 9.28m.

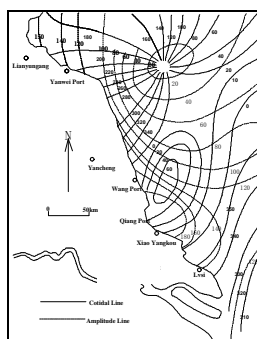


Figure 3: M_2 co-tidal chart in South Yellow Sea, China.

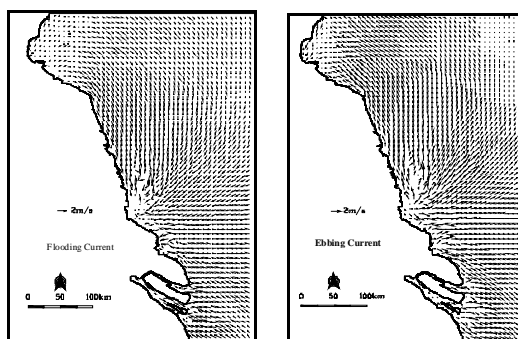


Figure 4: Tidal flow current pattern in South Yellow Sea, China.

Radial tidal current is supposed to be formed by the convergence of these two large tidal systems at the South Yellow Sea. The numerical simulation shows: the flooding currents from the north, northeast, east and southeast from the South Yellow Sea converge to the central point of the radial sand ridges, while the ebb currents diverge towards the outer sea (Figure 4). The ebb flow area make an angel of 150 degree from the central point. The flooding and ebbing tidal currents form two-directional flow patterns, while the currents in both directions either converge towards or diverge from the central point of the radial sand ridges. The numerical simulation also shows that even without the radial shape of sand ridges, the tidal current also presents a radial pattern. The converge-diverge tidal current pattern is

formed by the tidal wave propagated from the ocean along the East China Sea and the tide wave reflective by the Shandong Peninsula, with very limited influence from the changes of local bathymetry and land boundary. This special tidal pattern provides an essential force for the generation of the radial sand ridges.

During the flooding and ebbing currents along the tidal channel, the velocity distribution along the cross section is not uniform. Because the current speeds along the channel center are higher than the speed above the sand ridges due to a shallower water depth, velocity gradient along the cross sections is generated, leading to a secondary flow along the cross section. The surface currents flow from the sand ridges towards the deep tidal channel, as compensation, the bottom currents flow from the deep channel towards the sand ridges (Figure 5). Three dimensional numerical simulations show that, in the deep channels, the flooding and ebbing currents are mainly in two directions as high as 0.5 m/s to 2.5 m/s, while the circular current pattern also exists at the bottom of the deep channel. Most of the time, the secondary flow along the cross section exists in the tidal cycle (Figure 6). The normal components of the bottom velocity (perpendicular to the main current direction) could be higher than 0.5 m/s, strong enough to initiate bed materials, and to bring the sediment from the deep channel to the adjacent ridges, which leads to deeper channels and higher sand ridges.

In summary, the converge-diverge tidal current pattern, formed by the propagated tidal wave from the ocean along the East China Sea and the reflective tide wave by Shandong Peninsula, is regarded as the dominant force. Strong flooding and ebbing currents in two directions make the deep tidal channel, while the secondary flow in the tidal channels enhances the erosion of the channel and sedimentation on the sand ridges, resulting in the deep channel-wide ridge shape on cross sections.

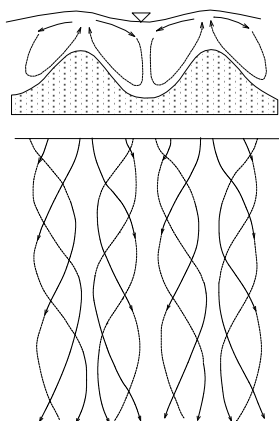


Figure 5: Sketch of the secondary flow pattern in tidal channels between sand ridges.

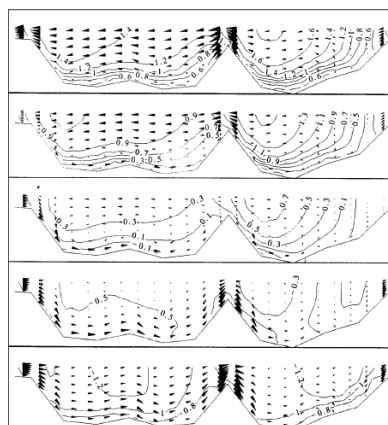


Figure 6: Dynamics of the secondary flow pattern in Xiyang Channel during a tidal cycle.

3. Hydrodynamics

3.1. Tides

The radial sand ridge area is known for its large tide range and strong tidal currents. Simultaneous in-site measurements during the recent 20 years in the areas show that the tidal wave belongs to standing wave. The tide belongs to regular semidiurnal tide. The maximum current velocity happens at MMWL. The tidal currents in deep channels are mainly in two directions along the channel directions while the tidal currents directions on sand ridges and shoals change with time. At the beginning of the flooding, the current pattern belongs to overland flow while at the end of the ebbing, the currents mainly belong to return flow, discharging to small channels on the ridges. The tidal current pattern within the sand ridge area is relatively stable, i.e. the current velocities in the deep channels are bigger than those on the ridges, and the velocities at the straight channels are bigger than those in the curved channels, implying that the morphology generally adapts well to the local hydrodynamic conditions.

The spatial pattern of the radial sand ridge area appears like a trumpet type with a wide mouth and a narrow inner area along the tidal channels. Because of bed friction and shoaling effects, tidal waves are transformed during the propagation, which results in higher tidal range and higher water level from the mouth towards the root area. The evidence came from the simultaneous measurement at 3 tidal stations at the Lanshayang channel at the mid south of the sand ridge area (Figure 7). From the mouth area towards the inner area, the distance between CW3 to CW2 is 24.5km and that between CW2 to CW1 is 20km. The tidal range at CW2 is 0.67 m higher than that at CW3 with a time lag of 11min, and the tidal range at CW1 inside the tidal channel, is 1.05 m higher than that at CW2 with a time lag of 20 min. The local morphology of the sand ridge system enhances the radial shape of the current pattern from the two large scale tidal wave systems.

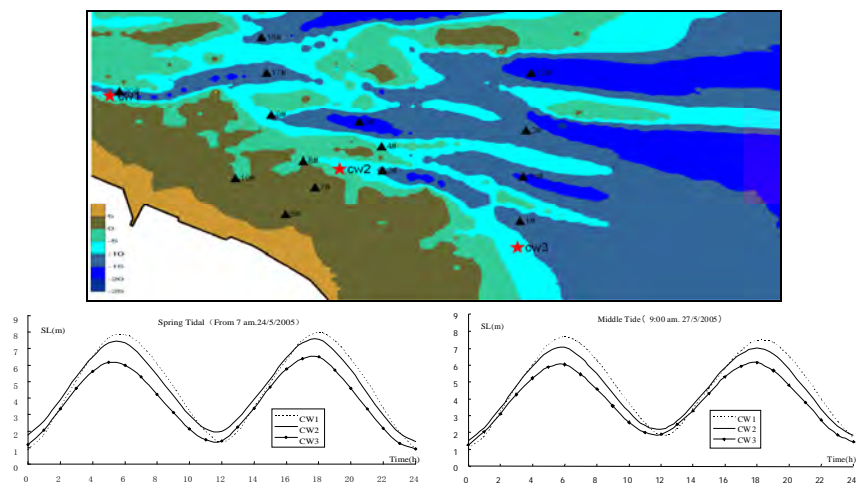


Figure 7: Position of the observing tidal stations along the Lansha Yang Channel and the water level measurements.

3.2. Waves

Waves are well sheltered by the massive sand ridges. Most of the wave energy from the outer sea is dissipated by wave-breaking and refraction caused by the complex bathymetry. In an area with a radius of 50km from the root of the radial sand ridge, the wave strength is mild, dominated by small amplitude waves. The measurement in the Xiaomiaohong tidal channel within the south of the sand ridge area during the recent 35 years shows that there is no wave 43% of the time. The average wave height from all directions in the long run is 0.48m (excluding calm days).

However, the shading effect varies with the change of tidal water level, thus wave propagation also varies accordingly. The results from the wave model show that, with high tide, bathymetry has the minimum effects on the wave propagation route. However, as water depth decreases during ebbing period, bathymetry has greater effects. At the minimum water level, waves can only propagate through the tidal channels towards the root of the sand ridge area. The numerical modeling also shows that short wave has less influence with the use of bathymetry. With higher wave periods, there are fewer wave propagation routes and the transport direction also deflects along the contour line.

Storm waves and big waves caused by typhoon also are affected by the tidal wave level. For example, measurement shows there was higher wave within the sand ridge area due to No. 9711 typhoon on August 18th of 1997. Measured significant wave height at West Taiyang Sha area is around 4.2m in average and 6.9m at most, and its average period is around 6s. The corresponding return period is around 50 years. Measurement confirmed the correlation between the significant wave height and water depth during No. 9711 typhoon in West Taiyang Sha area (Figure 8). The time window when the maximum wave height appears is corresponding to the time of HHWL. When water level, and the subsequent water depth, go down, wave height drops down rapidly, too. This results from the shading effects varying with the water level, and therefore, the big wave inside the sand ridge area is not consistent with time.

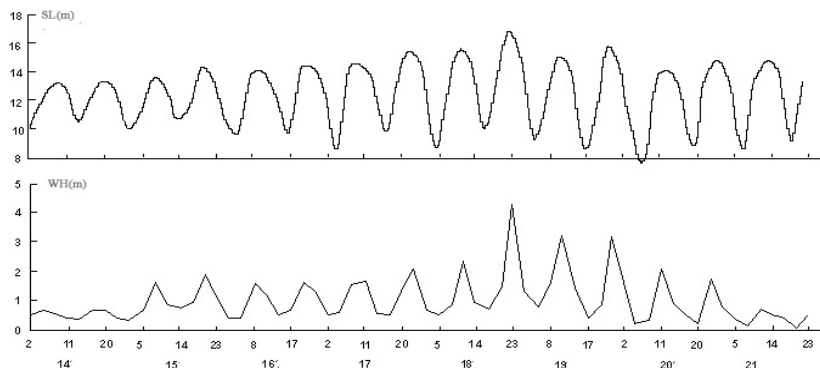


Figure 8: Corresponding wave height and water depth at the West Taiyang Sha area during No. 9711 typhoon.

4. Morphodynamics of the sand ridges

4.1. Stability in large scale

Research on the mechanism for the radial sand ridge shows that: 1) Tide is the driving force. The dominant tidal system in the sand ridge area is relatively stable, so that the driving force of the formation of the sand ridge is quite stable in large scale. 2) An analysis on the interactions of continental shelf components shows that, at present stage, there is hardly any sediment influx from the ambient environment. The radial sand ridge is regarded as a relatively independent morphological unit. Because the radial hydrodynamic pattern adapts well to the radial morphological features, i.e., sand ridge-tidal channel pattern, the morphological system is supposed to stay stable in the near future. The morphological pattern, the position of the main ridges, and the tidal channels will stay stable for quite some time.

4.2. Morphodynamics of the sand ridges

As a relatively independent morphodynamic unit, the morphological changes in the sand ridge stay in local subdivisions. The analysis based on the satellite images and field surveys during the recent 40 years shows that, on one hand, the outer blink of the sand ridges are under erosion, and the eroded sediment is transported landwards by the tidal current; on the other hand, some relatively smaller sand bodies between those main tidal channels tend to merge into a subgroup of sand ridge-channel systems. All the adjustments are regarded as local adaptations of the morphology to hydrodynamic forces.

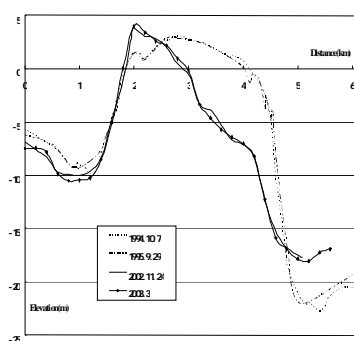


Figure 9: Corresponding erosion on the shore face and sedimentation in the channel at north of the West Taiyang Sha area after No. 9711 typhoon.

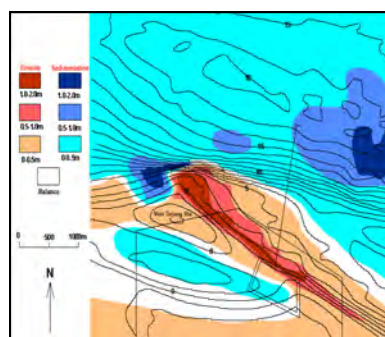


Figure 10: Corresponding erosion on the shore face and sedimentation in the channel at the West Taiyang Sha area caused by Matsa typhoon in Aug, 2005.

Furthermore, the middle and southern parts of the radial sand ridge show the trend of moving southwards in recent decades. Not only the southern part of sand ridges moves southwards, but also the axis of the deep tidal channels, such as Huangshayang Channel, Lanshayang Channel moves southwards for a few hundred of meters. The cross section in Xiaomiaohong Channel also shows the same tendency: erosions happened at the south bank and sedimentation at the north bank. The numerical simulations show that that might be caused by hydrodynamic changes. In the last two decades, the abandoned Yellow river delta, located in the north to the radial sand ridge area, have been under serious erosion and the coastal lines have retreated for around 20km. The underwater delta part has been eroded thoroughly, too. As a result, there is less blocking effect on the rotational tide wave from the north. The amphidromic point moves southwards correspondingly. The tidal wave from the north has more influence on the morphological change of the sand ridge area.

Morphological changes caused by storm surges are also significant. Three types of typhoon are classified in this area: from sea and northwards to the land, landing in the Yangtze estuary, or turning around on the sea. Big waves caused by the anti-clockwise typhoon usually propagate across the sand ridges in an angle, which usually causes serious erosion on the shallow ridges in a short period. As is mentioned above, due to the specific pattern of the sand ridges, erosion caused by wave always happens during HHWL. However, because for standing tidal wave, the current velocity is the minimum during HHWL, sediment particles due to the severe erosion caused by the big waves on the top of the sand ridges would not be transported for a long distance, but only settled in the deep channels close by. This is regarded as the causes of sudden erosion on the top of ridges and sudden sedimentation at the adjacent channels. A survey from Sept, 1995 to Nov, 2005 shows that the north bank of West Taiyang Sha was eroded to 8 meters at maximum and the channel adjacent got a deposition of 7 meters (Figure 9). A grain size analysis of the sediment in the channel shows the new deposition was transported from the shallow area, which happened in a short period and would be regarded as an episodic event. All the evidence shows that this episodic morphological event is related to No. 9711 typhoon and the consequent big waves. Furthermore, 1-2 meter erosion in the shallow front of the West Taiyang Sha and the corresponding sedimentation in the north adjacent deep channels, caused by the Matsa typhoon in August, 2005, also support this statement (Figure 10). The scaled model in laboratory driven by wave and tidal currents for the

West Taiyang Sha area also reproduced this phenomenon. This periodic erosion on the flats and sedimentation on the channels caused by storm surge waves are regarded as local sediment transport between the ridges and channels within this shallow water system.

4.3. Morphological Evolution

Tide is the driven force to form and maintain the sand ridge system, even though storm surges have strong capability to reform the morphology. However, the effects of storm surges are not continuous and stay short. Compared to tidal forces, the storm surges are supposed to be the secondary forces. The severe sedimentation and erosion caused by waves during storm period will be recovered and adjusted gradually back to the status before storm. There was no significant typhoon in the West Taiyang Sha area during the five years after Matsa typhoon in 2005. Field measurements were carried out in Nov, 2006, Dec, 2007, April, 2008, July, 2009, and in Dec, 2010. The measured data show that the north adjacent deep channels, which got serious sedimentation during the Matsa typhoon in 2005, are eroded gradually. In summary, the morphological evolutions show a cyclic trend from “tide form it” to “storm destroy it”, and to “tide recover it”, from an equilibrium status to a non-equilibrium status, then towards another new equilibrium.

5. Exploit of the resources in the sand ridge area

5.1. Land resource on the flat

The wide flat in the inner flank of the sand ridges area could be as wide as 30 km and still extending towards the seaside. The waterline under HHWL extends towards the seaside for around 200 meters every year in average. Furthermore, there are 10 more well-developed large sand bodies (the sand ridges) underwater. Each of these 10 km-wide sand ridges is longer than 100 km. Most of the ridges are above water level during low tide periods. More than 50 sand ridges have 1 km² area above water level. The area of the tidal flat above the LLWL over the whole area is as much as 2017.52 km², of which, the area above HHWL is around 307.47 km². This area is rich in land resources.

Since 1950, there has been tidal flat reclamation at more than 100 places with an area of 1700 km². The reclamation areas are mainly along the coastline at higher tidal flat above the mean sea level (Figure 11), which provides a huge amount of farming, harboring and industrial lands.

To exploit more land resources at the sand ridge area, there are plans to reclaim the area along the coastline and the top area of the offshore ridges in the coming 10 years. The area of 2 meters above LLWL, covering 1700 km², is going to be reclaimed. The area of 0 m above LLWL is planned to be exploited within 40 years (Figure 12). The numerical model results show that reclamation at the area of 2 m and 0 m above the LLWL would have limited effects on the converging tidal wave system. The systematic assessment on the effect of large scale land reclamation on ocean dynamics, the sand ridge and tidal channel system, the ecological system in the coastal wetlands, the nature reserve zones and fishery resources, are under way. Even though the tidal volume is essential to maintaining the tidal channel, the tidal flow patterns are quite different on the tidal flat and in the tidal channels. During the flooding and ebbing, only during the period when the water level lower than the middle water level, i.e. the beginning of the flooding, tidal currents are overland flow and at the end of the ebbing, the currents are mainly returning flow to the small channels on the ridges. Only that amount of tidal volume is effective to form and to maintain the tidal channels. Tidal volume at other periods, i.e. when water level higher than the middle water level, has little contribution to maintaining the tidal channel. Quite a part of the tidal volume in the tidal flat area is not effective to maintain the tidal channels. To understand this phenomenon, a scaled physical based tidal current and sediment transport model for the Xiaomiaohong Channel, located at the south wing of the sand ridge area, was setup (Figure 13). The partial reclamation of the south tidal flat scenario and the complete reclamation scenario were studied in detail.

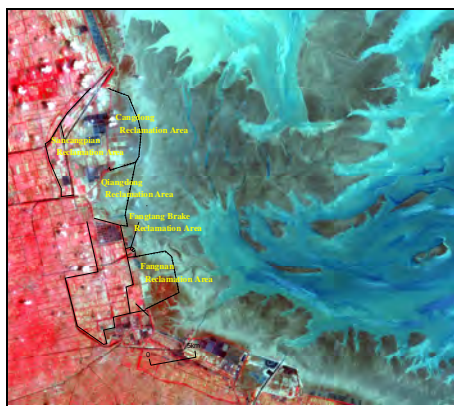


Figure 11: Land reclamation carried out at the land side of sand ridges area.

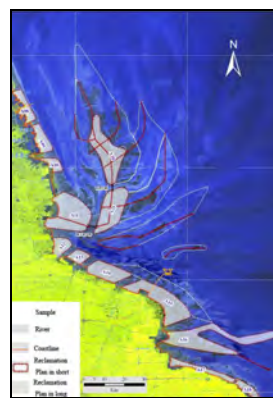


Figure 12: Reclamation plan in short, long term at the sand ridges area.

One of the experimental scenarios is to reclaim the tidal flat between the mean low water level and the middle water level, 3 km towards seaside at the inlet area of Xiaomiaohong Channel, with reclamation area around 3 km². Experiments show that the changes of hydrodynamic field caused by reclamation are limited in the shallow area within the -10 meter contour. No significant effects are found in the hydrodynamic structures. The morphological changes include local sedimentation at the fringe of reclamation area, and erosion in the front of the reclamation bank (Figure 14). The morphology got stable within 2 years after reclamation and there were hardly any effects on the natural change of tidal channel. The reclamation project was carried out in 2005. Field measurements at 2007, 2009 and 2010 presented the same trend. The local erosion and sedimentation patterns in the reclamation area were well reproduced by the scaled model experiments.

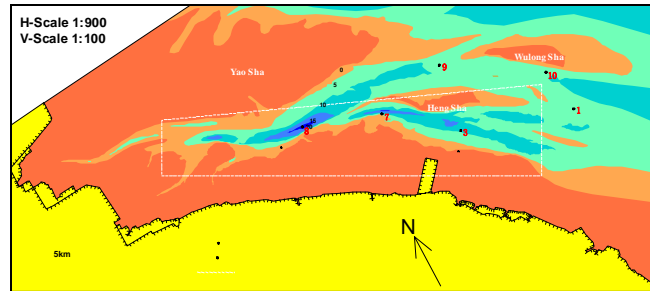


Figure 13: Physical based scaled model domain for tidal current and sediment transport in Xiaomiaohong channel, located at the south wing of the sand ridges.

Furthermore, scaled modeling experiments for reclamation over the overall southern tidal flat of Xiaomiaohong Channel were carried out in 2008. Even though the reclamation area is as much as 70 km², covering 11.8% of the horizontal tidal area, the reclaimed area are all above the MLWL and also 30% area are above the mean water level. Thus this reclamation scenario only reduced 3.1% of the effective tidal volume of the Xiaomiaohong Channel. This reclamation only effects on the hydrodynamics with -5 meter contour, thus there were very limited effects on the driven force to maintain the tidal channel. Morphology changes include the front of the tidal flat get sedimentation. The area is also limited within -5 meter contour (Figure 15), which would have very limited effects on the evolution of Xiaomiaohong Channel.

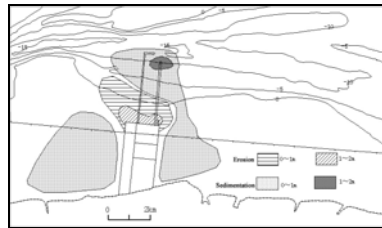


Figure 14: Local erosion and sedimentation pattern after partly reclamation along the south of Xiaomiaohong channel.

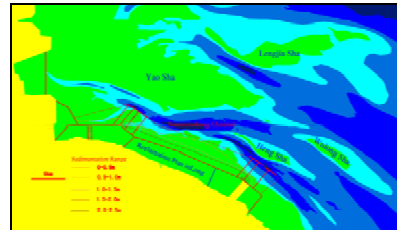


Figure 15: Local erosion and sedimentation pattern after full reclamation along the south of Xiaomiaohong channel.

5.2. Potential for harbor development

The tidal channels are natural navigation channels connecting the outer sea with the inner shore. Most of the channels are deeper than 10m. There is a great potential to develop a harbor by utilizing the natural deep tidal channels. As the natural conditions are fairly complicated, the sand ridges area was not suitable for harbor development. From the hydrodynamic point of view, the sand ridges area is the converge area for two tidal wave systems, with big tidal range and strong tidal current. The hydrodynamics in this area is quite complex. If the spatial pattern is taken into consideration, the tidal channels in this area are interconnected with each other. There are frequent exchanges of water and sediment within the tidal channels. Thus there is no fixed boundary for tidal channel system. Furthermore, the morphodynamics of the tidal channels are quite active. Sedimentation and erosion are dynamic. The bed materials here are mainly fine sand and silt, which are easy to be initiated. Thus, to develop harbors in this area, it is essential to understand the stability of the deep tidal channels and their evolution trends. In addition, it is crucial to understand the effect of harbor construction on the evolution of the tidal channels. In a short term, the local sedimentation and erosion on the tidal flat and channels resulting from storm surges are significant to harbor operation as well.

In the recent 20 years, systematic studies on harbors have been carried out, such as, 1) the Lvshi Harbor, which utilized the Xiaomiaohong Channel in the south, 2) Yangkou Harbor, which used the Lanshayang Channel in the middle of sand ridge area, 3) Dafeng Harbor, which used the Xiyang Channel in the north. Mainly from morphodynamic point of view, these studies are to reveal the local change of the deep tide channel while the overall sand ridges remain relatively stable. Approaches including numerical simulation and scaled physical model are applied

to studying the effect of harbor construction on the evolution of tidal channels. Also scaled model for sediment transport under wave and current interaction are used to study the local sedimentation in the channel and erosion at the tidal flat, morphodynamic effects on the harbor operation and measurements. Those studies provide good references for the planning and designing of the harbor construction in this area.

The key point to the exploit of the harbor development is how to design harbors so as to adapt to the natural trend of the tidal channel development and morphological change. The design procedure of Yangkou Harbor and the artificial island of West Taiyang Sha set a good example in this area.

Lanshayang Channel, located in the middle south of the sand ridge area, is used as the navigation channel for Yangkou harbor. West Taiyang Sha Island is exactly located at the converging point of three sub-tidal channels at the tail part of Lanshayang Channel. Scaled model experiments show that the proposed reclamation area at West Taiyang Sha is located in the shallow area with relatively weak current (Figure 16). The 2.5 km² reclamation will have very little effects on the tidal volume and diversion ratios, nor much effect on the hydrodynamic pattern, and will not introduce significant decreased or increased tidal currents in the adjacent tidal channels. The area with changes of current regime is limited within 500 meters in front of the structure of the artificial island. The area with hydrodynamic change is limited within 1.5 times the scale of the artificial island itself. Morphological changes including the erosion on the northeastern side and sedimentation on the southwestern side (Figure 17) are also limited locally around the artificial island, which have little influence on the large scale “tidal channel-sand ridges” morphological pattern. Scaled modeling experiments for sediment transport under wave and current interaction show that there are possibilities that 1-meter sedimentation in the north part of the harbor could take various combination of storm wave conditions. But it is not likely to have 2-meter sedimentation at the harbor basin during single storm condition (Figure 18).

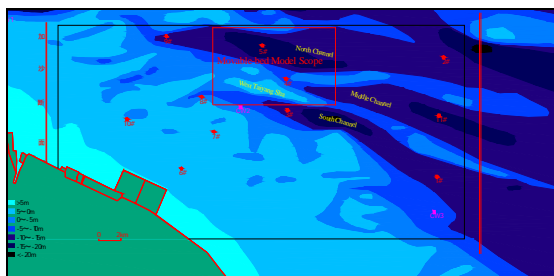


Figure 16: Physical based scaled model domain for tidal current, wave and sediment transport in Yangkou Harbor, located at the middle of the sand ridges.

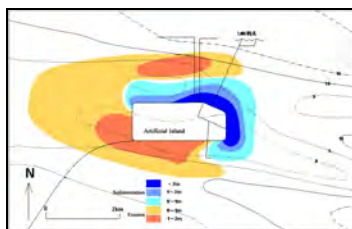


Figure 17: Local erosion and sedimentation pattern caused by construction of the artificial island in Yangkou Harbor.

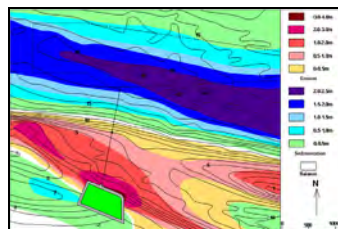


Figure 18: Erosion on the tidal flat and sedimentation at deep channels around the artificial island of Yangkou Harbor (after 2 days work of NE direction storm wave with return period of 50 years)

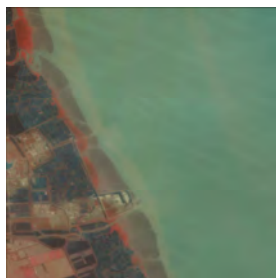


Figure 19: Dafeng Harbor, the berth for vessels of up to 50000 tonnes (satellite image).



Figure 20: Lvsi Harbor, the berth for vessels of up to 35000 tonnes (satellite image).



Figure 21: Yangkou Harbor, the artificial island (satellite image).

The above studies investigated the procedure and guideline for harbor designing in this area. Examples like Dafeng Harbor and Lvsi Harbor combined reclamation and jetty piers type; Yangkou Harbor used offshore artificial islands. So far, constructions of Dafeng Harbor (with a berth accommodating vessels of up to 50000 tonnes), Lvsi Harbor (with a berth accommodating vessels of up to 35000 tonnes), and the artificial islands for Yangkou Harbor have been finished (Figure 20~22). Field measurements after those constructions proved that the studies mentioned above captured the main trend. The finished constructions provided good engineering experience for further exploit of the tidal flat for harbor designing and constructions in this area.

Development of large scale harbors is somewhat limited by the wide tidal flat, and the deep channels are not approaching the coastal line directly. To avoid this limitation, there are ideas for dig-in dock basin (Figure 23~24). Systematic studies are carrying on. Furthermore, effects on the hydrodynamics, sediment transport, morphological change and corresponding engineering constructions by enormous human interferences in the sand ridges area are drawing more attention from researchers in coastal morphology, ocean dynamics, and coastal engineering disciplines.

6. Conclusions

Radial tidal current is the main force to form the radial sand ridge and it is the significant hydrodynamic characteristics of the sand ridge area. As a relatively independent morphological unit, the morphology of the radial sand ridge is stable. However, local adjustment between tidal flat area and tidal channels is active due to the complex hydrodynamics within the sand ridge area. There is significant potential for land, resources and harbor constructions in the sand ridge area. However, the exploit of land, resource and harbor development should adapt to the natural evolution of the hydrodynamics and morphodynamic change.

Acknowledgments

This study was supported by the Scientific Research Foundation of Public Sectors (Marine) under contract No. 200805082 and the Natural Science Foundation of China under contract No. 41006048.

References

1. Ren, M.E., 1986. Tidal mud flat. In: Ren, M.E. (Ed.), *Modern sedimentation in the coastal and nearshore zones of China*. China Ocean Press, Beijing, pp. 78–127.
2. Zhang, Renshun, Chen, Caijun (ed.) 1992. *The evolution of the sand ridges along Jiangsu coast and the possibility of Tiaozi Sand merging to mainland*. Ocean Science Press, China.
3. Liu, Zhenxia, and Xia Dongxin., 1995. Hydrodynamics in tidal current ridges area. *Yellow Sea and Bohai Sea*, 14(3). (in Chinese)
4. Zhu Yuliang., Y. X. Yan, and H. C. Xue 1998. Hydromechanics for the formation and development of radial sandbanks (I)-Plane characteristics of tidal flow, *Science in China*, 28(5), pp. 403-410 (in Chinese).
5. Song Zhi Yao, et al 1998. Hydromechanics for the formation and development of radial sandbanks (II)-Vertical characteristics of tidal flow, *Science in China*, 28(5) (in Chinese).
6. Zhang, dongshen, Zhang Junlun, and Zhang Changkuan, 1998. Tide forms it - storm destroy it -tide recover it, a preliminary study on the mechanism of generation and evolution of the radial shape sand ridges in Yellow Sea, *Science in China (series D)* 28(5), 394-402.
7. Lin, Hui et al, 2000, *Tidal system in Southeast China Sea and ocean dynamic simulations*, Science press, Beijing.
8. Lu, Peidong, 2006. *Guideline on the harbor design at the sand ridge area, Jiangsu*. Nanjing Hydraulic Research Institute, Technical Report.
9. Lu, Peidong, 2006. *Effects of the tidal flat reclamation on tidal current and sediment transport using scaled model for Lvsi Harbor, Jiangsu*. Nanjing Hydraulic Research Institute, Technical Report.
10. Lu, Peidong, 2006. *Analysis on the harbor design for the Petro-chemical industrial base at Lengjia Sha, Haimen, Jiangsu*. Nanjing Hydraulic Research Institute, Technical Report.
11. Lu, Peidong, 2006. *Effects of the artificial island on tidal current and sediment transport using scaled model for West Taiyang Sha, in Rudong, Jiangsu*. Nanjing Hydraulic Research Institute, Technical Report.
12. Lu, Peidong, 2006. *Sedimentation and erosion pattern at north of the artificial island using scaled model with mobile bed for West Taiyang Sha, in Rudong, Jiangsu*. Nanjing Hydraulic Research Institute, Technical Report.
13. *Guideline and planning on the reclamation and development along Jiangsu coast line (from 2010 to 2020)*, March 2010.
14. Lu, Peidong, 2006. *Stability analysis on the sand ridges for harbor construction in South Yellow Sea, China*. Nanjing Hydraulic Research Institute, Technical Report.
15. Lu, Peidong, 2005. *Study on tidal current and sediment transport for dig-in harbor basin in Lvsi, Rudong using numerical model and scaled model*. Nanjing Hydraulic Research Institute, Report, No. R05115.

About the speaker



Dr. Peidong Lu received in 2002 his Ph.D. degree in Coastal Engineering Environmental Studies from Nanjing Normal University, China. He is currently a senior engineer in the River and Harbor Engineering Department of Nanjing Hydraulic Research Institute, where he is also the Deputy Director of the Coastal Engineering Research Center. He is a member of the Advisory Committee of the Chinese Geographic Society, the Chinese Quaternary Research Society, and the Chinese Ocean Engineering Society. He has been in charge of more than 70 projects, accomplishing many achievements in the site development of new ports, coastal geomorphology, coastal sediment dynamics, and the physical model testing of waterways. He is currently looking into the geomorphology of radial sand ridges to find out conditions for the construction of harbors in the Yellow River Delta.

PERFORMANCE-BASED DESIGN OF CAISSON BREAKWATER INCORPORATING WAVE HEIGHT INCREASE DUE TO CLIMATE CHANGE

KYUNG-DUCK SUH

Department of Civil and Environmental Engineering, Seoul National University, 599 Gwanak-ro, Gwanak-gu, Seoul, 151-744, Republic of Korea

This paper describes several methods to incorporate wave height increase due to climate change in the performance-based design of a caisson breakwater and their application to the East Breakwater of the Port of Hitachinaka in Japan. When wave height increase was not included, the performance-based design methods calculated the same caisson width as that of the constructed breakwater, partly validating the consistency with the conventional deterministic methods. Wave height increase dictates an increase in caisson width of about 1.5 m and 0.5 m for linear and parabolic increases, respectively, which are about 6.8% and 2.3% of the present caisson width of 22 m. Finally, it is recommended that the caisson breakwater be designed using the projected wave height 30 years from construction, if the deterministic method is used and climate change impacts are to be taken into account.

1. Introduction

Recently reliability-based or performance-based design methods have been adopted in the design of coastal structures. The basic idea of a performance-based design is to allow a certain amount of damage unless it is so great as to stop the function of the structure. In the course of performance-based design, we have to consider the uncertainties of the design variables. However, the up-to-date performance-based design methods have not taken into account the uncertainties of the design variables associated with climate change. In this paper, several methods are presented that can incorporate the climate change impacts into the performance-based design of a caisson breakwater. The methods are applied to the East Breakwater of the Port of Hitachinaka in Japan. Only the sliding failure of a caisson is considered, which is the primary cause of damage of a caisson breakwater [1, 2]. Only wave height increase due to climate change is considered because the sea level rise is negligibly small compared with the water depth at the breakwater site.

2. Design Variables

In general, caisson sliding is caused by large waves on par with the design waves. The annual maximum wave height is considered sufficient for the design calculation. In this study, the Weibull distribution is used, whose cumulative distribution function is given by

$$F^*(x) = [F(x)]^\lambda = \left\{ 1 - \exp \left[- \left(\frac{x-B}{A} \right)^k \right] \right\}^\lambda \quad (1)$$

where x = annual maximum offshore significant wave height, A , B , and k = scale, location, and shape parameters, respectively, and λ = mean rate of the extreme wave heights. The wave height of return period of R is estimated by $x_R = B + A\{\ln[\lambda R]\}^{1/k}$.

Mori *et al.* [3] compared the present wave climate with the future extreme wave climate around Japan. The Weibull parameters offshore in the Pacific Ocean at the end of the 20th century are given by $A = 2.01$, $B = 7.34$, $k = 1.0$, $\lambda = 0.35$, and $x_{50} = 13.09$ m, while those at the end of the 21st century are given by $A = 2.71$, $B = 7.31$, $k = 1.0$, $\lambda = 0.46$, and $x_{50} = 15.81$ m.

On the other hand, the deepwater design wave height with a 50-year return period for the Port of Hitachinaka is given as $(H_s)_0 = 8.3$ m with a significant wave period of $T_s = 14.0$ s and the principal wave direction of 90° clockwise from north [4]. To calculate the deepwater wave height near the design site from the deep-ocean wave height, we use the method of Kim and Suh [5], which assumes the coefficient of variation of the 50-year wave height remains the same between the two locations. The Weibull parameters near the Port of Hitachinaka at the end of 20th century are then calculated as $A = 1.27$, $B = 4.65$, $k = 1.0$, $\lambda = 0.35$, and $x_{50} = 8.30$ m, while those at the end of the 21st century are calculated as $A = 1.72$, $B = 4.63$, $k = 1.0$, $\lambda = 0.46$, and $x_{50} = 10.02$ m.

The preceding estimation gives the wave information at the ends of the 20th and 21st centuries, but we do not know how the waves will change during this period. The location parameter, B , hardly changes during the period, while the scale parameter and the mean rate change significantly. If we assume a linear increase of them, i.e., $A(t) = 1.27 + 0.0045t$ and $\lambda(t) = 0.35 + 0.0011t$, where t = time in years, the 50-year return wave heights at $t = 0$, 50, and 100 years are 8.28 m, 9.15 m, and 10.04 m, respectively. If we assume a parabolic increase, i.e., $A(t) = 1.27 + 4.5 \times 10^{-5}t^2$ and $\lambda(t) = 0.35 + 1.1 \times 10^{-5}t^2$, they are 8.28 m, 8.71 m, and 10.04 m, respectively.

The wave period was calculated by the modified Goda [6] formula: $T_s = 3.69(H_s)_0^{0.63}$, which gives $T_s = 14.0$ s for $(H_s)_0 = 8.3$ m. An analysis of waves greater than 2 m in height gives the mean and standard deviation of wave direction as 0.0° and 26.5° , respectively, counterclockwise from the shore-normal direction (i.e., east).

Since the bottom topography near the Port of Hitachinaka is very simple, the approach of Goda [7] was applied to calculate the wave transformation from deepwater to the breakwater site. The Bretschneider-Mitsuyasu frequency spectrum and the Mitsuyasu-type directional spreading function were applied, with $s_p = 20$, which is the peak directional spreading parameter corresponding to the deepwater wave steepness of 0.027 at the Port of Hitachinaka.

With a tidal range of $\Delta\eta = 1.5$ m, the tide level η_t was simply assumed to vary sinusoidally between LWL ($\eta_t = 0$) to HWL ($\eta_t = \Delta\eta$). For simplicity, the effect of storm surge was taken into account by adding 10% of the deepwater significant wave height to the tide level. Since the increase of wave height due to climate change is taken into account, the influence of climate change on storm surge is also taken into account indirectly.

The water depth at the breakwater site is 24.2 m (below LWL), and the breakwater is located about 2.6 km from the shoreline. The breakwater is 6 km long, is oriented in north-south direction, and is parallel to the shoreline. The predominant wave direction is normal to the breakwater. The cross-section of the breakwater is given in Fig. 1, which is a typical sloping-top caisson breakwater. The bottom slope is 1:100, the caisson weight per unit length in air is 11,348 kN/m, and the buoyancy is 4,430 kN/m. The width of the caisson is 22.0 m. The mean and standard deviation of a design variable is represented by $\mu_x = (1 + \alpha_x)X$ and $\sigma_x = \gamma_x X$ where X , α_x and γ_x = characteristic value, bias, and coefficient of variation, respectively, of the design variable. The statistical characteristics of the design variables are given in Table 1.

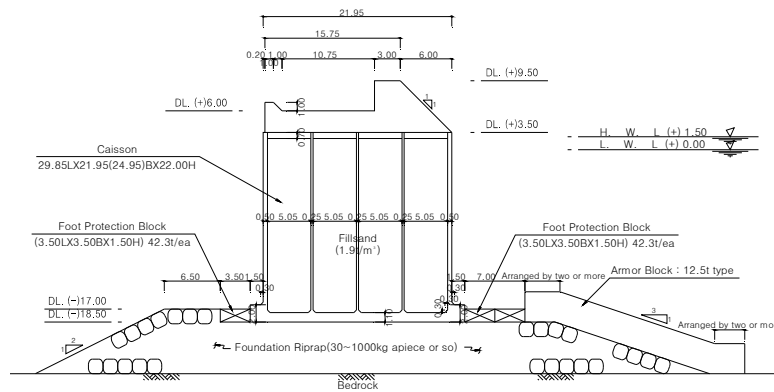


Figure 1. Cross-section IV of East Breakwater of the Port of Hitachinaka.

Table 1. Statistical characteristics of design variables.

Description	X	α_x	γ_x	Description	X	α_x	γ_x
Offshore wave height	various	0.0	0.1	Horizontal wave force	various	-0.09	0.19
Significant wave period	various	0.0	0.12	Vertical wave force	various	-0.23	0.20
Wave transformation	various	0.0	0.1	Friction coefficient	0.6	0.06	0.16

3. Time-Dependent Performance-Based Design

Three design criteria are used in the performance-based design of a caisson breakwater [8,9]: (1) expected sliding distance during the lifetime of the breakwater (ESD-L); (2) exceedance probability of total sliding distance during the lifetime (ExP); and (3) expected sliding distance by a storm event of a certain return period (ESD-S). The criteria depend on the importance of a breakwater, limit state, return period, and so on. Assuming that the breakwater is important and the return period is 50 years, ESD-L is 30 cm, ExP of 30 cm is 10%, and ESD-S by a 50-year storm event is 10 cm (restorability limit state).

In performance-based design, the caisson is designed so that the ESD or ExP is below a tolerable limit. The sliding distance is calculated with the model of Shimosako and Takahashi [10]. The computational procedure to calculate the ESD-L or ExP can be found in many papers [e.g. 10], and are not repeated here. The procedure to calculate the ESD-S is the same as that for ESD-L except that the offshore wave height is randomly sampled from a normal distribution instead of an extreme wave height distribution. The mean of the normal distribution is the wave height of the given return period (50 year in this study), and the coefficient of variation of 0.1 was used. Given an allowable sliding

distance, the ESD or ExP are estimated with Monte Carlo simulations to account for uncertainties in various design variables.

The previous performance-based design methods assume the wave climate is time-invariant. However, the method presented here expresses the wave climate as a function of time to account for climate change impacts. This method calculates time-dependent ESD and ExP over the service life of the breakwater $[0, T_L]$. Time-dependent ESD is the same as in the previous method, except it is calculated throughout the lifetime of the breakwater instead of at the end. Time-dependent ExP is expressed as $P_f(t) = \Pr[S(t) \geq S_i]$, where $\Pr[\bullet]$ denotes the probability of an event, $S(t)$ = accumulated sliding distance until year t , and S_i = acceptable total sliding distance, say, 30 cm. This is also different from the previous method which calculates $P_f(T_L)$.

In this study, the number of waves during a storm was assumed to be 1,000, which corresponds to about 3.2 hours for a design wave with $T_s = 14.0$ s. The maximum accumulated sliding distance during the lifetime of the breakwater was set to $S_{max} = b + W/2$, where b = rear berm width of the riprap foundation and W = caisson width. If the accumulated sliding distance exceeds S_{max} , then S_{max} was used as the accumulated sliding distance. S_{max} is the threshold sliding distance beyond which the caisson is judged as fallen from the mound. The number of Monte Carlo simulations was 50,000, which consists of 10,000 simulations with five different initial random seeds.

4. Results and Discussion

The construction of the East Breakwater of the Port of Hitachinaka began in 1989 with plans to build a 6,000 m breakwater; it is still under construction with 5,280 m completed as of April 2010. In this study, the breakwater was assumed to be completed in 2000, and the computations were made for $t = 0$ to 50 years, from 2000 to 2050.

Fig. 2 compares the temporal variations of ESD and ExP; the acceptable ESD and ExP are also illustrated. The ESD-S for no wave height increase is constant as 0.04 m and is not shown in the figure. A linear increase in wave height yields larger ESD and ExP values than a parabolic increase. Note that the linear increase produces larger wave heights than the parabolic increase because the wave heights in the two cases are the same in both 2000 and 2100. With ESD-L, the critical years when the acceptable sliding distance is exceeded are 46 years (no increase), 40 years (parabolic increase), and 32 years (linear increase). With ExP, the critical years increase by 4 years to 50, 44, and 36 years, respectively. With ESD-S, the critical years are longer than 50 years for the parabolic increase and 36 years for the linear increase. Therefore, the criterion for ESD-L is the most conservative. The criterion for ExP is more conservative than that for ESD-S for the parabolic increase, but they are the same for the linear increase.

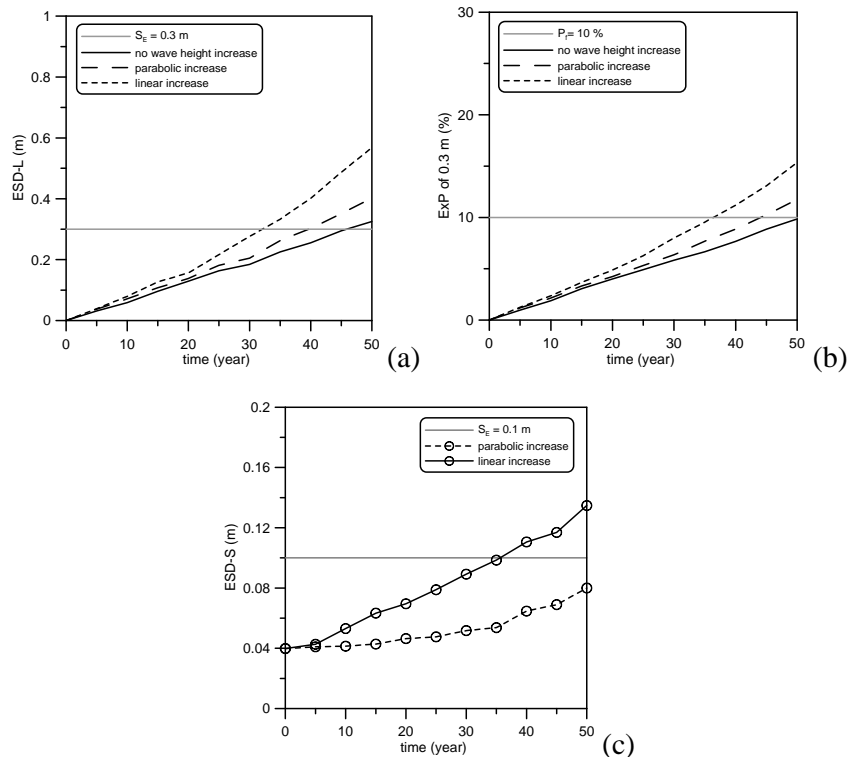


Figure 2. Temporal variation of (a) ESD-L, (b) ExP of 0.3 m, and (c) ESD-S.

The results presented previously concerned changing ESD or ExP relative to time. However, port engineers and managers may be more interested in how climate change impacts increase the required width of a caisson. Fig. 3 shows the variations of ESD-L and ExP relative to caisson width. A structure lifetime of 50 years was used. Both criteria dictate a required caisson width of 22 m when no climate change impact is taken into account. Surprisingly, this caisson width is the same as that of the constructed breakwater, which was designed using the conventional deterministic method. This partly validates that the performance-based design method is consistent with the conventional deterministic method. If the climate change impacts are taken into account, the required caisson widths are 22.7 m (parabolic increase) and 23.7 m (linear increase) with ESD-L, while they are 22.3 m and 23.3 m with ExP. On the other hand, Fig. 4 shows the temporal variation of the required caisson widths satisfying the ESD-S criterion, which are 21.3 m (parabolic increase) and 22.6 m (linear increase) at 50 years. Based on the criteria for ESD-L and ExP, the caisson width needs to increase by about 0.5 m for parabolic increase in wave height, and 1.5 m for linear increase.

On the other hand, Okayasu and Sakai [11] presented a method taking into account long-term sea level rise but still using the deterministic method. In this study, their method for wave height increase due to climate change is applied. The method calculates the optimal caisson width of the earliest year (i.e., the smallest wave height) satisfying the ESD-L or ExP criterion. The year with the optimal caisson width is defined as the optimal design year. If the optimal design year is known *a priori*, the caisson can be designed for the wave height of the optimal design year using the deterministic method. Fig. 5 shows the plots of caisson width versus design-base-year calculated using the ESD-L criterion and ESD-L versus design-base-year. Similar plots can be drawn for the ExP criterion but are not shown here due to the page limitation. For a linear increase of wave height, the optimal design years for the ESD-L and ExP criteria occur at years 28 and 29, respectively. For a parabolic increase, they occur at 37 and 38 years, respectively. Okayasu and Sakai [16] have shown that the optimal design years fall between 23 and 29 years for a linear increase of sea level rise, which is similar to the present result for a linear increase in wave height.

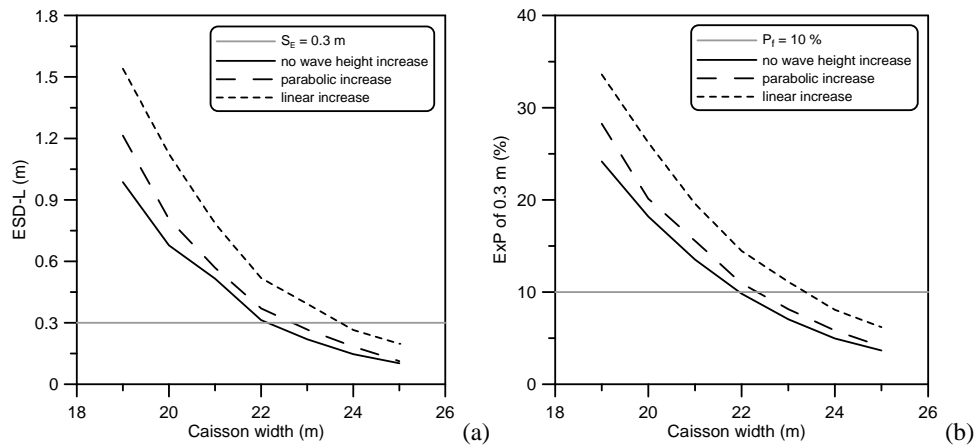


Figure 3. Variation of (a) ESD-L and (b) ExP of 0.3 m relative to caisson width.

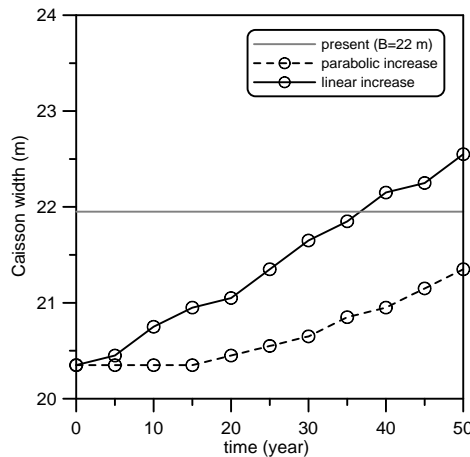


Figure 4. Temporal variation of required caisson widths satisfying ESD-S criterion.

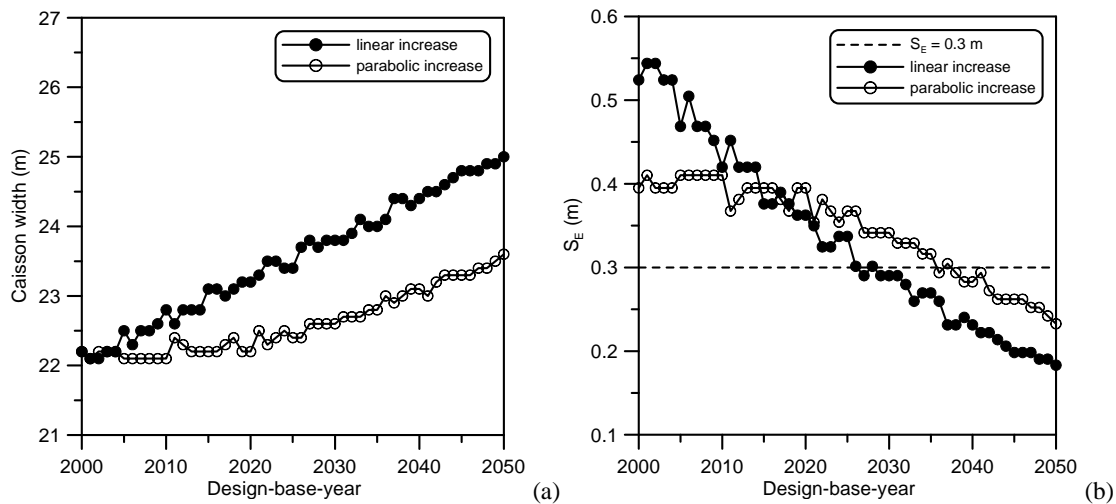


Figure 5. (a) Caisson width versus design-base-year calculated using ESD-L criterion and (b) ESD-L versus design-base-year.

5. Conclusion

In this study, we described how to incorporate the influence of wave height increase due to climate change into the performance-based design of a caisson breakwater. The method was applied to the East Breakwater of the Port of Hitachinaka in Japan. The ESD-L criterion was found to be most conservative, and those for ExP and ESD-S followed it. When wave height increase was not taken into account, the performance-based design method calculated the same caisson width as that of the constructed breakwater, partly validating the consistency between the conventional deterministic method and the performance-based design method. Wave height increase dictated an increase in caisson width of about 1.5 m and 0.5 m for linear and parabolic increases of wave height, respectively. Finally, to account for climate change impacts, the deterministic design method should be utilized to design the caisson breakwater, using the wave height and water level projected 30 years after the construction.

Acknowledgments

This work was supported by the National Research Foundation of Korea Grant funded by the Korean Government (NRF-2010-013-D00074) and the Kyoto University Global COE Program.

References

1. Y. Goda and H. Takagi, *Coastal Eng. J.* **42**, 357 (2000).
2. S. Takahashi, K. Shimosako, K. Kimura and K. Suzuki, Proc. 27th Int. Conf. Coastal Engineering, 1899 (2000).
3. N. Mori, Y. Shimura, T. Yasuda and H. Mase, *Ann. J. Coast. Eng.* **57**, 1231 (in Japanese) (2010).
4. E. Takata, K. Morohoshi, T. Hiraishi, T. Nagai and S. Takemura, *Tech. Note Nat. Ins. Land Infrastructure Management*, No. **88** (in Japanese) (2003).
5. S.-W. Kim and K.-D. Suh, *Coastal Eng. J.* **52**, 331 (2010).
6. Y. Goda, *J. Waterw., Port, Coast. Oc. Eng.* **129**, 93 (2003).
7. Y. Goda, *Random Seas and Design of Maritime Structures*, 2nd ed., World Scientific (2000).
8. Technical standards and commentaries for port and harbor facilities in Japan, Overseas Coastal Area Development Institute of Japan (2009).
9. S. Takahashi, K. Shimosako and M. Hanzawa, *Proc. Advanced Design of Maritime Structures in 21st Century*, 63 (2001).
10. K. Shimosako and S. Takahashi, *Proc. Int. Conf. Coastal Structures '99*, 363 (2000).
11. A. Okayasu and K. Sakai, *Proc. 30th Int. Conf. Coast. Eng.*, 4883 (2006).

About the speaker



Professor Kyung-Duck Suh received his Ph.D. Degree in Civil Engineering in 1989 from University of Delaware, USA. He is currently the professor in charge of the Coastal Engineering Laboratory in the Department of Civil and Environmental Engineering of Seoul National University, Republic of Korea. In 2008-2010, he was the Chair of his Department, and was also the Director of BK21 Social Infrastructure Research Group for Safe and Sustainable Development, Seoul National University. Prof. Suh and his group study various water wave problems and the interactions between waves and coastal structures. They are in particular interested in the study on wave deformation, perforated-wall structures, and reliability-based design of coastal structures. He is the recipient of many awards, the recent one being the Scientific Research Award from the Korean Society of Coastal and Ocean Engineers in 2010.

THE CHALLENGES TO BE ADDRESSED IF TIDAL ENERGY IS TO BECOME ECONOMICALLY VIABLE

CAMERON M. JOHNSTONE

Nautricity Ltd, 5 St. Vincent Place, Glasgow, G1 5GH, UK

The initial tidal energy technologies deployed to date have had limited success in demonstrating the cost effectiveness of generating power from tidal flows. The benchmark to achieving commercial acceptance is linked to the cost of energy associated with off-shore wind power. Due to the increased costs of the engineering systems adopted within these 'first mover' tidal technologies, this makes it difficult for these systems to demonstrate cost competitiveness in an energy market dominated by lower cost fossil fuels. In order for tidal systems to become cost competitive, greater efforts need to be made to reduce system capital and maintenance costs.

1. Drivers influencing future a future energy supply make up

With current concerns on the environmental impact of the increasing use of fossil fuels to satisfy our ever increasing energy demands, Governments are introducing policies which require greater capacities of renewable energy systems to be used within future energy supply make-up. The most popular renewable technologies being utilised at sufficiently large scale installations at present include: hydro power and wind power. However, in many applications there are major limitations associated with these systems. In the case of Hydro power: low head run of river systems result in seasonal variations in power output, which can be directly correlated to the seasonal rain fall of a specific geographical region; while high head systems require the construction of a dam causing flooding of large land areas resulting in considerable environmental and ecological damage. In the case of wind energy systems, the limitations are related to the variability of power output associated with the unpredictability of the wind. In order to maintain integrity of the power supply system there needs to be either stand by generating capacity to meet demand when there is low or no power output or demand management to flex large parts of the demand to match the output from the wind energy systems. In all cases, the stochastic power supplied from these systems increase the cost of generated electricity.

In order to be part of a future power generation portfolio make up, emerging generation technologies must at least perform above a certain threshold level in the context of cost of generated electricity; responsiveness of generating plant to demand; security of supply/ resource availability; environmental impact; and finally execution risk. Since the execution risk associated with any new technology entering the market is always going to be higher, they're required to have superior performance in the other areas of power supply performance to mitigate this risk. The tidal resource within our coastal waters has the potential to provide a consistency of energy supply which goes a long way to achieving this mitigation. In many places, bathymetric variation, complex shapes of coastal land forms and proximity to amphidromic centres serve to focus and phase these flows into a highly energetic resource which can be harvested to generate predictable and firm renewable power delivery. These tidal flows, and the resultant electrical power, are highly predictable and dependable offering significant advantages over both wind and wave generated power. The most energetic tidal sites are often avoided by both leisure and commercial marine users, reducing the impact tidal harvesting is likely to have on other activities. Within the UK the exploitable tidal energy resource has been estimated as being sufficient to generate 94TWh per year of electricity in water depths of 40 meters or less [1] - equivalent to about one quarter of the UK's annual electricity consumption. The global resource from tidal and other marine currents may exceed 1100TWh/y [2].

Tidal energy clearly scores highly compared to other renewable generating types in the existing UK generation portfolio in terms of availability of resource, security of supply, and arguably, environmental impact. Its predictability makes its energy attractive in a future renewable weighted electricity market when compared to wind and wave, which provide less certainty over the timing of their power generation. Although early stage demonstration devices have taken to the water with limited success, there is, as yet, no mature tidal generation device in production and generating electricity considered to be commercially viable. However, a number of projects are currently under development. A major challenge to be addressed is to deliver acceptable capital and operating costs and to establish a track record for reliable generation, driving down their cost of money. As tidal energy technology matures and for it to be considered cost competitive it needs to benchmark its self with the costs of equivalent technologies, the closest of which is offshore wind. In the development of a tidal energy industry, the technology needs to: demonstrate high reliability; and either match the costs associated with the development of offshore wind or better these.

2. The acceptable costs for power generation

In an effort to establish the costs for different power generation technologies you need to take into consideration the upfront capital cost for erecting and commissioning the plant and the operational costs over the engineering life for servicing and maintenance and fuelling costs for operation. These costs can be further elaborated when investigated as elements contributing to the generation of electrical power.

Elements of cost: When considering the cost of electricity, the total lifecycle cost of generation by any one plant should be considered, i.e. the total capital and operating costs of the plant divided by the total power it has generated.

There are several components to this cost: capital costs of the plant and equipment; cost of money on that capital over the term of the project; cost of maintenance and operations over the life of the project; and cost of fuel and other consumables.

The total life cycle cost of a system can be further viewed as either fixed costs, or variable costs. Looking at the preceding list in this way, we can assign the costs as follows:

Fixed costs:

1. The capital costs of the plant and equipment;
2. The cost of money on that capital over the term of the project;
3. The cost of maintenance and operations over the life of the project;

Variable costs:

4. The cost of fuel and other consumables.

The cost of money could be viewed as variable, however in most cases it is considered as a fixed commitment over the term of the project; and, calculated as the total interest payments that would accrue if the capital was borrowed at a typical interest rate of 10% and repaid so that the project was fully amortised by the end of its working life. Similarly, there are arguments that operations and maintenance could be a variable cost, either with time or with generation.

However, in practice generating plants run routine maintenance schemes until they are decommissioned and accordingly are viewed as a fixed cost commitment over the plant's lifetime, although the annual value of this cost can inflate with time.

3. Establishing cost associated with offshore wind

To date, progress in developing renewable energy generation capacity has focused on onshore and offshore wind farm development. This market has experienced significant growth in the last decade with installed global total capacity growing from 10,200MW in 1998 to 120,791MW in 2008. A considerable portion of recent growth has been in offshore wind which has grown from about 10,000MW installed capacity in 2003 to 58,000MW in 2008 with significant future growth forecast [3]. Since tidal energy is a renewable resource whose development shares many of the characteristics and challenges of offshore wind development, it seems reasonable to expect the tidal generation market to behave in a similar way to this mature market if:

- tidal devices can be build to a cost which compare favourably with the capital and operating costs of offshore wind generation; and
- develop a track record for operational reliability.

Both tidal and offshore wind installations should generate power for 30% to 40% of the time but, given the predictability and dependability of tidal generation, tidal energy should have a competitive advantage, all other things being equal. Published information on the development costs of offshore wind [3], as reported in Table 1, suggests that large installations are being developed at capital costs in the range of 1.2 million – 2.7 million Euros per megawatt (MW); and future forecasts seem to lie in the range of 2 – 2.2 million Euros per MW. An analysing of the capital cost breakdown for the Horns Rev and Nysted sites shows that about 20% of costs are associated with site planning and export to shore with the remaining 80% associated with the equipment and interconnection.

Table 1: Analysis of offshore wind developments and a digest of the related investment components. (Extract from the Economics of Wind Energy, EWEA).

	IN OPERATION	NUMBER OF TURBINES	TURBINE SIZE	CAPACITY MW	INVESTMENT COSTS € MILLION		INVESTMENTS 1000 €/MW	SHARE %
Middelgrunden (DK)	2001	20	2	40	47	Turbines ex works, including transport and erection	815	49
Horns Rev I (DK)	2002	80	2	160	272	Transformer station and main cable to coast	270	16
Samsoe (DK)	2003	10	2.3	23	30	Internal grid between turbines	65	5
North Hoyle (UK)	2003	30	2	60	121	Foundations	350	21
Nysted (DK)	2004	72	2.3	165	248	Design and project management	100	6
Scroby Sands (UK)	2004	30	2	60	121	Environmental analysis	50	3
Kentish Flats (UK)	2005	30	3	90	159	Miscellaneous	10	<1
Barrows (UK)	2006	30	3	90	-	TOTAL	1,680	-100
Burbo Bank (UK)	2007	24	3.6	90	181			
Lillgrunden (S)	2007	48	2.3	110	197			
Robin Rigg (UK)	2008	60	3	180	492			

This sets a useful capital costs target tidal devices should be aiming for. The cost of device and moorings should be competitive with the cost of an offshore wind turbine and its foundation. This sets a target capital cost of around 1.2 million Euros (or about £1million) per megawatt for the device and its mooring for devices built on a commercial scale. Obviously, technologies with the early stages of market development do not benefit from engineering cost optimization and economies of scale and therefore it is not unexpected that prototype and early batch devices will be more expensive. Moving from prototype to mass production, introduces scope to drive down the cost of many components and the assembly itself. Figure 1 illustrates operating expenditure (2006) for a number of offshore wind sites.

When compared with tidal energy production costs, the cost of money for developments should be competitive with wind once a track record has been established. Accordingly, investment related costs should be similar or less so long as capital costs per MW is similar or less as identified earlier. Balancing costs should arguable be less given the dependability of tidal energy flows, but in no case should be more. The focus should be on matching, or beating, operating and maintenance costs which for offshore wind are around €16/ MWh.

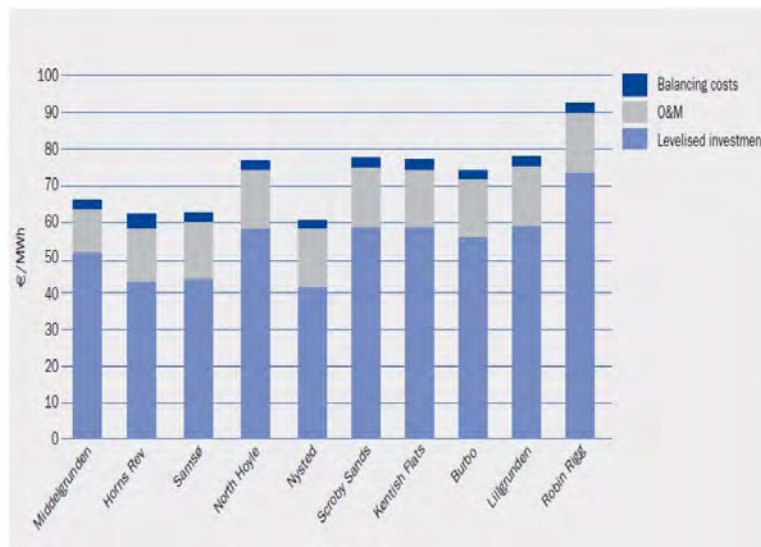


Figure 1. Offshore wind operating costs (⁴Extract from the Economics of Wind Energy, EWEA).

4. Establishing costs associated with tidal energy

A wide range of tidal devices have been proposed to include horizontal and vertical axis rotors, oscillating foils, other hydrodynamic shapes, and venture devices. Large scale impoundment of tidal height change has also been proposed. A few ‘first generation’ technologies have progressed to the large scale prototype stage, which look not dissimilar to ‘marinised’ wind turbines, as shown in Figure 2.



Figure 2: 1st Generation ‘marinised’ wind turbine technologies.

The Carbon Trust [4] has considered the costs of 1st generation tidal devices and published a summary of the capital cost breakdown for a typical device (Figure 3).

For devices under development, the Carbon Trust [5] concluded that the capital cost of tidal energy devices at prototype stage lay in a price band £5000 to £8000 per MW (Figure 4) and the likely cost of energy from devices under development lay in a range band 4 to 7 times higher than the current cost of combined cycle gas powered generation. Of the devices deployed to date, weight has been a major component which results in escalated device and installation costs. The majority of the 1st generation technologies which have been deployed, have weighed in at approximately 1000 tonnes/ MW. At such weights, installation of devices has to be undertaken by large, expensive marine vessels developed for the offshore oil and gas industry. These vessels can command charter rates in excess of £100K/ day. When you consider mobilization time, on-site operational time and standby time, the charter cost for installing such a unit can easily exceed £1million. If you then require a similar vessel to facilitate access for service and maintenance, this will considerably escalate the O&M costs associated with tidal device economics.

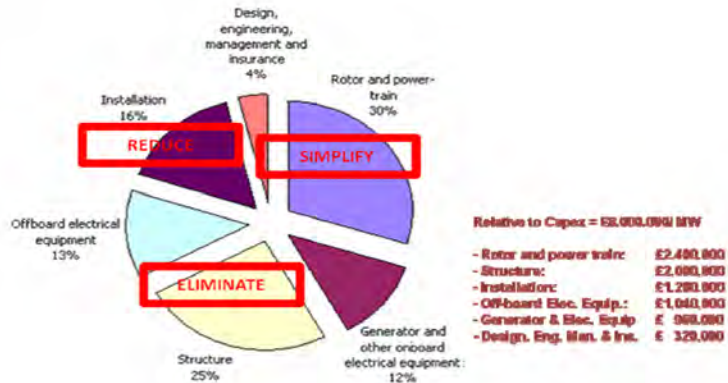


Figure 3: Breakdown of costs associated with 1st Generation tidal technologies.

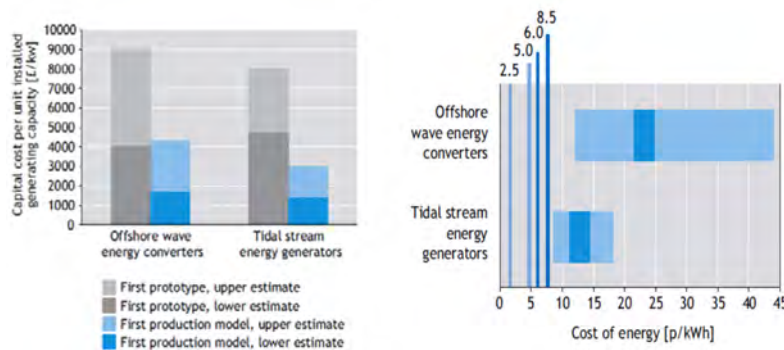


Figure 4: Device costs and related energy production costs today (⁶Extract from Carbon Trust Report on Wave and Tidal Energy).

For a technology to be considered commercially viable, it has to make a return on investment of 10%, therefore whether this can be achieved will be dictated by the capital cost of the plant together with the O&M costs; and the tariff received for the electricity generated [6]. In the UK today, when the wholesale price drops to £25/ MWh, plant capital costs need to be less than £500/ MW. Where an enhanced tariff is available, two Renewable Obligation Certificates (ROC's) are awarded per MWh, this equates to approx £120/ MWh and where three ROC's per MWh are awarded, this equates to £165/ MWh. In order for to facilitate the commercialisation of a tidal energy industry, the Scottish Government have introduced 3 ROC's for tidal energy. This has set a target figure of £3.5million/ MW for installed capacity, as shown in Figure 5.

In order to attain the targeted device cost for economic acceptance, new design concepts need to be considered which allow for significant cost savings in the previously identified areas to be realized. This is being achieved either by simplifying or eliminating major components within each of these categories. This is where the development of 2nd Generation tidal technologies has focused. One such system capitalising on this is the CoRMaT tidal generator system [7].

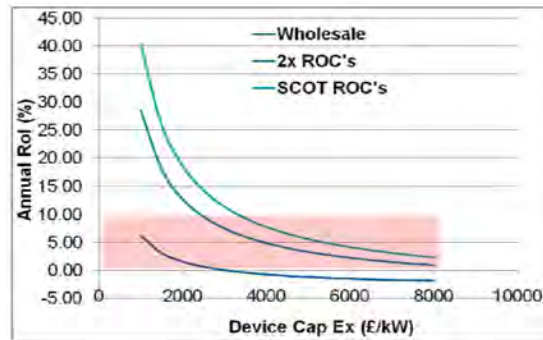


Figure 5. Target device cost to achieve commercial acceptance.

5. Next generation tidal technologies

Next generation (2nd Generation) tidal turbines have now evolved towards full scale commercial demonstration and show promise of substantively reducing the costs of tidal energy. The costs savings associated with 2nd Generation (2G) technologies are being achieved through: 1) eliminating the costly rigid supporting structure used for station keeping; and 2) reducing complexity and the number of components in the power capture and conversion drive train and power take off systems. Some 2G tidal technologies employ direct drive, permanent magnet generators (eliminating the need for a gearbox), passively yawing with the tidal current (eliminating the need for active yaw or pitch control) and use of a flexible mooring for station keeping (eliminating the need for a heavy, rigid mono-pile). The CoRMaT technology is an example of such a 2G system. This technology using two closely spaced, fixed pitch, contrarotating rotors. These capture energy from the tidal flow to directly drive a contra-rotating generator, as shown in Figure 6. The development and performance of this prototype system has been extensively reported [7, 8].

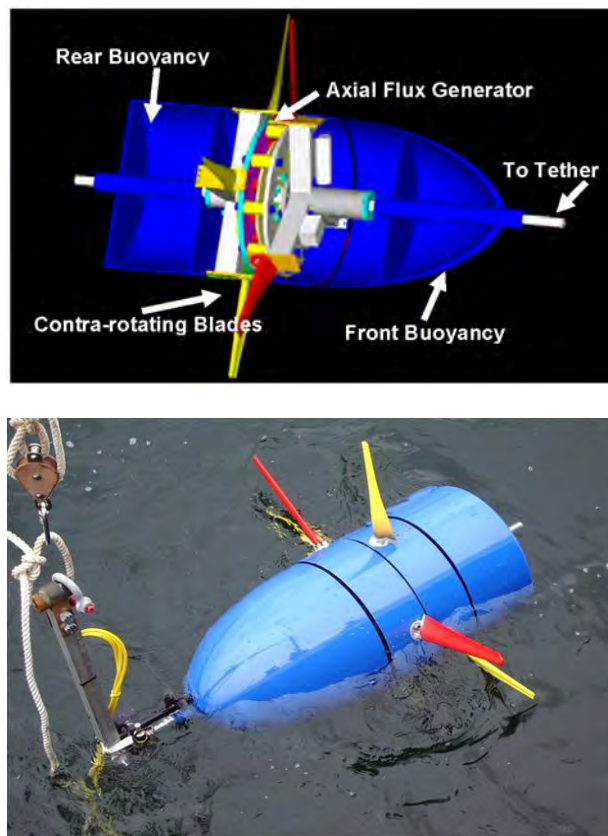


Figure 6: Visualisation of the CoRMaT tidal system.

First generation turbines produce wakes which persists for many rotor diameters downstream, however CoRMaT's contra-rotating rotors are designed to reduce the vorticity elements in the wake, having positive implications for the

packing density when deployed as a array of devices. These benefits arise from a smaller amount of seabed has to be rented to generate a given amount of electricity and the amount of inter-device cabling per MW can be as much as halved, with subsea cabling a significant expense.

Power transfer: The relatively slow prime mover rotational speed of a tidal turbine (a 250kW machine's rotors each rotate at around 23rpm) normally necessitates a gearbox to increase the speed suitably for a common multi-pole generator. The use of contra-rotation enables direct drive to contra-rotating generator with a large number of electrical poles. This results in:

1. complete elimination of a gearbox as the relative speed of the two contrarotating rotors effectively doubles the rotational speed in the generator;
2. higher overall drive-train/ take off efficiency of typically 90% near rated load, compared to around 80% for a costly multi-stage high torque gearbox (4- stage efficiency of 90%) and generator (90% efficiency);
3. elimination of mechanical linkage as the rotor blades are mounted directly onto the generator elements; and
4. increased reliability and a diminished maintenance requirement.

The benefits from next generation technologies lead to significant savings in capital expense and elimination of many sources of failure, offering potential reduction in operating expense. The design weight of the contra-rotating turbine is currently approximately 44 tonnes per Megawatt, driving cost savings in deployment, operations and maintenance through the need for smaller handling vessels. The device has followed a disciplined development through IEA-OES suggested development Technology Readiness Level stage gates and has successfully generated electricity at sea at 30th scale. Recent work building a supply chain and completing the engineering development of a range of device sizes for standalone community scale applications; distributed generation scale operations and large scale commercial tidal array deployment has yielded encouraging financial projections. It is now intended to build commercial 500kW devices to be deployed in an array to: prove operation of the device at a commercial generating scale; confirm inter-device research methodologies; and develop operating procedures and maintenance intervals for devices deployed in larger arrays. Such a deployment also establishes a track record, reducing the cost of capital for the eventual development of larger tidal arrays. Projections for the capital cost of early 500kW small batch construction are demonstrating a target figure of less than £3.5 million per MW being achieved.

6. Conclusions

This paper demonstrates that for tidal energy to be accepted as being cost effective it has to compete favourably with offshore wind in terms of capital and operational maintenance costs. Tidal is one of the few clean energy resources to allow a finite amount of daily supply to be firmly contracted. 1st Generation tidal technologies are so expensive that it is unlikely that they will achieve a cost level that will make them competitive. The development of 2nd Generation tidal technologies is showing promise in under-cutting the current targeted costs for tidal energy systems at this stage of technology maturity. As these develop, the capital and operational costs of emerging technologies are likely to fall. Therefore, at the current time tidal generation is an immature technology and second generation devices e.g. CoRMaT, etc offer the ability to make significant reductions to both capital and operating costs. This provides the ability for tidal power to produce electricity at a cost comparable to offshore wind.

References

1. Quantification of exploitable tidal energy resources in UK, npower juice, July 2007
2. Ocean Energy Systems Implementing Agreement: An International Collaborative Programme. IEA-OES. 2008
3. The Economics of Wind Energy, The European Wind Energy Association, March 2009)
4. Capital, operating and maintenance costs, The Carbon Trust at <http://www.carbontrust.co.uk/SiteCollectionDocuments/Various/Emerging%20technologies/Technology%20Directory/Marine/cost%20of%20energy/Capital,%20operating%20and%20maintenance%20costs.pdf>
5. Future Marine Energy, Results of the Marine Energy Challenge: Cost competitiveness and growth of wave and tidal stream energy, The Carbon Trust 2006.
6. C M Johnstone, D. Pratt, J A Clarke, A D Grant, 'A requirement for tidal energy to be cost competitive with offshore wind energy' Proc. 3rd International Conference on Ocean Energy 2010, Bilbao, Spain, October 2010.
7. J A Clarke, G Connor, A D Grant, C M Johnstone and S Ordonez-Sanchez 'Contra-rotating Marine Turbines: Single Point Tethered Floating System – Stability and Performance' Proceedings of the 8th European Wave and Tidal Energy Conference, Uppsala, Sweden, September 2009.
8. J A Clarke, G Connor, A D Grant, C M Johnstone and S Ordonez-Sanchez 'A Contra-rotating Marine Current Turbine on a Flexible Mooring: Development of a Scaled Prototype' Proc. 2nd International Conference on Ocean Energy 2008, Brest, France, October 2008.

About the speaker



Mr. Cameron Johnstone held the post of senior lecturer in the Department of Mechanical Engineering at the University of Strathclyde and is a director of the Energy Systems Research Unit, which was established in 1987 as a cross-discipline team concerned with new approaches to built environment energy demand reduction and the introduction of sustainable means of energy supply. Cameron has conducted extensive research into tidal power extraction focusing on flow analysis/ power transfer techniques and the development of control parameters for firm power delivery from multiple sites. He has investigated the performance optimization of tidal turbine systems to better facilitate power take-off and supply integration. Cameron is a member of the Energy Institute and is on the management team of the EU's Coordinated Action in Ocean Energy initiative and Equimarproject.

TSUNAMI AMPLIFICATION AND BREAKING ALONG A VERTICAL WALL

HARRY YEH, WENWEN LI

School of Civil & Construction Engineering, Oregon State University, Corvallis, Oregon 97331, USA

When a solitary wave (a model of tsunami in the nearshore shallow water) impinges on a reflective vertical wall, it can take the formation of Mach reflection (a geometrically similar reflection from acoustics). The mathematical theory predicts that the amplification at the reflection is not twice, but four times the incident wave amplitude. Evidently, this has an important implication to engineering design practice. Our laboratory experiments verify detailed features of the Mach reflection phenomenon, whereas contradict the theory in terms of the maximum four-fold amplification: the maximum amplification observed in the laboratory was 2.9, instead. The reason for the discrepancy is discussed. In addition, we show that a tsunami along the reflective wall can reach higher than the maximum solitary wave height. Once the wave breaking happens along the wall, the substantial increase in water-surface slope results along the wave crest away from the wall.

1. Introduction

In spite of active research in recent years, the coastal effects of tsunamis remain difficult to predict with adequate accuracy. It is because tsunami behavior near the shore is not sufficiently understood. Tsunamis are long waves; hence we tend to expect tsunami flooding to occur fairly uniformly along a coastline. Contrary to this perception, our field surveys often reveal otherwise: tsunami runup heights often deviate significantly within neighboring areas. This local variability is closely related to tsunami's reflective and refractive behaviors [1]. Wave reflection and refraction lead to obliquely-interacting multiple waves. When their amplitudes are sufficiently large, nonlinear effects can have striking effects on the resulting surface waves. Here we focus on the reflection of tsunamis obliquely incident onto a vertical wall. We use solitary waves as a model tsunami. According to the scaling analysis by Hammack and Segur [2], co-seismically generated tsunamis do not evolve to the exact form of solitary waves in any oceans on the Earth [3, 4] – the Earth is too small to make the complete evolution. Nonetheless, a solitary wave is a stable permanent-form wave and possesses the characteristics of soliton; hence it is convenient to use it in the laboratory experiments as a canonical tsunami form.

Reflection of solitary wave with oblique incidence along a vertical wall was first investigated experimentally by Perroud [5]. He demonstrated that the reflection pattern resembled the formation of a Mach stem that was known to exist for compressible shock waves [6]. The Mach reflection has features such that the apex of the incident and reflected wave separates away from the wall and is joined to it by a third solitary wave that perpendicularly intersects the wall (Fig. 1). Perroud's experimental realization of Mach reflection of the solitary wave is remarkable, although the governing equations for compressible fluids are similar to the shallow-water wave equations.

Miles [7] provided the first comprehensive analysis by extending his theory for obliquely interacting multiple KdV solitons [8] to the Mach reflection problem. His theory is based on the assumptions of shallow-but-finite water depth $(h_0/\lambda_0)^2 = O(\varepsilon)$, and small-but-finite wave amplitude to the lowest order $a_i/h_0 = O(\varepsilon)$, in which a_i is the incident wave amplitude, h_0 is the water depth at the quiescent state, λ_0 is the scale of wavelength, the parameter $\varepsilon \ll O(1)$, and ψ_i denotes the incident wave angle. Analyzing the resonant interaction of the incident, reflected, and stem waves for a small incident wave angle condition, $\psi_i^2 = O(\varepsilon)$, he found that no regular reflection of a solitary wave is possible when $0 < \psi_i^2 < 3a_i$, and derived quantitative prediction for Mach-stem wave amplification in the asymptotic state:

$$\alpha = \begin{cases} \frac{4}{1 + \sqrt{1 - k^2}} & \text{for } k^2 \geq 1 \\ (1 + k)^2 & \text{for } k^2 < 1 \end{cases} \quad (1)$$

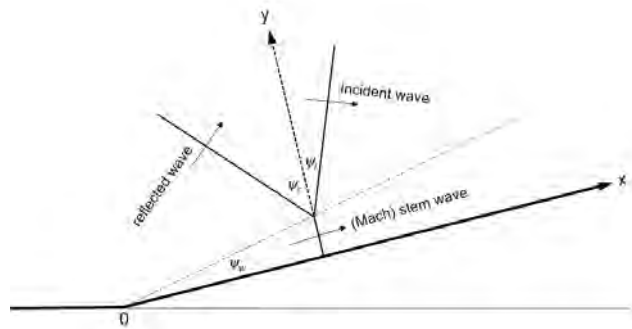


Figure 1. Definition sketch for Mach reflection: ψ_i , incident wave angle; ψ_r , reflected wave angle; ψ_w , angle of stem-wave development.

where k is the interaction parameter: $k = \psi_i / \sqrt{3a_i/h_0}$. In (1), the stem wave amplification α is the ratio of the stem-wave amplitude a_w at the wall to the incident wave amplitude a_i far offshore: $\alpha = a_w/a_i$. It is remarkable to point out that the maximum amplification is not double, but four-fold $\alpha = 4$, when $k = 1$.

This theoretical prediction of the four-fold amplification has not been verified experimentally. The laboratory experiments by Melville [9], could only achieve the maximum amplification $\alpha = 2.0$ at $k = 1.43$. As will be discussed, Melville's measurement location was not sufficient for the reflection to be fully developed. Tanaka [10] commented from his numerical experiments that it requires long propagation ($x/h_0 \sim 100 - 300$) to achieve the asymptotic condition in stem amplitude. Nevertheless, Tanaka also failed to numerically achieve the four-fold amplification; the simulated maximum stem-wave amplification was $\alpha = 2.897$ at $k = 0.695$.

2. Experiments

To examine wave amplification resulted from the reflection of obliquely incident solitary wave, laboratory experiments were performed in a wave tank (7.3 m long, 3.6 m wide, and 0.30 m deep). The laboratory apparatus is equipped with a 16-axis directional wavemaker along the 3.6-m long sidewall. The paddles are made of PVDF (Polyvinylidene fluoride) plates that are moved horizontally in piston-like motions. Each paddle has a maximum horizontal stroke of 55 cm – more than adequate to generate very long waves. An obliquely incident solitary wave was created in the water depth $h_0 = 6.0$ cm by placing a 2.54 cm thick Plexiglas plate vertically at a prescribed azimuth angle from the tank's sidewall (see Fig. 2). Solitary waves are generated using the algorithm based on KdV solitons [11].

The Laser Induced Fluorescent (LIF) method is used to extract temporal and spatial variations of water-surface profiles. A laser beam is converted to a thin laser sheet using a cylindrical lens: see Fig. 2. Two front surface mirrors direct the laser sheet to illuminate the vertical plane perpendicular to the wall. With the aid of fluorescein dye dissolved in water, the vertical laser-sheet illumination from above induces the dyed water to fluoresce and identifies the water-surface profile directly and non-intrusively. The illuminated images are recorded by a high-speed high-resolution video camera (1280 × 1024 pixels and 100 frames per sec.). The images are rectified and processed with the calibrated image. The LIF method is a highly accurate measurement technique to capture the spatiotemporal water-surface profiles in the non-intrusive manner.

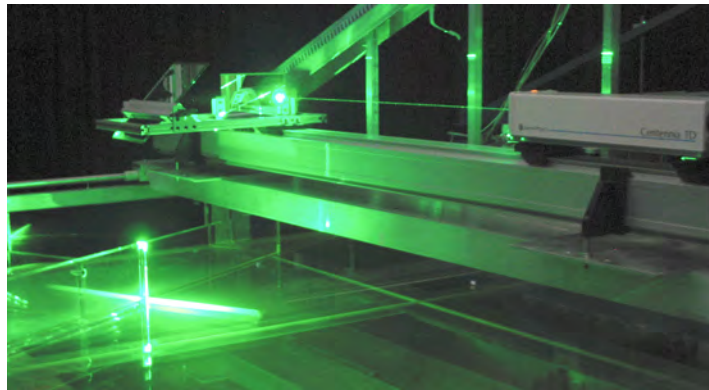


Figure 2. Laser-Induced Fluorescent (LIF) method comprised of the 5W laser, the cylindrical lens, and two front-surface mirrors. The water dyed with fluorescein (green) fluoresces when excited by the laser sheet.

3. Results

Our laboratory experiments of Mach reflection require measurements of small wave amplitudes (a few centimeters) in a large horizontal span (more than 75 cm). To achieve adequate resolution, we repeat LIF water-surface profiles on approximately 27 cm segments, and make a montage of the three-segment profiles to cover the 80 cm long transect perpendicular to the wall. This procedure is only possible with a laboratory apparatus that is capable of precise replication. An example of the resulting water-surface map in the $y-t$ plane is shown in Fig. 3. Because the LIF method permits measuring water-surface elevations non-intrusively, any uncertainty caused by meniscus contamination in the measurement often associated with wave gages is eliminated. Figure 3 represents the wave profile at $x/h_0 = 71.1$ for the case of the incident wave amplitude $a_i/h_0 = 0.277$ ($h_0 = 6.0$ cm) with the oblique wall $\psi_i = 30^\circ$. (The location $x/h_0 = 71.1$ is much farther than that of Melville's measurements [9], $x/h_0 = 26.7$.) The plot is made from 180 slices of the temporal profiles with approximately 3000-pixel resolution in the y -direction. As shown, the stem-wave formation is evidently realized, in which the apices of the incident and reflected waves separate away from the wall by the third wave that perpendicularly intersects the wall. Figure 3 also shows that the reflected wave amplitude is smaller than that of the

incident wave as anticipated for Mach reflection. We also found that the reflected wave angle $\psi_r = 41.6^\circ$: clearly, $\psi_i (= 30^\circ) < \psi_r$, that is one of the characteristics of Mach reflection.

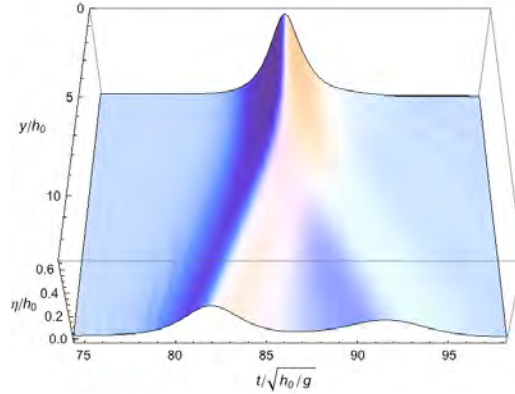


Figure 3. Temporal variation of the water-surface profile in the y -direction at $x/h_0 = 71.1$: the wall is located at $y = 0$, the water depth $h_0 = 6.0$ cm, the incident wave amplitude $a_i/h_0 = 0.277$, and the angle $\psi_i = 30^\circ$. The data were obtained by the LIF method.

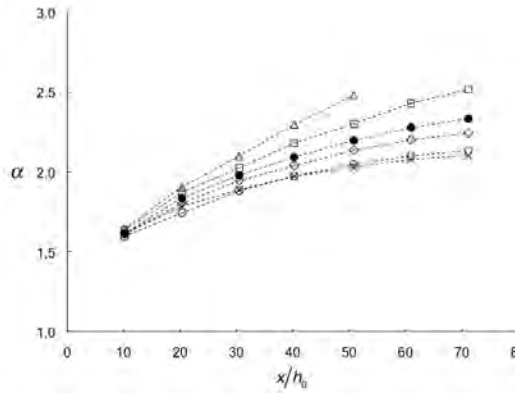


Figure 4. Amplification growth of the stem wave α for the conditions of $\psi_i = 30^\circ$, $h_0 = 6$ cm, and $-\times-$, $a_i/h_0 = 0.076$; $-o-$, 0.096 ; $-\diamond-$, 0.143 ; $-●-$, 0.188 ; $-\square-$, 0.277 ; $-\triangle-$, 0.367 .

Growing stem-wave amplifications $\alpha (= a_w/a_i)$ induced by a variety of incident waves with amplitudes $0.076 < a_i/h_0 < 0.367$ and $\psi_i = 30^\circ$ are presented in Fig. 4. No complete data are presented for the case of $a_i/h_0 = 0.367$ because of the wave breaking after $x/h_0 = 50.8$. The stem amplification continues to grow in the cases of larger-amplitude waves. On the other hand, the amplitude tends to approach its asymptotic value for the smaller amplitude cases. The continual growth indicates that limited physical dimension of the laboratory apparatus prevents the Mach stem from reaching its fully developed state. To circumvent this, we extend the experiment by generating the waveform measured at the furthest location ($x/h_0 = 71.1$) observed in the run. In other words, the effectively larger wave tank is achieved by patching the two experimental runs: the original ‘parent’ experimental run and the subsequent ‘extended’ run. Unlike the parent experimental run in which only an incident solitary wave was generated, the 2D waveform including the reflected and stem waves need to be generated for the extended run. This practice is made possible with the present wavemaker system that is capable of replication of the 2D waveform. It is cautioned nonetheless that this patching procedure induces some error because it is not possible to perfectly reproduce the wave measured in the parent experimental run with the 16-axis wavemaker system.

Figure 5 shows the stem wave amplification measured at $x/h_0 = 121.1$ by the extended experimental runs with $\psi_i = 20^\circ$ and 30° , and at $x/h_0 = 61.0$ with $\psi_i = 40^\circ$. (In the case of $\psi_i = 40^\circ$, the data at $x/h_0 = 71.1$ were contaminated due to the limited breadth of the wave tank, and the extended experiment for this case is not possible owing to its large oblique angle.) Also plotted in the figure are Miles’s theoretical prediction (1) and Tanaka’s numerical results [10] at $x/h_0 = 150$. It is emphasized that Tanaka’s numerical results were for a single incident wave amplitude, $a_i/h_0 = 0.30$ with a range of incident wave angles $\psi_i = 10 \sim 60^\circ$, whereas the present laboratory results are based on three incident wave angles with a range of incident wave amplitudes $a_i/h_0 = 0.076 \sim 0.277$. Disagreement with the theory (1) led Tanaka

(1993) to report that, instead of $k = 1$, the transition from Mach reflection to regular reflection occurs at $k = 0.695 < 1$ with the maximum amplification $\alpha = 2.897$, instead of 4.0. Figure 5 clearly exhibits the discrepancy in our laboratory data with both the theory and Tanaka's numerical results. Furthermore, the present data with different incident wave angles ψ_i do not yield unified data trend. The discrepancy that appears in Fig. 5 implies some missing factor(s) in the analysis.

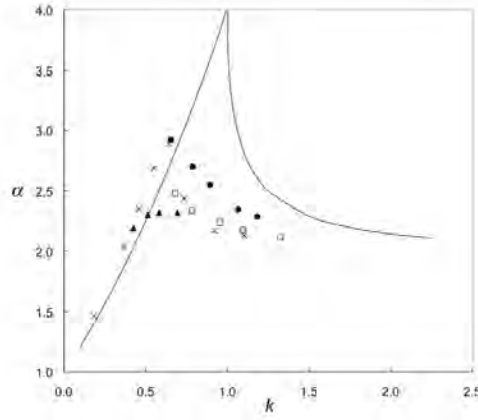


Figure 5. Comparison of the present data with (1) —, and Tanaka's numerical data \times . The present data are for $\psi_i = 20^\circ$, \blacktriangle and $\psi_i = 30^\circ$, \bullet at $x/h_0 = 121.1$. The data for $\psi_i = 40^\circ$, \square are at $x/h_0 = 61.0$.

Recall that the condition of small incident wave angle $\psi_i^2 = O(\varepsilon)$ imposed by Miles [7]. This condition in fact is violated for laboratory and numerical results. Our laboratory experiments are performed with the incident wave angle $\psi_i = 0.35 \sim 0.70$ radians ($20 \sim 40^\circ$) and Tanaka's numerical study [10] is with $\psi_i = 0.17 \sim 1.05$ radians ($10 \sim 60^\circ$). Recently, Yeh *et al.* [12] showed the treatment of oblique incident angle ψ_i in the Kadomtsev-Petviashvili (KP) equation [13]: the KP equation is equivalent to Miles's theory, assuming shallow-but-finite water depth $(h_0/\lambda_0)^2 = O(\varepsilon)$ and small-but-finite wave amplitude $a_i/h_0 = O(\varepsilon)$. Different from Miles's theory, the derivation of the KP equation requires the small oblique angle to be explicitly $\tan^2 \psi_i = O(\varepsilon)$, but not $\psi_i^2 = O(\varepsilon)$.

The KP equation in terms of the water-surface elevation η from the equilibrium state can be written in the dimensional form:

$$\left(\eta_t + c_0 \eta_x + \frac{3c_0}{2h_0} \eta \eta_x + \frac{c_0 h_0^2}{6} \eta_{xxx} \right)_x + \frac{c_0}{2} \eta_{yy} = 0 \quad (2)$$

where $c_0 = \sqrt{g h_0}$, the x -direction represents the primary wave propagation, and the weak transverse perturbation is in the y -direction. An exact solution to (2) is

$$\eta = a_0 \operatorname{sech}^2 \left[\sqrt{\frac{3a_0}{4h_0^3 \cos^2 \psi}} \left\{ x \cos \psi + y \sin \psi - c_0 \cos \psi \left(1 + \frac{1}{2} \frac{a_0}{h_0} + \frac{1}{2} \tan^2 \psi \right) t \right\} \right] \quad (3)$$

Taking the propagation direction of a line soliton to be $\xi = x \cos \psi + y \sin \psi$, and expanding $\cos \psi$ in the last term by $\cos \psi = 1 - \frac{1}{2} \tan^2 \psi + O(\varepsilon^2)$ yields

$$\eta = a_0 \operatorname{sech}^2 \left[\sqrt{\frac{3a_0}{4h_0^3 \cos^2 \psi}} \left\{ \xi - c_0 \left(1 + \frac{1}{2} \frac{a_0}{h_0} \right) t + O(\varepsilon^2) \right\} \right] \quad (4)$$

Rescaling the wave amplitude and water surface elevation with $a^* = a_0/\cos^2 \psi$ and $\eta^* = \eta/\cos^2 \psi$, we have the KdV soliton in the x -direction:

$$\eta^* = a^* \operatorname{sech}^2 \left[\sqrt{\frac{3a^*}{4h_0^3}} \left\{ \xi - c_0 \left(1 + \frac{1}{2} \frac{a^*}{h_0} \right) t + O(\varepsilon^2) \right\} \right] \quad (5)$$

This rescaling procedure results in the higher-order correction to the small angle approximation. It is emphasized that the amplitude a^* now represents the physical wave amplitude realized in the laboratory. While (5) is no longer the exact solution to the KP equation (2), it still remains valid within the KP limit. It is important to recognize that, instead

of the interaction parameter $k = \psi_i / \sqrt{3a_i/h_0}$ introduced by Miles [7] based on the assumption of $\psi_i^2 = O(\varepsilon)$, the modified parameter

$$\kappa = \frac{\tan \psi_i}{\sqrt{3a_i/h_0} \cos \psi_i} \quad (6)$$

should be used when the theory is compared with the experiments with the finite values of ψ_i and amplitude a_i .

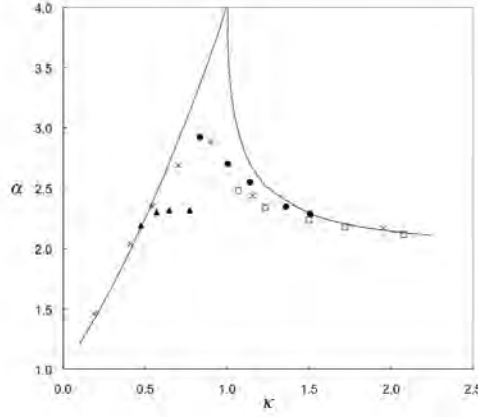


Figure 6. Comparison of the present data with (1) —, and Tanaka’s numerical data \times , using the modified interaction parameter κ . The present data are for $\psi_i = 20^\circ$, \blacktriangle and $\psi_i = 30^\circ$, \bullet at $x/h_0 = 121.1$. The data for $\psi_i = 40^\circ$, \square are at $x/h_0 = 61.0$.

With this corrected parameter κ , much improved agreement with the theory is presented in Fig. 6. On the contrary to Tanaka’s conclusion that stated discrepancies in many aspects, both laboratory and numerical experimental results now turn out to be in good agreement with Miles’s model, although the four-fold amplification at $\kappa = 1.0$ cannot be realized. The maximum amplification from the laboratory data is $\alpha = 2.922$ at $\kappa = 0.834$, and Tanaka’s numerical results now show $\alpha = 2.897$ at $\kappa = 1.03$. The discrepancy in the case of $\psi_i = 20^\circ$ remains due presumably to the limitation in propagation distance in the laboratory; however, the data clearly exhibit approaching the asymptotic state. The length of the stem formation at distant locations becomes too long to be reproduced by the wavemaker in the limited breadth of our laboratory tank, which disallows us to perform additional extended experiments beyond $x = 121.1$.

Figure 7 shows the temporal variation of incipient breaking waves along the wall at $x/h_0 = 61.0$ with the incident wave amplitude $a_i/h_0 = 0.351$ and angle $\psi_i = 30^\circ$. The wave profile was captured every 0.01 sec. using the LIF method of aligning the laser sheet parallel to the wall. Figure 7 exhibits gradual growth in wave amplitude prior to the incipience of wave breaking. The maximum wave height a_w/h_0 at the wall reaches 0.910, right at the incipience of the breaking. This Mach-stem height is higher than the highest plain solitary wave that is 0.827 [14]. The vertical-step-like appearance on the wave front in the last three time steps is the portion of overturning wave. Short spatial oscillations in front of the overturning water are capillary waves running down the steep front slope.

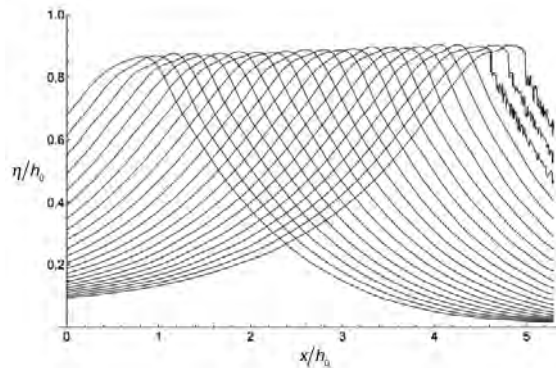


Figure 7. Temporal variation of wave profiles at the incipient breaking along the wall at $x/h_0 = 61.0$ with $\psi_i = 30^\circ$.

Figure 8 shows the breaking wave profiles in the y -direction at $x/h_0 = 61.0$ and 71.1 . For this, the LIF method is used aligning the laser sheet perpendicular to the wall. While the wave amplitude decreases near the wall due to energy dissipation, the amplitude continues to grow in the area away from the wall. The maximum wave amplitude at $x/h_0 = 71.1$ is $a/h_0 = 0.856$ at $y/h_0 = 3.17$. At the same offshore location but at $x/h_0 = 61.0$, the amplitude is $a/h_0 = 0.758$; that is 13% growth from $x/h_0 = 61.0$ to 71.1 . This growth rate is substantially faster than the growth rate of the Mach stem prior to wave breaking – Figure 4 shows a 6.9% increase in non-breaking-wave amplitude from $x/h_0 = 40.2$ to 50.8 at the wall. Perhaps more important, the water-surface slope facing the y -direction is substantially steeper at $x/h_0 = 71.1$ than at $x/h_0 = 61.0$. This amplitude growth cannot be explained with the growth of the stem length alone. One explanation for the faster increase in amplitude offshore is the increase in momentum in the y -direction near the wall due to turbulence induced by wave breaking.

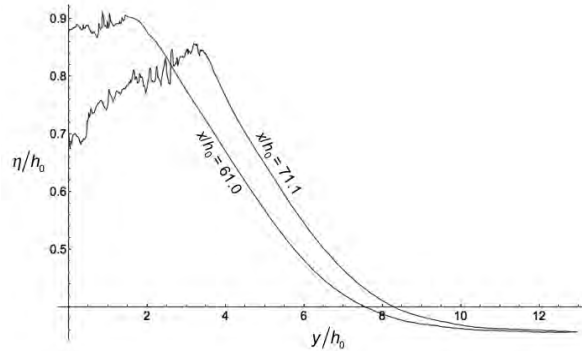


Figure 8. Breaking wave profiles in the plane perpendicular to the wall at $x/h_0 = 61.0$ and 71.1 with $\psi_i = 30^\circ$.

4. Summary and Conclusions

Reflection of an obliquely incident solitary wave along a vertical wall was investigated by performing the laboratory experiments. The temporal and spatial variations of water-surface were captured non-intrusively with the laser induced fluorescent method. The precise measurements demonstrate the realization of Mach reflection in the laboratory environment. The reflection is characterized by the Y-shape formation consisting of the incident, reflected, and stem waves. The reflected wave angle is larger than the incident wave angle, $\psi_r > \psi_i$, and the amplitude of the reflected wave is smaller than that of the incident wave, $a_r < a_i$. We found that our laboratory apparatus is too small to achieve the asymptotic state of the Mach reflection – recall that the theory [7] is for the three wave resonant interaction at the asymptotic state. To examine the evolution in an effectively longer distance than the limited size of the laboratory apparatus, we used a technique linking two separate experiments and patched the data. This could be achieved by generating the waveform measured at the farthest location, and observing the subsequent evolution of the generated waveform.

We showed, based on the KP theory, that the interaction parameter $k = \psi_i / \sqrt{3a_i/h_0}$ of the original form must be revised with $\kappa = \tan \psi_i / (\cos \psi_i \sqrt{3a_i/h_0})$ when the theory is verified with experiments. This is because the oblique angle of the incident wave is not infinitesimal, but finite in real-world experiments. The stem-wave amplification was found to be in good agreement with the asymptotic state of the theory except near the critical condition, $\kappa \approx 1.0$. The critical four-fold amplification at $\kappa = 1.0$ was not realized in the laboratory and also in the numerical simulation. Note that the gradient of (1) becomes singular as κ decreases toward unity. Therefore a small change in κ causes a substantial change in amplification. Therefore, the actual transition between the Mach reflection and the regular reflection is gradual, instead of the abrupt change at $\kappa = 1.0$, and the maximum amplification is lower than $\alpha = 4$. Our laboratory and Tanaka's numerical results suggest that the amplification factor of the stem wave is approximately $\alpha = 3$.

We also examined the maximum wave height of the Mach stem prior to its wave breaking and found that the maximum wave height of the stem wave $a/h_0 = 0.910$ exceeds the maximum height 0.827 of the plain solitary wave [14]: this result is consistent with Tanaka's numerical result [10]. After incipient breaking near the wall, the breaking broadens, shifting the location of the maximum water-surface elevation offshore. The water-surface elevation offshore grows faster. This behavior must be caused by an enhancement in momentum in the offshore direction near the wall, which must be resulted from turbulence induced by wave breaking.

The present results imply the following engineering consequences. First, the wave runup on a vertical wall can be amplified by threefold when a solitary wave is obliquely incident to the wall. (Intuition based on linear waves tells us

Keynote Lecture by Yeh

the twofold amplification for the normal incidence, and lower for the cases with an oblique incident angle.) This threefold amplification can occur when $\kappa \approx 1$, i.e. when the incidence angle is 'small'. For example, when the nonlinearity parameter of incident wave is $a_i/h_0 = 0.2$, the critical incidence angle would be 33° . The runup can climb up on the wall to $a_w/h_0 = 0.910$ without wave breaking. When the stem wave breaks, the profile toward offshore would be steepened (Fig. 8). Therefore, a boat that attempts to steer perpendicular to the wave crest could be in danger by the rolling action.

Acknowledgments

We are grateful to Yuji Kodama of Ohio State University for inspiring discussions. This work was supported by Oregon Sea Grant Program (NA06OAR4170010-NB154L and NA10OAR4170059-NA223L), and the Oregon State University Edwards Endowment.

References

1. SCOR 107, IOC Technical Series No 63, IOC, UNESCO, Paris, pp. 122 (2002).
2. J. L. Hammack, and H. Segur, *J. Fluid Mech.* **84**, 359 (1978).
3. H. Yeh, P. Liu, and C. Synolakis, *Long-Wave Runup Models*, World Scientific Publishing Co., Singapore, pp. 403 (1996).
4. P. A. Madsen, D. R. Fuhrman, and H. A. Schäffer, *J. Geophys. Res.* **113**, C12012, 1 (2008).
5. P. H. Perroud, Institute of Engineering Research, Wave Research Laboratory, Tech. Rep. 99/3, University of California, Berkeley, pp. 93 (1957).
6. J. Von Neumann, Explosives Research Rep. No. 12, Navy Dept. Bureau of Ordnance, Washington, D.C. (1943).
7. J. W. Miles, *J. Fluid Mech.*, **79**, 171 (1977).
8. J. W. Miles, *J. Fluid Mech.*, **79**, 157 (1977).
9. W. K. Melville, *J. Fluid Mech.*, **98**, 285 (1980).
10. M. Tanaka, *M. J. Fluid Mech.*, **248**, 637 (1993).
11. D. G. Goring, *Tsunami – the propagation of long waves onto a shelf*, PhD Thesis, Calif. Inst. Tech. (1979).
12. H. Yeh, W. Li, and Y. Kodama, *European Physical Journal*, **185**, 97 (2010).
13. B. B. Kadomtsev, and V. I. Petviashvili, *Sov. Phys. Doklady*, **15**, 53- (1970).
14. M. S. Longuet-Higgins, and J. D. Fenton, *Proc. R. Soc. Lond. Ser. A* **340**, 471 (1974).

About the speaker



Professor Harry Yeh received in 1983 his Ph.D. degree in Civil Engineering from University of California, Berkeley, USA. He is currently the Miles Lowell and Margaret Watt Edwards Distinguished Chair in Engineering of the School of Civil & Construction Engineering at Oregon State University. Prof. Yeh's research involves environmental fluid mechanics, ocean and coastal wave phenomena, flow-structure interactions, tsunami induced scour, wind turbulence, structure control (tuned liquid dampers), physical processes in lakes and oceans, and tsunami hazard mitigation. He is the recipient of many honors and awards and has published widely in the fields of wave hydrodynamics, natural hazards due to tsunamis, environmental fluid mechanics, and so on.

BOOK OF ABSTRACTS

Parallel Session 1
Wednesday, 14 December
Estuaries and Ports I
Ballroom C
Chair: Xiping Dou, Moonsu Kwak

14:00

Master plan of tidal flat reclamation along Jiangsu coastal zone

C.K. ZHANG, J. CHEN

College of Harbor, Coastal and Offshore Engineering, Hohai University, 1 Xi Kang Road, Nanjing, 210098, China

Jiangsu coastal zone is located in the center of coastal area of eastern China. Recently, "The Developing Plan for Jiangsu Coastal Zone" was approved by the Chinese Central Government, indicating that the development of Jiangsu coastal zone has been upgraded to be part of national development strategy. According to the Plan, about 1,800 km² of Jiangsu tidal flat is to be reclaimed during 2009-2020. A master plan of reclamation of Jiangsu tidal flat is made to ensure the reclamation in a scientific, comprehensive and efficient way. The main contents of the master plan, including the guidelines and principles of reclamation, the spatial layout of the reclaimed area, the procedure of implementation, the necessary construction of ancillary infrastructures as well as the environmental protection and financial safeguard measures for the reclamation, are presented in this paper.

14:30

Simulation of the hydrodynamic influence for the HZM bridge project in the estuarine areas of Pearl River

J. HE, W.J. XIN, J.Y. HOU

Nanjing Hydraulic Research Institute, Nanjing 210024, China

State Key Laboratory of Hydrology-Water Resource and Hydraulic Engineering, Nanjing 210024, China

The HZM (Hongkong-Zhuhai-Macao) bridge connects Hongkong, Zhuhai and Macao district, and it stretches across the Lingding sea in the Pearl River estuary. A lot of piers and three large artificial islands in the sea will have some influences on the hydrodynamic environment of the Pear River estuary. In this paper, a 2D tidal current numerical model is introduced to simulate the hydrodynamic impact from the HZM bridge. For the broad water area of the Lingding Sea, the water area covered by the model should be large as for as possible. And the lower limit of the pier is 2.0m. Thus the unstructured grids are selected to split the computed area. The grids could be enlarged far away from the HZM bridge, and the grids would be small in the bridge area. And the FVM (finite volume method) is adopted to solve the tidal current governing equation, for it can satisfy the control equation's conservation and has a high calculated precision. The simulated results show that the Hydrodynamic influence is concentrated on the 5.0 km range from downstream to upstream nearby the navigation zone

and the 1.0 km range of bridge site in not-navigation zone, and the tidal range reduction is limited 0.03m and the tidal prism reduction is not more than 1% in the Lingding Sea after the HZM bridge is constructed. Therefore, the HZM bridge has little influence on the distribution of hydrodynamic environment in the Pearl River estuary.

14:45

Tidal flat evolution at the central Jiangsu Coast, China

Z. GONG

State Key Laboratory of Hydrology-Water Resources and Hydraulic Engineering, Hohai University, No.1, Xikang Road, Nanjing, 210098, China

Z.B. WANG

Deltares, P.O.Box 177, Delft 2600 MH, The Netherlands
Faculty of Civil Engineering and Geosciences, Delft University of Technology, P.O. Box 5048, Delft 2600 GA, The Netherlands

M.J.F. STIVE

Faculty of Civil Engineering and Geosciences, Delft University of Technology, P.O. Box 5048, Delft 2600 GA, The Netherlands

C.K. ZHANG

College of Harbor, Coastal and Offshore Engineering, Hohai University, No.1, Xikang Road, Nanjing, 210098, China

A schematized process-based model of tidal flat evolution was constructed with dimensions similar to the tidal flats near the Wanggang Mouth at the central coast of Jiangsu, China. The simulated flow patterns agree qualitatively with field observations from literature, i.e. involving tidal asymmetry, current directions and tidal wave features. The analysis of the sediment fluxes depicts that deposition occurs from spring tide to neap tide and erosion from neap tide to spring tide. A sensitivity analysis test of the morphological acceleration factor shows that the ideal value is only 1, implying no acceleration factor. The long-term mudflat evolution has been simulated starting from an initial sand seabed. The simulated morphological characteristics, including the convex cross-shore profiles with steeper slope and the southern prograding coastline with slight higher accretion rate compared with the north side, are qualitatively consistent with reality. Most importantly, the creek patterns are roughly reproduced.

15:00

Analysis of the decadal change in the riverbed of the Tedor River, Japan and its correlation with neighboring coasts

M.H. DANG, S. UMEDA, R. MATSUDA, M. YUHI

Graduate School of Natural Science and Technology, Kanazawa University, Kakuma-machi, Kanazawa, Ishikawa, 920-1192, Japan

Long-term variations in the riverbed of the Tedor River, Japan, were investigated using a set of field surveys conducted over 30 years. The results revealed that the sediment volume of the entire study reach declined by $11.5 \times 10^6 \text{m}^3$ from 1950 to 1979. Correspondingly, the riverbed has undergone serious

and rapid erosion, lowering by 0.5 to 3.5 m as a result of erosion at a rate of 0.06-0.10 m/year. The temporal and spatial variation of the sediment volume and corresponding riverbed response were related to anthropogenic activities such as material mining and dam construction. These variations were effectively captured using empirical orthogonal function (EOF) analysis. A collation of EOF results between the river and the coast was conducted to fully realize the cumulative anthropogenic impacts on the river-coastal watershed.

Parallel Session 1
Wednesday, 14 December
Climate Change and Sea Level Rise I
Ballroom B
Chair: Tsung-Lin Lee, Hisamichi Nobuoka

14:00

Oceanic oscillation and rainfall distribution in the Indonesian Archipelago

T. YAMASHITA, HENDRI, T. OKAMOTO
Department of Development Technology, the Graduate School for International Development and Cooperation, Hiroshima University, 1-5-1 Kagamiyama, Higashi-Hiroshima 739-8529, Japan
T. IKEDA

Japan Port Consultants, Ltd. 8-3-6 Nishi-Gotanda, Shinagawa-ku, Tokyo 141-0031, Japan
Characteristics of rainfall in the Indonesian Archipelago are closely related to oceanic oscillations in the Pacific Ocean and Indian Ocean. In this study, the daily rainfall data of Global Summary Of The Day (GSOD) from the National Climatic Data Center (NCDC) were used with careful consideration of data availability. The daily rainfall data from August 1985 to January 2010 were analyzed at 10 observation points. The results showed that significant differences of rainfall characteristics exist and they are classified into three regions as follows: ①Sumatra: multi-annual rain seasons for five long are dominant. Sever dry one or two years appeared in between the multi-annual rain seasons (1990-1992, 1999). ②Java Sea coastal area: clear variation in the annual rain and dry seasons. ③ East Indonesia: multi-annual rain seasons same as Sumatra with clear annual fluctuation of wet and dry seasons.

These rainfall characteristics are discussed with the correlation of oceanic climate change indicators (DMI: Indian Ocean Dipole Mode Index, MEI: Pacific Ocean oscillation, PDO (Pacific Decadal Oscillation). Daily precipitation has high correlation with these indices in particular with MEI or PDO. Dry year appears in El Nino phase (PDO warm phase) and rainy year is the opposite. Dateline El Nino (CP El Nino) that warm seawater stays at the position of the International Date Line, is prone to extreme weather such as heavy rain. In fact, a significant rainfall occurs during the transition of MEI and PDO. The changes in average global temperature (IPCC), NAO (North Pacific Ocean oscillation index) and the PDO have the long-term

variations of about 30-40 years. Apparently temperature and these indices have clear changes in 1903, 1944, and 1977. PDO seems to be shifting to cool phase (La Nina dominant phase) after 2005 and rainfall in Indonesia is also on the increase.

14:15

Extreme wave climate change projection at the end of the 21st Century

TOMOYA SHIMURA
Graduate School of Engineering, Kyoto University, Katsura, Kyoto 615-8530, Japan
NOBUHITO MORI, SOTA NAKAJO, TOMOHRO YASUDA, HAJIME MASE
Disaster Prevention Research Institute, Kyoto University, Uji, Kyoto 611-0011, Japan

The influences of global climate change due to greenhouse effects on the earth environment will require impact assessment, mitigation and adaptation strategies for the future of our society. This study projects future ocean wave climate in comparison with present wave climate based on atmospheric general circulation model and global wave model. Future change of averaged wave height depends on latitude strongly. On the other hand, the extreme wave height in the future climate will be increased significantly in tropical cyclone areas.

14:30

Long term trends of the regional sea level changes in Hong Kong and the adjacent waters

K.W. LI, H.Y. MOK
Hong Kong Observatory, HKSARG
Hong Kong, China

Direct consequences of global warming are thermal expansion of sea water and melting of glaciers and ice caps. Both effects would lead to a rise of the mean sea level. According to the fourth assessment report (AR4) of the Intergovernmental Panel on Climate Change (IPCC), the global mean sea level rose at a rate of 1.8 mm per year for 1961-2003 and 3.1 mm per year for 1993-2003. The fourth assessment report also projects that the sea level could rise by 0.59 metre in the 21st century while some recent studies suggest that the amount could be even higher - at one to two metres. Located at the coast of the South China Sea, Hong Kong has experienced a rise in the sea level. Previous studies show that the sea level at the Victoria Harbour has risen significantly by about 2.6 mm per year since the 1950's. However, some other factors such as ocean currents, water discharge, subsidence and sedimentation are also influencing sea level at the regional scale. As the eastern side of Hong Kong is open to the Taiwan Strait and Luzon Strait, while the western side is at the Pearl River Estuary and the southern end is open to the South China Sea, the change in sea levels in Hong Kong and the adjacent waters would have regional variations. This study aims at determining the long term trends of the regional sea level changes in Hong Kong and the adjacent waters by examining the sea level data recorded since the 1950s by tide gauges at various coastal locations in Hong Kong and Macau. The

satellite altimetry data are also used to corroborate the sea level change in the South China Sea with those in the Hong Kong Waters.

14:45

Prediction of future tropical cyclone characteristics using global stochastic tropical cyclone model

SOTA NAKAJO, NOBUHITO MORI, TOMOHIRO

YASUDA, HAJIME MASE

Disaster Prevention Research Institute, Kyoto University, Gokasho, Uji, Kyoto, 611-0011, Japan

A Global Stochastic Tropical cyclone Model (GSTM) using Principle Component Analysis and Monte Carlo Simulation technique has been developed for assessment. Future change trends of tropical cyclone have been estimated from ensemble predictions of 8 different General Circulation Models and they were implemented in the GSTM. Consequently, future changes of tropical cyclone frequency and their intensity have been projected statistically and the effects of uncertainty of future change are also estimated.

15:00

Projection of future storm surge due to climate change and its uncertainty – a case study in the Tokyo Bay

TOMOHIRO YASUDA, NOBUHITO MORI, SOTA

NAKAJO, HAJIME MASE

Disaster Prevention Research Institute, Kyoto University Gokasho, Uji, Kyoto 611-0011, Japan

YUTA HAYASHI

Graduate School of Engineering, Kyoto University

Kyotodaigaku-Katsura, Nishikyo-ku, Kyoto 615-8540, Japan

YUICHIRO OKU

Osaka City Institute of Public Health and Environmental Sciences, 8-34, Tojo-cho, Tennoji-ku, Osaka 543-0026, Japan

It has been discussed that intensity of typhoon may increase in the future due to climate change. It is important to estimate the probable maximum magnitude of storm surges under the future climate for coastal disaster mitigation. In the present study, sensitivity of storm surge projection due to storm track in Tokyo Bay is discussed by employing the hundreds of different severe meteorological conditions generated by the potential vorticity inversion method. Ensemble numerical results show the most hazardous tropical cyclone track is different from most intense tropical cyclone track in Tokyo Bay. Estimated maximum storm surge in the Tokyo Bay is found to be 1.4 m which is the same level as the historical highest record.

15:15

Statistical downscaling of multi-site multivariate daily extreme temperature series for climate-related impact assessment studies

VAN-THANH-VAN NGUYEN, MALIKA KHALILI

Department of Civil Engineering and Applied Mechanics, McGill University, 817 Sherbrooke Street West, Montreal, Quebec, Canada H3A 2K6

Statistical downscaling methods for describing the linkage between global scale climate variables and local climatic conditions have been commonly used in various climate-related impact assessment studies. These downscaling techniques must be able to provide physically plausible projections of high-resolution climate information for a given location as well as for different sites simultaneously over a region of interest under different climate change scenarios. In particular, many previous works have been dealing with downscaling of climatic processes for a single site, but very few studies are concerned with the downscaling of these processes for multi-sites because of the complexity in describing accurately both observed at-site temporal persistence and observed spatial dependence between the different locations.

In the present study, an efficient multivariate statistical downscaling (SD) approach was developed for simulating simultaneously and concurrently daily maximum (Tmax) and minimum (Tmin) temperature series at many sites. The proposed approach consists of a combination of a multiple regression model to represent the linkage between global climate predictors and local Tmax and Tmin series, and a Singular Value Decomposition (SVD) technique to describe the observed statistical properties of the residual stochastic component. In particular, the use of the SVD method could provide an efficient procedure for the simulation of the temperature series for many sites because this method is quite suitable for the transformation of a large matrix of the residuals (due to a large number of sites considered) into a smaller matrix of its independent principal components for a more effective computational scheme.

The feasibility of the suggested multi-site multivariate downscaling method was assessed using observed daily extreme temperature data available at ten weather stations located in the southwest region of Quebec and southeast region of Ontario in Canada as well as climate predictors estimated from the National Centre for Environmental Prediction (NCEP) re-analysis data set for the period from 1961 to 1990. More specifically, a set of 100 simulated daily extreme temperature series was generated for the calibration period from 1961 to 1975, and for the validation period from 1976 to 1990 for this assessment. It was found that the proposed SD approach was able to describe accurately various Tmax and Tmin characteristics, including their spatial and temporal variation as well as their inter-annual anomalies. In particular, it has been shown that the proposed procedure was quite efficient in the simulation of daily temperature series for many sites because of the effective computation of its SVD component.

Parallel Session 1
Wednesday, 14 December
Coastal Management and Shore Protection I
Tang
Chair: Insik Chun, Onyx W.H. Wai

14:00

Feasibility study of coastal reservoir for water supply to Southeast Queensland, Australia

SHU-QING YANG

School of Civil, Ming and Environ. Eng. Univ. of Wollongong

Wollongong, NSW2522, Australia

21st century is the century of sea, this should also include the water resources development. Australia is the driest country in the world, its southeast Queensland is experiencing extreme water scarcity. Intensive research has been conducted and many solutions have been proposed in order to secure its water deficit that is 500GL/year in 2050, such as more inland reservoirs, wastewater recycle and reuse, and desalination plants etc. By analyzing the rainfall data (1200mm/year) and runoff data (10,000GL/year), it is found that the assumption in the existing proposals is not true, in this region the shortage is not water, rather a lack of storage capacity. Based on this discovery, the application of coastal reservoirs in this region has been discussed and analyzed in terms of water supply reliability and water quality. An innovative design of coastal reservoir is proposed to prevent the external pollution by seawater and land-based contaminants. The new solution has been compared with the previous proposals based on their sustainability, impacts on environment and ecosystem, construction and operation cost, and green-house gas emission. It is found that the strategy of coastal reservoirs meets the regional water demand well, and it is sustainable, environment-friendly and cost effective. Most importantly, the example shown in this paper shows that the proposed strategy may eliminate the need of desalination in other similar areas of Australia as well as the world.

14:15

Reliability analysis of quarter-circular caisson breakwater

L.W. QIE, Y.N. QIN, H.Q. DING, X. ZHANG

College of Civil Engineering, Hebei University, Baoding, China

X.L. JIANG

Tianjin Key Laboratory of Soft Soil Characteristics & Engineering Environment, Tianjin Institute of Urban Construction, Tianjin, China

The quarter-circular caisson breakwater (QCB) is a new-type breakwater, and it can be applied in deepwater. The stability of QCB under wave force action can be enhanced, and the rubble mound engineering can be less than that of semicircular breakwaters in deepwater.

In order to study the wave force distribution acting on the QCB, to find wave force formula for this type breakwater, firstly in this paper, the distribution

characteristics of the horizontal force, the downward vertical force and the uplift force on the breakwater have been gotten based on physical model wave flume experiments and on the analysis of the wave pressure experimental data. Based on a series of physical model tests acting by irregular waves, a kind of calculation method, which was modified from Goda Formula, was proposed to carry out the wave force on the QCB.

Secondly, the reliability method with correlated variables was adopted to analyze the QCB, considering the high correlation between wave forces or moments. Based on the observed wave data at engineering region, the reliability index and failure probability of QCB were obtained as well as the proposed partial coefficients of wave loadings. Finally, the design expressions of QCB for anti-sliding and anti-overturning were presented.

14:30

Directional wave spectrum in shallow water waves using an array of pixel brightness on video images

MUHAMMAD ZIKRA

Department of Maritime Engineering, Kyushu University 744 Motooka, Nishi-ku, Fukuoka city, 819-0395, Japan

NORIAKI HASHIMOTO

Dept. of Urban and Environmental Engineering, Kyushu University, 744 Motooka, Nishi-ku, Fukuoka city, 819-0395, Japan

MASAKI YOKOTA, MASARU YAMASHIRO

Dept. of Urban and Environmental Engineering, Kyushu University 744 Motooka, Nishi-ku, Fukuoka city, 819-0395, Japan

KOJIRO SUZUKI

Marine Environmental Information Group, Port and Harbour Research Institute, Ministry of Transport, 3-1-1 Nagase, Yokosuka 239, Japan

Analyses of the directional wave spectrum in shallow water area using video images data are presented. The technique is based on time series of the pixel brightness on video images. The study was examined using video images data at Hasaki beach in Japan. Determination of directional wave spectrum is examined using two different configurations of arrays. The result indicated that in shallow water wave directional spectrum derived from video images was the narrowest at peak frequency and direction.

14:45

Research on armor units stability in 3d and 2d physical model

CI-HENG ZHANG

Tianjin Research Institute for Water Transportation Engineering,

Key Laboratory of Engineering Sediment of Ministry Communications, Tianjin, China

ZIAUDDIN ABD LATIF

Ingenieur, Department of Irrigation and Drainage, Malaysia

HAN-BAO CHEN, YU-FEN CAO

Tianjin Research Institute for Water Transportation Engineering,

Key Laboratory of Engineering Sediment of Ministry Communications, Tianjin, China

Breakwater is a very important anti-wave structure in harbor and near shore engineering. The stability of

superstructure, armor unit, toe and apron is the major consideration during design. For the calculation on size of armor unit, Hudson's Formula is adopted in many countries' design standard. This formula is developed by extensive hydraulic model tests. But, due to the limitation of test condition, this formula can't reflect the nature situation completely. In actual design progress, the verification of armor unit size is always combining with 3D and 2D stability wave physical model. However, due to the test methodology difference between 3D and 2D model, the scope of application is also different: 2D physical model is suitable for trunk part of breakwater with normal incidence wave, 3D model is more suitable for complex wave condition. In this paper, based on some project of Malaya, from the comparison between original design and model test result, we can know that: the wave condition is very complex in head part of breakwater, 3D model result is more feasible for stability verification; For trunk part of breakwater, the test result of 2D model is quite similar with calculation result of Hudson's formula. But for slant incident wave, the wave forces are lower than those from direct orthogonal waves, the test wave conditions should be hence reduced with relevant angle.

15:00

Preliminary design of decision support system for seawall safety management

ZHENGPING ZHOU, QIHUA ZUO, CHI WANG

Nanjing Hydraulic Research Institute, No. 223 Guangzhou Road, Nanjing, Jiangsu, China.

The efficient management of seawall is essential to maintain a safe community in the coastal areas, and one practical way is to set up a reliable fundamental seawall information system to support seawall management decision. In this paper, the general management situation of seawall constructions along China coastal areas is introduced, and then a Decision Support System for Seawall Safety Management (DSS-SSM) based on Geographic Information System (GIS) and database technology is initially proposed and designed. The basic framework of DSS-SSM consists of three parts which are fundamental information database, model base and evaluation management system. Since all the models are incorporated together, disaster prevention and reduction departments can simulate various scenarios with different considerations, then evaluate seawall security situation and make decisions of coast protection more effectively.

15:15

Development of coastal observation system using a network camera and its application to Hachigasaki Beach, Japan

H. KUROSAKI

Division of Environmental Science and Engineering, Graduate School of Natural Science and Technology, Kanazawa University, Kakuma-machi, Kanazawa, 920-1192, Japan

M. YUHI

School of Environmental Design, College of Science and Engineering, Kanazawa University, Kakuma-machi, Kanazawa, 920-1192, Japan

A local remote sensing system was developed to monitor the morphological processes on sandy beaches. The monitoring station consists of a network camera and a host computer mounted on a high vantage point. The data acquisition procedure is fully automated so that photographic images can be recorded continuously in a cost-efficient way. The system has been applied to the field observation of Hachigasaki beach, Ishikawa, Japan. Continuous measurements have been conducted since November 2007 over an alongshore stretch of approximately 2 km. The accuracy of shoreline detection based on image processing has been confirmed through comparison with an in-situ survey using a total station. Quantitatively good agreements are obtained. Various morphological features have been captured such as the splitting of a sand bar as well as the formation of beach cusps. These results show the high capability of the developed system to remotely measure the coastal morphology on sandy beaches.

Parallel Session 2

Wednesday, 14 December

Estuaries and Ports II

Ballroom C

Chair: Changkuan Zhang

15:45

Influence on flood control when building tidal sluice in Mulan Creek Estuary, Fujian Province, China

X.D. ZHAO, X.M. WANG, X.S. XU

Nanjing Hydraulic Research Institute, 223 Guangzhou Road, Nanjing 210029, State Key Lab of Hydrology-water Resources and Hydraulic Engineering, China

G.H. CHEN

The Mulan Creek Authority for Flood Control Works, Putian 351100, Fujian, China

The tidal sluice was planned to build in the Mulan Creek estuary, but siltation in the rivers downstream sluices is universe in China, usually making the discharge capacity of rivers decrease obviously and threatening the flood control in the upper reaches. In order to study the influence on flood control when building tidal sluice in the Mulan Creek estuary, a physical model was constructed in NHRI, with the horizontal scale of 1/335 and vertical scale of 1/65 respectively. Hydrodynamic environmental change and sediment movement after building tidal sluice were studied, in order to predict the sedimentation rate and the influence on flood control after building tidal sluice.

16:00

Numerical study on the siltation in harbor area of the Hongqili Waterway, Pearl River Delta

C.W. XU, L.Q. ZUO, H.X. LIU

Nanjing Hydraulic Research Institute, Nanjing, China

The Hongqili waterway, one of the main navigation channel in the Pearl River estuarial network, locates in the southeastern part of the Pearl River Delta, where is right adjacent to the Lingding Ocean. Thus this waterway is under the strong influence of both runoff and tides, resulting in sophisticated hydrological environments and erosion & sedimentation variation. A harbor project named Dagang is going to be carried out in the Hongqili waterway in order to enhance the local transportation performance. More than twenty docks of 1000-t class (can be upgraded to 3000-t class) will be constructed according to the design so that large amounts of excavation and dredging will be required in the harbor district and its navigation channels. This paper calculated the future siltation amounts in the excavation and dredging areas after the accomplishment of Dagang harbor. A two-dimensional numerical model was established to achieve this purpose. In this model integrated datasets including hydraulic, tidal and sediment data were all put into consideration. The model verification was based on the data series of both flood seasons (July ~August in 2004) and non-flood seasons (April in 2008, January in 2009).

16:15

The evolution tendency of the south channel of the Changjiang River Estuary, China, in the past 150 years

HUI-MING HUANG, YI-GANG WANG, TONG-JUN YANG, JUAN ZHAO

Key Laboratory of Coastal Disaster and Defense, Ministry of Education, Hohai University, Nanjing 210098, China

The South Channel of the Changjiang River ranges from the lower part of the South Branch to the South and North Passage bifurcation, its evolution has important impacts on its upper and lower reach. In this paper, based on underwater topography data of the South Channel in many typical years from 1842 to 2004, the historical evolutions of the South Channel are studied. The results show that, (1) the South Channel has undergone 3 evolutionary stages, before 1950s, water and sediment could exchange freely between the South and North Channel, during 1950s~1960s, the South and North Channel completely separated, and after 1970s compound channel with separated flood and ebb tide river courses formed gradually; (2) the South Channel evolution is mainly impacted by natural power before 1950s, but human activity functions strengthened gradually after 1950s; (3) in recent years, evolutions of the South Channel mainly reflected in the development of the compound channel, but cross sections are basically stable as a whole.

15:45

Assessment of coastal vulnerability to sea level rise using remote sensing (RS) and geographic information systems (GIS): a case study of Bolinao, Pangasinan, Philippines

S.R. REYES, A.C. BLANCO

Department of Geodetic Engineering, University of the Philippines, Diliman Quezon City, 1101, Philippines

Recent studies have identified the Philippines as one of the Asian countries subject to the major effects of climate change. Provinces situated along the Philippine coasts are considered the most vulnerable to the immediate consequences of sea level rise. Researches have confirmed the varying trends in sea level in the South China Sea, which is one of the largest semi-enclosed marginal seas in the northwest Pacific Ocean. An integrated vulnerability assessment is required to determine the degree of risks and the extent of the potential effects of sea level rise in order to formulate effective and efficient policies/measures related to climate change adaptation. Bolinao, Pangasinan is a province located in northwestern Luzon and bounded on the west by the South China Sea. In this study, three coastal communities in Bolinao, Pangasinan, namely, barangays Luciente 1.0, Germinal and Concordia were assessed for their natural and socioeconomic vulnerability to sea level rise. The socioeconomic data from each barangay were obtained through a qualitative survey. The Socioeconomic Vulnerability Index (SVI) was computed based on population, age, gender, literacy, employment, source of income and household size. Additional parameters include the family's capacity to recover from damage caused by flooding and typhoons and the community's awareness to the changing coastal environment. The Coastal Vulnerability Index (CVI) is calculated using parameters that describe the natural conditions, which include sea level anomalies, coastal topography, tidal range, recorded significant wave heights and coastal geomorphology. Sea level anomalies recorded by satellite altimeters validate the trends in mean sea level for the past decade. Coastal topography was assessed using a digital elevation model (DEM) extracted from high resolution satellite images and elevation values obtained using a terrestrial laser scanner. The tidal range was obtained from existing tide gauge records. All the included parameters for the SVI and CVI are weighted, classified and combined in ArcGIS for the determination of the Total Vulnerability Index (TVI). The integrated vulnerability for the three barangays is characterized in five classes, from very low to very high vulnerability.

16:00

Application of artificial neural network to estimate the long term sea level in 2020

T.L. LEE

Department of Asset Management and Urban Planning, University of Kang Ning, Tainan 709, Taiwan, R.O.C.

**Parallel Session 2
Wednesday, 14 December
Climate Change and Sea Level Rise II
Ballroom B
Chair: Noriaki Hashimoto**

C.C. WEN

Department of Safety, Health and Environmental Engineering, Hungkuang University, Taichung, 433, Taiwan, R.O.C

C.J. HUANG, T.W. HSU

Department of Hydraulic and Ocean Engineering, National Cheng Kung University, Tainan 701, Taiwan, R.O.C.

The problem of climate change has become a hot issue around the world, and many countries are raise concern about this critical change. The United Nations International Strategy for Disaster Reduction (2007) reported that extreme climate will induced the increase the vulnerability of disaster, such as sea levels rise. This paper is aim to develop the neural network to evaluate the long term sea-level data and estimate the possible sea level in 2020 based on the observed tidal gauge data at Fukang Harbor, Taiwan. Comparing with other methods, it can be found that the neural network can be efficiently forecasted the long term sea-level using five years data and the sea level in 2020 has rise.

16:15

Vulnerability change in coastal zones of Vietnam and Japan

H. NOBUOKA

Urban and Civil engineering, Ibaraki University, 4-12-1 Naka-Narusawa, Hitachi, Ibaraki, 316-8511, Japan

M.V. CONG

Civil Engineering, Water Resources University, 175 Tay Son, Dong Da, Hanoi, Vietnam, Vietnam

Preparing of adaptation strategy against global warming is one of the important issues. The purpose of paper is to show the typical effect of adaptation and early adaptation for reducing vulnerability in developed country and developing countries. The quantitative results of vulnerability assessments following trial scenarios of adaptations show that effect of early adaptation is strong in developing courtiers in case of good economy growth.

Parallel Session 2

Wednesday, 14 December

Coastal Management and Shore Protection II

Tang

Chair: Han-Bao Chen, Luwen Qie

15:45

From dynamic sand beach to static rubble mound

FRANS RABUNG

Department of Civil Engineering, Hasanuddin University, Jl. Perintis Kemerdekaan KM 10 Makassar, South Sulawesi, Indonesia

JON B. HINWOOD

Department of Mechanical and Aerospace Engineering, Monash University, Wellington Rd., Clayton, Victoria 3168, Australia

Experience from construction of a self-adjusted rubble-mound breakwater at Grassy, King Island, in Bass Strait, where severe wave conditions was up to 7.6 meter incident waves, together with careful observation on large scale model tests (1:10 geometric Froude similitude without distortion) resulted in

conclusion that stability of rubble mounds depend on mass stability of the mounds. Although the function of individual armor rocks is still important to cover the core layer in order to achieve static stability, use of equilibrium beach profile principles in predicting final profiles will result in more effective use of overall available material and smaller armor rocks. This study combines observation on the prototype, development of equilibrium beach profile theories, progress in reshaped berm-breakwater design, and large scale model tests to define a new procedure for rubble-mound breakwater/revetment trunk design and to predict the future of Grassy breakwater.

16:00

Training work at the mouth of tidal inlet for protection of approach channel to fishing harbor

D.K. MAITI

West Bengal Fisheries Corporation Ltd.

GN 31, Sector- V, Salt Lake, Kolkata-700091, India

M.D. KUDALE, A.V. SITARAMA SARMA

Central Water and Power Research Station

Khadakwasla, Pune- 411024, India

Fishing harbours in India are mostly located in the tidal inlets, which provide natural shelter to the fishing boats. However, siltation near the mouths of tidal inlets and rivers is a perennial problem in the Gangetic Delta in Eastern India. Maintenance dredging involves huge expenditure. Shankarpur, situated along the coast of West Bengal is a traditional fishing area for more than four decades, where mechanized fishing vessels pass through the tidal inlet (locally known as Dubda Canal) for reaching the fishing harbor located inside the channel. Due to gradual accretion, sand spit had been formed at the inlet mouth thereby degrading navigability. Another critical problem was severe erosion on the western side of the channel mouth. Mathematical model studies were carried out to arrive at the suitable option for training works along with dredging of channel. A 425 m long groyne was suggested for the dual purpose of avoiding siltation in the mouth of the channel and to protect the eroding beach at Digha near the inlet. The suggested groyne is low crested and was economized by making it sloping, submerged and using stone-filled gabions in the armour. Later, the crest of the groyne was elevated and it was renovated by placing tetrapods in the armour layer. The design and the performance of the groyne, which highlights the model-prototype conformity has been discussed in the paper.

16:15

Development of deformable rubber membrane parapets

I. CHUN, S. KIM

Department of Civil Engineering, Konkuk University, 1

Hwayang-dong, Kwangjin-ku, Seoul, 143-701, Korea

It's been reported that the global warming effect has invoked the ever increasing typhoon intensity and long-term sea level rise which jointly cause severe wave overtopping of breakwaters or shore dykes. In this paper, **Deformable Rubber Membrane Parapets**

(DRMP) which not only suppress the wave overtopping in storm periods but also can retain coastal seascapes in normal days are presented. With numerical analyses using a nonlinear finite element program and hydraulic experiments, the air controlled expansion and contraction of the parapets are investigated together with their structural behaviors and stability against wave overtopping.

16:30

Analytical research on the reliability of sea dike structure safety

QING-JUN LIU, QI-HUA ZUO, DENG-TING WANG,
ZHENG-PING ZHOU, JIN WANG

Nanjing Hydraulic Research Institute, No. 225, Guangzhou Road, Nanjing, Jiangsu, China.

Safety of sea dike structures is related to several important factors, which usually have some uncertainties in engineering practice, sea dike structure safety by reliability analysis is initially studied in this paper. Firstly, the main influencing factors and the basic methods for the analysis of sea dike structure safety are reviewed, and then the basic framework of reliability analysis system is constructed. Secondly, several sea dike structures failure modes, such as excessive wave overtopping, failure of armor block, local scour of the sea dike toe, seepage, parapet wall failure and overall structure failure are analyzed and the corresponding performance functions are proposed. Finally, the reliabilities of those methods are applied to several engineering case studies.

Parallel Session 3
Thursday, 15 December
Marine Energy I
Ballroom C
Chair: Josie Close, Cameron M. Johnstone

09:30

Design of offshore wind farms

ANDRASS ZISKA DAVIDSEN, FLEMMING JAKOBSEN
*LIEngineering A/S, Ehlersvej 24, DK-2900 Hellerup
 Denmark*

An overview of the work involved in the design of an Offshore Wind Farm is presented. The main structural solution considered is the monopile foundation, but the jacket foundation is also touched upon.

The following structural analyses shall be made for the foundation:

1. In-place analysis: ULS (Ultimate Limit State); FLS (Fatigue Limit State); and ALS (Accidental Limit State, ship impact).
2. Analyses of installation issues (Fatigue damage due to pile driving); and
3. Serviceability Limit States (Comfort Analysis for substation if required).

A monopile foundation is a very dynamic structure. Therefore it shall be analysed by dynamic methods.

The analyses and related calculations are divided into the following topics for the primary steel:

- Pile driving and impact on monopile;
- p-y curves and calculation of soil springs;
- Analysis of natural frequencies;
- Hydrodynamic damping (viscous and radiation);
- SCF analysis for monopile and transition piece, including effect of misalignment and appurtenances;
- ULS and FLS response analyses with: 1. Deterministic analyses; 2. Frequency domain analyses; 3. Time-domain analyses;
- Check of VIV;
- Check of ringing for the steep wave trains;
- Comfort analyses;
- Scour protection;
- Cathodic protection;
- Lifting analyses; and
- Seafastening analyses.

10:00

Physical experiments on the discharge capability of the sluice caisson of tidal power plant

SANG-HO OH, DAL SOO LEE, KWANG SOO LEE, SE CHUL JANG

Coastal Engineering & Ocean Energy Department, Korea Ocean Research & Development Institute, 787 Haeanro

The performance of sluice caisson of tidal power plant was investigated by performing a laboratory experiment in a planar open channel. By installing 1/70 scale model of the sluice caisson in the planar open channel, with the sloping topography in front of and behind the sluice caisson, the water discharge capability was estimated with five different flow rates

and three different water level conditions. By analyzing the experimental results, the relationship among the flow rate, head difference, and the discharge coefficient was found. The obtained discharge coefficient values were significantly smaller compared to the result of a previous study performed in a two-dimensional open channel.

10:15

Upstream wake effect on performance of the horizontal axis tidal current power

C.H. JO, K.H. LEE, J.H. LEE

Naval Architecture & Ocean Engineering, INHA University, 253Yonghyun-dong, Nam-gu Incheon, 402-751, S. Korea

C. NICHITA

Electrical Engineering, University of Le Havre, Le Havre, 76063, France

The rotor initially converting the flow energy into rotational energy is a very important component that affects the efficiency of the entire system. The rotor performance is determined by various design variables. The power generation is strongly dependent on the incoming flow velocity and the size of the rotor. To extract a great quantity of power, the tidal current farm is necessary with multi-arrangement of devices in the ocean. However, the interactions between devices also contribute significantly to the total power capacity. Therefore, the rotor performance considering the interaction problems needs to be investigated to maximize the power generation in a limited available area. The downstream rotor efficiency is to be affected by the wake produced from upstream rotor. This paper introduces the performance of downstream rotor being affected by wakes from upstream rotor which demonstrates the interference for various gaps between devices.

10:30

Development of real-time control and monitoring system for wave energy converters

SHIN-YEOL PARK, BYUNG-HAK CHO, DONG-SOON YANG, KYUNG-SHIK CHOI

Korea Electric Power Research Institute, 65 Munjiro, Yuseonggu, Daejeon, 305-380, Korea

A control and monitoring system (CMS) for the real-time control and data acquisition of an oscillating body type wave energy converter (WEC) has been developed and tested successively. The 2kW class WEC is the prototype of 50kW class target system. The CMS of the WEC is designed to control and monitor the motion of the wave energy extracting bodies and power takeoff unit of the WEC. The CMS consists of local and remote systems, which communicates each other through a wireless local area network (LAN) and/or a commercial CDMA protocols. The local system of the CMS gathers data from the WEC and analyzes the data for the precise monitoring of the WEC condition, and then control the WEC by sending control signals to the actuators. The performance of the CMS has been verified through a series of sea trial tests.

Parallel Session 3
Thursday, 15 December
Estuaries and Ports III
Ballroom B

Chair: Zheng Gong, Masatoshi Yuhi

09:30

Preliminary analysis of the effects on the Yangtze Estuary after Three-Gorge Reservoir operation

X.P. DOU

Nanjing Hydraulic Research Institute, 223Guangzhou Road Nanjing, Jiangsu 210029, China

X.Q. CHEN, Y.X. YAN

Hohai University, State Key Lab. of Hydrology-water Resources and Hydraulic Eng.

Nanjing, Jiangsu 210098, China

In this paper, the topography and the characteristics of flow and sediment at the estuary are analyzed. By using the hydrology data measured at Datong Station, the long-term variations of flow and sand upstream Datong Station are also analyzed. The conclusions about the changes of flow, sand, salt intrusion and sandbank in the estuary are summarized according to the previous feasibility study for the Three-gorge Project (TGP). The data measured during TGP operation from 2003 to 2007 are also analyzed.

09:45

The research on hydrodynamic mechanism of morphology revolution of the Xiaomiaohong tidal channel in radial sand ridges, Jiangsu Province, China

K.F. CHEN

State Key Laboratory of Hydrology-Water Resources and Hydraulic Engineering, Hohai University, Nanjing 210098, China;

River and Harbor Engineering Department, NanJing Hydraulic Research Institute, Nanjing, 210024, China

L.L. YU

River and Harbor Engineering Department, NanJing Hydraulic Research Institute, Nanjing, 210024, China

The comparison of the recent 40 years' terrain dataset showed the entrance of XiaoMiaoHong channel had an evolutionary tendency of deposition at north and erosion at south waterway. The north trough silted constantly to disappear while the south trough developed adequately. This article discussed the mechanism of the change in deposition and erosion at different channels these years from the viewpoint of hydrodynamic, according to analysis of field data and the tidal current Mathematical model we established. The result showed XiaoMaoHong Tidal Inlet was mainly controlled by tidal. The reason, that XiaoMiaoHong channel exhibited a state of deposition at north and erosion at south recent years, has close connection with the tidal current characteristics at this area. The north channel, which exhibits deposition, is a channel that flood predominate, no matter according to its flood-ebb property or the direction of residual current. While the south channel, which exhibits erosion, is just the opposite.

10:00

Numerical simulation of tidal wave deformation in lower reach caused by floodgate in estuary

X.Z. ZHANG, X.P. DOU, X.M. WANG, X.D. ZHAO, X.S. XU

Nanjing Hydraulic Research Institute, 223 Guangzhou Road, Nanjing 210029, Key Lab of Port, Waterway and Sedimentation Engineering of the Ministry of Transport, China

Siltation in the rivers downstream of floodgates is serious in China, making the discharge capacity of rivers decrease obviously and threatening the flood control in upper rivers. Tidal wave deformation is one conclusive dynamic factor leading to siltation downstream of floodgates in estuaries. The hydrodynamic characteristics of tidal wave deformation are different with different river length downstream of floodgates, so the fluvial processes and morphology characteristics are also different. A 2-D numerical model is established to simulate the tidal wave deformation with different-length river downstream the floodgate. The changes of tidal level, flow velocity and phase difference are simulated before and after the construction of floodgate. The length of river downstream of floodgates influences tidal wave deformation obviously, and several conclusions are obtained in this paper which can provide some theoretical basis for the prediction and analysis of the siltation characteristics in lower reach caused by floodgates with different length in estuaries.

10:15

Flow change induced by shift and modification of submerged weir installed at Han River Estuary

KYONGOH BAEK

Department of Civil Engineering, Hankyong National University, 327 Chungang-ro, Anseong-si, Gyeonggi-do, Korea

An estuary is the wide part of a river where it joins the sea. It has an unique ecosystem and potential values for economics, whereas it is hard to control the water level and bed changes in an estuary due to a tidal movement. In this study, the flow characteristics of Han River Estuary located in Korea were investigated by using a two-dimensional numerical model according to the assumption of shift and modification of the Shingok submerged weir. The two-dimensional analysis has contributed to our understanding of the hydraulic effects induced by shift of the weir on the topography, especially wetlands. The tide and flow discharge of 2007 were adopted as an input data for the simulation. The tidal data contained both spring and neap tides, and the flow discharge condition was divided into monsoon and normal seasons. The boundaries of this study were Han River Bridge, Tongil Bridge, and Yu island. The numerical model which was used as a tool to simulate the flow field was calibrated and verified based on the measured data acquired from Jeonlyu station. The simulation results showed that influence area of seawater changed depending on the weir shift, and the water level at particular station fluctuated according to the condition

of tide and flow discharge. Especially the low-tide level increases seriously due to the weir shift at Janghang wetland located in Han River Estuary. Thus it is expected that the wetlands where an area of land consisting of soil saturated with moisture are transformed into completely submerged land. Also the tidal effects fall back to the downstream by means of weir shift.

Parallel Session 3
Thursday, 15 December
Marine Ecology and Environment I
Tang
Chair: Satoquo Seino, Wai Thoe

09:30

Capture and clogging behavior of organic mud in sand beds

N. TOUCH, N. SHINYA, T. HIBINO

Department of Civil and Environmental Engineering, Hiroshima University, 1-4-1 Kagamiyama, Higashi-Hiroshima City, 739-8527, Japan

S. FUKUOKA

Research and Development Initiative, Chuo University, 1-13-27 Kasuga Bunkyo-ku, Tokyo, 112-8551, Japan

The objective of this research is to present an experimental study of the capture and clogging behavior of organic mud in saturated sand beds. Such work has yielded a large body of information which can be used to understand the sludge-ization of tidal flats. Key aims are to delineate the decline in permeability due to the clogging of organic mud, and to understand the restoration of permeability due to the release of organic mud. It is obvious that the permeability decreases due to the clogging of organic mud, and that this permeability finally becomes constant if there is no deposition of organic mud on the surface of sand beds. Moreover, it was found that the residual organic mud could not be completely released from sand beds by infiltration flow; thus, the permeability could not be restored to the initial permeability.

09:45

Spatio-temporal patterns and the variation mechanism of nutrients in the Yangtze Estuary

Y. CUI, G. HUANG

RCEES Chinese Academy of Sciences, Shuangqing Road 18, Beijing 100085, China

Q. CHEN

China Three Gorges University, Yichang 433002, China

S. QU

Colleges of Hydrology and Water Resources, Hohai University, Nanjing, 210098, China

Basing on the data from four times surveys, the spatio-temporal distribution patterns and the variation mechanism of nutrients in the Yangtze estuary were analyzed. The nitrate and silicate concentration exhibited an eminent 'double tongue' pattern in summer and autumn, however, it moved southward along the shore in spring and winter. Phosphate concentration showed the similar 'double tongue'

pattern in summer and autumn, but the northeast frontal zone was more west comparing to that of the nitrate and silicate. The nitrate and total dissolved nitrogen (TDN) were positively correlated in all seasons; similarly the phosphate was positively correlated with total dissolved phosphorus (TDP) and total phosphorus (TP) in all seasons. It was also found that nitrate, silicate and phosphorus all had high negative correlation with salinity, which meant that the nutrient dynamics in the estuary was predominantly governed by the freshwater discharge. The Redfield ratio analyses revealed that SiO₃-Si/DIN was obviously higher in the far-shore area than the near-shore area. The DIN/PO₄-P was higher than the Redfield ratio 16 in the entire study area, and it gradually decreased from near-shore to far-shore.

10:00

The variation trend of nutrient flux from Yangtze River and related impact on Yangtze Estuary

G.X. HUANG, Q.W. CHEN, Y.P. CUI, F. YE

State Key Laboratory of Aquatic Chemistry, Research Center for Eco-Environmental Sciences, 18 Shuangqing Road, Haidian District, Beijing, 100085, China

B.D. WANG

Key Lab for Marine Ecological Science, the First Institute of Oceanography, State Oceanic Administration, 6 Xianxialing Road, Hi-Tech Industrial Park, Qingdao, 266061, China

Due to climate change and mankind activities, especially reservoirs' operation such as Three Gorge reservoirs (TGP) and pollutions from industry, agriculture and domestic sewage in the Yangtze River basin, the nutrient flux at Datong hydrological station has significant changes in recent years. Based on the data measured at Datong station in different period, the changing trend of nutrient flux including discharge, suspended solids (SS), total phosphorus (TP), total nitrogen (TN) are analyzed. Then a three-dimensional water quality model based partially on the open source code of Elfe, Wasp and EFDC are developed to simulate the C, N, P, Si cycling processes. The model is applied to the region from 120.6°E to 124.5°E and from 29.5 °N to 32.5 °N, including Yangtze estuary, Hangzhou bay and two important fishing grounds named Zhoushan and Lvsu. The upstream boundary condition at the Tianshenggang station in the 3D model are obtained by a 1D river water quality model which covers the region from Datong to Wusong using the related inflow at the Datong station. The downstream boundary conditions at open sea are given reasonably by a coarse grid model which including East China Sea. The measured data of Yangtze Estuary and Hangzhou Bay from 2004 to 2005 after TGP project are used to verify the model. The results show that the suspended sediment decreases continuously from annual value 4.6×10^8 to 2.6×10^8 in 2003 and then fall further to 1.3×10^8 ton in 2008. TP and TN have a rising trend because of increasing pollution load, especially from the middle and lower reach of Yangtze River in recent years. The variation of inflow flux of nutrient matter has great influence on the concentration of nutrients in the front of Yangtze delta where

confluence region of Yangtze main inflow and upwelling from the out sea exists.

10:15

Multivariate statistical analysis of the seasonal variation of chlorophyll distribution in the north Indian Ocean

SUSHANT DAS, GIRIJA JAYARAMAN

Centre for Atmospheric Sciences, Indian Institute of Technology, Hauz Khas, New Delhi 110016, India.

BEENA KUMARI

Marine and Earth Sciences Group, Space Applications

Centre (ISRO), Marine Ahmedabad, 380015, Gujarat, India

Marine ecosystems in general and Phytoplankton in particular are influenced by the variability in features such as sea surface temperature (SST), advective processes (upwelling and upper ocean mixing), mixed layer depth, horizontal and vertical transport, and ecological dynamics. Chlorophyll (chl-a), the major photosynthesis constituent in the phytoplankton influences the colour of ocean water. Remote sensing of ocean colour helps to monitor the variation in biological properties of the ocean on a larger spatial scale. The present study, related to north Indian ocean, deals with a multivariate statistical analysis to study the seasonal variation of chlorophyll with variables such as Sea Surface Temperature (SST), Mixed Layer Depth (MLD) and Nitrate. Remote sensed data was used for Chl-a (Sea-WiFS) and Sea Surface Temperature (MODIS-Terra) while for nitrate and mixed layer depth, NASA Ocean Biogeochemical Model (NOBM) derived data was used. The region of study corresponded to four different zones: i) North eastern Arabian Sea, ii) Southern Arabian Sea, iii) Western Bay of Bengal and iv) Andaman Sea. The region of Northeastern Arabian Sea was found to be biologically more productive compared to the Southern Arabian Sea during the winter monsoon (FMA) as it showed large variation of chlorophyll content mainly due to winter cooling and convection overturning. The region in the Southern Arabian Sea showed high chlorophyll content during the summer monsoon (JAS) mainly due to the upwelling. The region in the Bay of Bengal showed high chlorophyll content during the summer monsoon but much lesser than that of Arabian Sea due to the stratification of layers. The region in Andaman Sea showed high chlorophyll concentration during the winter monsoon mainly due to coastal upwelling. The time series monthly data from 2001-2006 of Chl-a, SST, MLD & nitrate was studied simultaneously in all the zones through a multivariate statistical analysis. The correlation between Chl-a and SST was negative in all the zones. The multivariate regression analysis using all the data variables showed improved correlation coefficient between the observed and regressed chl-a data in all the zones.

10:30

Impact of oil and gas production activities on cohesive sediment and biological adaptation

M. CHEN, S. WARTEL

Hydrology and Hydraulic Engineering, Vrije Universiteit Brussel, Pleinlaan 2, B-1050, Brussels, Belgium

F. FIERS

Recent Invertebrates, Royal Belgian Institute of Natural Sciences, Vautierstraat 29, B-1000, Brussels, Belgium

The potential impacts of oil and gas production activities on marine environment and ecological habitats are of growing concerns. This study presents the effect of oil and gas production activities induced mud contamination on meiobenthic community, and the interactions between meiobenthic and cohesive sediments in the Campeche Shelf, Yucatan, Mexico. The meiobenthic community has potential merits in environment monitoring, because it is not affected by physical disturbance to the same degree as macrofauna, and is more stable than macrofauna but with a shorter generation time, and moreover, its life cycle is spent entirely within the sediment. The field investigations and data analyses showed that one of the key factors seriously affecting the study area is the deposition of a cohesive clay layer, bentonite, introduced from the oil production sites. The occurrence of such bentonite clay significantly changed the natural sediment granulometry as observed in the grain-size frequency distribution where a narrow peak in the size fractions between 2 and 4 μm was predominant. Such peak occurred frequently in the area surrounding the oil production sites. Contrary to what may be expected, the increase of clay content had no influence or even had a negative influence on the density of nematodes. The nematode to copepod ratio normally would increase when the content of fine fractions increases (or with decreasing particle size). However this study showed that the nematode-copepod ratio increased with the decreasing clay content. The observed contradistinctions may be explained by the deposition of bentonite clay that was artificially imported to the study area by oil and gas production activities and caused a lagged impact on the meiobenthic community. This study showed that the interactions between meiofauna and cohesive sediments as an indicator can give valuable information on environmental changes and provide a better understanding of the impact of oil and gas production activities on the marine benthic realm.

Parallel Session 3

Thursday, 15 December

Hydrodynamics I

Ming II

Chair: Adrian Wing-Keung Law, Wataru Kioka

09:30

Experimental study on wave crest height on a gravity type complex structure

HAIYUAN LIU

Tianjin Research Institute for Water Transportation Engineering,

Key Laboratory of Engineering Sediment of Ministry Communications, Tianjin 300456, China

BAOYOU ZHENG, HANBAO CHEN, BAOLEI GENG
*Tianjin Research Institute for Water Transportation
 Engineering,*

*Key Laboratory of Engineering Sediment of Ministry
 Communications, Tianjin 300456, China*

By theory analysis and physical model test, the disciplinarian on wave crest height has been studied when waves act the single and group pile-gravity type complex structures. Get the relationships between the wave crest and wave height, wave length, wave period, dimension of pile-gravity type complex structure and wave incidence angle and put forward the calculation method on wave crest height of pile-gravity type complex structure. The method can be adopted to design the practical project for wharf surface elevation of pile-gravity type complex structure.

09:45

Wave-field flow structures developing around large-diameter vertical circular cylinder

G. ALFONSI, A. LAURIA, L. PRIMAVERA
*Fluid Dynamics Laboratory, Università della Calabria
 Via P. Bucci 42b, 87036 Rende (Cosenza), Italy*

In this work the issue of wave-induced flow structures that develop around a large-diameter surface-piercing vertical circular cylinder is addressed. A strictly-linear wave case is considered and simulated numerically, solving the Euler equations in primitive variables, and the results are compared with those obtained from the corresponding close-form velocity-potential solution. Then, the *swirling-strength* criterion for flow-structure education is applied to the primitive-variable Euler-equations-derived velocity field. It is found that differently-shaped flow structures develop at the free surface and under the free surface, in particular at the cylinder wall. This field of structures is not detectable from the potential-derived velocity field, due to the purely mathematical nature of the latter.

10:00

Analysis of wave interaction with a submerged slightly inclined porous plate with a partially reflecting sidewall

Y. LIU
*Shandong Provincial Key Lab of Ocean Engineering, Ocean
 University of China, Qingdao, 266100, China*

Y.C. LI
*State Key Lab of Coastal and Offshore Engineering, Dalian
 University of Technology, Dalian, 116024, China*

This study examines the reflection and transmission coefficients of a submerged slightly inclined porous plate with a partially reflecting sidewall. The multi-domain boundary element method (BEM) is used to obtain the solution. The effects of several main factors, including the plate inclined angle, the reflection coefficient of sidewall and the relative space between the plate and the sidewall, on the reflection and transmission coefficients of the porous plate breakwater are examined. Some significant results are presented to practical engineering.

10:15

Numerical modelling of wave-induced soil response around breakwater heads

D.-S. JENG, Y. ZHANG
*Center for Marine Geotechnical Engineering, State Key
 Laboratory of Ocean Engineering, Shanghai Jiao Tong
 University, Shanghai 200240 China*

J.-S. ZHANG, C. ZHANG
*State Key Laboratory of Hydrology-Water Resources and
 Hydraulic Engineering, Hohai University, Nanjing, China*
 P. L.-F. LIU
*School of Civil and Environmental Engineering, Cornell
 University, Ithaca, NY 14853, USA*

The evaluation of wave-induced pore pressures and effective stresses in a porous seabed near breakwater heads is important for coastal engineers involved in the design of coastal structures. Most previous studies have been limited to two-dimensional (2D) or three-dimensional (3D) cases in front of a breakwater. In this paper, a three-dimensional numerical model for the wave-induced seabed response around breakwater heads is developed. The 3-D wave model was based on the Navier-Stoke equation with wave generation model. The seabed is simulated by the Biot's poro-elastic dynamic model. Both models are linked together to form the PORO-WSSI (3D) model. Based on the newly model, the soil permeability and the degree of saturation significantly affect the wave-induced oscillatory pore pressures.

10:30

Coastal erosion caused by cavitation bubble implosion: micro-view on the bubble dynamics

Y.X. YANG
*DHI-NTU Centre and School of Civil and Environmental
 Engineering, Nanyang Technological University N1 -B1a-03,
 50 Nanyang Avenue, 639798, Singapore*

S.K. TAN
*Nanyang Environment and Water Research Institute and
 School of Civil and Environmental Engineering, Nanyang
 Technological University, N1- -B1a-03, 50 Nanyang Avenue,
 639798, Singapore*

Q.X. WANG
*School of Mathematics, the University of Birmingham,
 Watson Building, room 325, Edgbaston, B15 2TT
 Birmingham, United Kingdom*

Recently, coastal erosion in the form of inertial cavitation has been generally accepted. Air pockets in an incoming wave are forced into the surface of the coastal cliff, and then the force of the wave compresses the air pockets until the bubble implodes, giving off various forms of energy that erode the rock. This paper studies the behaviour of a cavitation bubble in a compressible liquid near a rigid boundary, when it is subjected to a harmonic wave. Because of the extremely short life time of the bubble, we assume the wave pressure acting on the bubble surface is constant. An approximate perturbation theory by using the method of matched asymptotic expansions is used to incorporate the influence of the compressibility of the liquid. The rigid boundary creates an asymmetry in the flow field that causes bubble to collapse non-spherically. A numerical model based on the mixed Eulerian-Lagrangian (MEL) method and the boundary

integral method (BIM) for bubble dynamics in a weakly compressible liquid is developed. The shock wave pressure caused by the high speed jet hitting on the rigid boundary is found to be of sufficient magnitude to initiate erosion of the loose boundary.

Parallel Session 3
Thursday, 15 December
Wave Loading
Sung I
Chair: Liang Cheng, Guohai Dong

09:30

Experimental investigation of wave loads on offshore platform with inverted cone column

JING ZHAO, YANLONG QIN, SHIPENG WANG
*Research Institute of Engineering Technology, CNPC
 CNPC Key Laboratory of Offshore Engineering Tanggu
 Jintang Road 40#, 300451, Tianjin, China*

The configurations of platform can affect its hydrodynamic characteristics and strength properties obviously. A new design of offshore platform, which with inverted cone column considering the frozen condition in winter, has been proven to improve its overall anti-ice performance. But little research has been conducted in the effect of wave loads on this type of structures. The analysis about the experimental of wave loads on inverted conic structure is carried out to discuss the pressure characteristics of structure under different experimental conditions such as wave height.

09:45

Research of wave force on the submerged caisson for pile-gravity complex wharf

B.L. GENG, B.Y. ZHENG, H.B. CHEN, H.Y. LIU
*Key Laboratory of Engineering Sediment of Ministry
 Communications, Tianjin Research Institute for Water
 Transportation Engineering, No.2618 Xingang Erhao Road,
 Tianjin, 300456, China*

The main objective of this study is to analysis the wave force on submerged caisson with pile-gravity composite structure. In this paper, formulas based on the modified Goda's formula about wave force on the vertical wall in Japan standard are given and wave crest action and wave trough action are considered respectively. A series of experiments with 1/50 scaled caisson model were carried out to determine the coefficients in former equations. The conclusions show that the calculated values are consistent with the test values, and those equations can be used to calculate the wave forces on single caisson as a semi-empirical method.

10:00

Numerical modelling of breaking wave impact pressure on a vertical wall

N. SENTHIL KUMAR, S.A. SANNASIRAJ
*Department of Ocean Engineering, Indian Institute of
 Technology Madras, Chennai, Tamilnadu, India*

Breaking waves impart higher impact pressures on coastal structures than non-breaking waves. An

estimation of breaking wave impact pressures on a vertical wall is important for its structural stability since such type of structures are frequently subjected to breaking wave impact. In the present study, the breaking wave impact on a vertical wall has been theoretically modelled using the pressure impulse theory. The pressure impulse formulation governed by the Laplace equation is solved numerically using finite element method. Numerical prediction of plunging wave impact pressures using measured pressure rise-fall time has been found to compare well with earlier experimental measurements. The maximum impact pressure occurs slightly above the still water level.

10:15

Experiment study on spectrum of wave and force on cylinder structure

HANBAO CHEN
*School of Civil Engineering, Tianjin University, Tianjin,
 China; Tianjin Research Institute for Water Transport
 Engineering, Tianjin 300456, China*

HAIYUAN LIU, HAICHENG LIU
*Tianjin Research Institute for Water Transport Engineering
 Tianjin 300456, China*

By the wave physical model, measure the wave force including the character value and process. Statistic parameter and spectrum of wave and wave force were analyzed respectively. The wave force spectrums were analyzed corresponding to swell and storm wave, compare the force spectrum and wave spectrum that is JONSWAP spectrum that adopted in wave simulation. A series of parameters were calculated to meet the measurement results. The relation between wave spectrum and force spectrum was obtained.

10:30

Wave induced pressures on crown wall of KOLOS armoured breakwater

A. ARUNJITH, S.A. SANNASIRAJ, V. SUNDAR
*Department of Ocean Engineering, Indian Institute of
 Technology Madras, Chennai, Tamil Nadu, 600036, India*

Breakwaters are designed as either overtopping or non-over topping structures. In case of a non-overtopping breakwater, it is not uncommon to provide concrete crown walls at the crest of the breakwater to minimize or avoid overtopping. The wave induced dynamic pressures on the crown wall is the most essential parameter which dictates its design. Several studies in the past have been on this aspect for crown walls of breakwaters armoured with different types of armour units, including natural rubbles stones and artificial units like ANTIFER, CUBIPODS etc. Recently introduced armour blocks "KOLOS", a modified version of DOLOS have been considered for a detailed investigation for its hydrodynamic characteristics. This paper presents the salient results on the pressures due to regular waves on the crown wall fronted by KOLOS through a well controlled experimental program.

Parallel Session 4
Thursday, 15 December
Marine Energy II
Ballroom C
Chair: Chul Hee Jo, Philippe Gourbeville

11:00

Tidal range and tidal current energy resources in neighboring seas of Korea

B.H. CHOI, B.I. MIN

Department of Civil and Environmental Engineering, Sungkyunkwan University, 300 Chencheon-dong, Jangan-gu, Suwon, Gyeonggi-do 400-746, Korea

The highest tides in South Korea are found along the northwest coast between latitudes 36-38 degrees and the number of possible sites for tidal range power barrages to create tidal basins is great due to irregular coastlines with numerous bays. At present Lake Sihwa tidal power plant is completed. The plant is consisted of 10 bulb type turbines with 8 sluice gates. The installed capacity of turbines and generators is 254MW and annual energy output expected is about 552.7 GWh taking flood flow generation scheme. Three other TPP projects are being progressed at Garolim Bay (20 turbines with 25.4MW capacity), Kangwha (28 turbines with 25.4MW capacity), Incheon (44 or 48 turbines with 30 MW capacity) and project features will be outlined. The introduction of tidal barrages into four major TPP projects along the Kyeonggi bay will render wide range of potential impacts. Preliminary attempts were performed to quantify these impacts using 2 D hydrodynamic model demonstrating the changes in tidal amplitude and phase under mean tidal condition, associated changes in residual circulation (indicator for SPM and pollutant dispersion), bottom stress (indicator for bedload movement), and tidal front (positional indicator for bio-productivity) in both shelf scale and local context. Tidal regime modeling system for ocean tides in the seas bordering the Korean Peninsula is designed to cover an area that is broad in scope and size, yet provide a high degree of resolution in strong tidal current region including off southwestern tip of the Peninsula (Uldolmok , Jangjuk, Wando-Hoenggan), Daebang Sudo (Channel) and Kyeonggi Bay. With this simulation system, real tidal time simulation of one-month (two spring-neap cycles) was performed to estimate spatial distribution of tidal current power potentials in terms of power density, energy density and then extrapolated annual energy density.

11:15

Morphological effect of flapping-type tidal power generator

J.H. KO, J.-S. PARK, K.-S. LEE

Korea Ocean Research & Development Institute, 787 Haean-Ro, Sangnok-Gu, Ansan, Korea

T.Q. LE, D. BYUN

Dept. of Aerospace and Information Engineering, 1 Hwayang-dong, Kwangjin-Gu, Seoul 143-701, Korea

Inspired by nature, flapping-type tidal power generators have been proposed since the early 21st

century. The improvement of power generation ability is one of key issues in commercializing the flapping-type generators. According to the researches of flapping-type propulsion, fluid-dynamic characteristics have been improved by morphologies such as the corrugation of scallops or the chamber of insect wings. In this study, we explore the effect of the corrugation and chamber, by mimicking a scallop, on the power generation ability. Two dimensional Navier-Stokes simulation is utilized for the numerical analysis of the morphological effects. From this analysis, we find that the morphological effects are also considerable in the flapping-type power generators, and suggest an optimal morphology in terms of the corrugation and chamber.

11:30

Performance of tidal stream turbine adapted to bridge pier protection structures

SANG-HO OH, JIN-HAK YI, SE CHUL JANG

Coastal Engineering & Ocean Energy Department, Korea Ocean Research & Development Institute, 787 Haeanro Ansan, 426-744, Republic of Korea

GUNWOO KIM

Division of Ocean System Engineering, Mokpo National Maritime University, 91 Haeyangdaehang-Ro, Mokpo, 530-729, Republic of Korea

SANG RYUL LEE

LeeWoos, 190-1 Sangdaewon-dong, Seongnam, 462-721, Republic of Korea

The preliminary results of physical and numerical experiment are presented for investigating the performance of the tidal stream turbine system, which is under development for application to the gap between the bridge protection structures. The advantage of this system is acquisition of high flow velocity due to flow acceleration at the gap which allows efficient power generation from the tidal stream turbine.

11:45

Study of the influence of tropical cyclone on offshore wind turbine generator system

LIANG PANG, ZHI-QIANG LI, HONG-RUI YANG

College of Engineering, Ocean University of China, Songling Road No.238, Qingdao, 266100, China

Offshore wind energy is one of the most important new energies that are developing fast in the world. There is an in-neglecting problem in offshore wind turbine system similar to other offshore structures that the offshore wind turbine system is in the severe sea states. Especially in the regions which influenced by tropical cyclones, the strong winds, surges and huge waves induced by storms will lead to the structure failures and make large losing. In meteorology field, more attentions are paid in the mechanism of the storm process than the effect of storms to the structures. While in engineering field, the combination of wind, wave and current with some return period is selected according to the design code, then the response analysis of structures will be performed. The influence of storm induced extreme sea environment factors to the wind turbine system is not considered reasonably. According to the previous research, Multivariate

Compound Extreme Value Distribution (MCEVD) is effective in the joint probability prediction of extreme sea states. It also can be used in the probability analysis of structure stress. And grey model is adaptive for the prediction based on short stochastic sample series. It can be used in reliability analysis of offshore structures. In this study, numerical simulation, probability analysis and prediction based on theory of grey system are used to propose a nested model for the reliability analysis of offshore wind turbine system. The model is consisted of MCEVD, Grey Markov Chain Model (GMCM) and structure dynamic response model. Using the nested model, the influence of tropical cyclone to the offshore wind turbine system in the South China Sea is analyzed.

12:00

Development of in-stream hydro power pilot plant in Korea

Y.C. PARK, C.S. MYUNG

ECOCEAN Co., Ltd., Unit 403, Industrial Technology R&D Center, 7-27, Songdodong, Yeonsugu Incheon 406-840, Rep. of Korea

KI-DAI YUM

Korea Ocean Research & Development Institute, Ansan P.O. Box 29, Seoul 425-600, Rep of Korea

SHIN TAEK JEONG

Division of Civil and Environmental Engineering, Wonkwang University, #22 Wonkwangdaehak-ro, Iksan, Jeonbuk, 570-749, Rep of Korea

In order to develop techniques for utilizing clean and renewable hydro energy, Korea has been conducting a study on in-stream hydro energy system. Field measurements have been performed in a discharge canal at the Hadong Power Plant Company. Helical-type hydro turbine has been selected on the basis of field conditions and results of preliminary experiments. The turbine jacket, kinetic energy transfer system and electrical facilities for the in-stream hydro energy system (IHES) are designed. The established IHES has been successfully operated. The present application to a discharge canal is advantageous since water current speed and temperature in the canal is decreased and adverse impacts on nearby ecosystem can be improved.

12:15

Experimental and numerical simulation tools for floating wind turbines

FERRANT PIERRE, ROUSSET JEAN-MARC, COURBOIS ADRIEN, PHILIPPE MAXIME

Laboratoire de Mécanique des Fluides, Ecole Centrale de Nantes, 1 rue de la Noe, BP 92101, 44321 Nantes – France

Wind energy business is moving offshore providing an alternative to land-based wind turbines. Many projects around European coasts have to deal with large water depths (50 -100 m) while gravity based wind turbines may not be a cost-effective solution. On the other hand, floating wind turbines could be able to overcome this main drawback and several different innovative systems are currently tested in labs to prove concepts and to improve the preliminary designs.

In fact the design of a floating wind turbine is not as easy as it could be expected. Hydrodynamic forces acting on the floating body and aerodynamic forces

acting on the wind turbine are interacting, the structural responses are complex and could have a negative influence on the power rate and the fatigue of the whole system.

Physical modelling and numerical modelling of floating wind turbines are then required to be as accurate and complete as possible. The present paper is presenting the tools which are under development at Ecole Centrale Nantes (France) in order to tackle challenges brought by marine wind turbines.

We describe first an innovative wind generation system over a wave basin which can simulate several characteristics of an offshore wind. Preliminary results are presented showing the ability to reproduce low frequency fluctuations with the fan RPM.

Concurrently numerical approaches are also evaluated, their results being compared to actual published data and to next experimental data from our wave basin. A comparison is performed in order to evaluate limitations of time and frequency domains simulations. As conclusion some significant aspects are highlighted in order to contribute to the establishment of good practises to test floating wind turbines in wave basins.

12:30

Assessment of wave energy source near Dangan Islands

ZHE MA, HONG DA SHI, ZHEN LIU

Department of Ocean Engineering, College of Engineering, Ocean University of China, Qingdao, China

The paper provides a wave resource assessment for region around the Dangan Islands located at the South China Sea. The spatial distributions for the seasonal and annual averaged wave power were obtained a Cartesian grid covering longitudes of 113.8-114.5°E and latitudes of 33.67-35°N. In order to obtain the wave power at project points, numerical simulations were performed with respect to the monthly averaged waves. The correlation between the significant wave height and energy period was considered to adjust the nearshore wave power obtained by the numerical simulation.

Parallel Session 4

Thursday, 15 December

Estuaries and Ports IV

Ballroom B

Chair: Keisuke Nakayama, Y.Y. Wan

11:00

Effect of large scale tidal flat reclamation on hydrodynamic circulation in Jiangsu coastal areas

J.F. TAO, T. YANG, F. XU

State Key Laboratory of Hydrology-Water Resources and Hydraulic Engineering, Hohai University, 1 Xikang Road, Nanjing, 210098, P. R. China

College of Harbor, Coastal and Offshore Engineering, Hohai University, 1 Xikang Road Nanjing, 210098, P. R. China

J. YAO

State Key Laboratory of Lake Science and Environment, Nanjing Institute of Geography and Limnology, Chinese

*Academy of Sciences, 73 East Beijing Road
Nanjing, 210008, P. R. China*

A process-based 3D hydrodynamic model was developed to study the changes in hydrodynamic circulation in Jiangsu coastal areas due to a large scale tidal flat reclamation planning project. The engineering sedimentation method was used to calculate the possible sediment siltation intensity in the vicinal sea area of reclamation project. It found that: the location of tide-free point of M2 tidal constituents moved about 3km from the present place to northeastward. The propagation velocity of tidal wave from Sheyang estuary to Jianggang is accelerated and tidal range is enlarged. After the completion of the first and second stage's reclamations, the peak velocity and unit tidal discharge in Xiyang tidal inlet increased about 20% and 5%~10%, respectively. But there were little changes in other tidal inlets due to beach reclamation near these tidal inlets. After the completion of the third stage's reclamation, both the peak velocity and unit tidal discharge in Xiyang tidal inlet further increased over 20%, however, decreased in Xiaomiaohong tidal inlet about 20% and 10%, respectively due to drastic reduction in tidal inlet width. The annual siltation intensity was about 30~50 cm/a near the tidal flat reclamation project.

11:15

Long-term hindcasting of wave climate for Jiangsu coast

Y.P. CHEN

State Key Laboratory of Hydrology-Water Resources and Hydraulic Engineering, Hohai University, 1 Xi Kang Road, Nanjing, 210098, China

C.K. ZHANG

College of Harbor, Coastal and Offshore Engineering, Hohai University,

1 Xi Kang Road, Nanjing, 210098, China

The latest version of the third generation spectral wave model, WAMC4, is adopted for the long-term hindcasting of wave climate for the Jiangsu coast. The model is driven by the NCEP/NCAR reanalysis wind data spanning the period of 1951-2010. A 3-level nested downscaling framework, covering the oceanic domain (Northwest Pacific Ocean), the regional domain (East China Sea) and the local domain (Jiangsu Coast), is established to simulate both wind and swell waves. Based on the long-term modeling results, the distributions of mean and extreme wave heights are obtained. Those results are valuable for the coastal engineering such as the large scale tidal flat reclamation project along the Jiangsu coast.

11:30

Measurements of tidal current and surface current in Tokyo Bay by HF radar

YUSUKE OZAWA

Civil Engineering, Tokyo City University Graduate School, 1-28-1 Tamadutsumi, Setagaya Ward, Tokyo, Japan

KAZUO MURAKAMI

Department of Urban and Civil Engineering, Tokyo City University,

1-28-1 Tamadutsumi, Setagaya Ward, Tokyo, Japan

Drifter garbage is transported by surface current. Surface current consists of tidal component and wind driven current. So we analyzed the data of surface current observed High Frequency Radar and ocean surface wind by means of multi-regression analysis in Tokyo Bay. The results of the analysis show that the horizontal distribution of wind driven current is influenced by bay topography. The wind effect estimated by numerical simulation is smaller than effect estimated by HFR data.

11:45

Investigation on overtopping rate of north bank seawall in Qiantang Estuary due to super typhoons

SHICHANG HUANG, JINCHUN HU, YALI XIE, XIN ZHAO

Zhejiang Institute of Hydraulics and Estuary, Hangzhou, Zhejiang Province, 310020, China

The numerical models containing estuarine and coastal numerical model (MIKE21) and wave propagation model (SWAN40.71) are used. Basing on the applicability of the validation, the storm tide and typhoon waves in front of the seawall along north bank of Qiantang Estuary in Zhejiang Province are simulated, which is caused by No.5612 typhoon that is most powerful typhoon landing China, and is selected as a typical super typhoon in this paper. Overtopping rate and its action on seawall are simulated in wave sluice. Simulation results show that: 1) Super typhoon lands at average annual highest tidal level along north route, overtopping rate of north bank can reach $0.4 \sim 1.4 \text{ m}^3/(\text{m}\cdot\text{s})$, and the outburst of seawall will occur. Landing at high tidal level of mean astronomical tide, overtopping rate of seawall from Gp to Zp can reach $0.17 \sim 0.5 \text{ m}^3/(\text{m}\cdot\text{s})$, the seawall will be seriously damaged, and then will burst. Landing at high tidal level of small astronomical tide, overtopping rate can reach $0.19 \text{ m}^3/(\text{m}\cdot\text{s})$ in some site from Gp to Zp, local damage of seawall will appear. 2) super typhoon lands in local average annual highest tidal level along middle-north route, it will cause overtopping rate of $0.11 \sim 0.46 \text{ m}^3/(\text{m}\cdot\text{s})$, seawall burst, but landing in high tidal level of mean astronomical tide, overtopping rate will drop to be $0.0 \sim 0.078 \text{ m}^3/(\text{m}\cdot\text{s})$, the inner slope of seawall remains stable basically. The results have practical significance for design of coastal engineering and minimization of damage during super typhoons.

12:00

Computer simulation of Yeong-II man new harbor for seiche reduction

M.S. KWAK

Civil Engineering, Myongji College, 134 Gajaro, Seodaemun, Seoul, 120-776 Korea

Y.H. MOON, C.K. PYUN

Civil and Environmental Engineering, Myongji University, 32 Namdong, Yongin, Kyunggi, 449-728 Korea

The seiche motion due to long waves at Young-il man new harbor in Korea have occurred frequently which produced undesirable wave and ship oscillation in the harbor, especially during the season with waves coming from the east-northeast direction. This paper

presents results of a computer simulation study for exploring seiche reduction measure at Yeong-il man new harbor. Several resonant modes are clearly seen from simulation results that resonant periods are 35s~45s and 6min~14min. This study make set up a target resonant periods for seiche reduction measure which is 35s~45s. These periods have a bad effect on small sized ship motion at Young-il man new harbor. It is seen that the seiche reduction measure is effective when the quay wall replace to the energy dissipating structure.

Parallel Session 4
Thursday, 15 December
Coastal Management and Shore Protection III
Tang
Chair: Xuelian Jiang, Shu-Qing Yang

11:00

Evacuation modelling to develop risk management strategies for the cities of Padang and Pariaman, West Sumatra

M. DI MAURO, K. MEGAWATI, Z.H. HUANG
Earth Observatory of Singapore, Nanyang Technological University, 639798, Singapore School of Civil and Environmental Engineering, Nanyang Technological University, 639798, Singapore

In 2007 an earthquake occurred along the Sunda Megathrust, caused by a partial rupture of the thrust along the Mentawai patch. Experts suggest that the stress released by this earthquake was only a fraction of the accumulated stress, thus another major earthquake is to be expected in the north-western segment of the patch in the near future. The area is facing the coast of West Sumatra Province, as well as the cities of Padang and Pariaman. In 2009, this area was affected by a 7.6 earthquake whose epicenter was located on the subducting Australian plate. Although this earthquake did not contribute in releasing the tension on the Mentawai patch, it showed the area's vulnerability to earthquakes, resulting in more than 2650 buildings damaged and more than a thousand of fatalities. The city of Pariaman was the closest to the epicenter, and suffered the loss of 37 lives as well as severe damage to its buildings and infrastructures. Whilst planning for such events have always been of great importance in West Sumatra, providing short-term feasible solutions is now extremely urgent. The work described in this paper is part of a research project looking at developing risk management strategies for the cities of Padang and Pariaman, West Sumatra. In particular, this paper focuses on the study carried out to assess evacuation scenarios. The analyzed scenarios depend on variables including: time of the day in which the event occurs; means of transportation; and possible behaviors of the evacuees. It is impractical, or rather impossible, to forecast such variables. Hence it is required to explore different scenarios to produce a comprehensive assessment, to enable the development of flexible solutions for a robust management of the risk. This study was carried

out including consultations with local authorities and emergency planners. The consultations provided an understanding of local risk perception and possible responses for building the models; enabled targeting the study to meet actual need; and contributed in developing solutions that could be actually implemented within the current policy framework. The models were developed by using different methods, including network analysis and agent-based techniques. The integration of the consultation with forefront modeling techniques contributed toward the development of feasible and scientifically-based solutions for managing the risk.

11:15

A dynamic 3-dimensional coastal information management system for the Pearl River Estuary, China

J.Z. LU, B.Y. CHEN

Department of Civil and Structural Engineering, the Hong Kong Polytechnic University, Kowloon, Hong Kong, China State Key Laboratory of Information Engineering in Surveying, Mapping and Remote Sensing, Wuhan University, Wuhan, 430079, China

ONYX W.H. WAI

Department of Civil and Structural Engineering, the Hong Kong Polytechnic University, Kowloon, Hong Kong, China

X.L. CHEN

State Key Laboratory of Information Engineering in Surveying, Mapping and Remote Sensing, Wuhan University, Wuhan, 430079, China

Coastal-related data are multi-dimensional varying in location, depth and time. In addition, coastal data are typically large in size with a vast volume of observation information. Management and visualization of these complex coastal data is a very challenging issue. This paper proposes a novel object-oriented spatiotemporal data model with efficient spatiotemporal operations to represent and manipulate such complex data. The proposed object-oriented is implemented in a Pearl River Estuary Coastal Information System (PRECIS). PRECIS can be used to assist coastal environmental engineers to mitigate the deteriorating water quality situation in the Pearl River estuary.

11:30

Monitoring coastal shoreline and bathymetry based on space imagery

SHOTARO FUNATAKE, YOSHIMITSU TAJIMA

Department of Civil Engineering, The University of Tokyo, Japan

WICKRAMAARCHCHI BANDULA

Coastal Conservation Department, Sri Lanka

SAMARAKOON LAL

Geoinformatics Center, Asian Institute of Technology, Thailand

SHINICHI SOBUE

Japan Aerospace Exploration Agency, Japan

This study newly develops a system for extraction of coastal shoreline and near-shore bathymetry based on the ALOS PALSAR image. Capturing the back-scattering of the radiated micro waves at the surface of the earth, PALSAR has strong advantage in that the

surface information is not interrupted by optical obstacles such as clouds. Comparisons of the image and measured shoreline data revealed that the shoreline can be detected where abrupt change of the horizontal distributions of backscattering is observed. The present system also estimates near-shore bathymetry based on the spatial distribution of wave crest lines observed in the image. The image is first filtered to remove noises and the local wave length is determined as a shifted distance that yields the peak correlation coefficient. The proposed system is applied to the north-west coast of Sri Lanka and, through comparisons with measured data, applicability of the system is investigated.

11:45

Wave run-up, run-down studies on berm breakwater with concrete cubes as armour units

SUBBA RAO, KIRAN G SHIRLAL

Department of Applied Mechanics and Hydraulics, National Institute of Technology Karnataka, Surathkal – 575 0205, India

BALAKRISHNA RAO K

Department of Civil Engineering, Manipal Institute of Technology, Manipal – 576 104, Karnataka, India

PRASHANTH JANARDHAN

Department of Applied Mechanics and Hydraulics, National Institute of Technology Karnataka, Surathkal – 575 025 India

The basic principle involved in the design of berm breakwater is provision of a wide berm at or around the water level with smaller size stones in the armour, which are allowed to move till an equilibrium slope is achieved. This paper presents the results of experimental studies conducted on the wave run-up, run-down characteristics of berm breakwater using concrete cube as artificial armour unit. The experiments were conducted under following conditions, berm width = 0.45m, water depths 0.37, 0.40 & 0.43m, breakwater slope 1:1.5. The weight of concrete cube is 79.5 gm. The wave heights used in the experiments are 0.10, 0.12, 0.14, and 0.16 m and wave periods are 1.6 and 2.0 sec. From the experimental study it is found that the run-up is more for longer period waves in comparison with the shorter period waves. With the increase in deep water wave steepness the run-up and run-down was found to decrease for all the water depths considered. The run-up values (Ru/Ho) vary from 0.52 to 1.08. The range of run-down values (Rd/Ho) varies from 0.45 to 0.88. In berm breakwater the run-up and run-down values were reduced by 35.91% and 23.81% when compared with conventional rubble mound breakwater.

12:00

The combination of low crested breakwater with mangroves to reduce the vulnerability of the coast due to climate change

MUHAMMAD ARSYAD THAHA

Civil Engineering Department, Hasanuddin University, Jl. Perintis Kemerdekaan km 10, Makassar 90245, Indonesia

A.B. MUHIDDIN

Civil Engineering Department, Hasanuddin University, Jl. Perintis Kemerdekaan km 10, Makassar 90245, Indonesia

The potential impacts of climate change on existing coastal hazards are likely to increase. During this century our coastline is likely to be impacted by climate change. Impacts such as sea level rise and an increase in frequency and severity of storm events are likely to lead to a greater coastal inundation and erosion. Hard approach protection has been used despite the expensive cost and less environmentally friendly. It is necessary to develop an eco-protection concept using vegetation or combination of vegetation with civil structures. Combined model is likely to be cheaper and is environmentally sounder. This paper presents the results of experimental research on the performance of mangroves as shore protection (Thaha, 2003) combined with a low crested rubble mound breakwater by Seabrook & Hall (1998) in Pilarczyk KW *et al.* (2003). The results showed a maximum wave transmission can be reduce 48% up to 85% for tidal ranges of 2.00 m for a 50 m width of composite structures with mangrove relative roots density in the range of 0.009 to 0.073. The increase of transmitted wave height through the LB-BW (without mangroves) due to the sea level rise can be reduced by combining it with mangrove forests where the mangrove wave damping capacity will increase by the growing of mangrove roots density. The combined equation of wave transmission coefficients consisting of both mangrove roots and low crest breakwater parameter is presented at the end of this paper.

12:15

Land use spatial model for building based on availability and capacity of land in territory of coastal city (case study: Palu City)

AMAR AKBAR ALI

Department of Civil Engineering, Hasanuddin University, Jl. Perintis Kemerdekaan Km 10 Makassar, South Sulawesi - 90245, Indonesia

MARY SELINTUNG

Departement of Civil Engineering, Hasanuddin University, Makassar, Indonesia

ROLAND A. BARKEY

Departement of Forestry, Hasanuddin University, Makassar, Indonesia

M. ARSYAD THAHA

Departement of Civil Engineering, Hasanuddin University, Makassar, Indonesia

The land use for building which keeps increasing in urban areas cause problems in the future, particularly related to the availability and capacity of land in urban areas, in fulfilling the need for development and sustainable urban development. The purpose of this research is to investigate the relationship between area of land use for building and time in the future, until when the land is capable of supporting the growth in the use for building, and how to deal with land use for building so that the land in the territory of Palu as a coastal city is capable of supporting the growth in the longer use. The research method used is the approach of quantitative method by using several analytical techniques, among others: land capacity analysis, regression analysis, projection analysis, and overlay analysis, and by using the help of some programs and

software to assist the analysis. The research data consists of spatial data including data on the number of land users of protected areas and cultivation areas obtained from the Revised Map of Spatial Planning of Palu City in 2010, and aspatial data including data on the number and population growth, the number and growth of the building in form of a time series of data obtained through document registration and GIS techniques. The results showed that the land use for building in Palu city on the future having growth average 2.50% per year; cultivation area will be full of buildings in the year 2212. In order to get the land in the territory of Palu as a coastal city is capable of supporting the growth of the land use for building much longer, some efforts are needed to be done through reducing the growth and the extensive land use for building per one user, controlling the population growth, adding the width of area, and planning storey buildings in certain zones.

Parallel Session 4
Thursday, 15 December
Hydrodynamics II
Ming II
Chair: Mohamed Ghidaoui, Dong-Sheng Jeng

11:00

Effects of pneumatic chambers on the performance of moored floating breakwaters: an experimental study

F. HE

School of Civil and Environmental Engineering, Nanyang Technological University, Singapore 639798

Z.H. HUANG

School of Civil and Environmental Engineering; Earth Observatory of Singapore, Nanyang Technological University, Singapore 639798;

A.W.K. LAW

School of Civil and Environmental Engineering; DHI-NTU Center, Nanyang Technological University, Singapore 639798

W.B. ZHANG

DHI-NTU Center, Nanyang Technological University, Singapore, 639798

An experimental study of the effects of pneumatic chambers on the performance of box-type floating breakwaters is reported. The floating breakwater is moored by a slack mooring system. It is found from our experiments that the pneumatic chambers can increase the energy dissipation and reduce the transmission coefficient significantly for medium and long waves, but have insignificant effects on short waves. Information on the motion responses and air chamber pressures are also reported.

11:15

Application of the wave pump concept to simulate tidal anomalies in Conjola Lake, NSW, Australia

THUY T.T. VU, P. NIELSEN, D.P. CALLAGHAN

School of Civil Engineering, University of Queensland, Brisbane, QLD 4072, Australia

D.J. HANSLOW

Office of Environment and Heritage, Newcastle, Australia

The present paper applies the wave pump concept to a flooding event at Lake Conjola, Australia. We explain how the raised water level in the lake was caused by waves with large height and very long period pumping water into the lagoon across a berm separating the lagoon from the ocean with the nominal wave set up effects. Outflow through the entrance channel, modeled as critical flow over a weir, results in less agreement with measurements compared to that of approximating it as a channel with finite length. An inverse analysis indicates that the entrance scoured out to become more efficient during the wave event, returning to normal cross section after the event. This insight was utilized to adjust the entrance area in a forward model to get optimal fit with measured water levels. Finally, the wave pump concept was confirmed using a two node model that reflected the actual surface areas of two lakes in series.

11:30

Vortex-induced vibration of a circular cylinder near a plane wall

X.K. WANG, S.K. TAN

Maritime Research Centre, Nanyang Technological University, 50 Nanyang Avenue, 639798, Singapore

Z. HAO

College of Logistics Engineering, Shanghai Maritime University, Shanghai, 200135, China

This paper presents an experimental study of the vortex-induced vibration (VIV) of a spring-supported rigid cylinder, which is placed near a plane wall and could vibrate in the transverse direction to the free stream. It is considered as an extension of the widely studied VIV phenomenon of a stand-alone cylinder in steady uniform flow. The effects of varying the gap height (defined as the distance between the cylinder bottom and the wall surface) on the VIV characteristics, including the vibrating frequency and amplitude of the cylinder, are examined in detail. The motion of the cylinder and its wake patterns have been measured using Particle Image Velocimetry (PIV), in conjunction with direct measurements of the hydrodynamic forces (drag and lift) on the cylinder using a piezoelectric load cell.

11:45

An introduction to O-tube

H. AN, C. LUO, L. CHENG

School of Civil and Resource Engineering, the University of Western Australia, 35 Stirling Highway, WA 6009, Australia

D. WHITE

Centre for Offshore Foundation Systems, the University of Western Australia, 35 Stirling Highway, WA 6009, Australia

T. BROWN

The University of Western Australia, 35 Stirling Highway, WA 6009, Australia

This paper describes the O-tube, which is a new facility for submarine pipeline stability research. The O-tube comprises of a closed loop channel of water driven by an impeller. The impeller runs at a constant speed to provide steady flow and at sinusoidal speeds to generate oscillatory flows. The O-tube combines the capabilities of a conventional open channel flume

(which provides steady current) with a U-tube (which provides oscillatory flow). The primary function of the facility is to physically model the stability of pipelines at a relatively large scale (typically 1/5) for large diameter pipelines (e.g. 40 inch gas trunklines) and at full scale for small diameter pipelines (< 10 inch). The specification of the motor and impeller is such that typical 100-year tropical storm conditions in 40 m to 80 m water depth on the North West Shelf (NWS) of Western Australia are comfortably generated within the performance envelope of the facility.

12:00

Bottom roughness and flow characteristics for combined near-orthogonal wave-current flows over smooth and rippled bottoms

KIAN YEW LIM

Department of Civil and Environmental Engineering, National University of Singapore, 1 Engineering Drive 2, EW1 03-01A, Singapore 117576

OLE SECHER MADSEN

Department of Civil and Environmental Engineering, Ralph M. Parsons Laboratory, 48-216C, MIT, Cambridge, MA 02139, USA

HIN FATT CHEONG

Department of Civil and Environmental Engineering, National University of Singapore, 1 Engineering Drive 2, E1A 07-03, Singapore 117576

Experiments for combined orthogonal wave-current flows over a movable sand bed have shown similar flow resistance when the current is parallel and perpendicular to the wave-formed ripples. This counter-intuitive observation motivated the present experiments, in which fixed artificial ripples are used to ensure a static and strictly 2D bottom roughness configuration during the experiments. An additional series of wave-current experiments over a smooth bed is also conducted in this study. The experimental results show that there is an increase in bottom roughness when the angle between ripple axis and current direction increases. The current also tends to align with the ripple axis as it approaches the bottom from above. When waves are present with near-orthogonal currents in a closed basin, it is observed that the steady current direction is 'forced' to change from its original mainstream direction, due to the presence of a wave-induced return current. This modification of current direction is inevitable due to mass transport associated with progressive waves, and should be considered when formulating and verifying models for wave-current interaction. For combined wave-current flows over a smooth bed, experimental results for angles of 60°, 90° and 120° between wave and current directions indicate an increase in the near-bottom mean flow when waves are present. However, the mean shear stress, when analyzed by the log profile method, is found to be smaller for combined wave-current flows than for currents alone.

12:15

A modeling approach of combined simulation of tide, wind and wave on the west coast of Korea

S.W. SUH, H.J. KIM, H.Y. LEE

Dept. of Coastal Construction Engineering, Kunsan National University, Kunsan, Jeonbuk, 573-701, Korea

To simulate typhoon induced surge for the west coast of Korea, an extended grid structure from Yellow Sea to North Western Pacific was established. Numerical simulations on the NWP grid were performed by using dynamical coupling of the two models pADCIRC and unSWAN on 64 parallel processors. Computed RMS error of tidal amplitudes and phases are in very good agreement. Coupling of wave model with asymmetric wind vortex give reasonable results showing water level jump up near landfall of typhoon.

Parallel Session 4

Thursday, 15 December

Tsunami and Storm Surge

Sung I

Chair: K.W. Chow, Seungbuhm Woo

11:00

Magnetic anomaly induced by tsunami waves in open oceans

B.L. WANG, H. LIU

Engineering Mechanics, Shanghai Jiao Tong University, 800# Dong Chuan Road, Shanghai, 200240, China

The magnetic anomaly induced by tsunami waves in open ocean is investigated with kinematic dynamo theory. Magnetic field will be induced by the velocity field of tsunami wave during its life cycle. Using long wave approximation, an integral solution of the dynamo problem is obtained based on the small dispersive parameter of water wave. The magnetic field induced by typical tsunami models, including single wave and N-wave, could be directly obtained from the integral solution. Through the analysis, the tsunami induced magnetic field magnitude is estimated at the order of 10 nano Tesla (nT) just over sea level and 1 nT at altitudes of several hundred kilometers respectively for 1m height waves, which also depends on other wave parameters and main earth magnetic field.

11:15

Numerical solution of landslide tsunami propagation over a uniformly sloping beach

S.N. SEO

Coastal Engineering Department, Korea Ocean Research & Development Institute, Ansan, Seoul 426-744, South Korea

P. L.-F. LIU

School of Civil and Environmental Engineering, Cornell University, Ithaca, NY 14853, USA

Linear shallow water equations with a prescribed forcing term are adopted to study landslide generated-tsunamis propagating on a plane beach. Seeking a solution valid for the life span of the tsunami, numerical methods are employed to evaluate integrals of the derived analytical solution. Numerical solutions are presented and discussed.

11:30

Rising seawall for prevention of tsunamis and storm surges

Y. KIMURA, M. INUI

Technical Research Institute, Hitachi Zosen Corporation, 2-11, Funamachi-2, Taisyo-ku, Osaka, 551-0022, Japan

K. NAKAYASU, Y. YAMAKAWA

Machinery & Infrastructure Headquarters, Hitachi Zosen Corporation, 5-1, Chikkoshinmachi-1, Nishi-ku, Sakai-shi, Osaka, 592-8331, Japan

T. HIRAISHI

Disaster Prevention Research Institute, Kyoto university, Higashinokuchi, Shimomisu, Yoko-oji, Fushimi-ku, Kyoto, 612-8235, Japan

H. MASE

Disaster Prevention Research Institute, Kyoto university, Gokasyo, Uji-shi, Kyoto, 611-0011, Japan

NEORISE is a new type structure for coastal disaster prevention against tsunamis or storm surges. It is installed on a mouth of tide embankments, and it is able to close the mouth by inundation flow without artificial operations and power sources when tsunami and surge occur. This study shows characteristics of the NEORISE's response against tsunamis, surges and waves through hydraulic model experiments. It was confirmed that the NEORISE blocks inundation flow properly.

11:45

Modelling of winds, precipitation, storm surge, and waves during the passage of typhoon Morakot using an atmosphere-waves-ocean coupled model

H.S. LEE, F. DING, HENDRI, T. YAMASHITA

Department of Development Technology, Graduate School for International Development and Cooperation, Hiroshima University, 1-5-1 Kagamiyama, Higashi-Hiroshima 739-8528, Hiroshima, Japan

H. MOHAMMED

Irrigation and Hydraulics Department, Faculty of Engineering, Cairo University, Egypt

Typhoon Morakot in 2009 was one of the deadliest typhoons ever in Taiwan due to extremely heavy rainfall during its landfall causing massive flooding and devastating mudslides in the southern Taiwan. In this study, we performed numerical simulations for the meteorological and oceanographic fields such as winds, pressure, precipitation, storm waves and storm surge during Typhoon Morakot using an atmosphere-wave-ocean modeling system. The simulated winds and pressure fields show good agreements with QuikSCAT observations and the simulated accumulated rainfall distribution agrees well with the rain gage observations. Four-day accumulated rainfalls at A-Li Shan station were 2,777mm and 2,850mm from observation and simulation, respectively. The simulated waves and storm surge fields also show reasonable results compared to observed values. The effects of waves-currents interactions in terms of momentum transfer through whitecapping and depth-induced wave breaking depict significant improvement in storm surge level on the west coast of Taiwan where the mild-sloped water depth is developed.

12:00

Tsunami induced shear stresses along submarine canyon off southeast coast of India

J.K. SEELAM, T.E. BALDOCK

School of Civil Engineering, The University of Queensland, St Lucia, QLD 4072, Australia

Tsunamis are a potential threat to submarine installations especially when the pipelines traverse the continental slope and shelf. Tsunami propagation simulation for the 26th December 2004 event was carried out for the southeastern shelf and slope regions of India. The velocities generated along the shelf and slope regions in the vicinity of canyons and the shear stresses derived from these velocities are evaluated. A 3D hydrodynamic model with initial surface elevation obtained from the earthquake details was used to drive the tsunami model. Shear stresses along select transects in the vicinity of submarine canyons are studied.

12:15

Influence of velocity distribution and density stratification on generation or propagation of tsunamis

T. KAKINUMA, K. NAKAMURA, K. YAMASHITA

Graduate School of Science and Engineering, Kagoshima University, 1-21-40 Korimoto, Kagoshima, Kagoshima 890-0065, Japan

K. NAKAYAMA

Department of Civil and Environmental Engineering, Kitami Institute of Technology, 165 Koen-cho, Kitami, Hokkaido 090-8507, Japan

A set of wave equations derived on the basis of a variational principle in consideration of both strong nonlinearity and strong dispersion of surface/internal waves is numerically solved to simulate generation and propagation of tsunamis in the vertical two-dimension. The velocity potential in each fluid layer is expanded into a power series of vertical position, such that the accuracy of vertical distribution of velocity depends on the number of expansion terms. Numerical results of surface displacement are compared with the existing experimental data, where tsunamis are generated by the seabed uplift. When the fundamental equations are reduced to nonlinear shallow water equations, the numerical model cannot represent propagation of a long wave group especially in distant-tsunami propagation, leading to overestimation of both the wave height and wave steepness of the first wave. The wave height becomes larger in the stratified ocean than that in a one-layer case, although the present density distribution hardly affects the tsunami phase over a long-distance travel.

Parallel Session 5
Thursday, 15 December
Beach Erosion and Morphodynamics I
Ballroom C
Chair: D.A. Suriamihardja, Jianping Gan

14:00

Beach nourishment projects in China

C.P. KUANG, Y. PAN, L.L. HE

Department of Hydraulic Engineering, College of Civil Engineering, Tongji University, Shanghai 200092, China
 Y.X. YANG

Qinhuangdao Mineral Resource and Hydrogeological Brigade, Hebei Geological Prospecting Bureau, Qinhuangdao, 066003, China

F. CAI

Third Institute of Oceanography, State Oceanic Administration, Xiamen, 361005, China

After 2005 there is a sharply increase in the quantities of beach nourishment in China. In this paper the beach nourishment projects in China are reviewed and discussed with respect to the project history, distribution, types, objectives, design, and evaluation. The designs and evaluations of two beach nourishment projects in Qinhuangdao are introduced briefly to provide a feature of current beach nourishment in China. It is inferred from the project review that the beach nourishment in China is on its beginning and the projects are initiated spontaneously by local governments and agencies with different technologies for economic benefits, better city image and the convenience of citizens. In the light of the review of beach nourishment projects some future prospects of the beach nourishment industry of China are proposed.

14:30

Modelling the change of beach profile under tsunami waves: a comparison of selected sediment transport models

L.L. LI

Earth Observatory of Singapore, Nanyang Technological University, 639798, Singapore

Z.H. HUANG

Earth Observatory of Singapore, Nanyang Technological University, 639798, Singapore School of Civil and Environmental Engineering, Nanyang Technological University, 639798, Singapore

Many different sediment transport formulas are available to estimate geomorphic changes in river and coastal environments. However, there have been few publications in the literature dealing primarily with sediment transport processes associated with tsunami waves. It is desirable to evaluate the performances of these existing formulas in modeling shoreline erosion due to tsunamis. The main objective of this study is to simulate, using six classical sediment transport formulas, the sediment transport under the action of solitary waves or tsunami-like waves and compare the numerical results with available measured data. By comparing the simulated and measured changes of bed profiles, the suitability of these models to simulate the tsunami induced shoreline changes is discussed. Our comparisons show that (i) the results obtained using

different sediment transport models often differ drastically from each other, and (ii) special care need to be taken when selecting model parameters for large waves which may generate bed shear stresses much larger than those normally encountered in open channel flows. The findings reported here will be useful for researchers working on tsunami hazard mitigation problems.

14:45

Effect of beach nourishment using gravel and tracking movement of gravel

T. ISHIKAWA, T. UDA

Public Works Research Center, 1-6-4 Taito, Taito, Tokyo 110-0016, Japan

T. SAN-NAMI

Coastal Engineering Laboratory Co., Ltd., 1-22-301 Wakaba, Shinjuku, Tokyo 160-0011, Japan

On the Hamamatsu-Shinohara coast facing the Pacific Ocean, beach has been severely eroded, resulting in the shoreline recession of 210 m between 1962 and 2004. As a measure against beach erosion, beach nourishment using a mixture of sand and gravel was begun in 2005. Since then, $3.5 \times 10^5 \text{ m}^3$ of sediment was supplied to the coast. Although the foreshore was widened by the beach nourishment, not only sand but also gravel was rapidly transported downcoast, resulting in the change in grain size of the beach material. In this study, the changes in the quality of the beach in terms of the grain size and transport process of gravel were investigated by field observation. Beach nourishment using coarser materials is effective for the shore protection, but it must be carefully used because of change in grain size.

15:00

Erosion of Hirota ruins due to storm waves associated with Typhoon 0514

T. UDA

Public Works Research Center, 1-6-4 TaitoTaito, Tokyo 110-0016, Japan

Y. KOWAKI, T. ISHIDO

Board of Education, Minamitane Town, 2793-1 Nakano-ue, Minamitane Town, Kumake-gun, Kagoshima 891-3792, Japan

The Hirota ruins are located in Minamitane Town on Tanegashima Island, 25 km south of Kyushu Island. The coastal sand dune containing these ruins has remained stable for approximately 1,400 years. In September 2005, Typhoon No. 14 passed very close to Tanegashima Island and the sand dune of the Hirota coast was eroded by storm waves, exposing the ruins. The causes of damage to the ruins were investigated using field data. It was found that the primary cause was the attack of the storm waves and the secondary cause was the truncation of the seawall at the north end.

Parallel Session 5
Thursday, 15 December
Estuaries and Ports V
Ballroom B
Chair: Jun Chen, Yongping Chen

14:00

Wetlands restoration and protection in Yellow River Delta, China

Y.Y. HUA, B.S. CUI, W.J. HE

State Key Joint Laboratory of Environmental Simulation and Pollution Control, School of Environment, Beijing Normal University, 19 Xijiekouwai Street, Haidian District Beijing, 100875, China

It has been 10 years since the wetlands restoration project that implemented in 2002 in Yellow River Delta, China. The project mainly aims to improve the natural habitat for rare birds through hydrological process's modification. A water volume-water level control technique was demonstrated and applied to prevent salinization by diverting freshwater into wetlands. In this study, we present the restoration effects and assess the rationality through bird-habitat responses based on monitoring data from 2001 to 2010. Results show that the restoration has achieved some positive effects, but lacks adjustment to unexpected situations. We propose that an establishment of water level-volume model and the calculation of appropriate ecological water requirement threshold are effective for wetland restoration and protection.

Acknowledgments

We appreciate financial supports from the National Natural Science Foundation (No. 41071330) and the Scientific Research Foundation of Beijing Normal University (No. 2009SD-24). We would like to acknowledge Yueliang Liu, Shuyu Zhu, Kai Shan from the Yellow River Delta Management Bureau for their help in historical data and field work.

14:15

A study on the seawater flow characteristics for various shrouds used in tidal current generation systems

J.W. KIM, Y.H. CHOI, S.H. LEE

Mechanical and Automotive Engineering, Wonkwang University, 570-749

Ik-san, Cheonbuk, Republic of Korea

The velocity of seawater flow has a strong influence on the power output of tidal current generation systems. Therefore, CFD (Computational Fluid Dynamics) analyses are performed to investigate the effect of shroud geometry variation on the flow characteristics for nozzle-diffuser and cylinder-diffuser type shrouds used for controlling seawater flow in horizontal axis tidal current turbine systems. Through these analyses, fluid velocity distributions and maximum velocity locations inside the shrouds are compared. Predicted results show that the flow fields and the peak velocity depend on the shroud angle. Especially fluid velocity in the cylinder-diffuser type is rather high in overall cylinder part while high velocity zone in nozzle-

diffuser type locally appears near the minimum sectional area. It can also be seen that fluid velocity at the centerline of cylinder-diffuser type shrouds increases near the entrance, and reaches a peak, and then decreases rapidly near the outlet before converging. Velocity variation with the shroud angle is much higher in cylinder-diffuser type, and maximum peak velocity is obtained for $\theta_2 = 0.315$ rad. These results can be applied to the optimal design of shroud in a tidal current power generation system for the development of the efficient systems.

14:30

Monitoring fluid mud in the north passage navigation channel of Yangtze Estuary, China

Y.Y. WAN

Estuarine and Coastal Science Research Center, Shanghai 201201, China

UNESCO-IHE Institute for Water Education, 2601 DA Delft, The Netherlands

J.A. ROELVINK

UNESCO-IHE Institute for Water Education, 2601 DA Delft, The Netherlands

Observations of longitudinal-channel fluid mud dynamics is conducted in the context of a cold-air wave on October of 2010 at the Yangtze Estuary, China. The measurement data reveals that just after the wind wave event, a large number of cohesive fine sediment particular materials are trapped as a status of fluid mud along the dredged navigation channel in the North Passage. The mechanism and transportation of the wave-forced fluid mud may be relate to both wave agitation and the spring-neap tidal variations. At the same time, some process-oriented sedimentary processes, such as, flocculation, stratification and trapping effects (sediment and salinity density flow), and the overall of flow regimes, tidal asymmetry (Shi, 2010) also may have some relationships with the formation and dynamics of fluid mud, but it need more evidences to discourse the occurrence of fluid mud in the river- and tidal- dominated estuary.

14:45

Advances in development and management of estuarine and coastal mudflats

Y.J. LU

State's Key Laboratory of Hydrology Water Resources and hydraulic Engineering Science, Nanjing Hydraulic Research Institute, Nanjing, Jiangsu, China

Q.Z. HOU

College of Geographical Science, Nanjing Normal University, Nanjing, Jiangsu, China

Y. LU, Y.H. WANG, C.W. XU, R.Y. JI

State's Key Laboratory of Hydrology Water Resources and hydraulic Engineering Science, Nanjing Hydraulic Research Institute, Nanjing, Jiangsu, China

With the rapid socioeconomic development and urbanization, reclamation of mudflat resources has become an important way to ease the contradiction between land supply and demand. Irrational exploitation of limited mudflat resources has seriously affected natural evolution of many estuarine and coastal areas, weakened the regeneration of these

resources, and threatened flood control, water security, and consequently the sustainable socioeconomic development in estuarine and coastal areas. Mudflat resources and their capacity are limited by the level of science and technology, in a certain period of time. Therefore, the ecological environmental health should be protected to ensure the sustainable development. This paper presents a review on the state-of-the-art knowledge concerning mudflats development and management, including development and utilization of mudflats and their impacts on environment, assessment of sustainable development, as well as construction of management system. Some necessary research fields and topics in the future are also recommended.

Parallel Session 5
Thursday, 15 December
Waves and Modelling I
Tang
Chair: Young-Taek Kim, Xiping Yu

14:00

Experimental research on computing method of wave pressure for immersed vertical barrier of open-type breakwater

L.H. JU, P. LI, Q.H. ZUO

Nanjing Hydraulic Research Institute, Nanjing, China

By making use of linear wave, this paper first presents a formula to calculate the wave pressure for immersed vertical barrier of open-type breakwater; then, a series of physical model experiments are carried out, based on different relative wave length, different relative wave height and different underwater penetrations of the barrier, for measuring the relative wave pressure of the barrier; and then the experiment results are compared with the calculated values, the result of comparison is analyzed; finally, an approximate computing method of the wave pressure for immersed vertical barrier of open-type breakwater is put forward for the use of design and reference.

14:15

Effects of diffraction and directional asymmetry of random wave loads on a long structure

J.-S. JUNG

Department of Civil and Environmental Engineering, Hanyang University, 222 Wangsimni-ro, Seongdong-gu, Seoul 133-791, South Korea

C. LEE

Department of Civil and Environmental Engineering, Sejong University, 98 Kunja-dong, Gwangjin-gu, Seoul 143-747, South Korea

Y.-S. CHO

Department of Civil and Environmental Engineering, Hanyang University, 222 Wangsimni-ro, Seongdong-gu, Seoul 133-791, South Korea

In this study, we consider diffraction effect in analyzing wave loads on a long structure. When waves are obliquely incident on a long structure, the diffracted wave give forces on the lee side of the structure. Thus, the wave loads increase with the existence of diffracted waves and also the phase

difference between the incident and diffracted waves. We further consider directional asymmetry effect in analyzing wave loads on a long structure. The force reduction parameters were analytically derived and verified with experimental data.

14:30

Particle trajectories in nonlinear interfacial water waves

H.C. HSU

Tainan Hydraulics Laboratory, National Cheng Kung University, Tainan 701, Taiwan

C.O. NG

Department of Mechanical Engineering, The University of Hong Kong, Hong Kong, China

H.H. HWUNG

Department of Hydraulic and Ocean Eng., National Cheng Kung University, Tainan 701, Taiwan

This paper presents a modified Euler-Lagrange transformation to obtain the third-order trajectory solution in a Lagrangian framework for the water particles in nonlinear interfacial waves. We impose the assumption that the Lagrangian wave frequency is a function of wave steepness and an arbitrary vertical position for each water particle. Expanding the unknown function in a small perturbation parameter and using a successive expansion in a Taylor series for the water particle path and the period of a particle motion, the third-order asymptotic expression for the Lagrangian particle trajectories, the mass transport velocity and the period of particle motion can be derived in a Lagrangian form. In particular, the Lagrangian mean level of the particle motion in Lagrangian form differs from that of the Eulerian.

14:45

Revision of regional frequency analysis method for extreme wave heights

Y. GODA, M. KUDAKA

ECOH CORPORATION, 2-6-4 Kita-Ueno, Taito-Ku, Tokyo 110-0014, Japan

H. KAWAI

Port and Airport Research Institute, 3-1-1 Nagase, Yokosuka, 239-0826, Japan

The method of regional frequency analysis with L -moments by Hosking and Wallis (1997) is revised with a new plotting position estimator and inclusion of the Weibull distribution as one of probable population distributions of extreme waves. Bias and efficiency of the L -moment method is examined through a large-scale numerical study. The revised method is applied to the POT wave data at 11 stations at the eastern coast of Japan Sea which cover the measurement period of 18 to 37 years.

15:00

Power of a piston wave maker by numerical method

H.B. GU, D.M. CAUSON, C.G. MINGHAM, L. QIAN, Z.H. MA

Centre for Mathematical Modelling and Flow Analysis, School of Computing, Mathematics and Digital Technology,

The Manchester Metropolitan University, Manchester M1 5GD, UK

HAN-BAO CHEN, ZILONG ZHENG

Tianjin Research Institute for Water Transportation Engineering, Key Laboratory of Engineering Sediment of Ministry Communications, Tianjin 300456, China

The piston-type wave maker is a very popular and important piece of equipment in coastal and ocean engineering physical wave model experiments. In this paper we use a numerical model to simulate the ability of the piston-type wave maker to generate a specified wave, which only can be done by theoretical analysis before under ideal conditions. Firstly, force on a wave board and its power is analyzed under different condition, and the power from numerical model is compared very well with the theoretical result under the same wave condition. Then the avoidance of using absorbers in a flume is studied by choosing a suitable position of the wave maker in the flume. This is of practical importance because the use of absorbers is often expensive and the effects are not very well when they are used.

Parallel Session 5

Thursday, 15 December

Hydrodynamics III

Ming II

Chair: Seungwon Suh, Xikun Wang

14:00

Numerical experiments on strong vertical mixing under strong winds in the coastal zone

NOBUHITO MORI, YUSUKE TANAKA, SOTA NAKAJO, TOMOHIRO YASUDA, HAJIME MASE

Kyoto Univ., DPRI, Gokasho, Uji, Kyoto, 611-0011, Japan

There are several bulk flux models for an ocean surface boundary layer of surface roughness and TKE flux at the ocean surface. However, these bulk flux models have not been calibrated at extreme conditions in detail. The validation for the parameterization of bulk flux models is carried out analyzing correlation between numerical and observed vertical distributions of temperature and velocity. The numerical experiments were conducted during the Typhoon Melor in 2009 at Tanabe Bay, Wakayama, Japan. It was found that the parameterization of the TKE flux has significant influences on temperature and velocity in the nearshore region. The calibrated model can be improved with the accuracy of temperature and currents against the observations about 10% to 30% near the ocean surface.

14:15

Experimental and numerical study on current velocities and vertical profiles of undertow over a submerged breakwater

SIDDIQUE MOHSIN, YOSHIMITSU TAJIMA, SHINJI SATO

Coastal Engineering Laboratory, Department of Civil Engineering, The University of Tokyo, 7-3-1 Hongo Bunkyo-ku, Tokyo 113-8656, Japan

This study focuses on better understandings and accurate predictions of the breaking and broken waves and associated undertow profiles especially over a submerged breakwater. Laboratory experiments are first performed in a 2D wave flume over 1:30 sloping beach with a submerged breakwater to capture the wave deformation, time-varying current velocities and vertical profiles of time-averaged undertow velocities. A newly developed numerical model is then tested against the experimental data sets. In contrast to the existing models, the present model accounts for mass conservation equations for determinations of the vertical profiles of undertow shear velocities. Furthermore, the model also introduces modified time-varying formulation of turbulent mixing length scale for turbulence closure scheme. While the laboratory experiments reveal the complex wave deformations and associated undertow properties around the submerged breakwater, the present model shows excellent predictive capabilities for simulation of the current fields under breaking and broken waves.

14:30

Oscillatory flow around a pair of cylinders of different diameters

K. YANG, H. AN, L. CHENG

School of Civil and Resource Engineering, the University of Western Australia, 35 Stirling Highway, Crawley WA 6009, Australia

M. ZHAO

School of Engineering, University of Western Sydney, Locked Bag 1797, Penrith, NSW 2751, Australia

This paper investigates sinusoidal oscillatory flow around a two-cylinder system numerically. The cylinder configuration comprises a pair of nearby cylinders of different diameters, with the small cylinder piggybacks on the big one. The configuration is often referred to as a "piggyback" cylinder system. The large cylinder is referred as the main cylinder and the piggyback cylinder is referred as the small cylinder. Flow structures around and hydrodynamic loadings acting on the main cylinder are expected to be influenced by the small cylinder due to the hydrodynamic interactions between the two cylinders. In order to find out the influences induced by the existence of the small cylinder at the proximity of the main cylinder, simulations are carried out both on an isolated cylinder and on the side-by-side piggyback configuration cases. The simulations are carried out at Reynolds number of 800 and Keulegan-Carpenter number of 8 (both based on the diameter of the main cylinder). In the two-cylinder cases, the small cylinder is located above the main cylinder and the gap to diameter ratio (g/D , where g is the gap and D is the diameter of the main cylinder) is in the range of 0.1 to 0.5 with a uniform increment of 0.1 to investigate the corresponding influences of the gap ratio. The diameter ratio (d/D , where d is the diameter of the piggyback cylinder) is 0.2 in the present study. Hydrodynamic forces and flow characteristics around the cylinders are investigated in detail. Flow structures near the two cylinders are investigated through flow visualization. It is found that the existence of the small

cylinder has profound effects on the flow structures around the main cylinder and hydrodynamic forces on the main cylinder.

14:45

The role of steady streaming in sheetflow transport
KYIKYI LWIN, HAIJIANG LIU, SHINJI SATO

Department of Civil Engineering, the University of Tokyo, 7-3-1 Hongo, Bunkyo-ku, Tokyo, 113-8656, Japan

To quantitatively evaluate the role of the onshore streaming, laboratory experiments were conducted under the combined asymmetric wave-current conditions. The asymmetric flows with a wave period of 5 s and a maximum onshore velocity u_{max} varying from 0.8 to 1.6 m/s have been applied for three well-sorted sands with different medium sand sizes. The sediment net transport rate was measured. Results show that except several cases, the onshore streaming enhanced the onshore sheetflow net transport by different extents. The streaming-induced net transport rate is found to be related to the free-stream velocity and the sand size.

15:00

The variation of water level and flow velocity in semi-closed water area by wind and boat wave
K. UNO, G. TSUJIMOTO, T. KAKINOKI

Department of Civil Engineering, Kobe City College of Technology, 8-3 Gakuen-Higashi, Kobe City, Hyogo Prefecture 651-2194, Japan

In this study, to clarify the relationship between water level variation and turbulence of flow, field observations were carried out in Omaehama beach, Nishinomiya City, Hyogo Prefecture, JAPAN. In each observation, wind speed and its direction, water level, wave height, flow velocity and its direction were measured in the vicinity of shoreline. The data of wave height was transformed to the velocity by using a liner filter theory and examined the effect of boat wave and wind one on turbulence of flow. The transferred velocity from wind wave was coincided with the turbulence of flow, however, that from boat wave was not so good. From the results of this study, we can see both boat wave and wind one are the significant factors of water level variation in urban semi-closed water area.

Parallel Session 5

Thursday, 15 December

Numerical Methods and Simulation I

Sung I

Chair: Hirohide Kiri, Benlong Wang

14:00

Potential and application of hydrodynamic modelling on unstructured grids
A. VERWEY, H.W.J. KERKAMP

Deltares, P.O. Box 177, 2600 MH Delft, the Netherlands

G.S. STELLING

Delft Technical University, Civil Engineering Department, Delft, the Netherlands

M.L. TSE

Mott MacDonald Hong Kong Limited, Hong Kong

W.C. LEUNG

Drainage Services Department, Government of the Hong Kong SAR

The use of unstructured grids in hydrological, hydraulic and water quality modelling offers great advantages in fitting complex model domains by applying combinations of linear, triangular, quadrilateral and higher order cell shapes. The flexibility of the approach is demonstrated by describing models developed for part of the Kam Tin Main Drainage Channel in Hong Kong and for the San Francisco Bay - Sacramento Delta in the USA.

14:15

RANS-VOF for a solitary wave flow around a 3D vertical cylinder

D.C. WAN, H.J. CAO, Y.C. LIU

State Key Laboratory of Ocean Engineering, School of Naval Architecture, Ocean and Civil Engineering, Shanghai Jiao Tong University, Dongchuan Road 800 Shanghai, 200240, China

A three-dimensional RANS (Reynolds-Averaged Navier-Stokes equations) - VOF (Volume of Fluids) model is presented for numerical simulations of a solitary wave flow around a fixed 3D vertical circular cylinder based on the OpenFOAM solver. The RANS equations with the blended SST $k-\omega$ turbulence model are solved by using the finite volume method. The free-surface is captured by the VOF method. The Pressure Implicit with Splitting of Operators (PISO) algorithm is used in the calculation procedure. The wave elevation within a cylinder radius distance around the cylinder is monitored at several particular positions. The flow field is investigated including the velocity and pressure distributions. The obtained numerical results of wave run-up and scattering around the cylinder are compared very well with the measurements from experiment model tests.

14:30

Three-dimensional numerical study on bore driven swash

B. DENG, C.B. JIANG, L.P. ZHAO

School of Hydraulic Engineering, Changsha University of Science & Technology, Changsha 410004, P.R. China

Human Province Key Laboratory of Water, Sediment Sciences & Flood Hazard Prevention, Changsha 410004, P.R. China

H.S. TANG

School of Hydraulic Engineering, Changsha University of Science & Technology, Changsha 410004, P.R. China

Department of Civil Engineering, The City College of New York, New York 10031, USA

The dynamics of flow involved with surge bore propagating over a slope is studied numerically using a fully three-dimensional (3D), incompressible, two-phase flow Navier-Stokes (NS) solver coupled to a LES turbulence model. A high-resolution STACS-VOF method is applied to capture the interface between the air and water phases. The computed uprush shoreline motion and the tip of runup water

surface compare favorably with experimental data. Numerical results are also presented for the instantaneous flow field, recirculation regions, vortex tubes, and maximal bed shear stress. The results indicate that the flow phenomena are very complicated after the bore breaks.

14:45

Internal generation of waves on an arced band in an unstructured grid system

G. KIM

Division of Ocean System Engineering, Mokpo National Maritime University, Mokpo City, Jeollanam-do, 530-729, Republic of Korea

C. LEE

Department of Civil and Environmental Engineering, Sejong University, 98 Gunja-Dong, Gwangjin-Gu, Seoul, 143-747, Korea

In this study, we developed Gaussian source functions on an arced band to generate incident waves in the extended mild-slope equation. Numerical experiments were conducted for waves propagating on a flat bottom and also waves scattered by a vertical cylinder. The numerical results showed that the technique of wave generation using on an arced band causes negligible diffraction problem near the sponge layer.

15:00

Numerical study on the water exchange of the Bohai Sea under the combined action of wave, tide and surge

BO XIA

School of Civil Engineering, Tianjin University, Tianjin, 300072, China

Changsha University of Science and Technology, Changsha, Hunan, 410114, China;

QINGHE ZHANG

School of Civil Engineering, Tianjin University, Tianjin, 300072, China

YUAN LI, CHANGBO JIANG

Changsha University of Science and Technology, Changsha, Hunan, 410114, China

The Bohai Sea is a semi-enclosed inland sea in northern China which has been polluted these years. The wave, tide and storm surge are the most important dynamic processes in the Bohai Sea, these three dynamic factors play an important role in the water exchange of the Bohai Sea, but few researches has been done about the influence of the wind on the water exchange in the Bohai Sea. In this study, some concepts and models for water exchange in the coastal sea are introduced. Half-life time, simulated by a dispersion model, is chose to represent the exchange ability of the Bohai Sea. Based on the FVM method and unstructured triangular mesh, a high resolution numerical model is established to study the tide and storm surge. This model coupled with SWAN model is applied to study the combined action of wave, tide and storm surge. The coupled model, verified by measured data from the southwest coast of the Bohai Sea, is used to simulate the water exchange process of the Bohai Sea. The results show that the wind in the Bohai Sea has significant influences on water exchange results. A

coupled numerical model of wave, tide and storm surge should be used when the water exchange process is simulated in the Bohai Sea.

Parallel Session 6

Thursday, 15 December

**Beach Erosion and Morphodynamics II
Ballroom C**

Chair: Yongjun Lu, Zheng Bing Wang

15:45

Prediction of long-term topographic changes of Tenryu River Delta associated with sand bypassing at dam in upper basin assuming no coastal facilities

S. MIYAHARA

Coastal Engineering Laboratory Co., Ltd., 1-22-301 Wakaba, Shinjuku, Tokyo 160-0011, Japan

T. UDA, T. ISHIKAWA

Public Works Research Center, 1-6-4 Taito, Taito, Tokyo 110-0016, Japan

K. FURUIKE, M. SERIZAWA

Coastal Engineering Laboratory Co., Ltd., 1-22-301 Wakaba, Shinjuku, Tokyo 160-0011, Japan

The long-term topographic changes of the Tenryu River delta were predicted using the contour-line-change model, in which changes in grain size are taken into account. Given the annual discharge of sediment with three grain sizes, the recovery of the delta topography and the effect of nourishment on the nearby coast were predicted. Under the hypothetical condition that no coastal structures had been constructed along the coast, the effect of artificial sand supply from the river mouth was studied. The model was applied to the coast with a 10 km length extending on each side of the river mouth, and the beach changes up to 100 years from the present were predicted.

16:00

Beach profile changes under the action of solitary waves: Boussinesq modeling and comparison with laboratorial measurements

J. CHEN^{1,2}, Z.H. HUANG^{3,4}, C.B. JIANG², L.L. LI⁴, H.T. NIE¹

¹*DHI-NTU Water & Environment Research Centre & Education Hub, Nanyang Technological University, Singapore 639798, Republic of Singapore*

²*School of Hydraulic Engineering, Changsha University of Science & Technology, Changsha 410004, P.R. China*

³*School of Civil and Environmental Engineering, Nanyang Technological University, Singapore 639798, Republic of Singapore*

⁴*Earth of Observatory of Singapore, Nanyang Technological University, Singapore 639798, Republic of Singapore*

A 1D numerical model is reported that has the capability of modeling solitary wave runup and rundown an erodible bed. We couple the highly nonlinear and weakly dispersive Boussinesq equations with a sediment transport module and morphological evolution module to study the sediment transport and morphological changes under solitary waves. The combined model is validated using available laboratory experiments on solitary waves attacking sandy beaches.

16:15

Long term extension of the sand spit and change of the surrounding coastal morphology around Damietta Promontory, Nile River Delta

MOSTAFA AHMED, YOSHIMITSU TAJIMA, SHINJI SATO

Department of Civil Engineering, The University of Tokyo, Hongo 7-3-1, Bunkyo-ku, Tokyo, 113-8656, Japan

Severe erosion is experienced around the Nile delta promontories. While the highest rate of erosion occurs around Rosetta promontory, less significant erosion rates are observed around Damietta promontory and accretion is also observed around the east side of the Damietta promontory. This accretion mainly forms sand spit and is still growing toward the south-east. The main goal of this study is to monitor the large scale morphology changes around Damietta promontory and to investigate the growing mechanism of sand spit through comparisons of shoreline profiles semi-automatically extracted from the land-sat data set. Extracted shorelines are quantitatively investigated based on the linear regression technique as well as the empirical orthogonal function analysis.

16:30

Beach erosion as long-term topographic response to avalanche and landslide associated with the 1923 Kanto Earthquake

T. SAN-NAMI

Coastal Engineering Laboratory Co., Ltd., 1-22-301 Wakaba Shinjuku, Tokyo 160-0011, Japan

T. ISHIKAWA, T. UDA

Public Works Research Center, 1-6-4 Taito, Taito, Tokyo 110-0016, Japan

T. HARUMI, K. AKITA

Odawara Public Works Office, Kanagawa Prefectural Government

5-2-58 Higashi-machi, Odawara, Kanagawa 250-0003, Japan

The Nebukawa coast is a typical shingle beach located on the east coast of Izu Peninsula, and therefore, its stability was believed to be high. However, the coast has been eroded in recent years. To investigate the cause, the shoreline changes were investigated. It was found that a large-scale avalanche of earth and rocks and landslide were triggered in this area by the 1923 Kanto Earthquake, and a large amount of gravel was supplied to the coast, forming shallow contours protruding offshore. Since then, this coastline has receded under the action of northward longshore sand transport. Thus, the beach erosion of this coast is closely related to the long-term beach changes after the earthquake.

15:45

Vertical spreading of surface jets

MANH TUAN NGUYEN

DHI-NTU Centre and School of Civil and Environmental Engineering, 50 Nanyang Avenue, Singapore 639798

SOON KEAT TAN

Maritime Research Centre and Nanyang Environment and Water Research Institute, 50 Nanyang Avenue, Singapore 639798

Free-surface jets play an important role in environmental engineering and have been incorporated in many engineering applications. Characteristics of the jet-induced water surface perturbation may be used for assessing the effect of pollutant discharge into watercourse (jet dilution), remotely detecting the wakes of ships, or improvement of water quality. Published studies are mainly focused on the hydraulic characteristics of surface jets in terms of both mean velocity and turbulence. In this study we aimed to utilize surface jets as a potential driver to enhance the re-aeration process so as to improve water quality throughout a water column, and specifically the concentration of dissolved oxygen (DO). This paper presents work done on the spreading characteristics of surface jets. Initially, an investigation on the effects of Reynolds number and air-water interface on the vertical spreading of surface jets was carried out. The Reynolds number (based on the circular jet diameter (d_0) of 6mm) ranged from 1,500 to 6,000, and the normalized jet depth (h/d_0) varied from 0.55 to 1.94, where h was the distance from air-water interface to jet centre line. The flow fields were measured using the Particle Image Velocimetry (PIV) technique, which had a resolution of 1600×1200 pixels and a frame rate of 15Hz. To characterize the jet-spreading behavior, we mapped the flow path traced by the core of the jet (enveloped by velocities, $u \geq 10\%$ of jet maximum velocity, U_m). This core was well-defined when presented in terms of d/d_m and x/x_m , where d_m and x_m were the jet maximum penetration depth and the corresponding distance from jet exit, respectively. The findings of this study show that an increase in Reynolds number results in an increase in the spreading width of the surface jet ($h/d_0 \leq 0.55$) in the downstream direction. The findings also revealed a well-defined relationship among the parameters investigated.

16:00

Turbulent jets: a comparative study of point-source and CFD simulation results

B.S. PANI, B.M. ARUNA

Civil Engineering Department, IIT Bombay, Powai Mumbai, 400076, India

Reichardt's momentum transport hypothesis is an interesting turbulent closure model which provides a theoretical basis for superposition of momentum flux from multiple sources of flow. The point-source method, an offshoot of Reichardt's hypothesis, can be applied to a variety of jet flows. The method has a distinct advantage over the conventional approach as it predicts the entire flow field based on a single spread

Parallel Session 6

Thursday, 15 December

Jets I

Ballroom B

Chair: K.M. Lam, Il Won Seo

coefficient. To use the method with confidence, the point source technique is being validated against CFD results of different kinds of jets.

16:15

Numerical study on flow characteristics of a single jet and four tandem jets in crossflow

Y. XIAO, H.W. TANG

State Key Laboratory of Hydrology-Water Resources and Hydraulic Engineering, Hohai University, Nanjing, 210098, China

College of Water Conservancy and Hydropower Engineering, Hohai University, Nanjing, 210098, China

National Engineering Research Center of Water Resources Efficient Utilization and Engineering Safety, Hohai University, Nanjing, 210098, China

D.F. LIANG

Department of Engineering, University of Cambridge, Cambridge, CB2 1PZ, UK

J.D. ZHANG

State Key Laboratory of Hydrology-Water Resources and Hydraulic Engineering, Hohai University, Nanjing, 210098, China

The flow dynamics of a single jet and four tandem jets in cross flow were simulated using the Computational Fluid Dynamics (CFD) code Fluent. The realizable $k-\epsilon$ model was used to close the Reynolds-Averaged equations. The flow characteristics of the jets, including jet trajectory, velocity field and turbulent kinetic energy, were compared at the jet to cross flow velocity ratio of $R = 2.38 - 17.88$. The single jet is found to penetrate slightly deeper than the first jet in a jet group at the same R , although discrepancy decreases with decreasing R . The way that the velocity decays along the centerline of the jet is similar for a single jet and the first jet in a group, and the speed of the decay increases with decreasing R . The downstream jets in a group behave differently due to the sheltering effect of the first jet in the group. Compared with the first jet, the downstream jets penetrate deeper into the cross flow, and the velocity decays slower. The circulation zone between the two most upstream jets is stronger than those formed between downstream jets.

16:30

Mean cross-sectional flow structures of oblique jets released in a moving ambient

X. WANG, G.A. KIKKERT

Department of Civil and Environmental Engineering, Hong Kong University of Science and Technology, Clear Water Bay, Kowloon, Hong Kong, China

An experimental investigation is carried out to determine the mean cross-sectional flow structures of oblique jets released in a moving ambient. The focus is on those initial discharge angles that neither produce the double-vortex pair structure of the momentum puff region or the axi-symmetric Gaussian of the weak-jet region. For an initial discharge angle of 30° , a stretched Gaussian can be used to represent the cross-sectional flow structure. The parameters defining the cross-sectional behaviour of the flow are related to important parameters of the mean flow, such as the rate of spread.

Parallel Session 6

Thursday, 15 December

Waves and Modelling II

Tang

Chair: Yong-Sik Cho, Hung-Chu Hsu

15:45

Study on characteristics of solitary wave simulation in laboratory

JIN WANG, DENG-TING WANG, QI-HUA ZUO, QING-JUN LIU

Nanjing Hydraulic Research Institute, Nanjing, China

Series of experiments on extreme solitary wave are carried out in a flume with 175 m length, 1.8 m height and 1.2 m width using the Collapsing water column method. The results show that the biggest ratio of wave height and water depth is up to 1.29. The dimension of water column has a significant and effective impact on the wave height of extreme solitary. Furthermore, based on the analysis of the relations the wave heights with respects to water column widths, water depths and water column heights, an empirical formula which can be used in future application is obtained in the scope of this experiment.

16:00

Laboratory study of breaking events of deep-water wave packets by Hilbert-Huang Transform

Y.L. HE, G.H. DONG, Y.C. LI, Y.X. MA, W. ZHANG

State Key Laboratory of Coastal and offshore Engineering, Dalian University of Technology, Dalian, 116023, China

Experiments for single wave packets evolution in deep-water were carried out to study the characteristics of wave breaking. The energy loss by breaking and the local characteristics of the breaking during the evolution were analyzed by Hilbert-Huang transform (HHT). The findings show that the main energy dissipation by wave breaking is the high frequency contents. And the instantaneous frequencies of the first intrinsic mode function for the breaking cases vary greatly around breaking locations.

16:15

Numerical study on the movement of muddy seabed under waves

X.J. NIU, X.P. YU

State Key Laboratory of Hydrosience and Engineering, Department of Hydraulic Engineering, Tsinghua University, Beijing, 100084, China

The complex rheological property of mud may play an important role in the response of muddy seabed to waves. In this study, the movement of the soft mud layer on the stationary seabed driven by waves and its resulting wave energy dissipation are studied numerically. The effects of the viscosity, the elasticity, and the plasticity of mud on the movement of the mud layer are discussed. The wave damping coefficient computed by the viscous model agrees well with the experimental data, except the case that the density of mud is large so that the elastic property and the plastic property may not be ignored. It is also found that the

elastic property may enhance the amplitude of mud movement, and the oscillating motion of mud shows nonlinear behavior corresponding with the plastic property of mud.

16:30

An experimental study on the wave control by environment-friendly artificial reef

K. KIM, S. SHIN, W. LIM

Waterfront and Coastal Research Center, Kwandong University, 522 Naegok-dong, Gangneung, Ganwon-do, 210-701, Republic of Korea

Y. MOON, C. PYUN

Dept. of Civil & Environmental Engineering, Myongji University, Nam-dong, Cheoin-gu, Yongin, Gyeonggi-do, 449-728, Republic of Korea

2-dimensional hydraulic model tests were conducted to investigate the wave control performance of the newly designed environment-friendly artificial reef in terms of a submerged breakwater with changing crest widths and freeboard heights. Transmission coefficients of the current model were inversely proportional to the crest width. The reflection coefficients were proportional to the freeboard heights. However, the coefficients were not so much changed with different crest widths. Especially, the model with the shorter crest width showed better performance in terms of wave control compared with the model from another study. However, the results showed that the performance of the submerged breakwater does not depend on the shape of individual block but the total shape of the submerged breakwater as the crest width increases.

than that observed in ocean. Anisotropic turbulence eddy viscosity is proposed to modify the CL-II formulation. The large horizontal eddy viscosity effectively dissipates LCs with large spanwise wave number and be able to predict preferred spanwise wave number well consistent with ocean.

16:00

Three dimensional model of the flow around a fishing plane net

Y.P. ZHAO, C.W. BI, G.H. DONG, Y.C. LI

State Key Lab of Coastal and Offshore Engineering, Dalian University of Technology Dalian 116024, China

A three-dimensional numerical model combined the Realizable $k-\varepsilon$ turbulence model and the porous media model is established to simulate the flow field around a fishing net under current. The unknown porous coefficients are determined from the experimental forces on the net and flow velocities and the attack angles using the least square method. Therefore, the porous media act the same water-blocking effect as the net. This numerical model is applied for the simulation of the flow field around a plane net under current and the numerical results are compared with the data obtained by physical model tests. The comparisons show that the velocity magnitude of the numerical simulation agrees well with the experimental data with different attack angles. It is indicated that this numerical model is applicable for the simulation of the flow field around a fishing net. This study can be valuable for better knowledge of the flow characteristics around fishing net cage.

Parallel Session 6

Thursday, 15 December

Hydrodynamics IV

Ming II

Chair: Changhoon Lee, Yong Liu

15:45

Spacing of Langmuir circulations in ocean

MING ZHAO

Department of Engineering Mechanics, Dalian University of Technology, PR China

MOHAMED S. GHIDAOUI

Department of Civil and Environmental Engineering, The Hong Kong University of Science and Technology, Hong Kong, PR China

ZHENHUA HUANG

School of Civil and Environmental Engineering, Nanyang Technological University, Singapore

An important primary mechanism for Langmuir circulations (LCs) is the Craik and Leibovich (CL-II) hydrodynamic instability mechanism. The widely accepted CL-II mechanism explains LCs as a consequence of current and wave interaction. However, the original stability analysis of CL-II mechanism quantitatively fails to predict the spacing (streaks occur where down-welling occurs and thus represent the spacing of two rolls) of LCs in ocean. The predicted preferred spanwise wave number corresponding to maximum growth rate of unstable mode is much larger

16:15

Dynamical analysis of a soft yoke moored FPSO in shallow waters

S.Q. WANG

College of Engineering, Ocean University of China, Qingdao, 266100, China

S.Y. LI, X.H. CHEN

China Petroleum & Chemical Corporation Gas Company, Qingdao, China

Multi-body dynamic simulation method is applied for the coupled dynamic analysis of a FPSO with soft yoke mooring system. In the analysis, the FPSO and soft yoke mooring system are modeled as four rigid bodies of six degrees of freedom. The transfer functions of the first- and second-order wave force and hydrodynamic coefficients of the FPSO are calculated in the frequency domain. Then, the coupled dynamic analysis of the soft yoke moored FPSO under wave environment is carried out in the time domain. To better understand the contribution of the second-order difference frequency force to the FPSO response motion, cases with different water depths and wave spectrum peak periods, are analyzed. Some useful conclusions could be drawn.

16:30

Diffraction of water waves by a modified V-shaped breakwater

K.H. CHANG

Hydrotech Research Institute, National Taiwan University, No. 1, Sec. 4, Roosevelt Road, Taipei, 10617, Taiwan, R.O.C.

D.H. TSAUR

Department of Harbor and River Engineering, National Taiwan Ocean University, No.2, Beining Road, Keelung, 20224, Taiwan, R.O.C.

L.H. HUANG

Department of Civil Engineering, and Hydrotech Research Institute, National Taiwan University, No. 1, Sec. 4, Roosevelt Road, Taipei, 10617, Taiwan, R.O.C.

As a supplement to the original concept of V-shaped breakwaters launched successfully by the U.S. Army in 1999, a modified model with wave screens is presented herein. Such a modified model allows flexibility in tuning a suitable screen structure to leave relatively calm water inside the breakwater. Consequently, the previous model is a special case of the present model. A dual series solution to the linearized diffraction problem under consideration is derived via the method of matched eigenfunction expansions. To further enhance the numerical efficiency and accuracy, a quickly convergent scheme is employed also. Comparisons between the computed results obtained by two proposed approaches are made.

Parallel Session 6

Thursday, 15 December

Numerical Methods and Simulation II

Sung I

Chair: Decheng Wan

15:45

Numerical simulation of sloshing in 2d rectangular tank based on SPH method with an improved boundary treatment approach

K. GONG

DHI-NTU Centre, Nanyang Environment and Water Research Institute, Nanyang Technological University, Singapore

H. LIU

Department of Engineering Mechanics, Shanghai Jiao Tong University, Shanghai, 200030, China

S.K. TAN

Maritime Research Centre and School of Civil and Environmental Engineering, Nanyang Technological University, Singapore

An improved boundary treatment approach for smoothed particle hydrodynamics is presented. In this approach, the pressure of a boundary particle is obtained by interpolation using the pressure of fluid particles in the near boundary area around it, and the boundary particle pressure is used to solve the momentum equations. This boundary treatment is applied in the SPH model to simulate nonlinear sloshing in a rectangular tank. The simulated free surface elevation is in good agreement with the experimental results. This paper also illustrate that the proposed approach is superior compared to earlier approach.

16:00

Optimum open boundary conditions for coupled numerical model of tide, surge and wave

S.Y. KIM, Y. MATSUMI

Department of Information, Management and Civil Engineering, Tottori University, 4-101, Koyama Minami, Tottori City, Tottori, 680-8552, Japan

T. YASUDA, H. MASE

Disaster Prevention Research Institute, Kyoto University, Gokasho, Uji, Kyoto, 611-0011, Japan

The present study suggests an estimate method of currents combined with surges and tides as values of open boundaries using the Flather's condition for a 2 dimensional coupled model of surge, wave and tide considering the wave-current interactions on the surface and bottom boundary layers. We found that the present method made an improvement in the reduction of spin-up calculation duration and was more stable in comparison between other radiation conditions with currents or water levels with either fixed or variable phase speeds.

16:15

Numerical experiments on a permeable breakwater by using numerical wave tank, CADMAS-SURF/3D

K. TAKAHASHI, K. ANNO, T. NISHIHATA, T. SEKIMOTO

Institute of Technology, Penta-Ocean Construction Co., Ltd., 1534-1 Yonku-cho, Nasushiobara-shi, Tochigi 329-2746, Japan

Although the 2-D numerical wave flumes have recently been applied to the wave-structure interaction system, 3-D configuration of permeable breakwaters cannot be reproduced in the method. In this study, CADMAS-SURF/3D which has been newly developed as 3-D numerical wave tank is applied to estimate the hydraulic performance of the permeable breakwater. The applicability is investigated from the comparison between experimental and calculation results, in which detailed wave absorption mechanism is also discussed.

Parallel Session 7
Friday, 16 December
Special Session: The 2011 East Japan Tsunami I
Ballroom C
Chair: Harry Yeh, Sung Bum Yoon

09:30

Overview of the 2011 Tohoku Earthquake Tsunami survey results

NOBUHITO MORI

*Disaster Prevention Research Institute, Kyoto University
Gokasho, Uji, Kyoto 611-0011, JAPAN*

THE 2011 TOHOKU EARTHQUAKE TSUNAMI JOINT SURVEY GROUP

<http://www.coastal.jp/tjt/>

At 14:46 local time on March 11, 2011, a magnitude 9.0 earthquake occurred off the coast of northeast Japan. This earthquake generated a tsunami that struck Japan as well as various locations around the Pacific Ocean. With the participation of researchers from throughout Japan, joint research groups conducted a tsunami survey along a 2000 km stretch of the Japanese coast. More than 5400 locations have been surveyed to date, generating the largest tsunami survey dataset in the world. The maximum run-up height measured to date was 40.4 m, resulting in the catastrophic destruction of towns and cities.

09:45

Field survey of the 2011 off the Pacific Coast of Tohoku Earthquake Tsunami disaster and future tsunami protection

TOMOYA SHIBAYAMA

Department of Civil and Environmental Eng., Waseda University, Okubo, Shinjuku-ku, Tokyo, 169-8555 Japan

On March 11, 2011, a large earthquake of magnitude 9.0 took place, generating a tsunami that caused a severe damage to the east coast of Japan. Field surveys were performed to know tsunami inundation heights and disasters in Iwate, Miyagi, Fukushima, Ibaraki and Chiba prefectures. The results of these surveys are reported. Inundation heights were more than 10 m in the north part of Miyagi, 5 to 10 m along the coast of Sendai Bay and around 5 m in Ibaraki and Chiba. Buildings, including reinforced concrete structures, were washed away and ships were stranded in land. Coastal structures such as dikes and coastal forests also suffered extensive damage. Possible evacuation measures are also discussed based on the observations.

10:00

Field survey of suffering appearances due to Tohoku Earthquake Tsunami

Y. KIMURA

Technical Research Institute, Hitachi Zosen Corporation, 2-11, Funamachi-2, Taisyo-ku, Osaka, 551-0022, Japan

Y. YAMAKAWA

Machinery & Infrastructure Headquarters, Hitachi Zosen Corporation, 5-1, Chikkoshinmachi-1, Nishi-ku, Sakai-shi, Osaka, 592-8331, Japan

H. MASE

Disaster Prevention Research Institute, Kyoto University, Gokasyo, Uji-shi, Kyoto, 611-0011, Japan

A huge earthquake occurred in the Pacific Ocean off Tohoku area, Japan, at 14:46 local time on March 11, 2011. Tsunamis due to this earthquake were the maximum in Japanese history and caused serious damage on extensive areas of Tohoku. In this study, field survey of suffering appearances due to tsunamis was carried out targeting 20 areas along coasts of Iwate and Miyagi Prefectures focusing on damage of coastal structures and effects of topography. As a result of survey, it was found that design conditions for coastal structures should be decided considering topography, especially areas of low-lying land, behind these structures.

10:15

A brief overview on the post-tsunami survey in the Sanriku Coast, Japan

HAIJING LIU¹, TOMOHIRO TAKAGAWA²,
YOSHIMITSU TAJIMA¹, SHINJI SATO¹, TAKENORI
SHIMOZONO³, AKIO OKAYASU³, HERMANN M.
FRITZ⁴

¹*Department of Civil Engineering, The University of Tokyo, 7-3-1 Hongo, Bunkyo-ku, Tokyo, 113-8656, Japan*

²*Port and Airport Research Institute, Asia-Pacific Center for Coastal Disaster Research, 3-1-1 Nagase, Yokosuka, Kanagawa, 239-0826, Japan*

³*Department of Ocean Sciences, Tokyo University of Marine Science and Technology, 4-5-7 Konan, Minato-ku, Tokyo 109-0075, Japan*

⁴*School of Civil and Environmental Engineering, Georgia Institute of Technology, Savannah, Georgia 31407, USA*

In the immediate aftermath of the 2011 Tohoku earthquake, we deployed a post-tsunami reconnaissance in the Sanriku Coast, Japan, where destructive damages caused by tsunami waves were demonstrated, as well as from the historical events. Significant land subsidence was observed with the ground level of harbor dock being inundated at high tide level after the earthquake. Damages on coastal structures, such as harbor jetty, seawall and breakwater, were also confirmed. Failure pattern of these structures exhibits a complex feature with respect to the tsunami height, current velocity and wave direction, the structure layout and its armoring effort.

Parallel Session 7
Friday, 16 December

Jets II
Ballroom B

Chair: Gustaaf Kikkert, Bidya Sagar Pani

09:30

Characteristic behaviours of a vertical round jet under different spectral waves

Z.S. XU

College of Harbor, Coastal and Offshore Engineering, Hohai University, 1 Xi Kang Road, Nanjing, 210098, China

Y.P. CHEN

State Key Laboratory of Hydrology-Water Resources and Hydraulic Engineering, Hohai University, 1Xi Kang Road, Nanjing, 210098, China

C.W. LI

Department of Civil and Structure Engineering, The Hong Kong Polytechnic University, Hong Kong

C.K. ZHANG

College of Harbor, Coastal and Offshore Engineering, Hohai University, 1 Xi Kang Road, Nanjing, 210098, China

A dynamic Large Eddy Simulation (LES) model is developed and applied to investigate the jet behaviours under three different kinds of waves, including regular (extremely narrow-band spectrum) waves, JONSWAP (narrow-band spectrum) random waves and P-M (wide-band spectrum) random waves. All the waves are 'energy equivalent', i.e., with the same energy density and energy flux. The quantitative comparison of jet characteristic parameters, such as the centerline velocity and the jet width, under those waves is performed. The results show that close to the discharge outlet the jet under the JONSWAP or P-M random waves exhibits a faster decay of centerline velocity and a wider lateral width compared to the jet under regular waves. However, with an increasing distance from the jet outlet, the decrease rate of centerline velocity for the jet under regular waves becomes faster, resulting in a wider jet width as compared to the jet under the random waves.

09:45

Two-phase velocity measurements in horizontally-discharging buoyant sediment jets

P. LIU, K.M. LAM

Department of Civil Engineering, The University of Hong Kong, Pokfulam Road, Hong Kong

Mixing of buoyant jets laden with solid sediments at different concentrations is studied in the laboratory. The jets discharge in an initial horizontal direction into an otherwise stagnant environment. The velocities of the fluid phase and the particle phase are measured simultaneously with particle-image velocimetry (PIV) using two cameras. Separation of the two phases is achieved by marking jet effluent fluid with fluorescent dye. Results suggest that mixing and rising of the buoyant jets are modified from the single-phase case when the sediment concentration increases. Some structures of the particle velocity fields are revealed. Discussion is made on the interaction between the particle phase and the jet flow phase.

10:00

Hydraulic characteristics of the submerged plane jet formed at the lee side of a silt screen

T.T. VU

School of Civil and Environmental Engineering and DHI-NTU Centre, Nanyang Technological University, Singapore 639798

S.K. TAN

Maritime Research Centre and Nanyang Environment and Water Research Institute, Nanyang Technological University, Singapore 639798

Silt screen is a flexible physical structure that has been widely employed to control sediment dispersal at dredging sites. Previous research showed that the water column is divided into two distinct flow regions in the immediate vicinity of a silt screen: a recirculation region in the upper water layer and a fast flow in the lower water layer. The fast flow at the lower water layer that emerges from below the silt screen strongly resembles a submerged plane jet. While the slow recirculation at the upper water layer may help facilitate sediment settling, the presence of such jet-flow of high velocity at the lower water layer raises concern about the potential of sediment re-entrainment and re-suspension.

This paper presents the analyses of the hydraulic characteristics of the submerged plane-jet flow that is formed at the lee side of a silt screen. The writers conducted both laboratory and numerical study to investigate the spatial development of the plane jet after it emerged from a silt screen. In the laboratory experiments, the technique of Particles Imaging Velocimetry (PIV) was used to capture the flow field in the vicinity of the silt screen. The results obtained showed that the effects of silt screen's configuration, in particular the silt screen's penetration depth, on the hydraulics parameters of the plane-jet – including velocity distribution, flow rate distribution and turbulence distribution are significant. In addition, the applicability of classical plane jet theory on describing the flow distribution of the silt screen's plane jet was also examined.

10:15

The near-field jet behavior of 60 degrees dense jets discharged into a perpendicular crossflow

CHRIS C.K. LAI

Department of Civil Engineering, The University of Hong Kong, Pokfulam, Hong Kong, China

JOSEPH H.W. LEE

Department of Civil Engineering, The Hong Kong University of Science and Technology, Clear Water Bay, Hong Kong, China

Wastewater effluents with a density higher than that of the environment are often discharged into coastal waters in the form of submerged dense jets. Examples include brine discharge from desalination plants and cooled water from liquefied natural gas plants. In general, there exists an ambient current which can approach the jet at an arbitrary angle; the resulting dense jet will then have a three-dimensional trajectory. We present an experimental investigation on 60° dense jets discharged into a perpendicular current. The tracer concentration field is measured at selected cross-sections using the Laser induced-fluorescence (LIF) method. Jet detrainment from the dense jet is observed; the detrained jet fluid is advected horizontally downstream by the crossflow. Compared to predictions of a validated integral jet model that does not account for jet detrainment, it is found that the horizontal jet penetration in the momentum plane is consistently under-predicted by about 35 percent, while the jet trajectory in the buoyancy plane and the near field

dilution in the bent-over dense jet are reasonably well-predicted.

knowledge obtained is useful in ocean fishery resource management.

Parallel Session 7
Friday, 16 December
Marine Ecology and Environment II
Tang
Chair: Margaret Chen, Tadashi Hibino

09:30

Influence of sea surface temperature on coastal urban area - case study in Osaka Bay, Japan

JUNICHI NINOMIYA

Graduate School of Engineering, Kyoto University, Gokasho, Uji, Kyoto, Japan

NOBUHITO MORI

Disaster Prevention Research Institute, Kyoto University, Gokasho, Uji, Kyoto, Japan

HIROYUKI KUSAKA

Center for Computational Sciences, University of Tsukuba, 1-1-1 Tennodai, Tsukuba, Ibaraki, Japan

This study simulates atmospheric environments at Osaka bay area of Japan using the numerical weather prediction with highly accurate sea surface temperature (SST) data from the satellite. A series of numerical experiments for understanding urban heat island at Osaka bay area is conducted considering latest information of land use classifications, SST and an urban canopy model. The accurate daily information of SST at Osaka bay improves the daily temperature at the center of Osaka city. In addition, the one degree SST increase has impact to 0.6 degree increase of maximum temperature at the center of Osaka city.

09:45

A study of pelagic plankton distribution patterns in the gulf of Alaska using a coupled population dynamics – physical mixing model

J. PENG

Department of Mechanical Engineering, University of Alaska Fairbanks, Fairbanks, AK 99775, USA

It is well known that plankton distribution patterns on the ocean surface are dependent on the coupling between plankton population dynamics and physical ocean mixing. The population dynamics describe the biological/ecological interactions among nutrient, phytoplankton and zooplankton. Physical advection by ocean currents affects location and concentration of the biota, which influences population growth. In this study, a model that couples plankton population growth and physical ocean mixing is used to simulate a plankton bloom in the Gulf of Alaska. The contributions of population growth and ocean mixing to the patterns and the evolution of spatial structures of plankton distribution are identified. The study found that the patterns of plankton structures on the large scale can be explained by mixing by ocean currents, whereas local distribution of plankton is more dependent on small-scale turbulence and plankton population dynamics. The method developed in this study provides a useful tool to monitor and study pelagic plankton distribution in the ocean and the

10:00

Monitoring topographic and habitat changes in natural sand dunes after setting back a seawall at Nakatsu tidal flat, Oita, Japan

S. SEINO

Dep. Urban and Environmental Eng., Graduate School of Eng., Kyushu University, 744 Moto-oka, Fukuoka, Fukuoka 819-0395, Japan

Y. ASHIKAGA

Nakatsu Waterfront Conservation Association, 2-8-35 Chuo, Nakatsu, Oita 871-0024, Japan

T. UDA

Public Works Research Center, 1-6-4 Taito, Taito, Tokyo 110-0016, Japan

H. MIHARA, S. WATANABE

Nakatsu Public Works Office, Oita Prefectural Government, 1-5-16 Chuo, Nakatsu, Oita Prefecture, 871-0024, Japan

A coastal dike for protecting the wetland was set back in 2004 near the mouth of the Maite River flowing into the Nakatsu tidal flat. Monitoring surveys were carried out between 2005 and 2009 after the setting back. During the observation period, Typhoon No. 5 hit the coast on August 2, 2007, resulting in the increase in tide level up to DL+4.7 m, which was a maximum since 2000. Owing to the storm surge, shoreward sand transport occurred and a high berm with a height of DL+5.02 m was formed with the recession of the foreshore by 5 m. No changes were observed in the wetland and its environment was maintained despite the storm surges, suggesting that the setting back was useful for protecting the wetland against storm surge.

10:15

Integrated use of electrical resistance tomography and radon monitoring for characterizing submarine groundwater discharge dynamics in a fringing reef

A.C. BLANCO

Department of Geodetic Engineering, University of the Philippines Diliman, Quezon City, 1101, Philippines

K. NADAOKA, A. WATANABE

Department of Mechanical and Environmental Informatics, Tokyo Institute of Technology, O-okayama, Meguro-ku, Tokyo-to, Japan

Submarine groundwater discharge (SGD) potentially contributes comparable amounts of nutrients compared with that of river runoff. It is imperative to understand the dynamics of SGD to be able to adequately quantify nutrient loading into coastal marine environment. Electrical resistivity tomography (ERT) and radon monitoring were used to characterize submarine groundwater discharge (SGD) dynamics in Shiraho Reef located in Ishigaki Island, Okinawa, Japan. Shore-parallel and shore-perpendicular ERT transect surveys were conducted to identify seepage zones. The ERT profiling was conducted repeatedly over high tide and low tide. Simultaneously, continuous radon monitoring was made in order to estimate SGD rates. These measurements were then compared against each other to elucidate on the possibility of estimating groundwater flux from ERT measurements alone.

Shore-parallel ER profiles showed the presence of several groundwater seepage zones during low tide only. These zones corresponded with relatively higher ^{222}Rn activities measured from grab samples taken along the ER transect. On the other hand, the shore-perpendicular ER profiles showed that SGD mainly occurs at the beach-nearshore reef interface, though seepage may also occur in pools of water formed in low tide. Comparing ERT and radon-estimated fluxes, increases in radon inventories corresponded well with higher increases in ER values.

Parallel Session 7

Friday, 16 December

Waves and Modelling III

Ming II

Chair: Keisuke Murakami, E Van Groesen

09:30

Large amplitude solitary waves due to solitary resonance

K. NAKAYAMA

Civil and Environmental Engineering, Kitami Institute of Technology, 165 Koen-cho Kitami City, 090-8507, Japan

T. KAKINUMA

Ocean Civil Engineering, Kagoshima University, 1-21-40 Koorimoto Kagoshima City, 890-0065, Japan

H. TSUJI

Research Institute for Applied Mechanics, Kyushu University, 6-1 Kasuga-koen Kasuga City, 816-8580, Japan

M. OIKAWA

Intelligent Mechanical Engineering, Fukuoka Institute of Technology, 3-30-1 Wajiro-higashi Higashiku Fukuoka City, 811-0295, Japan

A fully-nonlinear and strongly-dispersive internal wave equation model was used to investigate the interaction between internal solitary waves in a two-dimensional plane in order to clarify the resonance of fully-nonlinear internal solitary waves, which is one of the reasons for the occurrence of large amplitude solitary waves (LASW). The 3rd order theoretical solutions for internal waves in a two-layer system was used as initial conditions and a "stem" was confirmed to occur when the incident wave angle was less than certain critical angle. This study revealed the occurrence of LASW by using a fully-nonlinear and strongly-dispersive internal wave equation model.

09:45

Empirical formula for regular wave breaking over currents

Y. LIU, X.J. NIU, X.P. YU

State Key Laboratory of Hydrosience and Engineering, Department of Hydraulic Engineering, Tsinghua University, Beijing, 100084, China

The study is to improve the accuracy of the breaking index formula for waves against currents, based on the predictive formula for the incipient breaking of regular waves recently proposed by the authors. To include the effects of currents, a total number of 220 experimental cases reported by 5 different scholars are collected for comparison. Three existing formulas proposed by

Sakai [1,2] that take the currents into account are also examined, in addition to the widely used Miche's formula [3]. Then, a new approach adopting the concept of equivalent wave height H_e and equivalent water depth h_e is proposed and good agreement with experimental data is reached while applying H_e and h_e to the breaking criteria proposed by the author[4] with a minimum relative variance of 2.6%. None of additional empirical coefficients is included in this process. Further study also reveals that applying H_e and h_e to Miche's formula [3] and Goda's formula [18] also yields relatively good results.

10:00

Wave setup over fringing reef with a shallow reef crest: a hydraulic theory for flows under critical conditions

Z.H. HUANG

School of Civil & Environmental Engineering and Earth Observatory of Singapore, Nanyang Technological University, 50, Nanyang Avenue, Singapore, 639798, Singapore

Y. YAO

School of Civil & Environmental Engineering, Nanyang Technological University, 50, Nanyang Avenue, Singapore, 639798, Singapore

S.G. MONISMITH

Department of Civil and Environmental Engineering and Environmental Fluid Mechanics Laboratory, Stanford University, 473 Via Ortega, Stanford, CA, 94305, USA

E.Y.M. LO

School of Civil & Environmental Engineering, Nanyang Technological University, 50, Nanyang Avenue, Singapore, 639798, Singapore

An analytical solution based on the cross-shore mass balance is presented in this paper to seek a proper description of wave-induced setup for very shallow and complex reef crest. An empirical parameter is proposed to account for the effects of flow unsteadiness and bottom shape. Theoretical results show that non-dimensional mean water level on reef flat is a function of both offshore wave steepness and wave reflection coefficient. The analytic model is first validated by our experimental work, in which the role of the ridge in wave-induced setup over the reef was investigated by using an idealized rectangle ridge model at the reef crest. Good agreement is found between the model predictions and laboratory measurements for very shallow reef-crest submergences. The theory is also successfully applied to reproduce other published data with similar reef configurations.

10:15

Mild-slope equations for random waves inside and over porous layers

C. LEE, S. PARK

Department of Civil and Environmental Engineering, Sejong University, 98, Gunja-dong, Gwangjin-gu, Seoul 143-747, South Korea

H. MASE

Disaster Prevention Research Institute, Kyoto University, Gokasho, Kyoto 611-0011, Japan

In this study, we developed hyperbolic-type mild-slope equations for random waves inside and over multiple porous layers. Two types of the models were developed in terms of the seepage velocity and discharge velocity. We determined complex-valued wave numbers by solving the boundary value problem. Then, in Radder and Dingemans' (1985) mild-slope equations, we included the damping coefficient due to drag and inertial resistances which were determined from the imaginary wave number and the group velocity. Numerical experiments were conducted to verify and compare model equations for several cases of waves propagating through porous layers.

Parallel Session 7
Friday, 16 December
Numerical Methods and Simulation III
Sung I
Chair: Susumu Araki, Changbo Jiang

09:30

Three dimensional numerical simulation of flow around four circular cylinders in an in-line square configuration

F. TONG, L. CHENG

School of Civil and Resource Engineering, The University of Western Australia, 35 Stirling Highway, Crawley, WA 6009, Australia

M. ZHAO

School of Engineering, University of Western Sydney, Locked Bag 1797, Penrith, NSW 2751, Australia

X.B. CHEN

Research Department, BV, 92570, Neuilly-sur-Seine, France

Uniform flow past four circular cylinders in an in-line square configuration was studied numerically at Reynolds number of 270. The three-dimensional (3D) Navier-Stokes equations were solved using OpenFOAM, an open source code. The study was focused on the influence of multiple cylinders and their spacing ratio on the wake flow. The effects of gap between two neighbor cylinders on vortex shedding frequency and force coefficients are studied. Flow characteristics are observed through flow visualization of streamwise and spanwise vortices based on the numerical results. It was found that there exists remarkable repulsive force when cylinders are very close to each other, and this repulsive force disappears gradually with the increase of spacing ratio. Also, the critical Reynolds number for flow transiting from two-dimensional to three-dimension is different from that of an isolated cylinder and is dependent on gap among the cylinders.

09:45

Currents past gravity anchors astride offshore pipelines: a direct numerical simulation

X. ZHAO¹, M. ZHAO², L. CHENG¹, W. HE¹

¹*School of Civil and Resource Engineering, The University of Western Australia, 35 Stirling Highway, Crawley, WA 6009, Australia*

²*School of Engineering, University of Western Sydney, Locked Bag 1797, Penrith, NSW 2751, Australia*

Consisting of large arch-shaped precast concrete blocks positioned at intervals astride the pipeline, the gravity anchor system is engineered to provide secondary stabilization for large diameter offshore pipelines operating in severe metocean conditions. Bottom-seated on the seabed, however, the gravity anchor could subside into scour pits formed around it, imposing integrity risks on pipeline operations. With scour processes around gravity anchors correlating closely with the hydrodynamic behavior of flow, the present study concentrates on characterizing flow mechanisms around gravity anchors by means of direct numerical simulation. The three-dimensional Navier-Stokes equations were solved using the Petrov-Galerkin finite element method. Currents with a 90 degree angle of attack past a gravity anchor astride pipelines resting on a rigid bed was simulated at a pipe Reynolds number of 1000. The computed amplification of bed shear stresses was presented first, and compared with laboratory observations of scour patterns. Then, the responsible mean flow topology has been identified in two areas, comprising the horseshoe vortex upstream of the anchor and the lee-wake vortices.

10:00

Tidal current simulation of the Ariake Sea using the sigma-coordinate finite element model

H. KIRI, E. SHIRATANI, H. TANJI

National Agriculture and Food Research Organization, Institute for Rural Engineering, 2-1-6 Kannondai, Tsukuba, Ibaraki 305-8609, Japan

K. ISHITA

Kokusai Kogyo Co. Ltd., Kyushu Group, 3-6-3 Hakata Station East, Fukuoka-City, Fukuoka 812-0013, Japan

A three-dimensional finite element model was developed to simulate the tidal current of the Ariake Sea. This model has two features. One is its use of the sigma-coordinate system for the vertical direction and the other is its application of the finite element method that employs the bubble function element to perform analysis. The tidal current of the Ariake Sea in 2007 was simulated as a numerical model test. It was confirmed that the simulated tide level represents the observed tide by comparing the data at seven observation points. However, the amplification rate of the M2 component of the tide level from Kuchinotsu to Ooura was slightly small. The result of the comparison of current ellipses in January and August indicates that the proposed model can correctly simulate the tidal current of the Ariake Sea. The simulations of the distribution of the temperature and of the salinity of seawater were confirmed by comparing their results with the observation data.

10:15

Numerical simulation of free surface flow using a three-dimensional numerical model

J.W. LEE, K.-H. SEO, Y.-S. CHO

Department of Civil and Environmental Engineering, Hanyang University, 17 Haengdang-dong, Seongdong-gu, Seoul 133-791, Korea

In this study, three-dimensional hydrodynamic pressure model for free surface flows using a normalized vertical coordinate system is presented. Numerical models of free surface flow are developed to calculate the velocity components, the free surface elevations in the following three steps. At the first step, the vertical momentum equations are discretized by using an implicit method over the vertical direction. In the second step, the discrete horizontal momentum equations are projected on to the free surface equation. The predictor-corrector step method is used to calculate variations of free surface elevation and velocity. Finally, the hydrodynamic pressure and final velocity field are calculated. As the vertical velocity is not taken into account at the previous step, the velocity field may not satisfy the local mass conservation at each computational grid cell. In this step, the velocities and the free surface elevation obtained from the previous step are corrected to conserve the local mass balance by considering the hydrodynamic pressure in conjunction with the continuity equation. The developed model is applied to propagation and subsequent run-up process of nearshore solitary wave around a circular island carried out by Coastal Engineering Research Center (CERC), US Army Corps of Engineers. Computed results are then compared with laboratory measurements. Very reasonable agreements are observed.

Parallel Session 8
Friday, 16 December
Special Session: The 2011 East Japan Tsunami II
Ballroom C
Chair: Nobuhito Mori, Tomoya Shibayama

11:00

Hindcast simulation of 2011 great East Japan Earthquake Tsunami

B.I. MIN, B.H. CHOI

Department of Civil and Environmental Engineering, Sungkyunkwan University, 300 Chencheon-dong, Jangan-gu, Suwon, Gyeonggi-do 400-746, Korea.

K.O. KIM

Korea Ocean Research & Development, Ansan, 426-744, Korea

V.M. KAISTRENKO

Institute of Marine Geology and Geophysics Russian Academy of Sciences, Yuzhno-Sakhalinsk, 693022, Russia

E.N. PELINOVSKY

Department of Nonlinear Geophysical Processes, Institute of Applied Physics, Russian Academy of Sciences, Nizhny Novgorod, 603950, Russia

We proposed a rapid method for forecasting tsunami runup on the coasts combining 2-D numerical model and 1-D analytical runup theory. In the first step, the 2-D numerical simulations of tsunami generation and propagation are performed assuming impermeable boundary conditions of a 5-10m depth at the last sea points (equivalent to a wall). Then the time series of the water oscillations on the wall are used to calculate the runup heights using the analytical integral expression following from 1-D theory. The feasibility

of this approach was validated against the disastrous 2011 Great East Japan Earthquake Tsunami. We have demonstrated that the proposed approach is more reasonable and rapid method of forecasting than complicated coastal inundation models.

11:15

Numerical simulation of 2011 Tohoku Tsunami propagation over Pacific Ocean

JAE SEOK BAE, CHOONG HUN SHIN

Department of Civil Engineering, Hanyang University, 17 Haengdang-dong, Seongdong-gu, Seoul, 133-791, Korea

SUNG BUM YOON

Department of Civil & Environmental Engineering, Hanyang University, 1271 Sa-1-dong, Sangnok-gu, Ansan, Gyeonggi-do 426-791, Korea

In this study, initial wave field of the 2011 Tohoku tsunami was estimated by using waveform inversion method. And numerical simulations of the 2011 Tohoku tsunami were performed in order to analyze the propagation characteristics over the Pacific Ocean and to verify the waveform inversion method. Numerical results were compared with observed data of NOAA's DART buoy system and DONET system of JAMSTEC.

11:30

Propagation characteristics of 2011 North-East Japan Tsunamis towards Korean peninsula

SUNG BUM YOON

Department of Civil & Environmental Engineering, Hanyang University, 1271 Sa-1-dong, Sangnok-gu, Ansan, Gyeonggi-do 426-791, Korea

JAE SEOK BAE

Department of Civil Engineering, Hanyang University, 17 Haengdang-dong, Seongdong-gu, Seoul, 133-791, Korea

CHAE HO LIM

Oceanographic Division, Korea Hydrographic and Oceanographic Administration (KHOA), 1-17 Hang-dong 7 Street, Joong-gu, Incheon, 400-800, Korea

In the present study the effect of bathymetry near the south-west sea area of Korea on the propagation of 2011 North-East Japan Tsunami is analyzed based on the numerical simulation using the finite difference dispersion-correction model. It is found that the bathymetry from the source to Korean Peninsula, such as Nankai Trough, Ryukyu Islands and the topographical lens in the East China Sea, plays an important role to reduce the tsunami height along the south coast of Korea. The mechanism involved in the transformation of tsunamis over those topographies is discussed.

11:45

11 March 2011 great East Japan Tsunami inundation modelling of four coastal areas using simplified source descriptions

S. LESCHKA, O. LARSEN

DHI-NTU Water & Environment Research Centre & Education Hub, 200 Pandan Loop, #05-03 Pantech 21, Singapore, 128388, Singapore

N. SAKTI NINGRUM

*University of Nice S.A., Polytech Nice Sophia/EuroAqua,
930 route des colles Sophia Antipolis, 06903, France*

F. DUBONNET, P.S. RASCH

DHI Water & Environment Pte Ltd, 200 Pandan Loop, #08-03 Pantech 21, Singapore, 128388, Singapore

In tsunami modeling not all of physical phenomena, which occurs in reality, can be considered, especially with respect to source description and inundation. Empirical relations to describe earthquake deformations found in the literature differ considerably amongst each other, and so therefore does the subsequent inundation model results. In this paper it is tested if simplified source descriptions, still based on released earthquake energy, might lead to the same quality of inundation results. The test case selected is the 11 March 2011 Great East Japan Tsunami has been used to test such simplified source descriptions. The inundation modeled for four cities have been compared with observations. The results suggest that a simplification of the source description does not lead to lower quality in inundation modeling.

12:00

Waveform evolution of the 2011 East Japan Tsunami

HARRY YEH

School of Civil & Construction Engineering, Oregon State University, Corvallis, Oregon 97331, USA

SHINJI SATO, YOSHIMITSU TAJIMA

Department of Civil Engineering, the University of Tokyo, Hongo, Tokyo 113-8656, Japan

The 2011 East Japan Tsunami yielded a wealth of quality data and information. Here we focus on the waveform data recorded with the offshore gages at three locations along the east-to-west transect from the city of Kamaishi (39°16'N 141°53'E). The recorded data show the coherent waveform: the formation of a narrow spiky wave riding on the broader tsunami base at its rear side. This waveform resulted in the gradual initial rise and the strong second-stage runup, followed by the rapid drawdown. Our analysis shows that the linear water-wave theory can predict approximately the shoaling evolution, although some discrepancies in its propagation speed and amplification exist. Consequences of the tsunami waveform to the observed tsunami damage and human losses are discussed.

12:15

Aftermath of the 3/11 tsunami in Tohoku Region of Japan

A.W. JAYAWARDENA

International Centre for Water Hazard and Risk Management under the auspices of UNESCO, Public Works Research Institute, Tsukuba, Japan

On March 11, 2011 at 14:46, an earthquake measuring 9.0 on the Richter scale struck the north-east coastal region of Japan. The epicentre of the earthquake was approximately 70 km east of Oshika Peninsula of the Tohoku Region of Japan and the hypocentre at a depth of some 32 km in the ocean. It lasted for about 6

minutes and was the most powerful earthquake to hit Japan and one of the most powerful ones in the world. The tsunami triggered by this earthquake reached a maximum height of 40 m in Miyako in Iwate Prefecture and travelled up to about 10 km inland. Up to about 4.4 million people were without electricity and about 1.5 million without water for several days. According to National Police Agency of Japan, 15,836 people were killed and 3,650 missing as of November 11, 2011.

The earthquake shifted Honshu Island by 2.4 m eastwards and shifted the earth on its axis by 10-25 cm. It released surface energy which was dissipated as tsunami energy equivalent to approximately twice that of the 9.1 magnitude Indian Ocean Earthquake that killed over 230,000 people in 11 countries.

Although the tsunami disaster has been overshadowed by the nuclear accident in Fukushima that was triggered by the earthquake and tsunami, the main damage in terms of human casualties was from the former. From historical records of earthquake related disasters in Japan, the human casualties have been mainly due to accompanying disasters triggered by the earthquake. In the case of the Hanshin earthquake in 2005 that hit the Kobe area of Japan, it was the fire that took away many lives; in the Tohoku earthquake it is the tsunami that took away over 19,000 lives included those presumed dead.

Japan has lost a sizable chunk of land as a result of the nuclear accident which cannot be used productively for many years to come. People who lived within 20 km radius of the Fukushima No. 1 nuclear plant and within a radius of 10 km from Fukushima No.2 nuclear plant have lost their land, homes, livelihood and almost everything.

One contrasting observation when the Tohoku tsunami is compared with the 2004 Indian Ocean tsunami is the educational level, degree of preparedness and the experience of the affected people in the two regions. Japan is well aware of tsunamis, have experienced the consequences from past occurrences and is well prepared and disciplined to deal with disasters perhaps better than any other country in the world. The countries that were devastated by the Indian Ocean tsunami on the other hand had no knowledge of tsunamis, have never experienced before and were not prepared at all. For example, the Disaster Management Centre in Sri Lanka which is one of the countries affected and which lost over 35,000 lives was established by the Government only after the 2004 tsunami. Despite the high investments for disaster mitigation both in terms of structural and non-structural measures, Japan has lost a comparable number (taking all factors into consideration) of lives. An obvious question is whether it is practically possible to be prepared against an event of such magnitude. In other words, can human beings be prepared to expect the unexpected?

In this paper, an attempt will be made to compare and contrast the social, cultural and educational aspects, technological advances, early warning systems, access to information, investment policies in disaster

mitigation and management etc. of the countries affected by the 2004 Indian Ocean tsunami and the 2011 Tohoku tsunami including lessons to be learned, and explore the way forward to avoid disasters of unexpected severity.

Parallel Session 8
Friday, 16 December
Wastewater Disposal and Water Quality I
Ballroom B
Chair: Kazuo Murakami, Aijia Zhu

11:00

Assessment of seawater quality along northern coast of Oman

A. SANA, M. BAAWAIN

Department of Civil and Architectural Engineering, Sultan Qaboos University, PO Box 33, Al-Khoudh, Muscat, 123, Oman

Detailed studies on the extent of the ocean water pollution by oil-related sources in Gulf of Oman are scarce, so this study can be considered as a baseline study to assess seawater pollution along northern coast of Oman. Seawater samples were collected at 44 locations along the coast. In-situ measurements of temperature, salinity and dissolved oxygen profiles were carried out using a CTD probe at each location. The samples were analyzed using inductively coupled plasma-optical emission spectroscopy (ICP-OES). An average DO value of 5ppm was observed in most of the profiles. This value corresponds to the lower limit of a healthy marine life. The DO levels below this value put aquatic life under stress. Chemical analysis of the samples collected from the study area showed that lead concentrations are extremely high at some locations, especially the ones close to Sultan Qaboos Port, Muscat and Oman LNG plant. The maximum concentrations of lead and vanadium were found to be 50ppb and 6ppb, respectively. Both these trace metals are essential components of the petroleum, especially vanadium which is found to be a good indicator for the presence of oil in the environment.

11:15

Modelling dispersion characteristics in Rambler Channel

K.L. PUN, T.N. FUNG

Centre for Sustainable Environment, Chu Hai College of Higher Education, Hong Kong, China

X.L. CHEN, S.W. LU

Department of Civil Engineering, Chu Hai College of Higher Education, Hong Kong, China

A hydrodynamic model has been established to simulate three-dimensional tidal flow in Rambler Channel. The model consists of a coarse grid domain and a fine grid domain. The computations in both domains run in parallel. The model has successfully reproduced the tide levels recorded at two tide gauges during both the dry and wet seasons. Pollutant dispersion characteristics in relation to the uniqueness of the channel configuration are investigated at spring

and neap tides. Drogue tracking is used to simulate the dispersion pathways of pollutants discharged from two major stormwater box culverts in the channel. Flushing time in the typhoon shelter is also investigated by inert tracer simulations.

11:30

Hydrodynamic and water quality changes due to Saemangeum project in Korea

S.W. SUH, H.W. LEE, H.J. KIM

Dept. of Coastal Construction Engineering, Kunsan National University, Kunsan, Jeonbuk, 573-701, Korea

To understand hydrodynamic and water quality changes, numerical models ADCIRC and EFDC are applied. Lagrangian random walk particle tracking methods is applied to figure Saemangeum effects for the last two decades. Particle movement suddenly decreased during the dike construction with final gap of 2.7 km, and shows asymmetry of tidal currents yielding flood dominance. Inside water movement lessened severely and thus might act as adverse reasoning of water quality and ecosystem. Sudden stratification and stagnant environment can cause algae bloom and as a result of TSI test, eutrophication might be occurred. Tidal changes show decrease of M2 and S2 amplification in front of dike however it does not propagate to offshore.

11:45

Numerical tracking blue algal bloom in Taihu Lake based on fractional Brownian motion

C.P. KUANG, X.D. MAO, L. DENG, L.L. HE, J. HUANG

Department of Hydraulic Engineering, Tongji University, Shanghai, China

J. GU

College of Marine Sciences, Shanghai Ocean University, Shanghai, China

Taihu Lake Basin, one of the most developed regions of China for agriculture, industry and commerce, plays a critical role in water supply, tourism, fishery and navigation. However, it has suffered serious eutrophication, and the risks of sudden water pollution accidents increase in recent years, such as "water crisis event" in Wuxi in June, 2007 by blue algal blooms in Taihu Lake. In this paper, a numerical method to track blue algae trajectories, which are affected by the combination of advection and diffusion of water flow, are proposed. The wind-driven current is computed by Delft3D-Flow model, and the diffusion process is simulated by a discrete method to generate fractional Brownian motion (fBm) to illustrate super-diffusive transport due to that the trajectories of drifters on water surface have a fractal structure that is far from being described using ordinary Brownian motion. The improved model has been used to predict blue algae trajectories following the blue algal bloom that occurred in Taihu Lake in 2007. Compared with the observed trajectories and the results of traditional diffusion modeling, the numerical results based on the fBm model show that the improved model not only overcomes the shortcomings of the original fractional Brownian motion, but also affects the number of

particles in the cloud, so that the improved model based on the fBm model is encouraged to predict the trajectories of blue algal bloom.

12:00

Pollution control in urban drainage system - interception of dry weather flow in multi-cell box culvert

GABRIEL T.O. WOO, ELAINE Y.L. WONG
Drainage Services Department, the Government of HKSAR
KELVIN N.F. LAU, GLENN T.H. CHAN
Project Director, Black & Veatch Hong Kong Limited
Jordan Valley Box Culvert (JVBC) is a 7-cell stormwater box culvert serving a drainage catchment of about 5.9km² in the heart of East Kowloon, which is one of the densely populated urban areas in Hong Kong. In order to avoid any polluted runoff in the highly urbanised areas from discharging to the receiving water body through the JVBC, a dry weather flow interception (DWFI) system was proposed. Black & Veatch Hong Kong Limited (B&V) was commissioned by the Drainage Services Department (DSD) of the HKSAR Government to provide consulting services for the investigation, design and construction supervision of the DWFI system. This paper presents the principle of the DWFI and the considerations adopted and challenges in the design of the DWFI system.

12:15

Level 2 performance based design of coastal drainage pumping stations

HAJIME TANJI
National Institute for Rural Engineering, NARO, 2-1-6 Kannondai, Tsukuba, Ibaraki, 305-8609, Japan
HIROHIDE KIRI
National Institute for Rural Engineering, NARO, 2-1-6 Kannondai, Tsukuba, Ibaraki, 305-8609, Japan
Level II performance level design of coastal drainage pumping stations is proposed and actually examined taking drainage pump performance in low land of Saga prefecture as an example. The performance is modeled as the force counter force concept. Change of the inundation depth is examined as the safety index. For the level 2 method, rather than the actual inundation depth considering the expansion of the inundation area, the normalized inundation depth not considering inundation area is suitable. The safety index for the study area can be calculated based on this idea.

Parallel Session 8
Friday, 16 December
Sediment Transport I
Tang
Chair: Zhenhua Huang, Haijiang Liu

11:00

A study on sedimentation of tidal rivers and channels flowing into Deep Bay with a Delft3D model

Z.B. WANG
Delft University of Technology, Faculty of Civil Engineering and Geosciences, P.O. Box 177, 2600 MH Delft, The Netherlands

M.L. TSE
Mott MacDonald Hong Kong Limited, Hong Kong

S.C. LAU
Drainage Services Department (DSD), Government of the Hong Kong SAR

For supporting Drainage Services Department of the Government of the Hong Kong SAR to develop a comprehensive strategy for overall land drainage and flood control in Yuen Long and North Districts, 3D hydrodynamic and sediment transport model is set up. The model deploys Domain Decomposition technique and covers the whole Deep Bay (the estuary of the Shenzhen River), the tidal sections of the rivers and drainage channels including Shenzhen River, Kam Tin River, Shan Pui River and Tin Shui Wai Main Drainage Channel flowing into Deep Bay and a part of the Pearl Estuary. As driving forces, the model takes into account waves and flow driven by wind, tide, river discharge and salt intrusion. Field surveys for wind waves, sediment concentration and especially sediment properties have been conducted. The collected data are analysed together with the existing data and used as basis for the set up of the model. The model is calibrated especially against the development of sedimentation in the Lower Shenzhen River since 2000, after a major deepening of the river. The model can be applied to predict sedimentation in Shenzhen River and tidal drainage channels for different scenarios concerning dredging strategy and river discharge regimes. The study has improved insights into the complicated hydrodynamic and morphodynamic system of Deep Bay together with the rivers and channels flowing into it.

11:15

Estimating settling velocity of mud flocs using laser diffraction particle size analyzer

T. KOEDA, N. TOUCH, T. HIBINO
Department of Civil and Environmental Engineering, Hiroshima University, 1-4-1 Kagamiyama, Higashi-Hiroshima City, 739-8527, Japan

The objective of this study is to suggest a new method to estimate the settling velocity of mud flocs. The settling velocity is estimated based on the particle size distribution measured by a Laser Diffraction Particle Size Analyzer (SHIMADZU: SALD-2000J). The accuracy and validity of the suggested method were investigated by comparing the measured results with those obtained from a Monte Carlo simulation. The relative error is about 5 % when distilled water was used, and it becomes equal to 10% (by 20 min) when salted water was used. Therefore, it is considered that the accuracy of the suggested method is high; that is to say, the suggested method is valid for estimating the settling velocity of mud flocs that have different organic matter contents, both in distilled water and salted water conditions.

11:30

Simulation study on deposition downstream estuarine gates

X.P. DOU¹, H.L. QU², X.M. WANG¹, X.Z. ZHANG¹

¹Nanjing Hydraulic Research Institute, 223Guangzhou Road Nanjing, Jiangsu 210029, China

²Jiangsu Provincial Communications Planning and Design Institute Co., Nanjing, Jiangsu 210005, China

In this paper, simulation studies are conducted on hydrodynamic changes downstream of the estuarine gates of different irrigation channel lengths with a generalized physical model. According to the characteristics of seabed in silt coastal and estuarine areas with fluid mud layers, the impact of fluid mud is taken into account in the sediment-carrying capacity formula. The simulation studies are conducted on the characteristics and laws of deposition downstream of the estuarine gates of short approach channel-river course type, short approach channel-shoal strand type and long approach channel-river course type with a 3-D hydrodynamic and sediment transport model.

11:45

Model for predicting formation of slender sand bar due to shoreward sand transport on shallow tidal flats

M. SERIZAWA

Coastal Engineering Laboratory Co., Ltd., 1-22-301 Wakaba, Shinjuku, Tokyo 160-0011, Japan

T. UDA

Public Works Research Center, 1-6-4 Taito, Taito, Tokyo 110-0016, Japan

S. MIYAHARA

Coastal Engineering Laboratory Co., Ltd., 1-22-301 Wakaba, Shinjuku, Tokyo 160-0011, Japan

Shoreward transport of sand originally supplied from the offshore zone of the tidal flat, while forming a slender sand bar, and the landing of such sand were observed on the Kutsuo coast, where a very wide tidal flat develops. Although this landward sand movement due to waves on the shallow tidal flat is part of the returning process of sand transported offshore by river currents during floods, its mechanism has not yet been studied. We investigated this phenomenon by considering the Kutsuo coast as an example. Then, we performed numerical simulation using the BG model to predict such shoreward sand movement. The observed phenomena were successfully explained by the results of the numerical simulation.

12:00

Variation pattern analysis of the suspended sediment concentration in Busan New Port, Korea

H.Y. CHO

Marine Environments & Conservation Research Department, Korea Ocean R&D Institute, Ansan PO Box 29, Seoul, 425-600, Republic of Korea

J.W. CHAE, K.H. RYU, Y.M. OH

Coastal Development & Ocean Energy Research Department, Korea Ocean R&D Institute, Ansan PO Box 29, Seoul, 425-600, Republic of Korea

INBUS (Intelligent Buoy System) monitoring buoys have been operated to observe the real time suspended

sediment concentration (SSC) generated by the port construction works in the Busan New Port areas since 2006. The variation pattern and/or characteristic analysis of the SSC data are carried out using the natural and artificial data components roughly classified from the treated SSC data. It is clearly appeared three typical patterns of the SSC variation, which are affected by tidal advection, rainfall-runoff and dredging works, etc.

Parallel Session 8

Friday, 16 December

Waves and Modelling IV

Ming II

Chair: Kyung-Duck Suh, D.H. Zhang

11:00

Development of mild-slope equation for irregular waves over mud layers

T.H. JUNG

Department of Civil Engineering, Hanbat National University, San 16-1, Duckmyoung-dong, Daejeon, 305-719, South Korea

C. LEE

Department of Civil and Environmental Engineering, Sejong University, 98 Gunja-dong, Gwangjin-gu, Seoul, 143-747, South Korea

In this study, we derived the mild-slope equation for waves over mud layers. A complex wave number for multiple mud layers was calculated solving linear Navier-Stokes equations with matching conditions. Then, we develop Kubo et al.'s (1992) mild-slope equation for random waves with a damping coefficient which was determined by the imaginary wave number and the group velocity. The developed equations were verified by comparison of numerical solutions against analytical solutions.

11:15

Wind wave spectral analysis in north-central coastal waters of Jiangsu

W.B. FENG

Research Institute of Coastal and Ocean Engineering, Hohai University, 1 Xikang Road, Nanjing, 210098, China

B. YANG, J.S. XIA, Y.B. LI

Harbor, Coastal, and Offshore Engineering College of Hohai University, 1 Xikang Road, Nanjing, 210098, China

Based on the one-year wave surface data, three methods of the calculation of the spectrum were compared, and the Fast Fourier Transform was selected to figure out the smooth spectrum for the following calculating of dimensionless average spectrum. Then several spectral models were used to fit the measured dimensionless average spectrum resulting in a model of representative spectrum.

11:30

Ship wave crests in intermediate-depth water

C. LEE, B.W. LEE

Department of Civil and Environmental Engineering, Sejong University, 98 Gunja-dong, Gwangjin-gu, Seoul 143-747, Republic of Korea

Y.J. KIM

Maritime & Coastal Department, Saman Corporation, 546-4 Guui-dong, Gwangjin-gu, Seoul 143-824, Republic of Korea

K.O. KO
Department of Research and Development, Hyundai Engineering and Construction Company, 102-4 Mabuk-dong, Giheung-gu, Yongin-si, Kyeonggi-do 446-716, Republic of Korea

In this study, we predicted ship wave crest patterns in intermediate-depth water by extending Kelvin's theory with the recursive relation for the dispersion relation in intermediate-depth water. Using the FLOW-3D we tested for two cases that the relative water depths are $kh = 0.86\pi$ and 0.42π . The numerical results showed that, as the water depth became shallower, both the diverging and transverse wave crests were located further behind the ship and the cusp locus angle became larger as 19.60 and 24.81 degrees, respectively. These were because, in shallower water, the Froude number became higher. In other words, as the ship speed increased compared to the gravity-affected long wave speed, all the wave components were located further behind and outside.

11:45

Wave attenuation through an array of rigid circular cylinders: an experimental study

Z. H. HUANG

School of Civil and Environmental Engineering and Earth Observatory of Singapore Nanyang Technological University, 50 Nanyang Avenue, 639798, Singapore

W. B. ZHANG

DHI-NTU Center, Nanyang Technological University, 50 Nanyang Avenue, 639798, Singapore

Coastal vegetation has a special role in providing food and shelter for many organisms; it also protect coastal zones by dissipating wave energy. We report here a set of laboratory experiments on the interactions of monochromatic waves with emergent, rigid vegetation. The vegetation models are consisted of an array of rigid circular cylinders. The effects of water depth and wave period and height on the wave transmission and reflection coefficients are investigated for two vegetation configurations.

12:00

Wave transformation and breaking on gentle slope

P. LI, J.N. PAN, H.C. WANG

River and Harbor Engineering Department, Nanjing Hydraulic Research Institute, 34 Hujuguan Road Nanjing, Jiangsu Province/210024, China

The limit wave height, that is, breaking wave height, is usually adopted as the design wave height for the offshore structures that most build on very gentle slopes, hence the breaking height research is very important to engineering application. Based on other's research, especially the most representative methods of wave breaking indices are proposed by Goda, regular wave breaking indices are proposed and the changes of wave height after wave transformation on the gentle slope through the physical wave model test on 1/30, 1/200, 1/500, and based on the test data and Goda's methods, a modified Goda's formulas is yielded. And

based on the model test results, mathematic model on wave transformation in shallow water can be established, and it can be used in wave transformation after wave breaking in shallow water. And the results are applied in Fangchenggang harbor and waterway construction.

12:15

Time-accurate AB-simulations of irregular coastal waves above bathymetry

E. (BRENNY) VAN GROESEN

Applied Mathematics, University of Twente, Enschede 7500AE Netherlands

ANDONOWATI

LabMath-Indonesia, Bandung 40391 Indonesia

In this contribution the performance is shown of a hybrid spectral-spatial implementation of the AB model for uni-directional waves above varying bottom. For irregular waves of JONSWAP-type, with peak periods of 9 and 12[s], significant wave height of 3[m], running from 30 to 15[m] depth over a 1:20 slope, comparison with scaled experimental data show reasonable (for the 9[s] wave) to good (for the 12[s] wave) results in calculation times less than 15% of the physical time. Especially, the most extreme, freak-like, waves are well simulated for both cases.

Parallel Session 8

Friday, 16 December

Numerical Methods and Simulation IV

Sung I

Chair: Gunwoo Kim, Soo Youl Kim

11:00

Verification of numerical simulation method for motion of cubic armor block

SUSUMU ARAKI, SAKI FUJII, ICHIRO DEGUCHI

Civil Engineering, Osaka University, 2-1 Yamada-oka, Suita, Osaka 565-0871, Japan

The motions of cubic armor blocks are simulated with DEM in which the shape of each element is cube. The result simulated with DEM under a simple condition including a collision is compared with a measured result. The positions of vertices in a cubic armor block before and after the collision simulated with DEM almost agree with the measured result.

11:15

A new technique for nested boundary conditions in hydrodynamic modeling

QINGHUA YE, ROBIN MORELISSSEN, ERIK DE GOEDE,

MAARTEN VAN ORMONDT, JAN VAN KESTER
Deltares, Rotterdamseweg 185, Delft, 2629HD, the Netherlands

A new technique to choose open boundary conditions for model nesting in hydrodynamic modeling is presented. In addition to the traditional ways to configure the open conditions, a tangential velocity component is incorporated. To verify the technique, a schematic case and an engineering case are set up. The

results from overall models are well reproduced by the nested models with much less computational effort and higher resolution. The results show that the new technique has high potential to design simple, efficient and robust open boundary conditions for coastal area models.

11:30

Numerical simulation of hydrodynamic behavior on wave-flap structure interactions with a SPH model

D.W. CHEN, S.Y. TZANG, N.Y. ZENG

Department of Harbor & River Engineering, National Taiwan Ocean University 2nd Peining Rd. Keelung, 202, Taiwan

C.M. HSIEH

Institute of Maritime Information and Technology, National Kaohsiung Marine University 482th Zhongzhou 3rd Rd. Kaohsiung, 805, Taiwan

J.H. CHEN

Department of Systems Engineering & Naval Architecture, National Taiwan Ocean University, 2nd Peining Rd. Keelung, 202, Taiwan

R.R. HWANG

Institute of Physics, Academia Sinica, 128, Sec. 2, Academia Rd., Taipei, 115, Taiwan

In this study, a SPH model is preliminarily applied to estimate the interactions between a bottom-hinged wave energy converter (WEC) and free surface waves in a 2-D numerical wave flume. To estimate the capturing efficiency of a WEC in this flume, a monochromatic wave with height of 7.15 cm and period of 1.56 s based on a model scale of 1:20 of the in-situ wave conditions were adopted. The results show that the loading waves can cause the flapper to stably swing back and forth within average ranges of 16~18 degrees. The phases could directly influence the flapper's swinging and should potentially play a key role in capturing wave energy. Comparisons of the velocity profiles at different phases further illustrate that elliptical form of water particle trajectory could directly influence the rotations of flapper. When the flapper undergoes small rotations, most of the counterclockwise vortices in the weather side and clockwise ones in the lee side have occurred around the flapper. But when the flapper undergoes large rotations, those vortices would only occur near free-surface. Meanwhile, the circulations in the lee side of the flapper have increased while those in the weather side have decreased.

11:45

Numerical simulation of forces on particles in the oscillatory boundary layer flow over a rough bed using Lattice Boltzmann Method

L. DING, Q.H. ZHANG

State Key Laboratory of Hydraulic Engineering Simulation and Safety, Tianjin University, Tianjin, 300072, PR China

The 3-D fully resolved simulations of forces on particles in oscillatory boundary layer flow over a rough bed composed of a layer of spherical particles are carried out using the lattice Boltzmann (LB) method. Two types of bed pattern are considered, i.e., hexagonal packing and cubic packing. The variation of

ensemble-averaged force coefficients in one oscillatory period is investigated. The maximum of them as a function of amplitude Reynolds number and the ratio between particle diameter and the Stokes boundary layer thickness are also discussed. The expressions for them are suggested with introducing the porosity to characterize the effect of the bed pattern. Meanwhile, the role of spanwise force is shown.

12:00

Computation of wave overtopping on slope plate

H.S. KIM, C.H. JANG, H.J. YOO

Civil and Environmental Engineering, Kookmin University, Seoul, 136-702, Korea

M.S. SONG

Department of Harbor, Gunhwa Engineering, Seoul, 135-513, Korea

Numerical experiments were carried out to see the effect of the wave period on the overtopping rate over a sloped seawall with a small relative free-board. An existing numerical model, KU-2DV-Surf was used for the experiments. Regular waves were generated at an internal point in the numerical wave tank, computed results show that the effect of the wave period on the non-dimensional overtopping rate is non-negligible, while existing Owen's (1980) empirical formula predicts minor dependence of the non-dimensional overtopping rate on the mean wave period. The present numerical experiments are confined to a given cross-section, and a small relative free-board, and thus further experiments for small free-boards are needed for a wide range of variables in the future.

Parallel Session 9

Friday, 16 December

Beach Erosion and Morphodynamics III

Ballroom C

Chair: Hajime Mase, A.W. Jayawardena

14:00

Coral reef islands of Spermonde: morphodynamics and prospect

D.A. SURIAMIHARDJA

Study Program of Geophysics, Faculty of Sciences, University of Hasanuddin, Makassar 90245, Indonesia

Coral Reef Islands of Spermonde (Sangkarang) extends widely in southwest of South Sulawesi Province composed of coral reef islands which are functioning as natural breakwaters, and as coral reef islands providing biological production. This paper aims to describe some problems of coastlines of the islands due to exceeding exploitation from view points of morphogenetics and morphodynamics, and to prepare a policy in promoting the islands as tourist destinations. There is anxiety that once the islands have degraded, the west coast will be threatened by incoming waves during west monsoon. The proper utilizations of the islands might be considered and promoted as sustainable tourism, by which Regional governments should be able to identify potencies of its natural characteristics and cultural peculiarity to

formulate marketable tourist destinations and related facilities. The discussion will arrive at the need of a strong networking for cooperation, partnership, collaboration with various stakeholders who are accessible to the resources, and coordination among surrounding regional governments for smooth access and supporting needs. If the nature of the Spermonde Islands have been understood and completed with clear understanding and proper formulation to manage sustainable tourism, it will bring the area to be attractive as tourist destinations, from where the potency to maintain the islands will be prospective.

14:30

Prediction of deposition of sand on gravel layer formed by beach nourishment and onshore movement of gravel during storm

M. KOYA

Graduate School Student, Nihon University, College of Science & Technology, 7-24-1 Narashino-dai, Funabashi, Chiba 274-8501, Japan

A. KOBAYASHI

Nihon University, College of Science & Technology, 7-24-1 Narashino-dai, Funabashi, Chiba 274-8501, Japan

T. UDA

Public Works Research Center, 1-6-4 Taito, Taito, Tokyo 110-0016, Japan

Y. NOSHI

ICOMNET Ltd., 2-7-4 Aomi, Koto, Tokyo 135-0064, Japan

On the Akashi coast facing the Pacific Ocean, beach nourishment using gravel with grain sizes ranging between 2.5 and 13 mm was carried out. Beach changes were monitored by taking photographs from several fixed points. It was found that medium-grain-sized sand and fine sand were deposited on the gravel beach under calm wave conditions, whereas the nourishment gravel was transported onshore and deposited in front of the seawall under storm wave conditions. The deposition of fine and medium sand on the gravel layer under calm wave conditions was successfully explained on the basis of the increases in the equilibrium slopes of fine and medium sand due to the large percolation effect of the gravel layer using the contour-line-change model considering grain size changes.

14:45

Three-dimensional morphodynamic model to sandy beach with shore reef area

M. KUROIWA, Y. MATSUBARA

Department of Civil Engineering, Tottori University, Koyama

Tottori, 680-8552, Japan

N. YAMAMOTO

CTI Engineering, Co. Ltd., 1-14-6, Ueikizaki, Urawa-ku Saitama, 330-007, Japan

Y. ICHIMURA, T. KOIZUMI, K. YOSHIZU, M. SANNOH
Mikuniya Corporation, 3-25-10, Mizonokuchi, Takatsuku Kawasaki, Kanagawa, 213-0001, Japan

A numerical model for predicting three-dimensional beach evolution to sandy beach with hard sea bottom such as shore reef was developed. The change in the water depth was considering the thickness of sand layer over hard bottom, and then the exposing and

burring of shore reef were reproduced. Firstly, a model test associated with the morphodynamic at an idealized pocket beach with exposed shore reef area was carried out. Secondary, the numerical model was applied to morphodynamics around a small fishery port surrounded in the shore reef area, which is suffering from deposition due to waves and nearshore currents. Finally, the applicability of the model was discussed.

15:00

Experimental study on effects of the beach nourishment using the coarser sand

YOKO SHIBUTANI

JSPS Research Fellow, Tottori University, 4-101, Koyama-minami, Tottori, 680-8552, Japan

YUHEI MATSUBARA, MASAMITSU KUROIWA,

NORIKO YAO

Department of Management of Social Systems and Civil Engineering, Tottori University, 4-101, Koyama-minami, Tottori, 680-8552, Japan

The beach nourishments have been carried out. Especially, the method using coarser sand has been noticed in Japan. In this study, laboratory experiments were conducted on the performance of beach nourishment of three types of grain size sand on a fine sand beach. The nourished sands were placed at near breaking point. After that the three types of irregular wave were acted. The changes of the beach profile were measured using a laser displacement meter.

Parallel Session 9

Friday, 16 December

Wastewater Disposal and Water Quality II

Ballroom B

Chair: Cuiping Kuang, K.L. Pun

14:00

Effects of tidal flat on water quality improvement in the Tokyo Port wild bird park

NANA SASAKI, KAZUO MURAKAMI, YUSUKE

UMEDA

Department of Civil Engineering, Tokyo City University, Tamadutsumi, 1-28-1 Setagaya-ku Tokyo 158-8557, Japan

TOMOHIRO KUWAE, EIICHI MIYOSHI

Coastal and estuarine environment research group, Port and Airport Research Institute, 3-1-1 Nagase, Yokosuka, 239-0826, Japan

KOUTA NAKASE

Department of environmental, Penta-Ocean Construction CO.,LTD. 2-8 Koraku 2-chome, Bunkyo-ku, Tokyo 112-8576, Japan

The aim of this study is to measure the role of tidal flat in water quality improvement in the Tokyo Port Wild Bird Park. Results from the field measurement show that (1) the tidal flat has a role of a source of phosphorus and a sink of nitrogen in summer, but a sink of both nitrogen and phosphorus in winter, (2) the tidal flat absorbed NO_3^- into the sediment and the release of PO_4^{+3} to the overlying water in both summer and winter, (3) the amount of removed nutrients by water birds is negative because the abundance of the excreted nutrient by birds are greater than those of feeding within the flat, (4) Denitrification and

anamnox formed in the sediment are major factors explaining the nitrogen removal by the tidal flat sediment.

14:15

Biomonitoring of pollution status in the Daya bay using protozoan communities with the bottled PFU method

A.J. ZHU, Z.Z. XU, J.Q. LIU, H.D. FANG, C.G. HUANG
South China Sea Environmental Monitoring Center, State Oceanic Administration, No. 155 Xingangxi Road, Guangzhou, 510300, China

J.R. HUANG

School of Life Sciences, Sun Yat-sen University, No. 135 Xingangxi Road, Guangzhou, 510275, China

H.B. LI

National Marine Environmental Monitoring Center, State Oceanic Administration, No.42, Linghe Street, Dalian, 116023, China

Structural and functional parameters of protozoan communities were assessed as indicators of water quality in Daya Bay (South China Sea) in the summer of 2010 using the bottled polyurethane foam unit (BPFU) method. A total of 69 species protozoa, most of which might be recorded in the bay for the first time were observed at three stations (MT1, YP1 and YP2). The species number and the species composition of protozoa suggested that the water condition was worse in the port area (MT1) than that in the aquaculture area (YP1 and YP2). Moreover, the functional parameters further indicated that the water quality was the worst at station MT1. Besides, the functional parameters and the diversity index implied that the pollution stress might be stronger at YP2 than YP1. Such results coincided with the pollution status indicated by water chemical parameters.

14:30

Numerical analysis of dispersion characteristics of cooled water discharge from LNG plant

IL WON SEO, CHANG GEUN SONG, HWANG JUNG CHOI, IN HWAN PARK

Department of Civil and Environmental Engineering, Seoul National University, 1 Gwanak-ro, Gwanak-gu, Seoul 151-744, South Korea

To determine whether the temperature difference of cooled water discharge from open rack vaporizers conforms to environmental standard stating that the temperature decrease should be equal to or less than 3 °C within 100 meters of the discharge point, numerical simulations using CORMIX and VISJET were performed to investigate the near-field mixing behavior of staged diffuser by varying ambient currents, effluent discharges, port diameters, and discharging depths. The simulation results showed that the weak momentum and the negative buoyant properties induced the jet to change its direction to downward and to collide onto the sea bed. VISJET gives higher dilution compared with the value of dilution equation or CORMIX since the assumption of merging between adjacent jets is not adopted in VISJET model. The empirical equation tends to underestimate the dilution rate due to the assumption

of complete merging of the individual jets and unidirectional dispersion trajectory. Another dispersion analysis was made regarding the further dilution by ocean turbulence, and the effect of effluent discharge on canal conveyance was checked by the calculation of the decay of mean axial velocity along the longshore direction.

14:45

Real-time forecast of marine beach water quality in Hong Kong

W. THOE

Croucher Laboratory of Environmental Hydraulics, Department of Civil Engineering, The University of Hong Kong, Pokfulam Road, Hong Kong

J.H.W. LEE

Hong Kong University of Science and Technology, Clear Water Bay, Hong Kong

Bacterial concentration (*E. coli*) is adopted as the key indicator of beach water quality in Hong Kong. As *E. coli* level in a beach varies dynamically on a daily basis, the current beach management system which relies on past data may not be able to fully track the bacterial variation. This study develops a real-time system for four marine beaches in Hong Kong to forecast beach water quality on a daily basis. Multiple Linear Regression (MLR) models are developed and validated against daily data over three months in 2008. An overall accuracy of over 70% in predicting water quality compliance/exceedance can be achieved. For beaches significantly affected by local non-point source pollution, the model can predict 71% of observed exceedance, when compared to 0% by the current system. The predictive models are applied to give real-time beach water quality forecast over the entire bathing season in 2009. As salinity data is not available during real-time application, a general model is developed to first predict salinity using an ANN sub-model. An overall accuracy of 70-90% can be achieved in real-time beach water quality forecast. The real-time forecasting system is incorporated in the WATERMAN system to deliver daily beach water quality forecasts for Hong Kong beaches, to enhance protection of public health and the utilization of our marine beach resources.

15:00

Field studies of E. coli decay rate at a coastal beach in Hong Kong

Y.M. CHAN, W. THOE

Croucher Laboratory of Environmental Hydraulics, Department of Civil Engineering, The University of Hong Kong, Pokfulam Road, Hong Kong

J.H.W. LEE

Department of Civil and Environmental Engineering, The Hong Kong University of Science and Technology, Clear Water Bay, Hong Kong

E. coli is a commonly used bacterial water quality indicator due to its high correlation with swimming associated illnesses. The determination of *E. coli* decay rate is significant in many engineering applications. We have carried out the first systematic study of *E. coli* decay rate in subtropical Hong Kong coastal

waters. Field experiments are carried out at the Big Wave Bay beach during and after storm events to study the *E. coli* decay rate; a parallel tracer method (with *E. coli* and freshwater fraction as the two natural tracers) is used to obtain the in-situ *E. coli* decay rate. It is found that the in-situ *E. coli* decay rates range from 1.1 to 5.0 d⁻¹ (T_{90} - time required to have a 90% reduction of the initial bacteria level = 11.0 – 48.2 h) for episodic storm events. It takes about 1-2 days for *E. coli* to return to the level before the storm in strong sunshine. The results are consistent with independent laboratory studies and provide a basis for the determination of *E. coli* decay rate in environmental engineering applications.

Parallel Session 9

Friday, 16 December

Sediment Transport II

Tang

Chair: Mengguo Li, Ole S. Madsen

14:00

Innovative monitoring and 3d modeling of dredging induced sediment plumes in the port of Los Angeles

YING POON, SHERILYN KIMURA

Everest International Consultants, Inc., 444 West Ocean Blvd., Suite 1104, Long Beach, California 90802, U.S.A.

BRENT MARDIAN

AMEC Earth and Environmental Inc., 9210 Sky Park Court, Suite 200, San Diego, California 92123, U.S.A.

KATHRYN CURTIS, ANDREW JIRIK

Port of Los Angeles, 425 South Palos Verdes Street, San Pedro, California 90731, U.S.A.

The Port of Los Angeles conducted a pilot study in 2009 to test the use of LISST in providing real-time in-situ monitoring of dispersion of sediment plumes resulted from dredging activities. The results indicate that the LISST is a more reliable method to measure TSS compared to more traditional methods such as OBS and light transmittance. In addition, the pilot test data were used to demonstrate the use of a previously developed 3D EDFC hydrodynamic and transport model in simulating the dispersion of dredged-induced sediment plume with success.

14:15

Numerical study of sediment transport in Yangon River and Estuary

TOE TOE AUNG, TAKENORI SHIMOZONO, AKIO OKAYASU

Dept. of Ocean Sciences, Tokyo University of Marine Sci. and Tech., 4-5-7 Konan, Minato-ku, Tokyo 108-8477, Japan.

The aim of this paper is to clarify the basic mechanism of sediment transport in Yangon River, Myanmar. Two dimensional numerical model is used to predict the water flow and sediment transport. The models for the flow and sediment transport are described in this paper. The water depth, velocity, sediment concentration and the bed level change were calculated for 4 cases near the “Inner Bar” area. It was found that the tidal current has a great influence on the sediment transport and the

sediment concentration is higher at the ebb tide in both spring and neap tide condition. The flow velocities and the sediment concentration are verified against field data of Nelson (2000).

14:30

Wave shape effect on sheetflow sediment transport

LE PHUONG DONG, SHINJI SATO

Department of Civil engineering, The University of Tokyo, 7-3-1, Hongo, Bunkyo ku, Tokyo, 113-8656 Japan

During the research process, a great deal of experiments has been conducted with the caution to investigate the sheetflow sediment transport of uniform sands under different skewed-asymmetric oscillatory flows. The experiments shows that in most of the cases with fine sand, the “cancelling effect” which cancels the net transport rates of both pure velocity and acceleration asymmetric waves may occur for waves with mixed shapes. However, in some certain conditions with coarse sand, it is observed an onshore enhancement for the mixed shape. The image analysis technique is applied so as to explore major influences of the wave shape on sand transport. Accordingly, the mechanism of sand transport under oscillatory sheetflow conditions is also studied by comparing the maximum bed shear stress and the phase lag parameter at each half cycle.

14:45

Evaluation on the sediment movement along the Miyazaki coast in terms of feldspar luminescence features

HAIJIANG LIU, SHINJI SATO

Department of Civil Engineering, The University of Tokyo, 7-3-1 Hongo, Bunkyo-ku, Tokyo, 113-8656, Japan

In this study, nearshore sediment movement and mixing process with nourished sands along the Miyazaki coast, Japan, are investigated based on the feldspar thermoluminescence (TL) properties. Field sampling was conducted twice in Mar and Nov, 2010. River-originated nourished sand presents a larger TL intensity than that of the natural beach sand. Various sand sources are detected with respect to the TL properties. A relatively uniform TL longshore distribution was confirmed with several local TL peaks representing the sand mixing from the river supply or beach nourishment. Longshore sediment movement pattern was also revealed from the TL measurement.

15:00

Application of ROMS for simulating evolution and migration of tidal sand waves

Z.P. ZANG¹, L. CHENG², F.P. GAO¹

¹*Key Laboratory for Hydrodynamics and Ocean Engineering, Institute of Mechanics, Chinese Academy of Sciences, 15 North 4th Ring West Rd, Beijing, 100190, China*

²*School of Civil and Resource Engineering, The University of Western Australia, 35 Stirling HWY, Crawley, WA, 6009, Australia*

A three-dimensional morphodynamic numerical sand wave model is established based on an existing model, the Regional Oceanographic Modelling System

(ROMS). In the model, the vertical flow structure, which plays an important role in the formation and evolution of sand waves, is resolved by solving three dimensional (3D) Reynolds-averaged Navier-Stokes (RANS) equations with a $k-\epsilon$ turbulence closure. The bed slope effect on the bedload transport is considered in the model. The model is capable of capturing sand wave evolution and migration processes, which can not be modeled by conventional stability models. First, a sensitivity analysis of the model configuration is conducted, including the morphological factor, the time step and the grid size, to find out an optimal balance between the computational time and the accuracy of results. The effects of the water depth, flow velocity and sand grain size on the Fastest Growing Mode (FGM) are then studied. Finally, a migrating artificial sand wave is simulated and numerical results are presented.

15:15

Littoral transport estimate from the field measurement along north Chennai coast of Tamil Nadu, India

K.V. ANAND, V. SUNDAR, S.A. SANNASIRAJ, K. MURALI

Department of Ocean Engineering, Indian Institute of Technology Madras, Chennai, Tamil Nadu - 600036, India
V. RANGARAO, B.R. SUBRAMANIAN

ICMAM – Project Directorate, Ministry of Earth Sciences, NIOT Campus, Pallikarani, Chennai, Tamil Nadu - 601302, India

Among the hard measures to combat coastal erosion, construction of groin fields remain as one of the most widely adopted. The groin field has been increasingly adopted for the Indian coast. As it is important to understand its effectiveness in taming the waves and the alongshore currents, which are the driving force of the littoral drift, it is essential to monitor the behavior of the hydrodynamic characteristics of the wave and the flow field within a groin field after its implementation. In this paper, the results from a preliminary exercise of the measurement and analysis of the wave and flow fields in a groin field north of the major port of Chennai along the South East coast of India are presented and discussed. An attempt to derive the sediment transport rate from the measured parameters using the energy flux method is made. The predicted sediment transport rates are compared with measurements from a field study that adopted a sand trap for the said purpose.

Parallel Session 9

Friday, 16 December

Waves and Modelling V

Ming II

Chair: Taro Kakinuma, Dong-qiang Lu

14:00

Wave overtopping on flaring shaped seawall under oblique incident waves

KEISUKE MURAKAMI

Department of Civil and Environmental Engineering, University of Miyazaki, 1-1 Gakuen-Kibanadainishi, Miyazaki, 889-2192, Japan

DAISUKE MAKI

Faculty of Engineering, University of Miyazaki, 1-1 Gakuen-Kibanadainishi, Miyazaki, 889-2192, Japan

NAOTO TAKEHANA

Engineering Grope, Kobe Steel Ltd., 4-2-7 Iwaya-nakamachi, Nada-ku, Kobe, 657-0845, Japan

Flaring Shaped Seawall, which has a deep curved section on its front face, checks a wave overtopping quite effectively in comparison with other conventional seawalls. Hydraulic characters of this seawall have been investigated under the condition of incident waves that approach the seawall with right angle. The seawall checks the wave overtopping by overturning an incoming wave motion to offshore on its largely curved section. This distinctive interaction is influenced by an incident wave angle with respect to the seawall. This study clears the characteristics of wave overtopping on Flaring Shaped Seawall under oblique incident wave conditions.

14:15

Steep standing waves against a vertical wall on a sloping beach

W. KIOKA, T. KITANO, M. OKAJIMA, N. MIYABE

Dept of Civil and Environmental Eng., Nagoya Institute of Technology, Gokiso-cho, Showa-ku, Nagoya, 466-8555, Japan

The characteristics of highly nonlinear waves reflecting from a vertical wall in water of finite depths are investigated both experimentally and theoretically. In this study, we re-examine nonlinear interaction phenomena with a vertical wall on a sloping beach as the effects of slope, i.e. changing in water depth are not included in any previous studies. The results of regular-wave experiments indicate that the wave periods of individual standing waves become slightly longer than those of progressive waves. The periods of reflecting wave groups become also longer than those of progressive wave groups. In both cases, amplitude modulations in the reflected wave field are very significant for higher wave steepness while no amplitude modulation occurs in the progressive wave field.

14:30

Wave reflection and transmission by vertical slotted barrier

C.-H. JI, K.-D. SUH

Department of Civil & Environmental Engineering, Seoul National University, 599 Gwanak-ro, Gwanak-gu, Seoul, 151-744, Republic of Korea

B.H. KIM

Hyundai Development Company Engineering & Construction, 160 Samsung-dong, Gangnam-gu, Seoul, 135-881, Republic of Korea

In this paper, we compared the closed-form solution developed by Kim in 1998 for calculating the reflection and transmission coefficients of a vertical slotted barrier with other closed-form solutions

developed by different authors. It is shown that all the solution gives a wrong result for very long waves, i.e., complete reflection and zero transmission. It is also shown that the inertia term is important for intermediate-depth and deep water waves so that the solution including the inertial effect gives better prediction than those neglecting the inertial effect. The accuracy of the existing closed-form solutions is not satisfactory. We propose a hybrid solution several parameters of which are based on empirical formulas. The hybrid solution better predicts the reflection and transmission coefficients than the existing solutions. Moreover, it gives a correct result, i.e., zero reflection and complete transmission, for very long waves.

14:45

Wave overtopping of gentle slope revetment placed behind artificial reef

T. OTA, Y. MATSUMI

Dept. of Social Systems Eng., Tottori University, 4-101 Koyama Minami, Tottori, 680-8552, Japan

Y. KURATA

Fujita Corp., 4-25-2 Sendagaya Shibuya, Tokyo, 151-8570, Japan

K. OHNO

Information Media Center, Tottori University, 4-101 Koyama Minami, Tottori, 680-8552, Japan

This study deals with wave overtopping on a gentle slope revetment placed behind an artificial reef (wide-crested submerged breakwater). Laboratory experiments were conducted in a wave flume to measure the volume of overtopped water with various conditions of the gentle slope revetment. A time-averaged wave and overtopping model and a numerical wave flume are applied to the prediction of the overtopping rate. The experimental results showed that the long-period wave measured behind the artificial reef influenced the wave overtopping. The time-averaged model is modified to take into account the influence of the long-period wave. The time-averaged model and the numerical wave flume predict the overtopping rate reasonably well in the case of low crest height of the revetment and relatively large overtopping rate.

15:00

Study on the relationship between mooring force and wave period for a mooring oil tanker

XIANGWEI MENG, FENG GAO, YUNPENG JIANG,

HAICHENG LIU

Tianjin Research Institute for Water Transport Engineering, Key Laboratory of Engineering Sediment of Ministry of Communications, Tianjin 300456, China

In this paper mooring condition of a 315000DWT oil tanker under wave action was simulated and computed by ship-mooring analysis software. The mooring conditions include the six degrees of freedom, the cable and fender force. The wave period varies from 4s to 30s. The results indicated that the maximum mooring force has a positive relationship with wave period when wave height keeps the same and the extreme value appears when the peak period approaches the natural rolling period of the ship. When

the peak period approaches twice rolling period, the mooring force has a new extreme value, which is far beyond the allowed scope. In another aspect the ship motion has a similar discipline with the mooring force. Thus, the damage of resonance between ship and long wave period should be paid more attention in the berth design.

Parallel Session 9

Friday, 16 December

Properties of Materials

Sung I

Chair: In-Sung Jang, Inyeol Paik

14:00

Experimental research on constitutive model of the saturated clay with seepage

YUAN-ZHAN WANG, LIN-NAN HAO, ZHONG XIAO, XI CHENG

School of Civil Engineering, Tianjin Key Laboratory of Port and Ocean Engineering, Tianjin University Tianjin 300072, China

DIAN-GUANG MA

Key Laboratory of Engineering Sediment of Ministry of Communications; Tianjin Research Institute of Water Transport Engineering Tianjin 300456; China

Rapid drawdown is one of the key factors that lead to slope deformation and failure, and clay slope is easier deformed or unstable with rapid drawdown due to its poor permeability. In this paper, the investigations on the constitutive model of the saturated clay with seepage are carried out using the stress-strain controlled triaxial shear seepage tester in the conditions of three different confining pressures. Depending on the stress-strain curves, the results of the triaxial tests are fitted by Duncan-Chang $E-\mu$ model and the parameters are confirmed. There are eight parameters, cohesion c , friction angle ϕ , modulus parameter K_i , Modulus index n , break ratio R_f , related to the tangent modulus E_t , testing constant d , G and F related to the tangent modulus μ_t . It is shown that parameters of c , K_i , F , d decrease with the seepage pressure increasing. Parameter G increases with the seepage pressure increasing. The changes of ϕ , R_f , n are not obvious with seepage pressure variation. Finally, the non-linear elastic constitutive model of saturated clay with the seepage is proposed.

14:15

Investigation of chloride ion profiles of harbor concrete structure based on in-situ cores

S.H. HAN, W.S. PARK, J.W. CHAE

Coastal Engineering & Energy Department, KORDI, 1270 Sadong, Ansan, 426-744, Korea

In harbor concrete structures, the corrosion of steel by the damage of passivity layer around steel bars is a major source of durability problems. As chloride ion penetration is a major cause of destruction of passivity layer, the evaluation of concentration profile of chloride ion is the essential factor for the service-life estimation of concrete structure. To estimate chloride

ion penetration characteristics, this paper investigated the depth of critical chloride concentration and the concentration profile of chloride ion on the basis of in-situ core specimens. The core specimens are obtained at air-zone, splash zone, and tidal zone in Wando, Masan, Incheon, Gwangyang, and Donghae harbors. Colorimetric method measured the chloride ion penetration depth, and ASTM C 114 and RCT test proposed by Germann Instruments evaluated the concentration profile of chloride ion. Based on experimental data, the influence of harbor location and vertical exposure condition on chloride ion penetration is evaluated. The analysis of experimental data showed that the surface chloride ion concentration increased with age of structure and the average of test results of surface chloride ion was 13.1 kg/m^3 . Also, the chloride ion diffusion coefficient decreased with age. Surface chloride ion concentration and chloride ion diffusion coefficient were not influenced by vertical exposure condition.

14:30

Predicting the hydraulic conductivity of Makassar marine clay using field penetration test (CPTu) results

T. HARIANTO, L. SAMANG, A. ZUBAIR
Civil Engineering Department, Hasanuddin University, Jl. Perintis Kemerdekaan km.10, Makassar, South Sulawesi, Indonesia

D.A. SURIAMIHARDJA
Physics Department, Hasanuddin University, Jl. Perintis Kemerdekaan km.10, Makassar, South Sulawesi, Indonesia

T. HINO
Institute of Lowland and Marine Research, Saga University, Honjo 1, Saga, Saga, Japan

Recently, the Cone Penetration testing (CPT) is a rapid method for determining the mechanical and transport properties of soils. The CPT provides continuous profiles of soil characteristics that are reliable, fast, and economical. Moreover, the estimation of the hydraulic conductivity from the CPT is traditionally made from the pore pressure dissipation test data. The Hydraulic conductivity for clay soil is primarily determined by the laboratory test. The main objective of this research is to develop correlation between CPTu (field-laboratory) test data and hydraulic conductivity, and the determination of the hydraulic conductivity that can overcome the drawbacks of the conventional dissipation test method. The method proposed here is based on the analysis of the steady-state pore pressure during the piezocone penetration test, so that the full interaction between the piezocone and the soil is considered. The study area was located in the coastal area of Makassar city, Indonesia. The results indicate that the cone resistance as well as the sleeve friction exhibits a very good linear relationship with the hydraulic conductivity value of marine clay. Furthermore, the exponential relationship was found between the friction ratio and pore water pressure. The relationship between the cone resistance and hydraulic conductivity was also found to be exponential. However, the dissipation of pore water pressure shown linear relationship. Finally, The comparison between

results obtained this study shown that a good correlation obtained in order to predict the hydraulic conductivity based on the CPTu results and indicated that there is some potential of using this correlation value in engineering practice.

14:45

Influence of sea water on the mechanical properties of porous asphalt containing liquid asbuton

N. ALI, L. SAMANG, M.W. TJARONGE, A. RAHMAN
DJAMALUDDIN

Department of Civil Engineering, Hasanuddin University, Makassar 90245, Indonesia

The Buton Asphalt or Asbuton is natural rock asphalt that deposited on South Buton Island in southeast Sulawesi Island, Indonesia. The refining process reduces the mineral content to produce the liquid Asbuton. Porous asphalt is an asphalt pavement that has enough voids within to allow water to pass freely through it. This paper reports on experimental investigation conducted to determine the influence of sea water on the mechanical properties of porous asphalt containing liquid Asbuton. The specimens were immersed in sea water up to 40 minutes at temperature of 60°C . Content of liquid Asbuton was varied from 4.5% to 6.5% at 0.5% interval. After removed from sea water, the raveling resistance, stability and flow of porous concrete were investigated. Porous asphalt containing of 6.5% liquid Asbuton had the normal traffic load bearing capacity in sea water with hot temperature of 60°C .

15:00

Effect of sea water on the strength of porous concrete containing Portland composite cement and micro monofilament polypropylene fibre

M.W. TJARONGE, RUDY DJAMALUDDIN, FTRIADY, AMIRULLAH

Department of Civil Engineering, Hasanuddin University, Makassar 90245, Indonesia

The aim of this research is to study the influence of sea water on the strength of porous concrete containing Portland Composite cement and micro monofilament polypropylene fibre. The specimens of porous concrete were immersed in the sea water up to 28 days. The compressive strength test and flexural strength test were carried out at 3, 7 and 28 days in order to investigate the strength development. The test result indicated that the strength of porous concrete can develop in the sea water. It was revealed that there was no appreciable effect of sea water on the hydration process when porous concrete were immersed in the sea water. An excellent bond was established between the cement paste and the coarse aggregates, resulting in the good compressive and flexural load bearing capacity of porous concrete.

Parallel Session 10
Friday, 16 December
Beach Erosion and Morphodynamics IV
Ballroom C
Chair: Liancheng Sun

15:45

Short and medium-term evolution of the northern bank, Hangzhou Bay

Z.J. DAI, J.F. LI, X.L. ZHANG, H.Y. YAO

State Key Lab of Estuarine and Coastal Research, East China Normal University, Shanghai, 20006, China

Understanding of coastal change during the short and medium-term is necessary for proper management of coastal resources, particularly in light of widespread coastal retreat. In this study, based on analysis of field data and sea maps, the characteristic of the northern bank, Hangzhou bay (NBHZB) is of accretion in winter half year and erosion in summer half year, respectively, due to the impacts of seasonal wave climate actions. However, coastal morphodynamic processes during typhoon actions could be described as that the crest of submarine bar was cut down, runnel was filled up and submarine platform was eroded into several similar shape of small bar-runnel. In addition, coastal erosion had drastically occurred along NBHZB in recent 20 years, which could be induced by the abrupt decreased sediment from Yangtze River.

16:00

Study on dynamic process of tombolo topography at Chiringa-Shima Island by image data based on point camera observation

AKIO NAGAYAMA

Technical office, Kagoshima National College of Technology,

1460-1, Shinkou, Hayato-cho, Kirishima-city, Kagoshima 899-5102, Japan

TOSHIYUKI ASANO

Dept. Ocean Civil Engineering, Kagoshima University 1-21-40, Korimoto, Kagoshima, 890-0065, Japan

This study deals with the simulation of topographical changes conducted by image analysis, field survey and image data based on point camera observation in order to examine the dynamic process of topographical changes in formation, maintenance and disappearance of Chiringa-shima Island tombolo, which emerges between the Ibusuki beach and Chiringa-shima Island in Kagoshima Prefecture, Japan. This study was conducted to develop practicable point camera observation in the field for a long time by using a general digital camera and a solar panel. The point camera image data was converted into orthophotos that examine dynamic process of topographical changes Chiringa-shima Island tombolo throughout a year. The tombolo was found to be unique in that it has daily and yearly changes in formation.

16:15

Analysis of the causes of sediment loss at Golden Beach, Hong Kong

HAKEEM JOHNSON

Halcrow Group Ltd, Manchester, SK9 3FB, United Kingdom

PETER SHEK

Halcrow China Limited, Hong Kong, China

FRANCIS LEE

Civil Engineering and Development Department, Hong Kong, China

The causes of sediment loss at Golden Beach in Hong Kong have been studied by analysis of historical shorelines and numerical modeling of sediment transport processes. Analysis of historic shorelines from 1994 to 2008 shows erosion of up to 2m/yr at the eastern end and up to 1m/yr at the western end of the beach. The model results show that Golden Beach is very oblique to the prevailing wave climate. This results in high longshore sediment transport gradients along the beach (given that there is no sediment supply past the marina entrance to the beach). Thus, sand placed at Golden Beach is eroded very quickly due to the prevailing wave climate and beach configuration. This mechanism for erosion was confirmed in simulations with the shoreline evolution model and two-dimensional coastal area models.

Parallel Session 10
Friday, 16 December
Seawater Intrusion
Ballroom B
Chair: Elena Dolgoplova, Ken Wong

15:45

Water resource management in Macao SAR to tackle its sea water intrusion problem

K.M. MOK

Honours College, University of Macau, Av. Padre Tomas Pereira, Taipa, Macao SAR, China

H. WONG, X.J. FAN

The Macao Water Supply Company Limited, 718, Avenida do Conselheiro Borja, Macao SAR, China

Though locates at the Pearl River Delta and being a coastal city, Macao has been suffering from water shortage due to its small land area hence very limited catchment. With an increasing pace of social and economic development of the region recently, maintaining proper supply of potable water both in quality and quantity is a challenge, of which sea water intrusion during dry season is one needed to be tackled immediately. Management of the raw water resources is an urgent topic for the Pearl River Basin where Macao sits on its exit delta. Through analysis of the basin hydrological and related data, possible causes of the worsening saline-water-intrusion situation were identified. Approaches to solve this problem at basin level, delta level and local city level are being attempted; e.g. cooperating with the water conservancies in Mainland China, a new raw water intake for Macao was built further upstream, and a reservoir of high capacity is being constructed as a major supporting unit for fresh water supply during dry season. Nonetheless, a future plan including a centralized water resources and basin management system and related regulations is necessary.

16:00

Formation of tidal bore and its effect on sea water intrusion

E.N. DOLGOPOLOVA

Institute of Water Problems, Russian Academy of Sciences, Moscow 119333, Russia

Conditions of tidal bore formation in river mouths are studied. Existence of bore is determined by balance between the tidal range, river flow and morphology of the estuary. The same factors determine the intensity of mixing of fresh and salt waters and the distance of sea water intrusion. The types of water circulation and stratification in the river mouths, where bores are formed, are discussed. Characteristics of mouths of the rivers Amazon, Yangtze, Qiantang and Mezen are compared. Longitudinal bottom profile of an estuary is assumed to be one of the main factors influencing the occurrence of tidal bore.

16:15

Numerical study on impacts of discharge changes caused by major water conservancy projects on salinities at water intakes in the Changjiang Estuary

J. HUANG, C.P. KUANG, M.T. JIANG

Department of Hydraulic Engineering, College of Civil Engineering, Tongji University, No. 1239 Siping Road, Shanghai, 200092, China

J. GU

College of Marine Sciences, Shanghai Ocean University, No.999 Hucheng Ring Road, Shanghai, 201306, China

B. SUN

Hangzhou Plan Design and Research Institute of Communications, No. 8 Jiande Road, Hangzhou, 310006, China

A depth-averaged 2-D numerical model with Delft3D-FLOW is adopted to compute the salinity in the Changjiang Estuary. After well validated against the field measurements, the model is applied to simulate the salinity under the different discharges after the operations of Three Gorges Project (TGP) and Eastern Route of South-to-North Water Transfer Project (ERSNWTP) combined with various tidal ranges in the dry season. The results show the salinities decrease with the increased discharges, especially ERSNWTP with drawing 1,000m³/s water from the Changjiang, which has the highest salinity while under TGP operation the salinity is the lowest and that under the mutual effect of these two projects is between them. It demonstrates TGP can effectively alleviate the saline water intrusion while drawing 1,000m³/s water by ERSNWTP will be the opposite, but the combination of these two projects can still ease the saline water intrusion.

16:30

Numerical investigation of circulation and nutrient transport in the Mirs Bay

JIANPING GAN, LINLIN LIANG, TINGTING ZU

Division of Environment, The Hong Kong University of Science and Technology, Clearwater Bay, Kowloon, Hong Kong

The Mirs Bay is located to the east of Hong Kong Island and occupies about 50 % of total sea area of Hong Kong. Since nutrient rich Pearl River water is potentially limited by light and phosphate, most of red tides or algal blooms are originated in the eastern part of Hong Kong waters. Study of Mirs Bay circulation is crucial to scientifically understand the interactive dynamics of the coupled bay-shelf system as well as the associated biogeochemical response in Hong Kong waters. A coupled three-dimensional physical model and nitrogen-phosphate (NP)-based dissolved inorganic nitrogen, phosphate, phytoplankton, zooplankton, and detritus (NPPZD) ecosystem model was used to study the ecosystem responses to the circulation in the Mirs Bay. The circulation in the Mirs Bay is not isolated from the adjacent shelf processes. With a deep central channel in the bay and unique shelf/coastline topography in the adjacent shelf waters, Mirs Bay is closely influenced by the intrusion of dense and nutrient rich deep shelf waters, induced by the frictional bottom Ekman layer and by the amplified cross-isobath shoreward transport at the lee of the coastal promontory due to Hong Kong Island. The intrusive nutrient rich deep waters surface in the bay and subsequently transport to the rest part of Hong Kong waters by the shelf circulation. Both shelf and bay circulations are highly time- and space-dependent governed by variable wind and tidal forcing as well as by the local intrinsic hydrodynamics.

Parallel Session 10

Friday, 16 December

Marine Ecology and Environment III

Tang

Chair: H.J.S. Fernando, Girija Jayaraman

15:45

Durability of water environment restoration by covering layer of granulated coal ash in brackish-water lake

T. SAITO, J. HIRAOKA

Energia Eco Materia Co., 1-3-32 Nakaku Kokutajimachi, Hiroshima City, 730-0042, Hiroshima, Japan

T. HIBINO, N. TOUCH

Department of Civil and Environmental Engineering, Hiroshima University, 1-4-1 Kagamiyama, Higashi-Hiroshima City, 739-8527, Hiroshima, Japan

Granulated coal ash has been used as a covering material to restore the water environment in closed water areas in Japan, where the bottom sediment was heavily deteriorated by organic substances. Hydrogen sulfide content in pore water of granulated coal ash covering layer can be improved significantly. The numbers of bivalves, *Tapes japonica* and *Scapharca subcrenata* which are important fisheries resources, were significantly recovered 2-3 years after covering the granulated coal ash. This means, the oxygen condition can be kept by covering granulated coal ash. From these results, the granulated coal ash is an effective material to restore water environment and bivalve habitat condition.

16:00

Research about the effect of reclamation on marine ecology in the northeast of Zhoushan Island

MAOMING SUN, YONGQIANG NI, SHANSHAN WANG, LIHU XIONG

Zhejiang Institute of Hydraulics and Estuary, Hangzhou, Zhejiang Province, 310020, China

The reclamation in the northeast of Zs Island was begun in Dec 2004, consisting of sea embankment and sea filling. Until now sea embankment have been completed while sea filling engineering hasn't been implemented yet, resulting in the form of half-enclose bay. By analyzing the data of phytoplankton, zooplankton, benthos and intertidal benthos of 1981, 2003, 2006 and 2007, the changes of ecosystem and the wetland due to the construction of sea embankment were showed in this paper including species richness, dominant species, density, biomass, diversity index, evenness index and richness index etc. From 2003 to 2006, the species richness of zooplankton and benthos decreased, increasing from 2006 to 2007, the species richness of phytoplankton increased from 2006 to 2007, while the species richness of intertidal benthos increased consistently from 2003 to 2007. The cell abundance of phytoplankton and individual abundance of zooplankton decreased consistently from 2003 to 2007. The biomass of zooplankton, density and biomass of benthos increased from 2006 to 2007. There was a little difference in density of intertidal benthos between winter of 2006 and winter of 2007, but the biomass of intertidal benthos in winter of 2007 was much more than that in winter of 2006. Especially the density of intertidal benthos in winter of 2007 was much less than that in winter of 2003, but the biomass of intertidal benthos in winter of 2007 was more than that in 2003, which shows that the macro intertidal benthos could generate during the period of sea embankment construction. It is 2006 that is turning point for marine ecology in the northeast of Zs island. Phytoplankton, zooplankton, benthos and intertidal benthos began adapting the environment after 2006. With the construction of siltation promotion embankment, the boundary of wetland has been expanding, leading to a better living environment for the intertidal benthos. After making on-the-spot investigation, we find the turbid seawater with high suspended sediment concentration becomes clearer than the seawater before the construction of sea embankment. That is to say, constructing the sea embankment without sea filling engineering could create a better environment for some ecosystem in part comparatively. But the sea filling would transform the ocean environment to the terrestrial environment, resulting in the ocean ecosystem damaged thoroughly.

16:15

Properties of granulated coal ash and its effects on sludge purification

T. HIBINO, N. TOUCH

Department of Civil and Environmental Engineering, Hiroshima University, 1-4-1 Kagamiyama, Higashi-Hiroshima City, 739-8527, Japan

T. SAITO

Energia Eco Materia Co., 1-3-32 Nakaku Kokutajimachi, Hiroshima City, 730-0042, Japan

Shallow areas located along enclosed coastal zones and river deltas near densely-inhabited districts have been damaged and have become sludge areas, due to the deposition of organic mud. This paper aims to explain the properties of granulated coal ash, and to review some achievements of the application of granulated coal ash in the improvement of marine environment and the purification of sludge. It is obvious that granulated coal ash has a capacity in the reduction of malodorous components, such as hydrogen sulfide, and methyl sulfide. Furthermore, the purification of sludge, the regenerations of habitat condition of clams and coastal environment, appeared after the application of the developed methods using granulated coal ash.

16:30

Modeling chlorophyll a of Bohai Bay based on structural equation model and Bayesian networks

X.F. XU

School of Environmental Science and Engineering, Tianjin University, Tianjin, China

X.Q. XIANG

The National Marine Data and Information Service, Tianjin, China

J.H. TAO

School of Mechanical Engineering, Tianjin University Tianjin, China

In this paper, a SEM-BN model is established to model chlorophyll a in Bohai Bay. The structural equation model (SEM) method has the advantage to investigate complex networks of relationships and has the disadvantage to predict with new data. On the contrary, the Bayesian networks (BN) method can produce good prediction accuracy with incomplete data sets, but it is limited in identifying the true and false relationships among factors. In our study, the two emerging tools are combined to model chlorophyll a in Bohai Bay. By using SEM, the relationship between the phytoplankton dynamics and coastal environment variables during the summer period in Bohai Bay is hypothesized and tested. And by using the BN, which is built based on the structure of SEM, the concentration of chlorophyll a is simulated. The result of simulation shows that the SEM-BN model has great performance, and shows good promise for future environmental modeling efforts in other regions.

Parallel Session 10

Friday, 16 December

Waves and Modelling VI

Ming II

Chair: Jong-In Lee, Takao Ota

15:45

Random wave generation using the internal wave maker in the Navier-Stokes equation-based model

T. HA, J. KIM, Y.-S. CHO

*Department of Civil and Environmental Engineering,
Hanyang University, 17 Haengdang-dong, Seongdong-gu,
Seoul 133-791, Korea*

P. LIN

*State Key Laboratory of Hydraulics and Mountain River
Engineering, Sichuan University, Ke Hua Bei Lu, Chengdu,
Sichuan 610065, China*

Recently, numerical simulations of water surface waves using the Navier-Stokes equation models have been increased since these models surpass the depth-integrated equations-based wave models. However, random wave generation with the internal wave maker has been barely considered in the Navier-Stokes equation-based models. In this study, the internal wave maker for the Navier-Stokes equation-based model is applied to generate random waves and numerical results are compared with analytical solutions.

16:00

Numerical study of wave breaking over a muddy seabed

YI HU

*Department of Hydraulic Engineering, Tsinghua University,
Beijing, 100084, China*

YI LIU, XIN GUO, LIAN SHEN

*Department of Civil Engineering, Johns Hopkins University
Baltimore, 21218, USA*

Direct numerical simulation capability using a level set method is developed for the study of water surface wave interacting with bottom mud flow. Simulation of plunging breaker is performed to investigate the effect of muddy seabed on wave breaking. It is found that in the presence of mud, the intensity of wave breaking is reduced, the dissipation in water decreases, and the dissipation in mud plays an important role in wave energy evolution. Before the impingement of plunging jet on wave surface and after 2.5 wave periods when most of the wave energy is lost, dissipation in mud dominates that in water. During the wave breaking, dissipation in water increases sharply and exceeds that in mud.

16:15

Waves due to a disturbance in a two-layer fluid covered by an elastic plate

D.Q. LU, C.Z. SUN

*Shanghai Institute of Applied Mathematics and Mechanics,
Shanghai University, Yanchang Road, Shanghai 200072,
China*

The transient flexural-gravity waves due to an impulsive source in a two-layer fluid system are investigated analytically. The fluid is assumed to be inviscid and incompressible. The density of each of the two layers is constant. The upper fluid of finite depth is covered by an elastic plate. Based on the assumption of small-amplitude waves, a linear system is established. The integral solutions for the free-surface and interfacial waves are obtained by means of the Fourier-Laplace transform. The corresponding asymptotic representations are derived for large time with a fixed distance-to-time ratio by the Stokes and Scorer methods of stationary phase. The analytical

solutions show that there are two different modes, namely the free-surface and interfacial wave modes. The wave profiles observed depend on the relation between the distance-to-time ratio and the group velocities. For an observer moving with the speed larger than the minimal group velocity, there exist two trains of free-surface waves, namely the short flexural waves and the long gravity waves, the former riding on the latter.

Parallel Session 10

Friday, 16 December

Construction and Structures

Sung I

Chair: Sanghun Han

15:45

Experimental study on lateral behavior of DSCT column

TAEK HEE HAN

*Coastal Engineering and Ocean Energy Research
Department, Korea Ocean and Development Institute,
Ansan, 426-744, Republic of Korea*

JONG SUN KIM

*Research Institute of Technology, Lotte Engineering and
Construction, Seoul, 140-111, Republic of Korea*

DEOK HEE WON, YOUNG JONG KANG

*Department of Architectural, Civil and Environmental
Engineering, Seoul, 136-701, Republic of Korea*

A double skinned composite tubular (DSCT) column, which is composed of two concentric steel tubes and concrete between them, was studied for its behavior under lateral loading. Quasi-static tests were performed by applying cyclic lateral loadings to two DSCT columns. One DSCT column had a flat inner tube (DSCT-FT) and the other had a corrugated inner tube (DSCT-CT). Test results were compared with those of a solid RC column and two hollow RC columns from other research. The compared two hollow RC columns had internal tubes and similar geometric and material properties with the DSCT columns. Test results showed that the DSCT columns had superior performance than other columns in terms of strength, yield energy, ultimate energy, and energy absorbing capacity. Owing to their superior moment capacities, the DSCT columns absorbed about 50% more energy than the solid RC column. However the DSCT columns showed lower energy ductility factors than the solid RC column because of their high yield energy.

16:00

Development of unmanned underwater excavation equipment for port construction

I.S. JANG, W.T. KIM, J.H. KO

*Coastal Engineering & Ocean Energy Research Department,
Korea Ocean Research & Development Institute, Ansan,
426-744, Republic of Korea*

T.S. KIM, K.W. PARK

*Research Institutes of Mechatronics, Changwon National
University, Changwon, 641-773, Republic of Korea*

M.K. LEE

Department of Control and Instrumentation Eng., Changwon National University, Changwon, 641-773, Republic of Korea

Underwater construction works in port areas have mostly depended on divers. It is necessary to develop a new type of mechanized underwater equipment for economical, effective and safe utilization for port construction, which complements a traditional method using divers, especially for underwater leveling works of rubble mound. A project in Korea recently commenced to develop and make practicable unmanned underwater excavation equipment, monitoring system for the underwater environment, and underwater management system. In this study, the specification of the equipment and attached apparatus was determined, and conceptual design of the underwater excavation equipment with underwater monitoring system, underwater management system was performed. An onshore type of remotely controlled system was fabricated and the performance of the equipment was verified in a field condition. The results of this research can be expected to increase the effectiveness of underwater works and to practically utilize to the real fields after performing various field tests with the developed equipment.

16:15

Experimental study on seismic performance of non-dispersible underwater concrete short columns

WEI-QIU ZHONG

School of Civil Engineering, Dalian University of Technology, No.2, Ling gong Road, Dalian, 116023, China

ZHI-WEI ZHANG

Tianjin Cement Industry Design & Research Institute, Tianjin, 300400, China

YE MA

Faculty of Infrastructure Engineering, Dalian University of Technology, No.2, Ling gong Road, Dalian, 116023, China

The mechanical properties of non-dispersible underwater concrete short columns and the common concrete short columns under low cyclic reversed loading were carried out by experimentation in this paper. The results showed that, the seismic performance of non-dispersible underwater concrete short columns and the common concrete short columns are similar, so the seismic performance of non-dispersible underwater concrete short columns can be calculated by the seismic theoretical of the common concrete short columns.

Poster Session 1
Thursday, 15 December
Ballroom A

Morphodynamics responses of the Erfenshui beach ridge on the Tiaozini sandbank in Jiangsu coast, China

JUN CHEN, XIAOQING WEI, YONG ZHOU
College of Harbour, Coastal and Offshore Engineering, Hohai University, 1 Xikang Road, Nanjing, Jiangsu Province 210098, China

The Jiangsu coast area is controlled by the East China Sea progressive tidal wave and the Southern Yellow Sea rotary tidal wave. The two tidal wave systems coming from the opposite direction converge near the middle of the Radiative Sandy Ridge. Under this special hydrodynamic condition, a large geomorphologic dynamic response system formed in the Tiaozini sandbank which is named Erfenshui water-dividing beach ridge. Using in situ measurements and some remote sensing satellite images, this paper discusses the geomorphologic characteristics, sedimentary characteristics, hydrodynamic characteristics and historical evolution pattern of the Erfenshui water-dividing beach ridge. Its ridge width is about 1km and the average height is about 0.5 m. The slope is about 0.64‰. It separates the Tiaozini sandbank into two parts. The surface sediment type is mostly sandy silt. The ebb average current velocity is larger than the flood during the measurement period. The maximum velocity occurred at the surface layer and decreased gradually from the surface to bottom. The flood suspended sediment concentration is greater than the ebb. The maximum sediment concentration occurred at the bottom, which increased gradually from surface to bottom. The average sediment discharge of per unit width is 1.30 kg/m³ during the flood and is 1.07 kg/m³ during the ebb, which shows that the sediment source is sufficient and the Erfenshui water-dividing beach ridge is in the deposition environment. The location of the Erfenshui sandy beach ridge is not fixed. It moved from south to north about 14.5 km because of the typhoon storm surge in 1974 and moved from north to south about 6 km because of the coastal reclamation.

Hydraulic model test and field experiment on beach nourishment at large scale tidal flat beach

GIL-PYO HONG
Civil Eng., Kwandong University, 522 Naegok, Gangneung, Gangwon, 210-701, Korea, Korea Port Engineering Corp., 73-4 6, Jeo-Dong 2Ga, Jung-Gu, Seoul, 100-032, Korea
 KEE-SOK YANG, BYEONG-KYU KIM, JUNG-SEOK MOON

Korea Port Engineering Corp., 73-4 6, Jeo-Dong 2Ga, Jung-Gu, Seoul, 100-032, Korea

The west coast of Korean Peninsula has large tidal range about 9 to 4 meters. And there are large scale tidal flat beach. Recently, many sandy beaches connecting the tidal flat beach make use of the human resorts, and severe beach erosion has been occurred since 1980s due to the effect of constructing the facilities of resorts. Particularly, the erosion of the

sandy beach connecting the tidal flat beach has taken place with some kind of the difference mechanism to the traditional theory of beach erosion; that is thought of the swell surging on the top of the slope face of sandy beach that is connected the large scale tidal flat beach. Considering the like those of hydraulic phenomena, hydraulic model test and field experiment carried out for the purpose of the beach nourishment. It was found that the nourishment profile at the large scale tidal flat beaches are dominated mainly the scale of off shore return flow along to the slope face of the beach. That is supposed to be caused by the swell surging in case of high tides.

Evaluation of coastal erosion in the Nandu River Delta

L.Q. SHI
Second Institute of Oceanography, SOA, State Research Centre for Island Exploitation and Management, 36 North Baochu Road, Hangzhou, 310012, China

G. HU
Qingdao Institute of Marine Geology, Ministry of Land and Resources of the People's Republic of China, 62 Fuzhou Road, Qingdao, 266071, China

S.H. ZUO
Tianjin Research Institute for Water Transport Engineering, Key Laboratory of Engineering Sediment of Ministry of Communications, 2 Xingang Road, Tianjin, 300456, China

J.X. WU
Hainan Marine Development Plan and Design Institute, 15 North Longkun Road, Haikou, 570125, China

Significant coastal erosion of the Nandu River Delta in Hainan Province has occurred in recent decades, caused by the compound actions of natural factor, such as the waves, tides, storm surges, and rising sea levels, and human activities like reservoir construction and river dredging. In this study, the stability of the shore was analyzed based on the measured depth from March 2008 to March 2009 and the charts of the Nandu River Delta during the years 1984 to 2007. Several evaluation factors, such as annual erosion rate of shoreline, down-cutting rate of beach surface, and erosion rate of the shoreline, were adopted to calculate erosion hazard. The results showed that the eastern, northern, and western coasts were in a state of serious erosion or erosion and silting. Additionally, the results of hazard analysis of the coasts using the coastal erosion hazard evaluation index system showed that the coasts were all at the medium hazard level.

Impact of sea level rise on Semarang coastal city Indonesia

IR SUHELMI
Research and Development Centre for Marine and Coastal Resources, Ministry Of Marine Affairs Republic of Indonesia Pasir Putih Street No 1 Ancol Jakarta

Semarang topography tends to flat with some area as height as the sea level and even in some places below him. Various environmental problems faced by Semarang related to coastal and ocean dynamics are tidal inundation, land subsidence, and floods in the rainy season. This study was conducted to model the locations that vulnerable to inundated due to sea level rise. The calculation of sea level rise according to

IPCC prediction. The data processing using Geographis Information System (GIS). Detailed Digital Elevation Models are very important to describe the distribution of inundated area caused by sea level rise phenomena. The results show that, the coastal Semarang have a high level of vulnerability to inundation due to sea level rise. The indications of the extent of area are affected by tidal inundation from 3.9% to 5.9% in one hundred years. Tidal inundation increase in the intensity and spreading along with the increase of subsidence. The modeling and monitoring of the vulnerable area very useful in the coastal zone management in Semarang City.

Effectiveness of GFRP-bar reinforcement on performance of new wave dissipating block

I.Y. PAIK

University Department, Kyungwon University, San 65 Bokjong, Songnam, Kyunggi, 461-701, Korea

Y.M. OH

Korea Ocean Research and Development Institute, Ansan, Kyunggi, 426-600, Korea

In this study the static load carrying capacity of a new wave dissipating concrete block is estimated by performing numerical analysis and static load test. The fiber reinforced plastic bar is used to supplement the capacity of the concrete block. The amount and the location of the reinforcement are decided by referencing the numerical analysis results. The load test is conducted by applying static load at the top of the concrete block. The fracture occurs at the load level of 350kN which is about 6.2 times of the weight of the block. Also, the test blocks show strength capacity of over 900 kN.

Wave period effects on wave overtopping of vertical structure

YOUNG-TAEK KIM

River, Coastal and Harbor Research Division, Korea Institute of Construction Technology, 1190 Simindae-Ro, Ilsanseo-Gu, Goyang, Gyeonggi-do, 411-712, Republic of Korea

JONG-IN LEE

Department of Marine and Civil Engineering, Chonnam National University, 50 Daehak-Ro, Yeosu, Jeonnam, 550-749, Republic of Korea

Wave overtopping is one of the most important design parameters which effects on the harbor calmness, operation and structural stability. Therefore the reliable estimation of wave overtopping is indispensable for designing the coastal structures. Recently, it is known that EurOtop (2007) is the most widely and newest design manual for the estimation of wave overtopping. In this study, the wave overtopping for vertical structures are measured and the empirical formula will be suggested concerning the wave period effect as well as the wave spectrum. The effect of wave periods will be analyzed using the relative water depth, kh .

An analysis of causes of downtime in Pohang new harbor through long-term investigation of waves and winds

K.-H. RYU

Department of Civil & Environmental Engineering at Ansan, Hanyang University

Ansan, Kyonggi-do, 426-791, Republic of Korea

W. JEONG, W.-D. BAEK

Coastal Engineering & Ocean Energy Research Department,

Korea Ocean Research & Development Institute, Ansan,

Kyonggi-do, 426-744, Republic of Korea

G. KIM

Division of Ocean System Engineering, Mokpo National

Maritime University, Mokpo city, Jeollanam-do, 530-729,

Republic of Korea

The reason for the occurrence of downtime problems in Pohang New harbor was analyzed by using the extensive field measurement data of short and long period waves and winds for more than one year, the precipitation data provided by KMA(Korea Meteorological Agency), and the downtime records during the measurement period. It was found that downtimes occur because of the short period wave of which height is higher than loading criteria and the swell with even smaller wave height but longer period(more than 10 sec) and fig-waves of which height is higher than loading criteria. Long period components(more than 5 min.) is seems to be related with the downtime problems. This study shows what was able to improve harbor calmness if short period waves and swells were blocked effectively.

Tide asymmetry in Mokpo coastal zone

TAE SUNG JUNG

Department of Civil & Environmental Engineering, Hannam

University, Daejeon 306-791, South Korea

JONG HWA CHOI

Department of Civil Environmental Engineering, Hannam

University, Daejeon 306-791, South Korea

In Mokpo coastal zone, physical factors generating ebb-dominant flow were reviewed by observed data and numerical modeling. Influence of critical depth for wetting and drying, bottom shear stress, coastal reclamation, tidal amplitude, and nonlinear tide at open boundaries on the change of ebb-dominant flow was investigated by applying a two-dimensional hydrodynamic model. The simulation results for a variety of conditions showed that critical depth for wetting and drying has little impact on the generation of asymmetric flow, but large bottom friction stresses generates ebb-dominant flow. Conversion of tidal flats into land swells ebb-dominant flow, but conversion of tidal flats into sea lessens ebb-dominant flow. Nonlinear tides at open boundaries play a decisive role in the generation of asymmetrical tidal flow.

Effect of stopping flow in one branch of bifurcated tidal estuary on hydrodynamic sediment environment

MENGGUO LI, WENDAN LI

Key Laboratory of Engineering Sediment of Ministry of

Communications, Tianjin Research Institute of Water

Transport Engineering, Tianjin 300456, China

Taking stopping flow in the South Branch of Oujiang Estuary as an example, tidal current and sediment problems related to stopping flow in one bifurcated branch of a complex tidal estuary are studied in this paper. A numerical model of tidal current and sediment

movement under the combined action of wave and current are set up with irregular triangular grid. The model is verified with in situ data, and the results show that the calculated water elevations at 19 stations, currents, suspended sediment at 19 vertical lines and seabed evolution are all in good agreement with measured data. This numerical model is applied in the tidal current and sediment movement simulations in stopping flow transport through the South Branch of the Oujiang Estuary and the feasibility to cut off the flow in the South Branch of the Oujiang Estuary is demonstrated by numerical simulation experiments. The results show that flow cutoff in the South Branch by heightening the present submerged dyke is technically feasible as far as its impact on hydrodynamic sediment environment is concerned.

Ebb-dominant tidal currents characteristics in the Han-River Estuary, South Korea

B.I. YOON, S.B. WOO

Department of Oceanography, College of Natural Science, Inha University, 253 Yonghyun-dong, Nam-gu, Incheon, Korea

Y.S. SONG

GeoSystemResearch Corp. #306, Hanlim Human Tower 1-40, Geumjeong-dong, Gunposi, Gyeonggi-do, Korea

Several field measurements were conducted to study the characteristics of tidal circulation in the Han River estuary (HRE) on the western coast of Korea. The HRE is macro-tidal coastal zone with a mean depth less than 10 m and a tidal range varying 3.5 (neap) to 8.0 m (spring). The tidal amplitude to depth ratio is large enough to generate non-linearity in the tidal wave. The harmonic analysis results at HRE indicate that relative phases of ($2M_2 - M_4$) are less than 180° for most of measured points. Hence, the analysis of relative phases is shown that HRE type is flood dominant. But this method is typically based on the non-linear distortion of the tidal current in tidal lagoon system where freshwater discharge is assumed to be relatively small. We investigated the tidal current from 3 periods (December, 2005, September, 2007 and May, 2010) at the nearby station over a 15 days or 35 days. The statistical methods of ebb and flood used to characterize the tidal circulation were as follows: the duration of ebb and flood currents; the time to slack water of ebb and flood current; and the magnitude of the mean and maximum ebb flood currents. Both the maximum and mean current velocities during ebb exceed the corresponding velocities during flood. The averaged duration-difference during 3 observation period was ebb dominant. The duration percent of ebb is larger than that of flood. HRE has ebb dominance that is stronger and longer than flood. Such asymmetry can be explained in terms of the hydraulic current generated by the continuously changing tidal ranges and phases at different points (e.g. T0 and T8).

The characteristic of mass flux at Yeomha channel, Gyeonggi Bay

D.H. LEE, S.B. WOO

Department of Oceanography, College of Natural Science, Inha University, 253 Yonghyun-dong, Nam-gu, Incheon, Korea

To calculate the total mass flux that change in time and space in the Yeomha Channel of Gyeonggi Bay, the 13 hour bottom tracking observation was performed from the entrance (Line1) of the Yeomha Channel and the southern extremity (Line2) during the spring and neap tidal cycles. The value of the total mass flux (Lagrange flux) was calculated as the sum of the Eulerian flux value and stroke drift value and the tidal residual flow was harmonically analyzed through the least-squares method. Moreover, the average during the tidal cycle is essential to calculate the mass flux and the tidal residual flow and there is the need to equate the lattice of repeatedly observed data. Nevertheless, due to the great differences in the studied region, the number of vertical lattice tends to change according to time and since the horizontal lattice differs according to the transport speed of the ship as a characteristic of the bottom tracking observation, differences occur in the horizontal and vertical lattice for each hour. Hence, the present study has vertically and horizontally normalized (sigma coordinate) to equate the lattice per each hour. When compared to the z-level coordinate system, the Sigma coordinate system was evaluated to have no irrationalities in data analysis with 3~5% of error. As a result of the analysis, the tidal residual flow displayed the flow pattern of sagging in the both ends in the main waterway direction of Line2. In Line1, it was confirmed that the tidal residual flow was dominated by favorable pressure caused by the differences in height of the sea surface. As a result of the total mass flux, the ebb properties of 576cms and 67cms were observed during spring and neap tides, respectively. This is the intertidal region between Youngjong-do and Ganghwa-do and estimated to outpour approximately 935cms during the spring tides and approximately 315cms during the neap tides.

Mathematical modeling of the effect of constructing LNG terminal on hydrodynamic environment

WENDAN LI, MENG GUO LI

Tianjin Research Institute for Water Transport Engineering, Tianjin, China

WEI LIU

Tianjin Port Engineering Design & Consultancy Co. Ltd., Tianjin, China

According to the feature of the project and the sea area where the LNG terminal project lies, a 2-D tidal current mathematical model with irregular triangular grids is set up in this paper. Verification and validation are carried out fully against the measured data of 2009. A numerical simulation of tidal current is made after the project of LNG terminal in Yuedong area. In this paper, we analysis the detailed variation of the tidal current after the implementation of the project, such as: local flow field、 flow condition in front of wharf、 current velocity and direction in harbor basin and channel、 influence scope、 flow along the dike、 cross flow in channel. We master the flow field of present situation and the flow field after the implementation of

the project to provide the scientific basis for feasibility of the LNG terminal project. The results show that: though the project's effect on local flow field is obvious with the decreasing of the current velocity in the east and west of the dike and the increasing in the south of the dike, its effect on surrounding environment is limited, so it is feasible to construct the project.

Verification of rip current simulation using HAECUM compared with field observational data

J.Y. LEE, J.L. LEE

Department of Civil and Environmental Engineering, Sungkyunkwan University, Suwon, 440-746, Korea

I.C. KIM

Division of Architecture and Civil Engineering, Dongseo University, Busan, 617-716, Korea

Recently, rip current became a well-known technical term in Korea. At Haeundae beach which is located on the southeastern corner of Korean Peninsula, more than 50 people were swept away by the fast-moving seaward current and rescued, on July 29 and 30, 2010. Haeundae beach draws one million visitors and more than 50 people are rescued due to rip currents every summer season. The holidaymakers, who are enjoying the waves on tubes near the shore, are unexpectedly carried away seawards, floating as far as 50 ~ 100 meters away from the shore where swimming is restricted for safety reasons. A similar situation takes place more than 3 times every summer. Therefore, rescuers have strengthened lookout measures at several spots where dangerous rip currents have occurred.

It is generally accepted that rip currents arise mostly from alongshore a variation in wave height due to wave refraction over alongshore inhomogeneous bathymetry. The field measurement for clarifying the generation mechanism was performed in Haeundae beach. In this study, we verify a rip current forecasting model, HAECUM which was installed for Haeundae beach and using incident wave conditions, we set up a rip current predictive guidance which included in the HAECUM.

Experimental study on hydraulic characteristics and vorticity interactions of floating breakwaters

J. YOON, D. NAMGUNG

Department of Civil and Environmental Engineering, Hanyang University 17 Haengdang-dong, Seongdong-gu, Seoul 133-791, Korea

Y.-S. CHO

Department of Civil and Environmental Engineering, Hanyang University 17 Haengdang-dong, Seongdong-gu, Seoul 133-791, Korea

In this study, laboratory experiments are conducted to investigate flow fields around floating breakwaters by using the LDV (Laser Doppler Velocimetry) system. The LDV system is a well-known equipment to measure fluid particle velocities in laboratory experiments. Although the system requires great efforts and enormous time for measurements, it can provide precise velocity fields comparing to other available equipments. Various types of drafts and shapes for breakwaters are employed in laboratory experiments to analyze a relation between flow-fields

and vortex. A series of numerical experiments are also carried out by using a two-dimensional Navier-Stokes equations model. Numerically predicted results are compared with experimental measurements.

Hydrodynamic analysis of heave plates of the truss spar platform

XUELIANG JIANG

College of Engineering, Ocean University of China, Qingdao 266100

SONG SANG

College of Engineering, Ocean University of China, Qingdao 266100, State Key Laboratory of Hydraulics and Mountain River Engineering, Chengdu 610065

State Key Laboratory of Coastal and Offshore Engineering, Dalian 116024

In the time domain and frequency domain, the paper studies the influence of the heave plate geometric parameters and layout changes to the Truss Spar's hydrodynamic performance. First, it introduces the basic theory and method which are used in solving the hydrodynamic loads, the hydrodynamic coefficient and the nonlinear time domain response. And then, a number of different heave plate structures of Truss Spar Platform 3D hydrodynamic models are established. These model's hydrodynamic characteristics are discussed and the hydrodynamic coefficients are obtained by using three-dimensional potential flow theory. The relationships between the changes of quantity, distance, thickness of the heave plates and the platform's hydrodynamic coefficients is discovered by analyzing the information. At the same time, it gives coupled analysis to the Spar platform under regular wave in time domain, and also gives analysis to the influence of heave plates' parameter changes on platform's time domain motion. This paper can provide technical guidance for the optimal layout of heave plate and has a certain practical reference value.

Luo-Xia model and numerical simulations of dual synthetic jets

Z.B. LUO, Z.X. XIA, L. WANG, B. LIU, Q.H. ZENG

College of Aerospace and Material Engineering, National University of Defense Technology, Changsha, 410073, China

The flow-field of a dual synthetic jets actuator is numerically simulated based upon the LUO-XIA model. The results indicate the lower pressure region plays an important role on the interactions of the dual jets. The dual synthetic jets actuator produces two counter-rotating vortex pairs fore and aft. The vorticity of vortex pairs contribute to the pressure difference. The pressure in the domain of the main vortex pairs is lower than other flow domains. The stronger the vortex, the lower the pressure will be. In the near field downstream, the two jets vortex pairs are strong and entrain fluid around them and interact with each other, the saddle points are formed and the flow field is complex. And there is a phenomenon of "self-support" between the dual synthetic jets, which is owed to the pressure difference between the adjacent slots. In the far field downstream, the two jets vortex pairs are weak and the two jets merge a single, more stable jet.

The model can be used to predict pollutant plumes in coastal waters.

Interaction between hydrodynamics and salt marsh dynamics: an example from Jiangsu coast

Z. HU, M.J.F. STIVE, T.J. ZITMAN

Department of Hydraulic Engineering, Delft University of Technology, Stevinweg 1, Delft, 2628 CN, the Netherlands

Q.H. YE, Z.B. WANG, A. LUIJENDIJK

Deltares, Rotterdamseweg 185, Delft, 2629 HD, the Netherlands

Z. GONG

State Key Laboratory of Hydrology-Water Resources and Hydraulic Engineering, Hohai University, Xikang Road 1, Nanjing, 210098, China

T. SUZUKI

Ghent University / Flanders Hydraulics Research, Berchemlei 115 Antwerp, B-2140, Belgium

Salt marshes are distributed along more than 400 km of the Jiangsu coast in Eastern China, which are regarded as important habitats and serve as coastal protection as well. Previous research has proven that salt-marsh vegetation can reduce current velocity and dampen waves by its stems and leaves. Reversely, hydrodynamic forces also have a significant influence on the growth of salt-marsh vegetation. To study the interaction between hydrodynamics and salt-marsh development on the Jiangsu coast, a 2D schematized model has been built by using a new interactive structure between flow, wave and vegetation modules of the process-based model Delft3D. In the hydrodynamic simulations, the impact of vegetation on waves and currents is quantified. In the vegetation growth module, the development of salt marshes is influenced by inundation time and shear stress from hydrodynamic simulations. The feedback loop is completed by hydrodynamic modules receiving the newly updated data of salt-marsh field from the vegetation growth module. The results show that wave height and current velocity are significantly influenced by vegetation. Reversely, the dynamics of marsh vegetation greatly rely on hydrodynamic conditions. Consequently, this interaction between hydrodynamics and salt marsh induces temporal variations of each other. In the model, the salt marsh is especially sensitive to the waves. Though wave height is relatively small on the Jiangsu coast, in terms of bed shear stress, waves may be of great importance to the development of salt marsh.

Modelling chlorophyll a of Bohai bay based on CA-SVM using remote sensing data

XIANQUAN XIANG

School of Environmental Science and Engineering, Tianjin University, Tianjin, China, The National Marine Data and Information Service, Tianjin, China

XIAOFU XU, JIANHUA TAO

School of Environmental Science and Engineering, Tianjin University, Tianjin, China

In this research, an integrated cellular automata (CA) and support vector machine (SVM) model was developed to model the concentration of chlorophyll a in Bohai Bay using remote sensing data. In order to take into account the spatial heterogeneity and local

interaction of the blooms, cellular automata paradigm was implemented. The SVM was used here to constructing nonlinear transition rules for CA, for its better capacity of dealing with nonlinear complex relationships. The CA-SVM model was established with three different cases, which reflect the effect of 8-neighbouring cell of chlorophyll a concentration, the spatial position of the cell, and external factors such as SDD, SSC, SST. The model was calibrated and verified by remote sensing data of Bohai Bay. Through this study, it is shown that the spatial position, and external factors such as SDD, SSC, SST have a great effect on the distribution of chlorophyll a, and the proposed CA-SVM model could be preferably to simulate and predict the concentration of chlorophyll a in Bohai Bay, and capture the non-linear information in ecological processes.

Experimental study on wave energy concentration and control measures in limited sheltered basin area

HAI-CHENG LIU

Tianjin Research Institute for Water Transport Engineering, Tianjin 300456, China

YUN-JIANG WANG

CCCC First Harbor Engineering Company Ltd., Tianjin 300456, China

Based on wave physical model test of Yantai West Port, the wave energy concentration phenomenon and control measures in limited sheltered basin area are introduced. The mooring conditions are not improved as expected and deterioration in part region in Yantai West Port after the outside breakwater constructed. Even some slide and other facilities construction are damaged by the wave. Through physical model test and theoretical analysis, the reasons of the construction damaged are found, that is the wave energy concentration. The previous research shows that the wave energy concentration has related with many factors that include the rate of sheltered area scale (a) and wave length (L), the formation of construction, reflection wave and stem wave, etc. In this physical model, the port has already been constructed, so the rate of a/L can't be altered and other ways must be found to reduce or remove the wave energy concentration. During the test, the stem wave appears near the LPG berth, and it is the main wave energy that diffusing into the limited sheltered basin. The different control measures are studied that includes the way to reduce wave energy diffusing into the limited sheltered basin area and the way to absorb wave energy at the wave energy concentration area, in the physical model. And by the two ways, wave energy concentration disappears, and wave becomes calmness in the limited sheltered basin area. It may serve as reference for similar projects.

Numerical investigation on water discharge capability of sluice caisson of tidal power plant

G. KIM

Division of Ocean System Engineering, Mokpo National Maritime University, Mokpo city, Jeollanam-do, 530-729, Republic of Korea

S.-H. OH, K.S. LEE, I.S. HAN, J.W. CHAE

*Coastal Engineering & Ocean Energy Research Department,
Korea Ocean Research and Development Institute, 787
Haeanlo, Ansan, Gyeonggi-do 426-744, Korea*

S.-J. AHN

*GeoSystem Research, 1-40 Keumjung-Dong, Kunpo,
Gyeonggi-do, Korea*

The design methodology of the sluice caisson structure is one of important factor that is close related to the efficiency in tidal power generation. When the sluice caisson is designed to maximize the water discharge capability, it is possible to minimize the number of sluice caissons for attaining the water amount required for achieving the target power generation, which results in reduction of the construction cost for the sluice caisson structure. The discharge capability of sluice caisson is dependent on the geometrical conditions of an apron structure which is placed in both sides of the sluice caisson. In this study, we investigated numerically the variation of water discharge capability of sluice caisson according to the geometrical conditions of apron. Flow fields are simulated with FLOW-3D software using VOF method.

Poster Session 2
Friday, 16 December
Ballroom A

Mooring line dynamics for a floating wave energy converter

D.H. JUNG, S.H. SHIN, H.J. KIM, H.S. LEE
Daejeon branches, Korea Ocean Research & Development Institute, KOREA #171, Jang-dong, Yuseung-ku, Daejeon, Korea

Dynamic behavior characteristics for the mooring line of a floating wave energy converter with the numerical study are analyzed. The case studies for the different top excitation in the horizontal and axial direction induced by surge and pitch motion of a floater are carried out. On the operational condition, the height of tension variation of a mooring line by the top excitation in the axial direction at the top of a mooring line shows almost 2.5 times than it in the horizontal direction. That can be an important parameter to determine the connection point between a floater and top point of mooring line. It is found that the top excitation with long period by slow drift motion of a floater induces the large excursion resulting in large top tension of a mooring line. In the design of a mooring system point of view, the different natural frequencies according to excursion distance and static configuration should carefully be considered.

Design and control of a 50kw class rotating body type wave energy converter

BYUNG-HAK CHO, SHIN-YEOL PARK, DONG-SOON YANG, KYUNG-SHIK CHOI, BYUNG-CHUL PARK
Korea Electric Power Research Institute, 65 Munjiro, Yuseonggu, Daejeon, 305-380, Korea

A 50kW class rotating body type wave energy converter (WEC) composed of two floating bodies and a power takeoff (PTO) unit is designed based on the experimental and simulation studies. As a wave energy extractor, the body is equipped with a variable liquid-column oscillator (VLCO) having a liquid filled U-tube and air chambers. The PTO converts the rotational moment introduced from the relative motion of the hinged bodies to a hydraulic power by means of a cylinder. A high pressure accumulator, a hydraulic motor and a generator are provided for the PTO to convert the hydraulic power to a high quality electric power. Control laws for adjusting the oscillation period of the VLCO, and regulating the pressure and flow rate of the working oil pumped by the cylinder are proposed for the efficient operation of the WEC.

Dam break simulation using level-set finite volume method for solving two phase incompressible flows

KIL SEONG LEE, KIDOO PARK, WOO YEON SUNWOO
Dept. of Civil and Environmental Engineering, Seoul National University, 599 Gwanak-ro Gwanak-gu, Seoul, 151-744, Korea

In order to analyze incompressible two-phase flow, level-set method is applied on the artificial compressibility (AC) method in which the incompressible Navier-Stokes (INS) equations are directly solved for velocity components and pressure. Level-set function is defined as a signed distance

function from the interface between gas and liquid. Numerical model for a two-phase flow is developed on general curvilinear coordinate. The numerical study is applied for a dam break problem and the numerical result is in overall agreement.

Direct numerical simulation of wave deformation around submerged structures using IB method

MIN-JI KIM, JUNG-HYUN PARK, YONG-WON SEO, DO-SAM KIM

Department of Civil Engineering, Korea Maritime University, 727 Taejon-ro, Yeongdo-Gu, Busan, 606-791, South Korea

KWANG-HO LEE, NORIMI MIZUTANI
Department of Civil Engineering, Nagoya University, 1 Furo-cho, Chikusa-ku, Nagoya, 464-8603, Japan

In this work, we employed the immersed boundary method and volume of fluid method to simulate the interactions between free-surface waves and submerged fixed structures. The immersed boundary method is applied to handle solid object boundaries that are replaced with a proper force in the Navier-Stokes equations imposed on the body surface. Submerged obstacles of different shapes such as trapezoids, and semicircles are investigated to validate the ability of the numerical model to simulate fluid-structure problems. The comparison between the results of the developed numerical model, available experimental data, and numerical estimations reveal a favorable agreement.

Numerical study on the tidal effect of seawater intrusion in Liao Dong Bay coastal plain, China

F. DING, T. YAMASHITA, H. S. LEE, M. HAGGAG
Graduate School for International Development and Cooperation, Hiroshima University, 1-5-1 Kagamiyama, Higashi-Hiroshima, Japan

In 2007, the State Oceanic Administration of People's Republic of China started monitoring the seawater intrusion in China. The results showed that seawater intrusion area in the coastal plain of Liao Dong Bay already encroached more than 4,000 km² of land area with nearly 1,500 km² of area in serious condition. The most remote region of seawater intrusion was situated 68 km inland from the shore of Pan Jing City. To analyze the tidal effect on seawater intrusion, a three-dimensional numerical model of density-dependent groundwater flow and miscible salt transport was developed based on SEAWAT code which combined the two commonly used groundwater flow and solute transport modeling programs of MODFLOW and MT3DMS. A simulation of 55 months (from October 2004 to April 2009) in the coastal plain of Liao Dong Bay (140 km x 119.997 km) was conducted by this numerical code. After model calibration, two prediction cases were conducted considering no-tidal and with-tidal effect for an extension of continuous 40 years starting April 2009 based on the calibration model. The results of the two cases showed that seawater intrusion area will increase in all layers and that seawater intrusion into the Quaternary layer will be significantly faster than that of the Minhuazhen group layer. In addition, most of the Quaternary layer chlorine content of with-tidal case

will be higher than those under the no-tide case, especially in the area located within 20 km from the coast. The extension of seawater intrusion area encroached nearly 10 km deep in the Quaternary layer and 3 km in the Minhuazhen group layer.

Spatial and temporal variations and hydrodynamics explanation to suspended sediment concentration in the Changjiang (Yangtze) estuary, China

S.H. ZUO

Key laboratory of Engineering Sediment of Ministry of Communications, Tianjin Research Institute of Water Transport Engineering, Tianjin 300456, China; State Key Laboratory of Coastal and Offshore Engineering, Dalian University of Technology, Dalian 116024

J.F. LI

State Key Laboratory of Estuarine and coastal Research, East China Normal University, Shanghai 20062, China

L.Q. SHI

The Second Institute of Oceanography, Hangzhou 310012, China

Large-scale hydrological observations in the Yangtze Estuary in China have been carried out in February and July, 2003. Based on these data, temporal and spatial variations of suspended sediment concentration in the Yangtze Estuary are studied from the upriver sites to the mouth sites with the multi-methods of hydrology and statistics. The results show that (1) the reach of upriver, in whose suspended sediment concentration is stable oppositely, is controlled mainly by the runoff current; (2) suspended sediment concentration of downstream to the mouth bar is effected by some factors, for example runoff, tide, landform etc, and its variation is complicated; (3) during a tidal cycle, suspended sediment concentration is related to the current velocity, but lags to the current velocity about one or two hours. The sediment transport flux exists space-time change complexly due to the runoff and tidal current. Also the process of sediment re-suspension is more complicated in the South Passage and North Passage than other passages in respect to the salinity, and the re-suspension process is an important source of suspended sediment for maximum turbid zone. Suspended sediment re-suspension is related to the critical velocity and the eddy diffusion coefficient.

Research on sediment deposition in deep-water compound navigation channel

LIANCHENG SUN, NA ZHANG

Key laboratory of Engineering Sediment of Ministry of Communications, Tianjin Research Institute of Water Transport Engineering, Ministry of Communications, Tianjin, China

The port of Tianjin is located at a muddy coast in the western Bohai Bay. Based on field measured data and former research achievements, 3-dimension tidal flow and sediment mathematical model is set up and is used to compute sediment deposition of 300,000-ton deep-water compound navigation channel. In the paper, an empirical formula of computing sediment deposition of compound navigation channel is presented. Both methods have been applied to engineering practice.

The results from empirical formula and mathematical model show that the error is about 10%.

Three-dimensional numerical simulation of cohesive sediment transport due to a typhoon

NA ZHANG, HUA YANG, BING YAN, HONGBO ZHAO

Key Laboratory of Engineering Sediment of Ministry of Communications, Tianjin Research Institute of Water Transport Engineering, Ministry of Communications, Tianjin, China

In the paper, wind wave field, tidal current field and suspend sediment concentration field and the deposition in the channel in Lianyungang sea area are simulated based on MOHID 3D tidal current and sediment mathematical model, SWAN wind wave model. Wind field during Typhoon Wipha is simulated using the method of the Fujita.T formula and Takahashi formula. The computed results and the field measured data is compared and verification. The computed results are compared with measured data. The verification shows that the simulated result tallies well with the field observation data, thus the forecasts may serve engineering practice.

Diagnosis and improvement for status and problems of dredging and ocean disposal of coastal sediment in Korea

KI-HYUK EOM, DAE-IN LEE, GUI-YOUNG KIM

Marine Environmental Impact Assessment Center, National Fisheries Research & Development Institute, Busan, 619-705, Korea

To minimize negative impacts of dredging and ocean disposal of coastal sediment on marine ecosystem and potential strife among coastal users, we suggest 1) in development projects involving ocean disposal, it should be mandatory to propose careful reuse plans in the land, and 2) guidelines of environmental assessment and consequence management programs should be developed and implemented. As a consequence, different assessment fields need to be emphasized for evaluation of the impact that both dredging and dumping might have on the sites involved. The status of current assessment procedures is examined and its problems are diagnosed. Following checklists of core assessment items are proposed as part of a revamped review process, along with improvements to the assessment system.

On the wintertime abnormal storm waves along the east coast of Korea

H.S. LEE, T. YAMASHITA

Department of Development Technology, Graduate School for International Development and Cooperation, Hiroshima University, 1-5-1 Kagamiyama, Higashi-Hiroshima 739-8528, Hiroshima, Japan

In the winter East Sea/Japan Sea (EJS), the abnormal high waves due to the East Asian monsoon and winter storms (extratropical cyclones) are often reported and causes large coastal damages around the EJS. Along the east coast of Korea, there were large coastal damages in Oct. 2005 and Oct. 2006 due to the swell induced by winter storms passing through the EJS from Korean Peninsular to the east and the southeast, respectively. In this study, we investigated the

abnormal storm waves in the winter EJS to find out their generation mechanism based on the atmospheric systems and performed numerical simulations of two events in 2005 and 2006 by using a WRF-WWIII modeling system since the timely and accurate forecast of the atmospheric and wave fields is one of the key factors to reduce related coastal disasters. In the numerical simulations, the wind input and whitecapping source terms were investigated in detail to evaluate the performance of available source terms in WWIII. The results of Hsig and Tsig from three source terms show high correlation coefficient with the observed values, while the differences among the three terms remain small. The atmospheric systems were categorized into three patterns based on their movements and the modeling results showed good agreements with the observed wave parameters.

Evaluation of tsunami fluid force acting on a bridge deck subjected to plunging breaker bores and surging breaker bores

G. SHOJI, Y. HIRAKI

Department of Engineering Mechanics and Energy, University of Tsukuba, Japan

The 2011 off the Pacific Coast of Tohoku earthquake tsunami caused the catastrophic damage of infrastructures such as coastal structures, utilities and transportation facilities. Among infrastructures evaluation of tsunami fluid force acting on a bridge deck is urgently required for designing a tsunami-proof bridge structure. Authors carried out hydraulic experiments to clarify a tsunami wave load on a bridge deck subjected to plunging breaker bores and surging breaker bores, focusing on the relationship between the position of a bridge deck against wave height and the occurrence of wave forces acting on a bridge deck.

Discussion on calculation of wave forces on submerged quarter circular breakwater under irregular waves

X.L. JIANG

Department of Civil Engineering, Tianjin Institute of Urban Construction, Tianjin, China

Y.B. LI

School of Civil Engineering, Tianjin University, Tianjin, China

L.W. QIE

School of Civil Engineering, Hebei University, Baoding, Hebei, China

A series of irregular wave experiments were carried out to study the hydraulics of submerged quarter circular breakwater (QCB) focusing on horizontal wave forces. First, the methodology of model experiments is introduced in brief. Then, the frequency spectrum analysis is performed to learn about the interior characteristics of irregular dynamic pressures on submerged QCB and semi-circular breakwater (SCB). Next, the horizontal wave forces on QCB calculated with the empirical formulas are compared with the experimental data. Finally, the difference between the horizontal wave forces on SCB and QCB are explored by both comparing the synchronal pressure distributions on both breakwaters and simulating the fluid fields around both breakwaters.

Steady streaming and set-ups due to gravity-capillary waves in a viscous fluid

C.O. NG

Department of Mechanical Engineering, The University of Hong Kong, Hong Kong, China

H.C. HSU

Tainan Hydraulics Laboratory, National Cheng Kung University, Tainan 701, Taiwan

This paper presents a theoretical study on the mass transport and set-ups due to partially standing gravity-capillary waves in a domain that can be closed or open ended. Based on Lagrangian coordinates, a perturbation analysis is carried out to the second order to find the mean Lagrangian drift and the free surface set-ups, which expression is shown to be different when described by the Eulerian and Lagrangian approached. This solution can be reduced to a second-order pure partial standing wave solution obtained by Ng [1].

Numerical analysis of abnormal long wave “abiki” generated by local meteorological disturbance

HENDRI, T. YAMASHITA

Department of Development Technology, Graduate School for International Development and Cooperation, Hiroshima University, 1-5-1 Kagamiyama, Higashi-Hiroshima 739-8529, Japan

T. KOMAGUCHI

Blue Wave Institute of Technology, Co. Ltd, Tokyo, Japan

“Abiki” is a Japanese local name of abnormal long waves that cause disasters of flooding and damages to aquaculture facilities mainly in inner bay. In July 2009, an extraordinary phenomenon happened in Hagi and Hamada City. This time, Abiki phenomenon was generated off Japan Sea and affected the city with a maximum wind speed of 13.8 m/s as reported by JMA (2009). By focusing on a possible cause of wet microburst onto the sea surface, this study conducted the numerical simulation of downburst and long wave generation using the models of ocean model (POM) and atmosphere model (cloud resolving simulation model, CReSS) for the case of Abiki, off Hagi and Hamada in 2009. From the weather chart (Japan Meteorological Agency, JMA (2009)), warm air on the upper layer and cold air on the lower layer mixed just after the disappearance of the stationary front that is formed by cold air in low pressure zone, and warm and moist air which is fed by the high pressure over the Pacific Ocean. CReSS simulation was conducted using the background data from JMA’s reanalysis (GPV-MSM) data with 3 km horizontal resolution (240×240 grids) and 300 m vertical resolution in 53 layers. The resulting sea surface pressure and wind parameters were then transferred to POM for long wave simulation. Simulation results showed that immediately after the disappearance of the stationary front with 5 hPa pressure difference, a low pressure disturbance moving slowly westward was reproduced. This result explains the atmospheric pressure changes observed at Hagi and Hamada city. However, downburst was not clearly reproduced. The wave height off Hagi and Hamada as computed by POM was a several centimeters high with the period of 75-100

min. On the other hand the observed Abiki height in the inner bay of Susa with complex topography was 30-40 cm with the same wave period as offshore waves.

Numerical study for waves propagating over submerged porous breakwater

YONGZHOU CHENG, CHENGXIANG LIU, YUN PAN, QINGFENG LI

School of Hydraulic Engineering, Changsha University of Science & Technology, 960, 2nd Section, Wanjiashi South RD, Changsha, Hunan 410004, China

The coupling numerical model is used to study the interaction between the water waves and submerged porous breakwater. Based on the calculation results, the influences of submerged trapezoidal porous breakwater height, crown width and porosity on transmission coefficients are analyzed. The results denote that wave damping increase with submerged crown width and breakwater height increased. Wave reflection, transmission and dissipation coefficients have a balance point at the porosity $n=0.6$ which the porous breakwater has good performance for wave-damping. The velocity field around the breakwater is also investigated, and compared with impermeable breakwater on the slope bed.

Study on the wave making and wake washes of trimaran

L. ZHOU, G. GAO

School of Transportation, Wuhan University of Technology, Heping Avenue 1040# Wuhan, 430063, China

The washes generated from the high speed ships are becoming a serious problem with the speed up of the ships, how to reduce the wake washes or the effects of the wake washes are challenges for coastal and ship engineers. Predicting the wash accurately and finding the laws of the washes is the first step to solve these problems, and it's the aim of this paper.

A combined near/far-field method is used to calculate the waves of trimaran in deep water, a raised Rankine-source panel method based on NURBS is used to calculate the near field waves of trimaran, and then a wave spectrum analysis method is used to calculate the far field waves based on the results of the near field. The law of wake washes of trimaran is discussed according to the numerical results together with the experimental results, and the effects of the displacement of side bodies and hull spacing between main body and side body on the wave-making resistance and washes of trimaran are also investigated. The maximum wave height criterion is used in the paper.

For the trimaran calculated in this paper, maximum wave heights at the same lateral distance decrease with the increase of transverse spacing Y_s ; the maximum wave heights with the side hull at the middle of main hull are lower than the ones with the side hull at the aft of main hull; the wave making resistance changes in a similar way.

When the side hull located at the aft of the main hull, the wave-making resistance decreases with the increase of the displacement of the side hull with relatively lower Froude numbers; when the side hull

located at the middle of the main hull, the resistance of trimaran with side hull displacement of 2.8% is smaller than the one with side hull displacement of 3.6%.

Wave calculations for seawall rehabilitation in Hangzhou Bay

JINHAI ZHENG, SHANGFEI LIN

State Key Laboratory of Hydrology-Water Resources and Hydraulic Engineering, Hohai University, 1 Xikang Road, Nanjing 210098, China

College of Harbor Coastal and Offshore Engineering, Hohai University, 1 Xikang Road, Nanjing 210098, China

The WABED wave model is applied to predict design wave parameters for the project of breaking a seawall in Lingang New Planning District, Shanghai, China. By applying Putian wind-wave formulas to calculate the wave parameters along the water depth contour of 8-9m, the design wave parameters at initial section are chosen from the larger result of the Energy-fetch Method and the Surface-to-shore Fetch Method. Wave predictions are obtained through calculation of 12 combinations with different design tide levels and wind velocities. Results show that the security of the project is controlled by waves from the south-east and south directions.

Numerical modelling of Kandy Lake, Sri-Lanka in preparation for water quality improvement

J.H. PU¹, K.B.S.N. JINADASA², W.J. NG¹, S.K. WERAGODA³, C. DEVENDRA⁴, S. K. TAN¹

¹*Nanyang Environmental and Water Research Institute (NEWRI), Nanyang Technological University, 639798 Singapore*

²*Department of Civil Engineering, University of Peradeniya, 20400 Sri Lanka*

³*National Water Supply and Drainage Board, Kandy, 20400 Sri Lanka*

⁴*Irrigation Department, Regional Director's Office, Kandy, 20000 Sri Lanka*

Kandy City is recognised by UNESCO as a world heritage city because of its history and cultural treasures. In the centre of the city is Kandy Lake, a 0.25 km² man-made waterbody. Urbanisation and consequent inadequate waste management facilities have resulted in deterioration of the lake's water quality. This study investigates issues related to water discharges into the lake and flow patterns therein. The hydraulic study utilises Delft3D software as the computational tool. Flow 'dead-zones' which can be locations of lower water quality and accumulation of debris are identified using the model. A number of possible mitigation solutions are discussed in the paper. These include diversion of existing drainage channels to other less sensitive locations in the lake.

Evaluation of the vertical and horizontal undrained bearing capacities of suction buckets for wind turbines in clay

CHI HUNG LE, SUNGRYUL KIM

Civil Engineering Department, Dong-A University, 840 Hadan-2dong, Saha-gu, Busan, 604-714, South Korea

MYOUNGHAK OH

Coastal Engineering & Ocean Energy Research Department, Korean Ocean Research & Development Institute

Three-dimensional finite element analyses were performed to evaluate the undrained bearing capacities of suction bucket foundations in homogenous clay. The loading conditions were vertical (V), horizontal (H), and combined (V-H). The effect of the aspect ratios (skirt length to diameter ratios, L/D) of a suction bucket on the bearing capacities was investigated. Dimensionless and normalized failure envelopes in a V-H load space were developed. The sizes and shapes of failure envelopes, as well as the failure mechanism, were clearly shown to be dependent on the aspect ratios of the foundations.

Application of cement stabilization sediment dredged as subgrade road of rigid pavement

HAMZAH YUSUF, MUHAMMAD SALEH PALLU,
LAWALENNA SAMANG, M.WIHARDI TJARONGE,
AMAR AKBAR ALI

*Departement of Civil Engineering, Hasanuddin University,
Makassar, Indonesia*

On March 26, in 2004, some areas of Mount Bawakaraeng landslide, carrying an expected avalanche of material about 230 million cubic meters of sediment in the upstream, due to the effect on the future ruins of multi-purpose reservoir located Bili-bili +30 km downstream from caldera. There are around 75 million cubic meters of fine sediment that had accumulated in the bottom of reservoirs and nearly reaches the intake. Therefore, the effort is needed in order to maintain the stability of sediment dredging reservoir function. The purpose of this study is to examine the behavior of sediment dredging Bili-bili Dam with cement stabilization for rigid pavement and give solutions to optimize the Bili-bili Dam function in a way to dredge the sediments around the intake. The method used to achieve this objective is by dredging sediments around the intake dam, but the impact on the accumulation of material (material dumping) and damage the environment. While the other parties would need the land for road construction is increasing, but the soil is limited and expensive. By looking at the problem, this study tries to make an assessment of sediment dredging to be used as a soil base (subgrade). The improvement of the sediment was conducted with a number of tests such as physical tests, chemical, and minerals to determine the characteristics of actual dredging sediment continued with stabilization of the soil sample, namely mixing with cement binder percentage and curing time, and then conducted laboratory tests to look at mechanical index. Results of laboratory tests were then conducted the test model with rigid pavement loading, to find a large decline in sediment material from the subgrade, cement stabilization of loading, the results of the analysis in the form of graphs the relationship between the modulus of subgrade reaction (k) with some of the CBR as a model validation data.



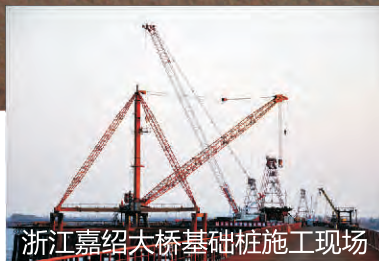
8000HP多用途拖轮



起重打桩船



海供船



浙江嘉绍大桥基础桩施工现场



水泥砼拌和船



广东省长大公路工程有限公司

GUANGDONG PROVINCIAL CHANGDA HIGHWAY ENGINEERING CO.,LTD

广东省长大公路工程有限公司具备国家公路工程施工总承包特级资质，并拥有对外经营权。是一家集施工、设计、养护、科研、资本运作于一体的工程总承包企业，公司总资产超过100亿元，年土建施工能力100亿元。

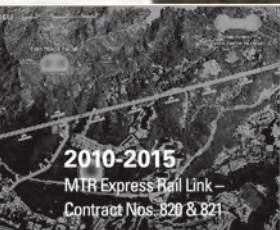
公司成立以来，先后进入了9个国家和地区以及国内11个省的公路建设市场，建成水上特大型、大中型桥梁200多座。公司在大跨度悬索桥、斜拉桥、连续刚构桥、连续梁桥、拱桥等施工技术达到了国内领先水平。在施工工艺、产品质量、科技进步等方面获得国家科技进步奖、国家级工法、国家发明专利、中国土木工程詹天佑奖、鲁班奖、国家优质工程银质奖共20项。公司通过了广东省高新技术企业、广东省“省级工程技术研究开发中心”、广东省“省级企业技术中心”的评审认证，荣获广东省十大创新企业提名奖。

公司拥有新材料、新技术、新工艺生产研发基地和船舶设备基地，投资建造和购置了国内外先进的大型水上施工设备、路面施工拌和、摊铺设备及隧道施工设备等超过30亿元，拥有先进的计算机辅助设计、施工和管理系统，实现了大型化、专业化、机械化工程项目施工。

长期以来，公司依法经营、诚信经营。公司良好的信誉和企业形象赢得了各界褒奖，先后获得了“全国施工技术先进单位”、“全国交通运输系统先进集体”、“全国五一劳动奖状”、“全国工人先锋号”等称号。2006年被评为中国交通建设“十大桥梁英雄团队”，“九五”以来，被列为“全国百强建筑企业”。



SHAPING THE CITY FOR OVER 50 YEARS



2010-2015
MTR Express Rail Link –
Contract Nos. B20 & B21



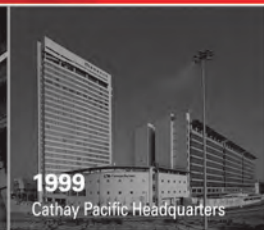
2010-2013
Kai Tak Cruise Terminal Building



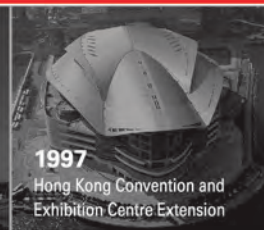
2005
AsiaWorld-Expo



2003
KCRC - Kwai Tsing Tunnels



1999
Cathay Pacific Headquarters



1997
Hong Kong Convention and
Exhibition Centre Extension



1994
Hong Kong Stadium
Redevelopment



1991
Pacific Place - Phase II



1982
Central MTR Station



1975/1964
Lion Rock Tunnels



1968
Plover Cove Reservoir



1958
Kai Tak Airport Runway